energies

Special Issue Reprint

Sustainable Energy Development in Liquid Waste and Biomass

Edited by
Timothy Sibanda

mdpi.com/journal/energies

MDPI

Sustainable Energy Development in Liquid Waste and Biomass

Sustainable Energy Development in Liquid Waste and Biomass

Guest Editor

Timothy Sibanda

MDPI

Basel • Beijing • Wuhan • Barcelona • Belgrade • Novi Sad • Cluj • Manchester

Guest Editor
Timothy Sibanda
School of Molecular and Cell
Biology
University of the
Witwatersrand
Johannesburg
South Africa

Editorial Office
MDPI AG
Grosspeteranlage 5
4052 Basel, Switzerland

This is a reprint of the Special Issue, published open access by the journal *Energies* (ISSN 1996-1073), freely accessible at: https://www.mdpi.com/journal/energies/special_issues/H7LLW5K23J.

For citation purposes, cite each article independently as indicated on the article page online and as indicated below:

Lastname, A.A.; Lastname, B.B. Article Title. *Journal Name* **Year**, *Volume Number*, Page Range.

ISBN 978-3-7258-4561-3 (Hbk)
ISBN 978-3-7258-4562-0 (PDF)
https://doi.org/10.3390/books978-3-7258-4562-0

Contents

Preface

This Special Issue reprint explores the sustainable energy potential of liquid waste and biomass through a multidisciplinary lens. Aimed at advancing both scientific and practical understanding of waste-to-energy systems, it responds to the urgent need for low-carbon energy solutions. Intended for researchers, students, and policymakers, the volume promotes innovation, circularity, and environmental responsibility.

Timothy Sibanda
Guest Editor

energies

MDPI

Article

Calorific Value Prediction Model Using Structure Composition of Heat-Treated Lignocellulosic Biomass

Sunyong Park [1], Seon Yeop Kim [2], Ha Eun Kim [2], Kwang Cheol Oh [3], Seok Jun Kim [1], La Hoon Cho [1], Young Kwang Jeon [1] and DaeHyun Kim [1,3,*]

[1] Department of Interdisciplinary Program in Smart Agriculture, Kangwon National University, Hyoja 2 Dong 192-1, Chuncheon-si 24341, Republic of Korea; psy0712@kangwon.ac.kr (S.P.)
[2] Department of Biosystems Engineering, Kangwon National University, Hyoja 2 Dong 192-1, Chuncheon-si 24341, Republic of Korea
[3] Agriculture and Life Science Research Institute, Kangwon National University, Hyoja 2 Dong 192-1, Chuncheon-si 24341, Republic of Korea
* Correspondence: daekim@kangwon.ac.kr; Tel.: +82-33-250-6496

Abstract: This study aims to identify an equation for predicting the calorific value for heat-treated biomass using structural analysis. Different models were constructed using 129 samples of cellulose, hemicellulose, and lignin, and calorific values obtained from previous studies. These models were validated using 41 additional datasets, and an optimal model was identified using its results and following performance metrics: the coefficient of determination (R^2), mean absolute error (MAE), root-mean-squared error (RMSE), average absolute error (AAE), and average bias error (ABE). Finally, the model was verified using 25 additional data points. For the overall dataset, R^2 was ~0.52, and the RMSE range was 1.46–1.77. For woody biomass, the R^2 range was 0.78–0.83, and the RMSE range was 0.9626–1.2810. For herbaceous biomass, the R^2 range was 0.5251–0.6001, and the RMSE range was 1.1822–1.3957. The validation results showed similar or slightly poorer performances. The optimal model was then tested using the test data. For overall biomass and woody biomass, the performance metrics of the obtained model were superior to those in previous studies, whereas for herbaceous biomass, lower performance metrics were observed. The identified model demonstrated equal or superior performance compared to linear models. Further improvements are required based on a wider range of structural biomass data.

Keywords: woody biomass; herbaceous biomass; prediction model; calorific value

1. Introduction

Biomass is used as a countermeasure against environmental pollution. Research has been conducted to use biomass as fuel [1], remove environmental pollution [2], or use it as an environmental improvement agent [3]. These biomass can be analysed using various methods, including elemental, proximate, and structural analyses. In the context of biomass composition, structural analysis refers to the method of analysing the contents of cellulose, hemicellulose, and lignin, which make up the biomass [4–6]. Cellulose is represented as $[C_6H_{10}O_5]_n$ and consists of linear chains composed of hundreds to thousands of D-glucose units connected by beta (1→4) glycosidic bonds, as shown in Figure 1. Hemicellulose is composed of hexose sugars, such as glucose, mannose, galactose, and rhamnose, and pentose sugars, such as arabinose and xylose. They are classified based on the main sugar residues in their backbones, which can be xylan, mannan, or glucan, as shown in Figure 2. Lignin refers to hydrophobic phenolic molecules found in various components of woody plants, such as conifers and hardwoods. Precursor molecules like p-coumaryl alcohol (H), coniferyl alcohol (G), and sinapyl alcohol (S) (Figure 3) form complex three-dimensional polymer structures via β-O-4 or carbon-carbon linkages [7,8].

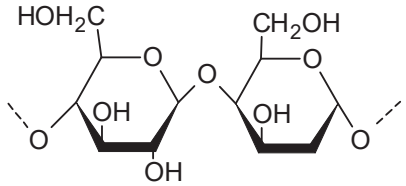

Figure 1. Structure of cellulose.

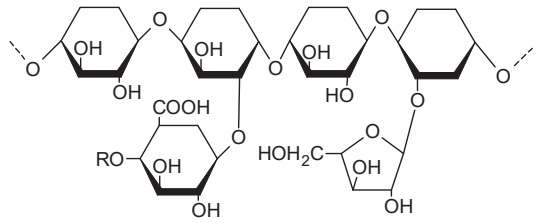

Figure 2. Structure of hemicellulose (arabinoglucuronoxylans).

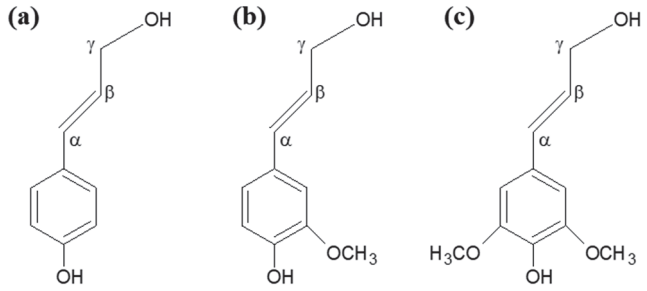

Figure 3. Structure of (**a**) p-coumaryl alcohol; (**b**) coniferyl alcohol; and (**c**) sinapyl alcohol.

Previous studies have predicted calorific values of different biomass considering based on their structural characteristics. Howard [9] investigated the variation in calorific values based on different parts of pinewood and highlighted the correlation between extractives and calorific values. Tillman [10] utilised a single variable in a model to estimate the higher heating value (HHV) of wood, which was expressed as dry weight as well as on a dry ash-free basis. White [11] introduced four equations, one of which calculated the calorific value of wood-containing extractives, whereas the other three calculated the calorific values of woods without extractives. Additionally, White proposed a fifth equation inspired by Tillman's work. Callejón-Ferre et al. [12] predicted a correlation between the structural analysis and calorific values of plant residues within greenhouses in Almería, Spain. Subsequently, predictive equations for the heating value based on structural analysis were also proposed for various biomass and thermally treated biomass. Table 1 summarizes some of the previous studies that predicted HHV by analysing the structure.

Table 1. Models used in previous studies to predict a higher heating value (HHV) using structure analysis.

Model	Biomass	Reference
$HHV = 19.307 + 0.118[E]$	Pine	[9]
$HHV = 0.17389[Ho] + 0.26629(100 - [Ho])$	Extractive-free wood	[10]
$HHV^B = 17.9017 + 0.0744[L] + 0.0661\ [E]$	Unextracted wood, four softwoods and four hardwoods	[11]
$HHV^B = 17.7481 + 0.0800[L^*](100 - [E]) + 0.0886[E]$		
$HHV^B = 17.6132 + 0.0853[L^*]$	Extractive-free wood	
$HHV^B = 17.4458 + 0.0907[L^*]$	Extractive-free softwood	
$HHV^B = 18.0831 + 0.0637[L^*]$	Extractive-free hardwood	

Table 1. *Cont.*

Model	Biomass	Reference
$HHV^B = 0.0889[L] + 16.8218$	Extractive-free wood and non-wood	[13]
$HHV^B = 0.0893[L] + 16.9742$	Extractive-free lignocellulosic materials	
$HHV^B = 0.0877[L] + 16.4951$	Extractive-free non-wood	
$HHV^B = 0.0864[L] + 16.6922$	Extractive-free sunflower shells, almond shells, hazelnut shells, wood bark, olive husks, hazelnut kernel husks, and walnut shells	[14]
$HHV = 0.0979[L] + 16.292$	Corn stover, corn cobs, sunflower shells, beech wood, Ailanthus wood, hazelnut shells, wood bark, olive husks, and walnut shells	[15]
$HHV = 10.955 + 0.692[L]$	Greenhouse crops	[12]
$HHV = 8.211 + 0.150[H] + 0.767[L]$		
$HHV = 7.405 + 0.163[H] + 0.065[C] + 0.682[L]$		
$HHV = 16.1964 + 0.0555[L]$	Twenty biomass samples of agro-forestry wastes and industrial wastes	[16]
$HHV = 17.0704 - 0.0202[H] + 0.0449[L]$		
$HHV = 19.393 + 0.039[E]$	Tree species from Oaxaca, Mexico	[17]
$HHV = 23.527 - 0.059[C]$		
$HHV = 22.582 - 0.051[C] + 0.032[E]$		
$HHV = 17.893 + 0.068[L]$	Mixture of eight untreated and heat-treated woods	[18]

[B] converted from Btu/lb; * extractive free; [C] cellulose; [H] hemicellulose; [L] lignin; [E] extractive.

Equations for predicting the calorific value of heat-treated biomass have been proposed for elemental and proximate analyses [19,20]. However, few equations are available to predict the calorific value of heat-treated biomass based on structural analyses. Therefore, in this study, we aimed to present an equation for predicting the calorific value of heat-treated biomass based on structural analysis.

2. Materials and Methods

2.1. Collection of Data

From previous studies, 111 structural analyses and calorific value data were collated for 59 woody and herbaceous biomass samples of 52 herbaceous plants [21–35]. All data are summarised in Table S1. The distributions of the structural composition and calorific value of the biomass are shown in Figures 4 and 5.

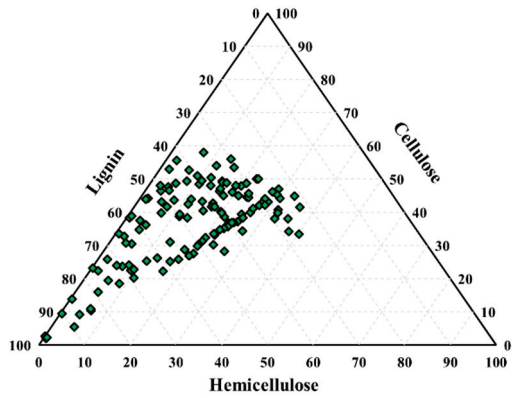

Figure 4. Scatter plot of structural composition of biomass.

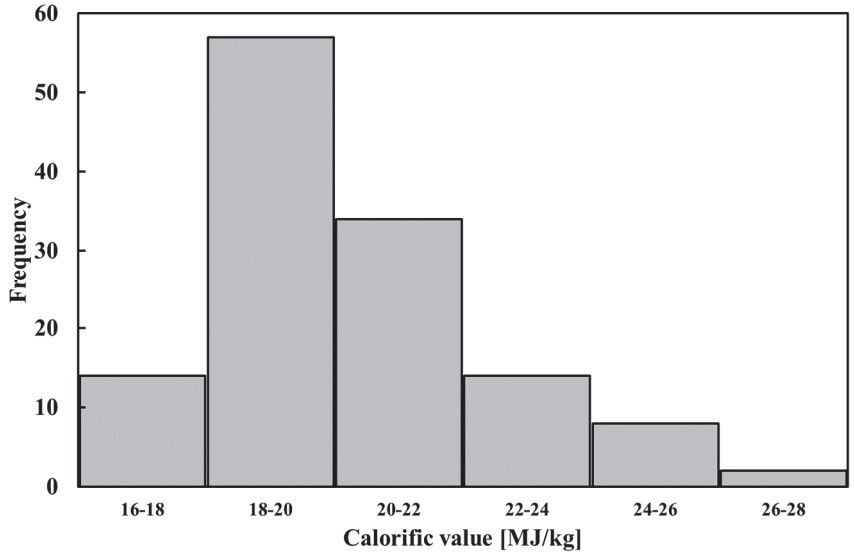

Figure 5. Histogram of calorific value.

2.2. Pearson Correlation Coefficient

The study employed the Pearson correlation coefficient (Equation (1)) to assess the relationships compositional (Cell, Hemi, and Lig) analyses and calorific value. This coefficient, as defined in Equation (1), was employed to evaluate the extent of correlation between two sets of data. It ranges from -1 to 1, where positive and negative values indicate a direct and inverse relationship, respectively. Values closer to -1 or 1 signify a stronger linear correlation, while those closer to 0 suggest a weaker correlation [36]. The analysis involved deriving correlation equations with varying goodness-of-fit values through linear and non-linear regressions applied to the final analysis data using IBM SPSS version 22.0. However, for exponential and logarithmic regression models, they were not applied due to the possibility of certain structural components becoming zero during thermal treatment. The data analysis in this study employed a combination of the "stepwise" and "enter" methods within the SPSS software. The input variables included C, H, L, squared (C^2, H^2, and L^2), and squared roots ($C^{0.5}$, $H^{0.5}$, and $L^{0.5}$).

$$R = \frac{\left(\sum_{i=1}^{n}\left(X_i - \overline{X}\right)\left(Y_i - \overline{Y}\right)\right)}{\sqrt{\sum_{i=1}^{n}\left(X_i - \overline{X}\right)^2}\sqrt{\sum_{i=1}^{n}\left(Y_i - \overline{Y}\right)^2}} \quad (1)$$

2.2.1. Linear Regression

Linear regression is a statistical approach frequently employed to ascertain the value of a dependent variable using an independent variable [37]. This method relies on a mathematical equation that yields a single value by considering a combination of input characteristics. The linear regression equation is represented as follows [38]:

$$\hat{y} = \beta_O + x_1\beta_1 + x_2\beta_2 + x_3\beta_3 + \ldots + x_n\beta_n \quad (2)$$

2.2.2. Polynomial Regression

Polynomial regression is a statistical technique in which data are approximated using a polynomial function [39]. It entails the incorporation of higher-order terms of variables to estimate the polynomial regression and construct a curved response surface [40]. As there is no universally applicable polynomial equation, the equation should be derived based on the specific problem under consideration. The general expression for a polynomial function is as follows [38]:

$$f(x) = c_o + c_1x + c_2x^2 + \ldots + c_nx^n \quad (3)$$

2.3. Model Evaluation

The suitability of the model was assessed using different performance metrics. Four performance metrics were used, namely the coefficient of determination (R^2), mean absolute error (MAE), root-mean-squared error (RMSE), average absolute error (AAE), and average bias error (ABE). R^2 was employed because of its advantage in facilitating relative performance comparisons using Equation (4). This quantifies the proportion of variance in the dependent variable that is predictable from the independent variables [39]. MAE was used because it measures the absolute difference between the observed and predicted values in the same units (Equation (5)), which makes it intuitive and straightforward to interpret. RMSE has the advantage of reducing the distortion in the values resulting from squaring the errors (Equation (6)). However, its drawback is that errors < 1 become even smaller owing to squaring, whereas errors > 1 become larger. AAE and ABE represent the average errors in the correlation equation (Equations (7) and (8)). ABE is evaluated such that positive values are rated higher, indicating a better fit, whereas negative values suggest a somewhat lower fit [37,38]. These metrics provide a comprehensive evaluation of the performance of a model by considering different aspects of its accuracy and fit.

$$R^2 = 1 - \frac{\sum_{i=1}^{n} \mathrm{Value_M} - \mathrm{Value_P}}{\sum_{i=1}^{n} \mathrm{Value_M} - \overline{\mathrm{Value_P}}}, \quad (4)$$

$$\mathrm{MAE} = \frac{\sum_{i=1}^{n} (\mathrm{Valule_M} - \mathrm{Value_P})}{n}, \quad (5)$$

$$\mathrm{RMSE} = \sqrt{\left(\frac{1}{n}\right) \sum_{i=1}^{n} (\mathrm{Value_M} - \mathrm{Value_P})^2} \quad (6)$$

$$\mathrm{AAE} = \frac{1}{n} \sum_{i=1}^{n} \left| \frac{\mathrm{Value_P} - \mathrm{Value_M}}{\mathrm{Value_M}} \right|, \quad (7)$$

$$\mathrm{ABE} = \frac{1}{n} \sum_{i=1}^{n} \left[\frac{\mathrm{Value_P} - \mathrm{Value_M}}{\mathrm{Value_M}} \right], \quad (8)$$

Validation of the optimal conditions was conducted based on the performance metrics mentioned above, using the data listed in Table 2.

Table 2. Validation data for suggested model.

Biomass	Type	Cell [%]	Hemi [%]	Lig [%]	HHV [MJ/kg]	Ref.
Mixed waste wood	Woody	38.30	25.50	22.00	17.50	[27]
Torrefied mixed waste wood (200 °C)	Woody	41.10	26.30	26.50	19.20	
Torrefied mixed waste wood (250 °C)	Woody	43.70	7.70	31.40	19.90	
Torrefied mixed waste wood (300 °C)	Woody	36.20	5.30	43.70	20.80	
Oak waste wood	Woody	38.30	25.50	22.00	18.60	
Torrefied Oak waste wood (200 °C)	Woody	41.10	26.30	26.50	19.10	
Torrefied Oak waste wood (250 °C)	Woody	43.70	7.70	31.40	21.20	
Torrefied Oak waste wood (300 °C)	Woody	36.20	5.30	43.70	22.50	
Miscanthus	Herbaceous	41.40	19.70	22.60	16.41	
Torrefied miscanthus (200 °C)	Herbaceous	41.90	21.20	23.10	19.15	
Torrefied miscanthus (250 °C)	Herbaceous	44.10	8.40	41.60	21.10	
Torrefied miscanthus (300 °C)	Herbaceous	35.00	3.20	52.30	21.28	

Table 2. *Cont.*

Biomass	Type	Cell [%]	Hemi [%]	Lig [%]	HHV [MJ/kg]	Ref.
Hops	Herbaceous	42.2	0	26.20	16.59	
Torrefied hops (200 °C)	Herbaceous	42.9	0	26.80	18.80	
Torrefied hops (250 °C)	Herbaceous	47.00	0	35.10	18.90	
Torrefied hops (300 °C)	Herbaceous	39.90	0	38.70	20.70	
Torrefied pine chip (225 °C)	Woody	41.23	12.87	38.42	19.48	
Torrefied pine chip (250 °C)	Woody	41.90	6.93	45.70	20.08	
Torrefied pine chip (275 °C)	Woody	39.54	0.99	53.30	21.82	
Torrefied pine chip (300 °C)	Woody	12.84	0.56	79.99	25.38	
Logging residue chip	Woody	37.49	13.26	26.15	18.79	[41]
Torrefied logging residue chip (225 °C)	Woody	41.04	14.77	33.20	19.79	
Torrefied logging residue chip (250 °C)	Woody	38.57	5.87	42.49	21.21	
Torrefied logging residue chip (275 °C)	Woody	34.08	5.23	52.80	22.03	
Torrefied logging residue chip (300 °C)	Woody	6.10	1.04	85.06	26.41	
Torrefied Cotton Balls	Herbaceous	29.44	24.22	34.20	18.73	[42]
Torrefied Sunflower	Herbaceous	31.00	29.35	24.73	19.65	
Wet torrefied bamboo (180 °C 30 min 0 M HCl)	Herbaceous	42.61	25	23.18	17.79	
Wet torrefied bamboo (180 °C 15 min 0.2 M HCl)	Herbaceous	34.97	0	33.94	24.19	[43]
Wet torrefied bamboo (180 °C 30 min 0.2 M HCl)	Herbaceous	13.96	0	36.98	24.86	
Corn straw	Herbaceous	39.12	30.95	10.73	18.61	
Torrefied corn straw (160 °C)	Herbaceous	38.03	28.86	10.12	19.17	[44]
Torrefied corn straw (180 °C)	Herbaceous	37.11	28.12	9.87	19.79	
Torrefied oat hull (285 °C)	Herbaceous	33.52	0.72	45.65	22.45	[29]
Torrefied bamboo (280 °C 10 min)	Herbaceous	49.76	8.60	39.79	19.88	
Torrefied bamboo (280 °C 30 min)	Herbaceous	49.40	5.56	43.12	20.11	[45]
Torrefied bamboo (280 °C 60 min)	Herbaceous	47.40	2.03	50.40	20.42	
Sweet sorghum bagasse	Herbaceous	29.80	24.40	5.24	17.30	
Torrefaction sweet sorghum bagasse	Herbaceous	19.90	4.80	16	23	[46]

To compare the optimal model selected based on the validation data with those of previous studies, we used the test dataset provided in Table 3 for verification.

Table 3. Verification test dataset for comparison validation model and previous studies.

Biomass	Type	Cell [%]	Hemi [%]	Lig [%]	HHV [MJ/kg]	Ref.
Softwood	Woody	47.40	13.80	23.50	18.00	
Torrefied softwood	Woody	36.60	2.65	23.20	22.30	[47]
Torrefied hardwood	Woody	46.70	1.20	15.70	22.40	

Table 3. *Cont.*

Biomass	Type	Cell [%]	Hemi [%]	Lig [%]	HHV [MJ/kg]	Ref.
Norway spruce	Woody	41.70	26.00	30.90	20.37	[46]
Torrefied Norway spruce (260 °C 8 min)	Woody	42.30	23.20	30.40	20.65	
Torrefied Norway spruce (260 °C 25 min)	Woody	40.10	13.50	33.90	21.51	
Corn straw	Herbaceous	39.12	30.95	10.73	18.61	[44]
Torrefied corn straw (160 °C)	Herbaceous	38.03	28.86	10.12	19.17	
Torrefied miscanthus (230 °C 15 min)	Herbaceous	44.50	18.50	26.80	19.30	[48]
Torrefied miscanthus (250 °C 15 min)	Herbaceous	44.90	12.20	32.80	19.70	
Torrefied miscanthus (250 °C 30 min)	Herbaceous	43.30	9.90	36.20	19.90	
Torrefied willow (230 °C 15 min)	Woody	39.70	18.10	28.70	19.60	
Torrefied willow (250 °C 15 min)	Woody	40.50	15.30	30.30	19.90	
Torrefied willow (270 °C 15 min)	Woody	41.10	12.90	33.40	20.20	
Torrefied willow (230 °C 30 min)	Woody	39.30	16.80	29.60	19.60	
Torrefied willow (250 °C 30 min)	Woody	40.30	14.70	31.40	19.80	
Torrefied willow (270 °C 30 min)	Woody	41.60	14.20	32.90	20.50	
Bamboo	Herbaceous	48.03	24.13	27.83	19.00	[49]
Wet torrefied bamboo (200 °C)	Herbaceous	50.22	22.68	27.10	19.40	
Wet torrefied bamboo (220 °C)	Herbaceous	49.88	25.09	25.03	19.60	
Dry torrefied bamboo (180 °C)	Herbaceous	43.13	25.04	31.84	19.10	
Dry torrefied bamboo (200 °C)	Herbaceous	36.78	27.96	35.25	19.40	

3. Results and Discussion

3.1. Result of Pearson Correlation Coefficient

The results of the Pearson's correlation coefficient are summarized in Figure 6. In the case of cellulose, a positive correlation was observed with hemicellulose, while a negative correlation was found with calorific value. The reason for the positive correlation between hemicellulose and cellulose is likely because they share precursor structures composed of pentose or hexose sugar monomers. For hemicellulose, there was a negative correlation with calorific value and lignin. Particularly, the strong negative correlation of -0.7668 with lignin suggests that in heat-treated samples, the presence of hemicellulose decreases while the lignin content increases due to the decomposition of hemicellulose. In the case of cellulose, it decomposes at high temperatures and decreases like hemicellulose, which is inversely proportional to the increase in HHV. However, due to lower decomposition rate compared with hemicellulose, it has a negative correlation, but it appears to be a weaker correlation than the correlation between hemicellulose and HHV. Lignin, on the other hand, exhibited a strong positive correlation of 0.6518 with the calorific value. This can be attributed to the fact that lignin is a polymer with a high carbon content, and in heat-treated samples, the lignin content tends to be higher, leading to an increase in calorific value.

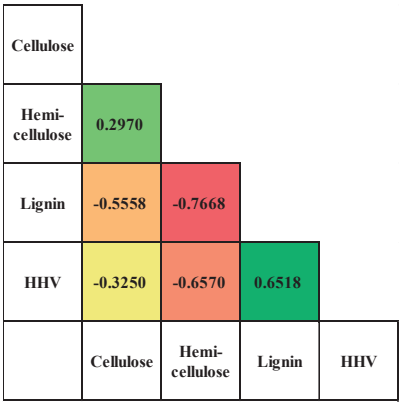

Figure 6. Result of Pearson correlation coefficient.

3.2. Prediction Model Using Total Biomass

The equations for predicting the calorific value of the overall biomass are summarised in Table 4. Given the diverse characteristics of the various biomass samples, they exhibited substantial variations, which likely contributed to the lower R^2 values. Various input variables were applied, and the highest R^2_P value of 0.5814 was obtained for T3.

Table 4. Calorific value prediction model using overall lignocellulosic biomass.

No.	Equation	R^2_P [-] [1]	$RMSE_P$ [-] [2]	MAE_P [%] [3]	AAE_P [%] [4]	ABE_P [%] [5]
T1	$HHV = 22.011 - 0.649H^{0.5} + 0.0000424L^2$	0.5423	1.3858	1.1006	5.3455	0.4302
T2	$HHV = -4.205$ $-0.003C^2 + 0.576C - 1.931C^{0.5}$ $+0.003H^2 - 0.589H + 7.491H^{0.5}$ $+0.007L^2 - 1.337L + 10.134L^{0.5}$ $+0.013CH - 1.313CH^{0.5}$	0.5719	1.5215	1.1764	5. 7280	2.1895
T3	$HHV = -2.918$ $+0.228C - 0.269H + 5.553H^{0.5}$ $-1.115L + 0.006L^2 + 8.469L^{0.5}$ $+0.01CH - 1.138CH^{0.5}$	0.5814	1.5455	1.1924	5.8641	2.9964

[1] coefficient of determination, [2] root mean square error, [3] mean absolute error, [4] average absolute error, [5] average bias error.

T1 and T2 had an R^2_P value of 0.5423 and 0.5719, respectively. T3 had the highest value of $RMSE_P$ at 1.5455, whereas T1 had the lowest $RMSE_P$ of 1.3858. AAE_P for T1 was calculated as 5.3455%. However, T2 and T3 exhibited an error rate of 5.7280% and 5.8641%, respectively. Furthermore, among the prediction models that used the overall biomass, the predicted values were higher, resulting in positive ABE_P values. T1 exhibited the lowest ABE_P of 0.4302%. Hence, T2 predicted more accurately than the ABE_P of T2 and T3, which were 2.1895% and 2.9964%, respectively. Given that the performance metrics did not meet the desired level of accuracy, a decision was made to enhance the model's performance by separating the predictions for woody and herbaceous biomass. This separation was undertaken as the simultaneous prediction of both hardwoods and softwoods may have contributed to the reduced accuracy observed in the model.

3.3. Prediction Model Using Woody Biomass

Three prediction models for woody biomass are presented in Table 5. When compared to the previous prediction models for lignocellulosic biomass, the R^2_P values for woody biomass were notably higher, ranging from 0.82 to 0.83. Similarly, the $RMSE_P$ values for these models fell within the range of 0.96 to 1.18.

Table 5. Calorific value prediction model using woody biomass.

No.	Equation	R^2_P [-]	$RMSE_P$ [-]	MAE_P [%]	AAE_P [%]	ABE_P [%]
W1	$HHV = 31.257 - 0.039C + 0.001C^2 - 0.88C^{0.5} + 0.074H - 0.001H^2 - 1.738H^{0.5} - 0.001L^2 + 0.463L^{0.5}$	0.7811	1.2810	1.0860	5.3534	2.8879
W2	$HHV = 31.027 + 0.000316C^2 - 1.118C^{0.5} - 1.398H^{0.5} - 0.001L^2 + 0.462L^{0.5}$	0.8222	1.1888	0.8724	4.0008	−1.7930
W3	$HHV = 27.567 - 0.28C^{0.5} - 1.333H^{0.5}$	0.8392	0.9626	0.7238	3.5106	0.2286

Interestingly, in most cases, an increase in the number of input variables tended to result in higher R^2_P values, which could indicate a risk of overfitting. However, it is worth noting that for the prediction models of woody biomass, the model with the highest number of input variables, W1, exhibited the lowest R^2_P value and the highest $RMSE_P$. On the contrary, the model with the fewest input variables, W3, demonstrated reasonable performance, boasting an R^2_P of 0.8392 and an $RMSE_P$ of 0.9626.

3.4. Prediction Model for Herbaceous Biomass

The prediction models for herbaceous biomass are outlined in Table 6. The R^2_P values for these models varied in the range of 0.82 to 0.87. Interestingly, the model with the fewest input variables, H1, had the lowest R^2_P, whereas the model with the most input variables, H3, had the highest R^2_P. However, when considering the $RMSE_P$, H1 had the highest value at 1.2958. In terms of ABE_P, only H2 had a positive value, while H1 and H3 had negative values, indicating an underestimation in the latter cases. The reason for the low accuracy of herbaceous biomass was due to be extractive and non-uniformity compared with woody biomass. In general, it is known that the extractive and ash content of herbaceous biomass is higher than that of woody biomass [50,51]. Because this was not considered in this study, it was determined to be low.

Table 6. Calorific value prediction model using herbaceous biomass.

No.	Equation	R^2_P [-]	$RMSE_P$ [-]	MAE_P [%]	AAE_P [%]	ABE_P [%]
H1	$HHV = 24.918 + 0.002Ho^2 - 1.36Ho^{0.5} + 2.813H^{0.5} - 0.003L^2 + 0.165L - 0.67CH^{0.5}$	0.8256	1.2958	1.1723	5.9563	−5.8252
H2	$HHV = 15.513 + 0.002C^2 - 1.283C^{0.5} - 0.297H + 0.007H^2 + 2.688H^{0.5} - 0.388L + 4.23L^{0.5} + 0.003CH - 0.504CH^{0.5}$	0.8561	0.6294	0.5243	2.7030	1.8674
H3	$HHV = 14.738 + 0.002C^2 - 1.246C^{0.5} + 0.007H^2 - 0.31H + 2.8H^{0.5} - 0.429L + 4.524L^{0.5} + 0.003CH - 0.521CH^{0.5}$	0.8739	0.4836	0.3698	1.8929	−0.2333

3.5. Validation of Calorific Value Prediction Models

A validation process was carried out to determine the most suitable model among the presented models. Table 7 displays the validation outcomes for overall lignocellulosic biomass. The validation results reveal that T2 achieved the highest R^2_{CV}, standing at 0.7870. However, it also displayed the lowest $RMSE_{CV}$, which was 1.1258. Both T1 and T3 demonstrated R^2_{CV} values of approximately 0.4920. Comparing MAE_{CV} and AAE_{CV}, T2 demonstrated satisfactory performances. In conclusion, based on the validation results, T2 emerged as the optimal model.

Table 7. Validation of the results obtained from the model using overall lignocellulosic biomass.

	R^2_{CV} [-]	$RMSE_{CV}$ [-]	MAE_{CV} [%]	AAE_{CV} [%]	ABE_{CV} [%]
T1	0.4920	1.9178	1.3871	6.6409	0.3278
T2	0.7870	1.1258	0.9180	4.3728	0.3878
T3	0.4902	1.9198	1.4490	7.0107	1.2695

Regarding woody biomass (Table 8), most models displayed R^2_{CV} values within the range of 0.60 to 0.69. However, W3 stood out with the highest R^2_{CV} value of 0.8108. The $RMSE_{CV}$ values generally fell between 1.44 and 1.45 for most models, although W1 had a slightly higher $RMSE_{CV}$ at 2.0387. When considering ABE_{CV}, W3 had the highest value, reaching 5.2810, compared to W1 and W2 with values of 3.7659. Despite its higher ABE_{CV}, W3 was deemed the optimal choice due to its combination of a high R^2_{CV}, low $RMSE_{CV}$, and a reduced number of input variables.

Table 8. Validation of the results obtained from the model using woody biomass.

	R^2_{CV} [-]	$RMSE_{CV}$ [-]	MAE_{CV} [%]	AAE_{CV} [%]	ABE_{CV} [%]
W1	0.6217	2.0387	1.8632	9.1077	7.6093
W2	0.6933	1.4568	1.2382	5.9518	3.7659
W3	0.8108	1.4423	1.2070	5.9422	5.2810

In the case of herbaceous biomass (Table 9), the R^2_{CV} values were notably higher, increasing within the range of 0.528 to 0.8959. Additionally, their $RMSE_{CV}$ values ranged from 1.3266 to 2.1312, respectively. The R^2_{cv} of H1 was the highest at 0.8959, but $RMSE_{CV}$ was 2.1312, higher than H2's 1.3266. H2 and H3 showed better performance in $RMSE_{CV}$, MAE_{CV}, AAE_{CV}, and ABE_{CV}. Despite a lower R^2_{cv}, H2 was determined to be optimal.

Table 9. Validation of the results obtained from the model using woody biomass.

	R^2_{CV} [-]	$RMSE_{CV}$ [-]	MAE_{CV} [%]	AAE_{CV} [%]	ABE_{CV} [%]
H1	0.8959	2.1312	1.9740	9.4032	−9.3217
H2	0.8528	1.3266	1.0707	5.0002	−3.5535
H3	0.8672	1.5457	1.3415	6.2997	−5.3494

3.6. Comparison of the Model with Previous Models

Using a verification dataset, we conducted a comparison between the calorific value prediction model developed in our study and models from previous research. For this study, we chose the model by Demirbaş [13], which was based on non-wood biomass, and the model by Domingos et al. [18], which utilized equations formulated using heat-treated biomass.

The biomass test results are outlined in Table 10. The RMSE values for T2, Demirbaş [13], and Domingos et al. [18] were recorded as 0.7702, 1.3534, and 1.1298, respectively. The T2 model proposed in our study exhibited the lowest RMSE. In the case of torrefied biomass, Domingos et al. [18] displayed a lower RMSE compared to Demirbaş [13]. The R^2 values were relatively low due to the variations in biomass properties, with a notably low R^2 value of 0.0059 observed in previous studies. Since both previous studies predicted only lignin as a variable, R^2 was observed to have the same value. In the case of previous studies, it was predicted based on lignin alone, but other studies indicate that there are other properties that have significant weight in changes in HHV in addition to lignin [50,52]. Through actual analysis, it was confirmed that cellulose and hemicellulose affected HHV. In all model, a negative ABE was noted, indicating an underestimation, as depicted in Figure 7a.

Table 10. Validation of the results obtained from the model using overall biomass.

	Equation	R^2	RMSE	MAE	AAE	ABE
T2	$HHV = -4.205$ $-0.003C^2 + 0.576C - 1.931C^{0.5}$ $+0.003H^2 - 0.589H + 7.491H^{0.5}$ $+0.007L^2 - 1.337L + 10.134L^{0.5}$ $+0.013CH - 1.313CH^{0.5}$	0.5171	0.7702	0.5768	2.9346	−0.2742
Demirbaş [13]	$HHV^B = 0.0877[L] + 16.4951$	0.0058	1.3534	0.8719	4.2037	−3.1029
Domingos et al. [18]	$HHV = 17.893 + 0.068[L]$	0.0058	1.1299	0.7384	3.5927	−0.4441

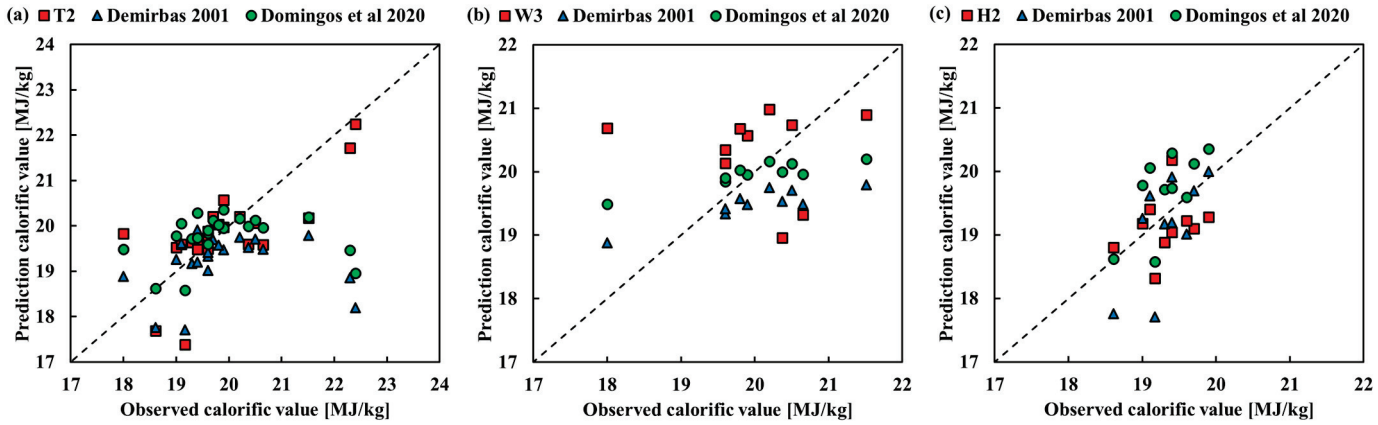

Figure 7. Scatter plot for predicted and observed calorific values when different biomass types were used: (**a**) overall lignocellulosic biomass, (**b**) woody biomass, (**c**) herbaceous biomass [13,18].

In the case of woody biomass (Table 11), the W3 model proposed in our study displayed the lowest RMSE. Conversely, the Demirbaş equation had a higher RMSE of 1.7427 compared to the other two equations. Also, the R^2 value was higher for W3, measuring 0.4152. When considering ABE, W3 was the only equation with a positive value, while that of Demirbaş exhibited a significantly negative value of −4.8843%, indicating an underestimation. Consequently, as depicted in Figure 7b, W3 is represented by a positive trendline, whereas the two equations from previous studies exhibit negative trends.

Table 11. Comparison of the model with those defined in previous studies by using woody biomass test dataset.

	Equation	R^2	RMSE	MAE	AAE	ABE
W3	$HHV = 27.567 - 0.28C^{0.5} - 1.333H^{0.5}$	0.4152	1.2668	1.0902	5.3992	2.7024
Demirbaş [13]	$HHV^B = 0.0877[L] + 16.4951$	0.0894	1.7427	1.2145	5.7017	−4.8843
Domingos et al. [18]	$HHV = 17.893 + 0.068[L]$	0.0894	1.4359	0.9479	4.4850	−2.3996

For herbaceous biomass (Table 12), H1 showed an RMSE of 0.5176, whereas Domingos et al. [18] reported an RMSE of 0.5784. The Demirbaş equation exhibited the highest RMSE among the three at 0.6208. However, the R^2 value for the Demirbaş and Domingos et al. equation was the highest. Regarding the ABE, only the H1 and Demirbaş equation showed negative values, whereas the Domingos et al. equation had positive values. This is illustrated in Figure 7c. The trend line of Domingos et al. exhibited an upward positive trend, suggesting that predictions from the equations tended to overestimate the values. In contrast, the Demirbaş equation and H1 resulted in an underestimation.

Table 12. Comparison of the model with those defined in previous studies by using herbaceous biomass test dataset.

	Equation	R^2	RMSE	MAE	AAE	ABE
H1	$HHV = 15.513 \quad +0.002C^2 - 1.283C^{0.5} - 0.297H$ $+0.007H^2 + 2.688H^{0.5}$ $-0.388L + 4.23L^{0.5} + 0.003CH$ $-0.504CH^{0.5}$	0.0830	0.5176	0.4677	2.4114	−0.8891
Demirbaş [13]	$HHV^B = 0.0877[L] + 16.4951$	0.4382	0.6208	0.4608	2.4060	−0.9652
Domingos et al. [18]	$HHV = 17.893 + 0.068[L]$	0.4382	0.5784	0.4869	2.5220	1.9026

4. Conclusions

In this study, the calorific value of lignocellulose using structural analyses was predicted. Building on previous research, we predicted the calorific value by classifying biomass as overall lignocellulose biomass, woody biomass, and herbaceous biomass. When using the overall biomass dataset, the presented models yielded relatively low R^2_P values, ranging from 0.5423 to 0.5814. However, when analysing the models separately for woody and herbaceous biomass, R^2 values of woody biomass ranged from 0.7811 to 0.8392, and those of herbaceous biomass ranged from 0.8256 to 0.8739.

The optimal model was identified after validation. Equations (9)–(11) were identified as the optimal model equations.

$$HHV = -4.205 \quad -0.003C^2 + 0.576C - 1.931C^{0.5} + 0.003H^2 - 0.589H \\ +7.491H^{0.5} + 0.007L^2 - 1.337L + 10.134L^{0.5} + 0.013CH \\ -1.313CH^{0.5} \tag{9}$$

$$HHV = 27.567 - 0.28C^{0.5} - 1.333H^{0.5} \tag{10}$$

$$HHV = 24.918 \quad +0.002Ho^2 - 1.36Ho^{0.5} + 2.813H^{0.5} - 0.003L^2 + 0.165L \\ -0.67CH^{0.5} \tag{11}$$

Furthermore, the chosen equations were assessed using a test dataset, revealing that T1 and W3 exhibited improved performance compared to previous studies, while H1 showed lower performance compared to prior research. Although the R^2 of H1 was low, the RMSE was low compared to previous studies, so it is seemed to be sufficiently usable. In the case of other studies, they were conducted in an extractive-free biomass, but it is important to note that this study presented a calorific value prediction model that did not consider extractive-free biomass. Also, the accuracy of the model using cellulose, hemicellulose, and lignin was confirmed to be higher than that of the conventional lignin-based calorific value prediction model.

This study aimed to encompass various biomass types but was based on a dataset of 111 biomass samples for model construction. However, the prediction rates for calorific values were relatively low for herbaceous and lignocellulosic biomass datasets. Future research should prioritize the development of models capable of predicting cellulose, hemicellulose, lignin, and calorific values across various biomass types and a wide range of heat treatment conditions.

Supplementary Materials: The following supporting information can be downloaded at: https://www.mdpi.com/article/10.3390/en16237896/s1, Table S1: Data from previous studies, 111 structural analyses and calorific value data.

Author Contributions: Conceptualization, S.P., S.Y.K., H.E.K. and D.K.; methodology, S.P., S.Y.K. and H.E.K.; validation, S.P., K.C.O., S.Y.K. and H.E.K.; investigation, S.P., K.C.O., Y.K.J. and L.H.C.; formal analysis, S.P., S.J.K. and K.C.O.; writing—original draft, S.P. and D.K.; writing—review and editing, S.P., K.C.O. and D.K.; data curation, S.P. and K.C.O.; writing—review and editing, D.K.; supervision, D.K. All authors have read and agreed to the published version of the manuscript.

Funding: This study was carried out with the supported of a research grant of Kangwon National University in 2023. Also, this work was supported by Korea Institute of Planning and Evaluation for Technology in Food, Agriculture and Forestry (IPET) through Agriculture, Food and Rural Affairs Convergence Technologies Program for Educating Creative Global Leader, funded by Ministry of Agriculture, Food and Rural Affairs (MAFRA) (Project No. 320001-4), Republic of Korea. This research was supported by Basic Science Research Program through the National Research Foundation of Korea (NRF) funded by the Ministry of Education (2021R1A6A1A0304424211).

Data Availability Statement: Data are contained within the article.

Conflicts of Interest: The authors declare no conflict of interest.

References

1. Park, S.; Kim, S.J.; Oh, K.C.; Jeon, Y.K.; Kim, Y.; Cho, A.Y.; Lee, D.; Jang, C.S.; Kim, D.H. Biochar from Agro-Byproducts for Use as a Soil Amendment and Solid Biofuel. *J. Biosyst. Eng.* **2023**, *48*, 93–103. [CrossRef]
2. Jia, L.; Cheng, P.; Yu, Y.; Chen, S.-H.; Wang, C.-X.; He, L.; Nie, H.-T.; Wang, J.-C.; Zhang, J.-C.; Fan, B.-G.; et al. Regeneration Mechanism of a Novel High-Performance Biochar Mercury Adsorbent Directionally Modified by Multimetal Multilayer Loading. *J. Environ. Manag.* **2023**, *326*, 116790. [CrossRef]
3. Park, S.; Kim, S.J.; Cho, A.Y.; Kim, Y.; Lee, D.H.; Oh, K.C.; Jang, C.S.; Kim, D.H. Effect of Agro-byproduct Biochar Fertilization on Cherry Tomato Growth and Carbon Sequestration. *J. Agric. Life Environ. Sci.* **2022**, *34*, 229–237. [CrossRef]
4. Motta, I.L.; Miranda, N.T.; Maciel Filho, R.; Wolf Maciel, M.R. Biomass Gasification in Fluidized Beds: A Review of Biomass Moisture Content and Operating Pressure Effects. *Renew. Sustain. Energy Rev.* **2018**, *94*, 998–1023. [CrossRef]
5. Gardner, K.H.; Blackwell, J. The Structure of Native Cellulose. *Biopolymers* **1974**, *13*, 1975–2001. [CrossRef]
6. Yeo, J.Y.; Chin, B.L.F.; Tan, J.K.; Loh, Y.S. Comparative Studies on the Pyrolysis of Cellulose, Hemicellulose, and Lignin Based on Combined Kinetics. *J. Energy Inst.* **2019**, *92*, 27–37. [CrossRef]
7. Ralph, J.; Lapierre, C.; Boerjan, W. Lignin Engineering-Special Issue for Lignin Structure and Its Engineering. *Curr. Opin. Biotechnol.* **2019**, *56*, 240–249. [CrossRef]
8. Vanholme, R.; Morreel, K.; Ralph, J.; Boerjan, W. Lignin Engineering. *Curr. Opin. Plant Biol.* **2008**, *11*, 278–285. [CrossRef]
9. Howard, E.T. Heat of Combustion of Various Southern Pine Materials. *Wood Sci.* **1973**, *5*, 194–197.
10. Tillman, D.A. *Wood as an Energy Resource*; Academic Press: New York, NY, USA, 1978.
11. White, R.H. Effect of lignin content and extractives on the higher heating value of wood. *Wood Fiber. Sci.* **1987**, *19*, 446–452.
12. Callejón-Ferre, A.J.; Carreño-Sánchez, J.; Suárez-Medina, F.J.; Pérez-Alonso, J.; Velázquez-Martí, B. Prediction Models for Higher Heating Value Based on the Structural Analysis of the Biomass of Plant Remains from the Greenhouses of Almería (Spain). *Fuel* **2014**, *116*, 377–387. [CrossRef]
13. Demirbas, A. Relationships between Lignin Contents and Heating Values of Biomass. *Energy Convers. Manag.* **2001**, *42*, 183–188. [CrossRef]
14. Demirbaş, A. Biodiesel Fuels from Vegetable Oils via Catalytic and Non-Catalytic Supercritical Alcohol Transesterifications and Other Methods: A Survey. *Energy Convers. Manag.* **2003**, *44*, 2093–2109. [CrossRef]
15. Acar, S.; Ayanoglu, A. Determination of Higher Heating Values (HHVs) of Biomass Fuels. *Energy Educ. Sci. Technol. Part A Energy Sci. Res.* **2012**, *28*, 749–758.
16. Álvarez, A.; Pizarro, C.; García, R.; Bueno, J.L. Spanish Biofuels Heating Value Estimation Based on Structural Analysis. *Ind. Crops Prod.* **2015**, *77*, 983–991. [CrossRef]
17. Ruiz-Aquino, F.; Ruiz-Ángel, S.; Feria-Reyes, R.; Santiago-García, W.; Suárez-Mota, M.E.; Rutiaga-Quiñones, J.G. Wood Chemical Composition of Five Tree Species from Oaxaca, Mexico. *Bioresources* **2019**, *14*, 9826–9839. [CrossRef]
18. Domingos, I.; Ayata, U.; Ferreira, J.; Cruz-Lopes, L.; Sen, A.; Sahin, S.; Esteves, B. Calorific Power Improvement of Wood by Heat Treatment and Its Relation to Chemical Composition. *Energies* **2020**, *13*, 5322. [CrossRef]
19. Qian, C.; Li, Q.; Zhang, Z.; Wang, X.; Hu, J.; Cao, W. Prediction of Higher Heating Values of Biochar from Proximate and Ultimate Analysis. *Fuel* **2020**, *265*, 116925. [CrossRef]
20. Oh, K.C.; Kim, J.; Park, S.Y.; Kim, S.J.; Cho, L.H.; Lee, C.G.; Roh, J.; Kim, D.H. Development and Validation of Torrefaction Optimization Model Applied Element Content Prediction of Biomass. *Energy* **2021**, *214*, 119027. [CrossRef]
21. Ben, H.; Ragauskas, A.J. Torrefaction of Loblolly Pine. *Green Chem.* **2012**, *14*, 72–76. [CrossRef]
22. Cahyanti, M.N.; Doddapaneni, T.R.K.C.; Madissoo, M.; Pärn, L.; Virro, I.; Kikas, T. Torrefaction of Agricultural and Wood Waste: Comparative Analysis of Selected Fuel Characteristics. *Energies* **2021**, *14*, 2774. [CrossRef]

23. Lin, Y.Y.; Chen, W.H.; Colin, B.; Pétrissans, A.; Lopes Quirino, R.; Pétrissans, M. Thermodegradation Characterization of Hardwoods and Softwoods in Torrefaction and Transition Zone between Torrefaction and Pyrolysis. *Fuel* **2022**, *310*, 122281. [CrossRef]
24. Reza, M.T.; Uddin, M.H.; Lynam, J.G.; Coronella, C.J. Engineered Pellets from Dry Torrefied and HTC Biochar Blends. *Biomass Bioenergy* **2014**, *63*, 229–238. [CrossRef]
25. Arous, S.; Koubaa, A.; Bouafif, H.; Bouslimi, B.; Braghiroli, F.L.; Bradai, C. Effect of Pyrolysis Temperature and Wood Species on the Properties of Biochar Pellets. *Energies* **2021**, *14*, 6529. [CrossRef]
26. Chin, K.L.; H'ng, P.S.; Go, W.Z.; Wong, W.Z.; Lim, T.W.; Maminski, M.; Paridah, M.T.; Luqman, A.C. Optimization of Torrefaction Conditions for High Energy Density Solid Biofuel from Oil Palm Biomass and Fast Growing Species Available in Malaysia. *Ind. Crops Prod.* **2013**, *49*, 768–774. [CrossRef]
27. Ivanovski, M.; Goricanec, D.; Krope, J.; Urbancl, D. Torrefaction Pretreatment of Lignocellulosic Biomass for Sustainable Solid Biofuel Production. *Energy* **2022**, *240*, 122483. [CrossRef]
28. Chen, W.H.; Hsu, H.C.; Lu, K.M.; Lee, W.J.; Lin, T.C. Thermal Pretreatment of Wood (Lauan) Block by Torrefaction and Its Influence on the Properties of the Biomass. *Energy* **2011**, *36*, 3012–3021. [CrossRef]
29. Valdez, E.; Tabil, L.G.; Mupondwa, E.; Cree, D.; Moazed, H. Microwave Torrefaction of Oat Hull: Effect of Temperature and Residence Time. *Energies* **2021**, *14*, 4298. [CrossRef]
30. Granados, D.A.; Ruiz, R.A.; Vega, L.Y.; Chejne, F. Study of Reactivity Reduction in Sugarcane Bagasse as Consequence of a Torrefaction Process. *Energy* **2017**, *139*, 818–827. [CrossRef]
31. Ma, Z.; Zhang, Y.; Shen, Y.; Wang, J.; Yang, Y.; Zhang, W.; Wang, S. Oxygen Migration Characteristics during Bamboo Torrefaction Process Based on the Properties of Torrefied Solid, Gaseous, and Liquid Products. *Biomass Bioenergy* **2019**, *128*, 105300. [CrossRef]
32. Kanwal, S.; Chaudhry, N.; Munir, S.; Sana, H. Effect of Torrefaction Conditions on the Physicochemical Characterization of Agricultural Waste (Sugarcane Bagasse). *Waste Manag.* **2019**, *88*, 280–290. [CrossRef]
33. Xu, F.; Linnebur, K.; Wang, D. Torrefaction of Conservation Reserve Program Biomass: A Techno-Economic Evaluation. *Ind. Crops Prod.* **2014**, *61*, 382–387. [CrossRef]
34. Joshi, Y.; Di Marcello, M.; De Jong, W. Torrefaction: Mechanistic Study of Constituent Transformations in Herbaceous Biomass. *J. Anal. Appl. Pyrolysis* **2015**, *115*, 353–361. [CrossRef]
35. Chen, C.; Qu, B.; Wang, W.; Wang, W.; Ji, G.; Li, A. Rice Husk and Rice Straw Torrefaction: Properties and Pyrolysis Kinetics of Raw and Torrefied Biomass. *Environ. Technol. Innov.* **2021**, *24*, 101872. [CrossRef]
36. Chicco, D.; Warrens, M.J.; Jurman, G. The Coefficient of Determination R-Squared Is More Informative than SMAPE, MAE, MAPE, MSE and RMSE in Regression Analysis Evaluation. *PeerJ Comput. Sci.* **2021**, *7*, e623. [CrossRef]
37. Majumder, A.K.; Jain, R.; Banerjee, P.; Barnwal, J.P. Development of a New Proximate Analysis Based Correlation to Predict Calorific Value of Coal. *Fuel* **2008**, *87*, 3077–3081. [CrossRef]
38. Elmaz, F.; Yücel, Ö.; Mutlu, A.Y. Makine Öğrenmesi Ile Kısa ve Elemental Analiz Kullanarak Katı Yakıtların Üst Isı Değerinin Tahmin Edilmesi. *Int. J. Adv. Eng. Pure Sci.* **2020**, *32*, 145–151. [CrossRef]
39. Zhang, T.; Zhang, Q.; Wang, Q. Model Detection for Functional Polynomial Regression. *Comput. Stat. Data Anal.* **2014**, *70*, 183–197. [CrossRef]
40. Gendy, T.S.; El-Shiekh, T.M.; Zakhary, A.S. A Polynomial Regression Model for Stabilized Turbulent Confined Jet Diffusion Flames Using Bluff Body Burners. *Egypt. J. Pet.* **2015**, *24*, 445–453. [CrossRef]
41. Phanphanich, M.; Mani, S. Impact of Torrefaction on the Grindability and Fuel Characteristics of Forest Biomass. *Bioresour. Technol.* **2011**, *102*, 1246–1253. [CrossRef]
42. Akhtar, J.; Imran, M.; Ali, A.M.; Nawaz, Z.; Muhammad, A.; Butt, R.K.; Jillani, M.S.; Naeem, H.A. Torrefaction and Thermochemical Properties of Agriculture Residues. *Energies* **2021**, *14*, 4218. [CrossRef]
43. Li, M.F.; Shen, Y.; Sun, J.K.; Bian, J.; Chen, C.Z.; Sun, R.C. Wet Torrefaction of Bamboo in Hydrochloric Acid Solution by Microwave Heating. *ACS Sustain. Chem. Eng.* **2015**, *3*, 2022–2029. [CrossRef]
44. Li, Y.; Fan, X.; Zhang, H.; Ai, F.; Jiao, Y.; Zhang, Q.; Zhang, Z. Pretreatment of Corn Stover by Torrefaction for Improving Reducing Sugar and Biohydrogen Production. *Bioresour. Technol.* **2022**, *351*, 126905. [CrossRef] [PubMed]
45. Li, M.F.; Chen, C.Z.; Li, X.; Shen, Y.; Bian, J.; Sun, R.C. Torrefaction of Bamboo under Nitrogen Atmosphere: Influence of Temperature and Time on the Structure and Properties of the Solid Product. *Fuel* **2015**, *161*, 193–196. [CrossRef]
46. Strandberg, M.; Olofsson, I.; Pommer, L.; Wiklund-Lindström, S.; Åberg, K.; Nordin, A. Effects of Temperature and Residence Time on Continuous Torrefaction of Spruce Wood. *Fuel Process. Technol.* **2015**, *134*, 387–398. [CrossRef]
47. Mafu, L.D.; Neomagus, H.W.J.P.; Everson, R.C.; Carrier, M.; Strydom, C.A.; Bunt, J.R. Structural and Chemical Modifications of Typical South African Biomasses during Torrefaction. *Bioresour. Technol.* **2016**, *202*, 192–197. [CrossRef] [PubMed]
48. Grams, J.; Kwapińska, M.; Jędrzejczyk, M.; Rzeźnicka, I.; Leahy, J.J.; Ruppert, A.M. Surface Characterization of Miscanthus × Giganteus and Willow Subjected to Torrefaction. *J. Anal. Appl. Pyrolysis* **2019**, *138*, 231–241. [CrossRef]
49. Yang, W.; Wu, S.; Wang, H.; Ma, P.; Shimanouchi, T.; Kimura, Y.; Zhou, J. Effect of Wet and Dry Torrefaction Process on Fuel Properties of Solid Fuels Derived from Bamboo and Japanese Cedar. *Bioresources* **2017**, *12*, 8629–8640. [CrossRef]
50. Smit, A.; Huijgen, W. Effective Fractionation of Lignocellulose in Herbaceous Biomass and Hardwood Using a Mild Acetone Organosolv Process. *Green Chem.* **2017**, *19*, 5505–5514. [CrossRef]

51. Thammasouk, K.; Tandjo, D.; Penner, M.H. Influence of Extractives on the Analysis of Herbaceous Biomass†. *J. Agric. Food Chem.* **1997**, *45*, 437–443. [CrossRef]
52. Enes, T.; Aranha, J.; Fonseca, T.; Lopes, D.; Alves, A.; Lousada, J. Thermal Properties of Residual Agroforestry Biomass of Northern Portugal. *Energies* **2019**, *12*, 1418. [CrossRef]

energies

MDPI

Article

Effect of Ash from *Salix viminalis* on the Biomass and Heating Value of *Zea mays* and on the Biochemical and Physicochemical Properties of Soils

Edyta Boros-Lajszner, Jadwiga Wyszkowska * and Jan Kucharski

Department of Soil Science and Microbiology, University of Warmia and Mazury in Olsztyn, Plac Łódzki 3, 10-727 Olsztyn, Poland; edyta.boros@uwm.edu.pl (E.B.-L.); jan.kucharski@uwm.edu.pl (J.K.)
* Correspondence: jadwiga.wyszkowska@uwm.edu.pl

Abstract: Wood ash is sometimes used as an alternative to mineral fertilizers; however, there is still a paucity of reliable data concerning its effect on plants—and on biological properties of soil. The present study aimed to determine the possible extent of soil pollution with ash from *Salix viminalis* that does not disturb the growth of *Zea mays* L., intended for energetic purposes, in order to identify how the increasing ash doses affect biochemical and physicochemical properties of soil and to finally to establish the neutralizing effects of soil additives, i.e., compost and HumiAgra preparation, on this soil pollutant. The study demonstrated that the heating value of *Zea mays* L. was stable and not modified by the excess content of ash from *Salix viminalis* in the soil. This finding points to the feasibility of *Zea mays* L. cultivation on soils contaminated with ash from *Salix viminalis* and its use in bio-power engineering. The biomass of the aboveground parts of *Zea mays* L. was significantly reduced after soil contamination with *Salix viminalis* ash dose of 20 g kg^{-1} d.m. soil, whereas the smaller ash doses tested (5–10 g kg^{-1} d.m. soil) did not impair either the growth or the development of *Zea mays* L. The ash inhibited activities of all analyzed soil enzymes but increased soil pH and sorption capacity. Fertilization with compost proved more effective in neutralizing the adverse effect of ash on enzymatic activity of the soil.

Keywords: ash; soil; plant; soil enzymes; heat of combustion; heating value

1. Introduction

Zea mays L. belongs to the *Poaceae* family. Due to its high yield potential and nutritional value, it is cultivated in many regions across the world for food and feed production purposes [1,2]. It is also commonly used as a main energy crop for biogas production. In a major part of Europe, it is treated as a "green energy" for biogas plants [3,4]. In addition, it may be grown for energetic purposes [5] on marginal soil and under stress-triggering conditions [6]. These stress conditions may be induced by excessive soil fertilization with wood ash obtained from, e.g., osier (*Salix viminalis*). *S. viminalis* is a fast-growing species with few soil requirements [7]. It may be cultivated in areas of low agricultural productivity and wastelands [5]. Finally, osier (*Salix viminalis*) has been reported to ensure the best performance among the energy crops [8] and has also been found effective in soil remediation [9].

Wood ash is a product of the combustion of wood materials containing organic and inorganic compounds [10,11]. Ash from biomass has strongly alkaline pH values (pH > 12.5) and is enriched with specified forms of minerals (like quartz and calcite) and nutrients (P, K, Ca, Mg) [12–15]. It contains oxides, hydroxides, carbonates, and silicates but is poor in nitrogen, which volatilizes during combustion [16]. In addition, its fine-grained (powdered) structure (some fractions are even smaller than <1 μm) ensures a very large reactive surface capable of interacting with heavy metals (cadmium, zinc, copper) [14].

Furthermore, ash exhibits various properties, depending on the type and origin of combusted biomass [17–19]. In general, wood-based ashes (the so-called type C ashes) have higher contents of calcium, magnesium, and manganese and higher pH values than those from annual plants (the so-called type K ashes) enriched in potassium, phosphorus, sulfur, and chlorine [20]. Ashes from wood biomass may differ significantly in terms of elemental composition (heavy metals) [18] and content of organic compounds (e.g., PAHs) [21,22]. Apart from essential nutrients, like phosphorus, potassium, calcium, and magnesium, which play an important physiological role in the synthesis of chlorophyll; nucleotides; phosphatides; alkaloids; and multiple enzymes, hormones, and vitamins [23], ash contains certain toxic substances, including organic compounds (chlorobenzenes, PAHs, and chlorophenols), as well as radioactive (^{137}Cs) and toxic (arsenic, cobalt, copper, nickel, lead, zinc) elements, which adversely affect the natural environment [24] and may be toxic to plants [25,26]. Due to its high toxicity and mobility, cadmium has been claimed the most hazardous metal in wood ash [27,28]. Therefore, soil amendment with high doses of ash may disturb nutrient cycling, which regulates organic matter content, and by this means may adversely affect plant growth and development [29]. Given these vast differences in ashes, great caution should be exercised when applying them as soil quality promoters, especially in agrosystems, because—under specified conditions—they may pose a threat to the natural environment (e.g., elution of heavy metals) [18,20] or may exert adverse health effects (e.g., increased uptake of heavy metals from soil by plants) [21,22].

The effects of applying wood-based ashes resemble those of calcium-based fertilizers, namely, they both regulate soil pH, but the ash offers an additional advantage, as it provides nutrients. However, both the wood-based ash and calcium fertilizers are strongly alkaline and may cause damage to crops when applied in excess doses [30]. The use of ash in crop cultivation may elicit both positive and negative outcomes. A study conducted by Liu et al. [1] demonstrated its positive effect when applied to soil in doses of 20 and 40 g kg^{-1} d.m. soil on the growth of *Zea mays* L. and the enzymatic activity of lead-polluted soil. Romdhane et al. [31] also demonstrated its positive impact (26 g kg^{-1} d.m. soil) on shoot growth and leaf number in two analyzed hybrids of *Zea mays* L. In turn, Pukalchik et al. [32] showed that an ash dose of 44.1 g kg^{-1} d.m. soil negatively affected the enzymatic activity of soil. The positive effects of ash may be ascribed to the greater availability of its P and K, whereas its adverse effects may be due to the reduced N content [13]. Given the high pH and chemical composition of wood-based ash, its application in agriculture has been studied for years [33,34]. Its deposition and irrational use in agriculture may result in environmental contamination [35,36].

In view of the above, an innovation of the present study was the application of ash from *Salix viminalis* aimed to establish the doses eliciting positive effects on plants as well as enzymatic activity and physicochemical properties of soil, and also to determine the doses causing soil contamination. In addition, compost and HumiAgra were applied to determine their efficacy in neutralizing the potential adverse effect of ash from *Salix viminalis*.

Taking into account the above data, the following research hypotheses were formulated: (a) up to a certain level (dose), ash from *Salix viminalis* exerts a positive effect on the biomass of aboveground parts and roots, heat of combustion, and heating value of *Zea mays* L. as well as on the activities of soil enzymes and physicochemical properties of soil; (b) once a certain level (dose) of osier ash is exceeded, it becomes a contaminant and elicits adverse effects on plants as well as enzymatic activity and physicochemical properties of soil; and (c) the adverse effects of high doses of ash on *Zea mays* L. biomass and activity of soil enzymes may be neutralized by soil amendment with compost and HumiAgra.

The major goal of this study was to evaluate the effect of ash from *Salix viminalis* on the growth and development of *Zea mays* L. and its heating value. Additional study aims were to determine the impact of increasing ash doses on the biochemical and physicochemical properties of soil and to establish the usability of soil fertilization with compost and HumiAgra preparation on the neutralization of the adverse effects of ash.

2. Materials and Methods

2.1. Characteristics of Soil and Composition of Ash from Salix viminalis, Compost, and Humic Acids

The soil used to establish the experiment was collected form the arable-humus horizon (0–20 cm) of soil in Tomaszkowo village, Olsztyn commune, Warmia and Mazury Province, Poland (53.7161° N, 20.4167° E). The soil was air-dried and sieved through a screen with 0.5 cm mesh diameter. Then, it was assessed for its fraction size composition and basic chemical and physicochemical properties. Soil properties and the design of the vegetation pot experiment are presented in Table 1.

Table 1. Design of the experiment.

Type of Analysis	Pot Vegetation Experiment
Soil characteristics	Sandy clay: sand 69.41%, silt 27.71%, clay 2.88%; Contents: organic carbon—6.18 g kg^{-1} d.m. soil, total nitrogen—1.27 g kg^{-1} d.m. soil; pH_{KCl}—6.09; Hydrolytic acidity (HAC)—8.81 mmol(+) kg^{-1} d.m. soil; Sum of exchangeable base cations (EBC)—24.00 mmol(+) kg^{-1} d.m. soil; Cation exchange capacity (CEC)—32.81 mmol(+) kg^{-1} d.m. soil; Extent of saturation with base cations (BS)—73.14%.
The mass of soil in the pot	3.5 kg
Experimental plant	*Zea mays* L. variety LG 32.58 (4 plants in one pot)
Fertilization in mg kg^{-1} d.m. of soil	N—150 in the form of $CO(NH_2)_2$ P—70 in the form of KH_2PO_4 K—120 in the form of KCl + KH_2PO_4 Mg—15 in the form of $MgSO_4 \times 7H_2O$
Dose of ash from *Salix viminalis* in g kg^{-1} d.m. of soil	0, 5, 10, 20
The content of elements in the ash (Figure 1a) in % d.m.	C—51.04, H—5.87, S—0.02, N—0.38; Cl—0.02; P—0.09; K—0.17; Mg—0.03; Ca—0.41; Na—0.009
pH in KCl	12.50
Compost	Manufacturer: Ekokonsorcjum-Effekt company (Cracow, Poland; license no. 21/02) from green waste (grass, bushes) gathered in parks, squares, and home gardens; fruit and vegetables picked at market squares; and organic waste from food processing plants. Chemical composition in % of d.m.: C_{org}—23.20; N_{Total}—1.30; P—0.26; K—1.24; Mg—0.30; and Ca—1.43.
HumiAgra	Manufacturer: AgraPlant, Kielce, Poland. Chemical composition in % of d.m.: 90% humic acids (50% humins and 50% fulvic acids), 6% K, and 3% S.
Dose of compost and HumiAgra in g kg^{-1} d.m. of soil	0 and 2.5
Experiment duration in days	60
Number of replications	Four repetitions per combination
Conditions in the vegetation hall	The average temperature was 17.5 °C, air humidity reached 78.5%, and day length was from 13 h 4 min to 15 h 30 min. The soil moisture content—50% of the water capillary capacity.

Investigations conducted by Romdhane et al. [31], Błońska et al. [36], Mundała et al. [37], and Núñez-Delgado et al. [38] have demonstrated that the content of cobalt in wood ash ranged from 3.37 to 5.00 mg kg^{-1}, that of chromium from 12.70 to 28.0 mg kg^{-1}, that of copper from 82.50 to 129 mg kg^{-1}, that of nickel from 5.28 to 27.30 mg kg^{-1}, that of lead from 23.30 to 527.00 mg kg^{-1}, that of zinc from 281.60 to 732 mg kg^{-1}, and that of cadmium from 0.22 to 0.55 mg kg^{-1}. According to Someshwar [39], the content of organic substances,

including biphenyl, naphthalene, and phenanthrene, in wood ash is negligible and does not pose threat to the natural environment.

2.2. Study Design

Zea mays L. (Figure 1b) was harvested on day 60 of the experiment (at the BBCH 39 stage) and assessed for the biomass yield of aboveground parts and roots. The aboveground parts of *Zea mays* L. were also analyzed for the heat of combustion and heating value. The leaf greenness index of *Zea mays* L. was evaluated three times throughout the experimental period. In turn, selected soil samples were analyzed for activities of soil enzymes: dehydrogenases, catalase, urease, acid phosphatase, alkaline phosphatase, β-glucosidase, and arylsulfatase. In addition, after crop harvest, the soil samples were analyzed for the following chemical properties: contents of organic carbon (C_{org}) and total nitrogen, and for the following physicochemical properties: pH, hydrolytic acidity (HAC), sum of exchangeable base cations (EBC), total cation exchange capacity (CEC), and extent of saturation with base cations (BS).

(**a**) (**b**)

Figure 1. (**a**) Ash from *Salix viminalis*. (**b**) View of the experiment with *Zea mays* L. in the vegetation hall.

2.3. Biochemical, Chemical, and Physicochemical Analyses of Soil

The experiment included determinations of the activity of soil enzymes as well as basic chemical and physicochemical properties of soil. Analyses of the biochemical soil properties included determinations of activities of: dehydrogenases (Deh) —with Lenhard's method modified by Öhlinger [40]; catalase (Cat)—with Alef and Nannipieri's method [41]; urease (Ure)—with Alef and Nannipieri's method [41]; acid phosphatase (Pac) and alkaline phosphatase (Pal)—with Alef and Nannipieri's method [41]; arylsulfatase (Aryl)—with Alef and Nannipieri's method [41], and β-glucosidase (Glu)—with Alef and Nannipieri's method [41]. Analyses of the chemical properties of soil included determinations of the contents of organic carbon (C_{org}) and total nitrogen (N_{Total}) by means of the Vario MaxCube CN elemental microanalyzer (Hanau, Germany). In turn, the physicochemical soil properties analyzed included: pH—with the potentiometric method in a 1 mol·dm^{-3} aqueous KCl solution, hydrolytic acidity (HAC), and sum of exchangeable base cations (EBC) with the Kappen's method [42]. The HAC and EBC values obtained were used to determine the total cation exchange capacity of soil (CEC) and the extent of its saturation with base cations (BS).

The heating value of *Zea mays* L. was estimated with the combustion method in a C-2000 calorimeter (IKA WERKE, Northchase Pkwy Se, Wilmington, USA). The heat of combustion (Q) was determined acc. to the Polish standard PN-EN ISO 18125:2017 IKA C2000 [43], and the heating value acc. to Kopetz et al. [44]. Contents of carbon, hydrogen, and sulfur were determined by means of an ELTRA CHS 500 automatic analyzer (Neuss, Germany), following PN-G-04584 and PN-G-04517 standard methods [45]. Nitro-

gen content was determined with the Kjeldahl method (ISO 11261) [46]. Contents of P, K, Mg, and Ca levels in *Salix viminalis* wood ash were determined using inductively coupled plasma (ICP) spectroscopy (ICP—OES ThermoiCAP 6500 DUO, ThermoFisher Scientific, Cambridge, UK), after sample mineralization in a mixture of concentrated nitrogen and perchloric acid. The leaf greenness index was determined using a Spectrum Technologies, Inc., Chlorophyll Meter (KONICA MINOLTA, Inc., Chiyoda, Japan).

Biochemical, chemical, and physicochemical analyses were conducted in three replications. A detailed procedure for enzymatic activity determination was provided in a work by Zaborowska et al. [47], whereas the procedures of determinations of chemical and physicochemical parameters were provided in our previous works [48,49]. In turn, the heating value of *Zea mays* L. was described in the study by Wyszkowska et al. [50].

2.4. Computations and Statistical Analysis

One of the computations included calculating the index of the *Salix viminalis* ash effect on activities of soil enzymes. A detailed description of its concept was provided in our previous works [51,52]. Using analysis of variance (ANOVA), the obtained data were statistically analyzed at the significance level of $p \leq 0.05$ using the STATISTICA 13 program [53]. Homogenous groups were computed using the Tukey's test for the following variables: biomass yield of the aboveground parts and roots of *Zea mays* L., heat of combustion, and heating value. Coefficients of the linear Pearson's correlation between the variables were computed, and the coefficient of percentage variability of all analyzed variables (η^2) was calculated by means of the analysis of variance (ANOVA). In turn, the principal component analysis (PCA) was applied to analyze activities of soil enzymes.

3. Results

3.1. Biomass and Heating Value of Zea mays L. Cultivated in Soil with the Addition of Ash from Salix viminalis

The percentage distribution of variable factors revealed the strongest effect (50.51%) of *Salix viminalis* ash dose on the yield of *Zea mays* L. roots. In turn, the aboveground parts of the experimental plant were most strongly affected (as much as 54.83%) by soil amendment with compost and HumiAgra (Table 2).

Table 2. Coefficient of observed variation η^2 (%).

Variable Factors	Plant Yield *		Enzymes **						
	AP	**R**	**Deh**	**Cat**	**Ure**	**Pac**	**Pal**	**Glu**	**Aryl**
Ash dose	26.23	50.51	93.47	80.84	87.01	95.64	68.42	92.92	57.13
Additives	54.83	31.47	2.64	15.85	5.00	3.15	21.99	4.69	36.22
Ash * Additives	7.95	5.50	1.07	2.72	7.89	0.93	6.04	2.19	6.55
Error	10.97	12.51	2.83	0.59	0.10	0.28	3.55	0.20	0.10

* AP—aboveground parts; R—roots; ** Deh—dehydrogenases; Cat—catalase; Ure—urease; Pac—acid phosphatase; Pal—alkaline phosphatase; Glu—β-glucosidase; Aryl—arylsulfatase.

A significant decrease in the biomass of aboveground parts of *Zea mays* L. was noted after soil treatment with a *Salix viminalis* ash dose of 20 g kg^{-1} d.m. soil (Figure 2a,b). Smaller ash doses tested (5–10 g kg^{-1} d.m. soil) did not impair *Zea mays* L. yield. In turn, its root biomass was significantly decreased by all analyzed doses of ash, i.e., 5–20 g kg^{-1} d.m. soil. The fertilization of control soil (without ash addition) with compost stimulated the growth and development of both aboveground parts and roots of *Zea mays* L., whereas soil amendment with HumiAgra showed a promoting effect on roots only. Both organic substances partly neutralized the adverse effect of the 20 g per kg soil ash dose on *Zea mays* L.

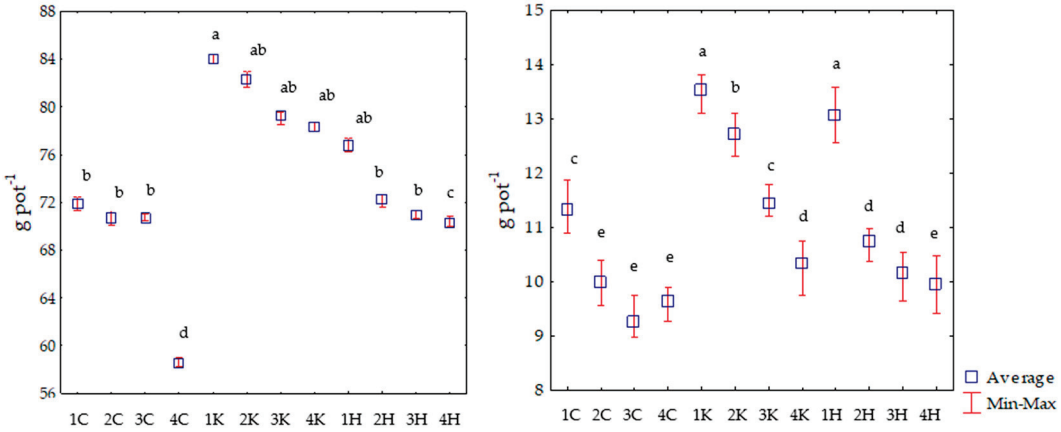

Figure 2. Dry weight of aboveground parts (**a**) and roots (**b**) of *Zea mays* from soil contaminated with *Salix viminalis* ash in g pot^{-1}. Explanations: 1–4 ash dose g kg^{-1} d.m. soil: 1—0; 2—5; 3—10; 4—20; C—soil without compost and HumiAgra, K—soil with compost, H—soil with HumiAgra. Homogeneous groups (a–e) were created separately for aboveground parts and roots.

The application of ash, compost, both, and HumiAgra to the soil had no significant effect on the leaf greenness index (SPAD) of *Zea mays* L. (Table 3). Its values decreased significantly along with *Zea mays* L. age, i.e., the highest value was recorded on day 14 of crop vegetation and the lowest on day 42. These correlations were determined in the non-fertilized soil and the soil fertilized with compost and HumiAgra.

Table 3. The effect of ash from *Salix viminalis* on the leaf greenness index (SPAD) of *Zea mays* L.

Ash Dose, g kg^{-1} d.m. Soil	14 Days	28 Days	42 Days
Without Additives			
0	43.02 ^{a} ± 1.73	36.71 ^{bcd} ± 2.47	26.03 ^{f} ± 2.23
5	42.37 ^{a} ± 1.47	35.12 ^{cde} ± 1.02	25.37 ^{f} ± 2.17
10	41.23 ^{ab} ± 0.60	35.07 ^{cde} ± 0.69	25.21 ^{f} ± 1.58
20	40.55 ^{ab} ± 0.40	31.43 ^{e} ± 2.56	24.78 ^{f} ± 2.08
$\overline{X}$	41.80 ^{B}	34.58 ^{D}	25.35 ^{F}
r	−0.96 *	−0.97 *	−0.96 *
Compost			
0	43.55 ^{a} ± 2.14	34.49 ^{cde} ± 1.98	24.58 ^{f} ± 3.58
5	43.43 ^{a} ± 1.57	34.07 ^{cde} ± 2.30	24.13 ^{f} ± 1.02
10	42.68 ^{a} ± 1.02	33.58 ^{de} ± 2.43	22.90 ^{f} ± 1.95
20	42.14 ^{a} ± 0.33	33.59 ^{de} ± 1.92	22.69 ^{f} ± 0.75
$\overline{X}$	42.93 ^{A}	33.950 ^{E}	23.58 ^{E}
r	−0.98 *	−0.87 *	−0.97 *
HumiAgra			
0	43.670 ^{a} ± 1.07	38.95 ^{abc} ± 0.63	26.31 ^{f} ± 0.91
5	43.07 ^{a} ± 1.08	35.56 ^{cde} ± 0.97	26.25 ^{f} ± 1.51
10	42.07 ^{a} ± 0.97	34.73 ^{cde} ± 1.56	25.99 ^{f} ± 0.61
20	42.14 ^{a} ± 1.29	34.55 ^{cde} ± 2.11	25.69 ^{f} ± 1.03
$\overline{X}$	42.75 ^{A}	35.95 ^{C}	26.05 ^{F}
r	−0.88 *	−0.80	−1.00 *

* r—correlation coefficient significant at $p = 0.05$; Homogeneous groups ($^{a–f}$) for three terms of the leaf greenness index assessment; homogeneous groups for means were calculated for three terms of the leaf greenness index assessment ($^{A–F}$).

The heat of combustion of *Zea mays* L. ranged from 17.86 MJ kg^{-1} p.dm. in the plants grown on the soil polluted with ash from *Salix viminalis* at a dose of 20 g kg^{-1} d.m. soil in the experimental series with HumiAgra to 18.42 MJ kg^{-1} p.dm. in the plants from the control pot without additives (Table 4), whereas the heating value ranged from 15.93 in the case of plants grown on the soil polluted with ash from *Salix viminalis* to 16.500 MJ kg^{-1} p.dm. in the case grown on the non-polluted soil. The energy obtained from *Zea mays* L. biomass produced from 1 kg of soil amended with compost and HumiAgra was higher than the variants without these additives. These correlations were observed in both the control soil and soil polluted with *Salix viminalis* ash.

Table 4. The effect of ash from *Salix viminalis* on the heat of combustion and heating value of *Zea mays* L.

Ash Dose, g kg^{-1} d.m. Soil	Heat of Combustion	Heating Value	Energy Production MJ kg^{-1}
	MJ kg^{-1} Air-Dried Plant Matter		
Without Additives			
0	18.42 ^{a} ± 0.04	16.50 ^{a} ± 0.03	0.340 ^{b} ± 0.02
20	17.91 ^{c} ± 0.03	15.93 ^{c} ± 0.02	0.27 ^{c} ± 0.02
Compost			
0	18.29 ^{b} ± 0.02	16.44 ^{a} ± 0.03	0.40 ^{a} ± 0.03
20	17.94 ^{c} ± 0.02	16.13 ^{b} ± 0.03	0.36 ^{ab} ± 0.02
HumiAgra			
0	17.90 ^{c} ± 0.05	16.17 ^{b} ± 0.02	0.36 ^{ab} ± 0.04
20	17.86 ^{c} ± 0.02	16.10 ^{b} ± 0.03	0.32 ^{b} ± 0.03

Homogeneous groups ($^{a–c}$) were created separately for columns.

3.2. Biochemical and Physicochemical Properties of Soil

Activities of all soil enzymes were affected to a greater extent (from 57.131% for arylsulfatase to 95.643% for acid phosphatase) by soil treatment with *Salix viminalis* ash than by its fertilization with compost and HumiAgra (from 2.635% for dehydrogenases to 36.220% for arylsulfatase) (Table 2). The results of PCA enabled illustration of the effect of ash from *Salix viminalis* on the soil enzymes (Figure 3). The figure presents the distribution of the analyzed samples in the system of two principal components. The activity of dehydrogenases, catalase, urease, acid phosphatase, alkaline phosphatase, β-glucosidase, and arylsulfatase was negatively correlated with the first principal component explaining 89.24% of the analyzed variability. The *Salix viminalis* ash doses of 5, 10, and 20 g kg^{-1} d.m. soil inhibited activities of the soil enzymes, as indicated by the distribution of cases on the plane. The reciprocal arrangement of vectors describing urease, β-glucosidase, acid phosphatase, dehydrogenases, and catalase indicates their similar response to the soil amendment with *Salix viminalis* ash. In turn, arylsulfatase and alkaline phosphatase formed one group; however, they were more sensitive to the negative effect of the ash. In addition, the distribution of cases in relation to vectors enables concluding that compost was more effective in mitigating the adverse effects of ash from *Salix viminalis* on the biochemical activity of soil than HumiAgra.

The inhibiting effect of ash on the soil enzymes was reflected in the values of the index of the *Salix viminalis* ash effect (IF_{Ash}) on the biochemical activity of the soil. Considering the IF_{Ash} values, the analyzed enzymes were ordered as follows (from the most to the least sensitive to *Salix viminalis* ash): Ure > Pac > Glu > Deh > Pal > Cat > Aryl (Table 5).

The adverse effects of *Salix viminalis* ash were noticed even in the soil samples polluted with its lowest dose (5 g kg^{-1} d.m.) and aggravated along with increasing ash doses, regardless of soil amendment with compost and HumiAgra.

The effect of soil treatment with the organic substances is well reflected in the values of the indices of compost influence (IF_K) and HumiAgra influence (IF_H) on the activities of soil enzymes (Figure 4a,b).

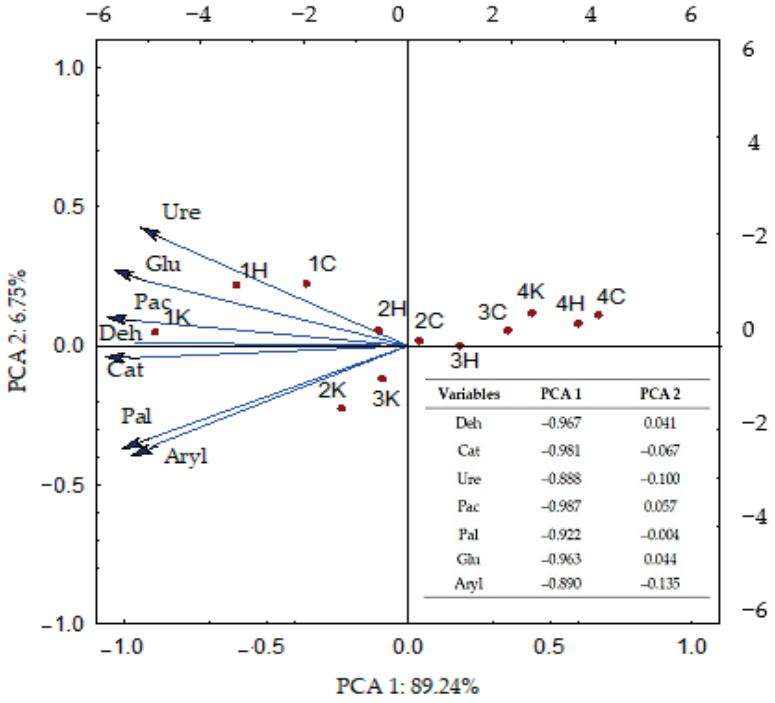

Figure 3. Enzyme activity in soil contaminated with *Salix viminalis* ash presented based on PCA. Explanations: 1–4 ash dose g kg^{-1} d.m. soil: 1—0; 2—5; 3—10; 4—20; C—soil without compost and HumiAgra, K—soil with compost, H—soil with HumiAgra; enzyme abbreviations are provided under Table 2.

Table 5. Index of the effect of *Salix viminalis* ash on the activity of soil enzymes.

Ash Dose, g kg^{-1} d.m. Soil	Deh	Cat	Ure	Pac	Pal	Glu	Aryl
			Without Additives				
5	$-0.23^{a} \pm 0.03$	$-0.111^{a} \pm 0.03$	$-0.42^{b} \pm 0.07$	$-0.25^{a} \pm 0.03$	$-0.04^{a} \pm 0.01$	$-0.26^{a} \pm 0.03$	$-0.030^{a} \pm 0.03$
10	$-0.26^{a} \pm 0.04$	$-0.254^{d} \pm 0.02$	$-0.51^{c} \pm 0.05$	$-0.47^{c} \pm 0.07$	$-0.30^{e} \pm 0.02$	$-0.40^{d} \pm 0.02$	$-0.06^{a} \pm 0.01$
20	$-0.61^{c} \pm 0.05$	$-0.31^{ef} \pm 0.02$	$-0.56^{d} \pm 0.02$	$-0.60^{d} \pm 0.05$	$-0.39^{f} \pm 0.04$	$-0.53^{f} \pm 0.04$	$-0.23^{e} \pm 0.02$
$\overline{X}$	-0.37^{A}	-0.23^{B}	-0.50^{B}	-0.44^{B}	-0.24^{B}	-0.40^{B}	-0.11^{A}
			Compost				
5	$-0.29^{b} \pm 0.08$	$-0.15^{b} \pm 0.01$	$-0.62^{f} \pm 0.08$	$-0.23^{a} \pm 0.02$	$-0.10^{b} \pm 0.02$	$-0.29^{ab} \pm 0.02$	$-0.10^{b} \pm 0.01$
10	$-0.31^{b} \pm 0.07$	$-0.18^{c} \pm 0.03$	$-0.57^{d} \pm 0.04$	$-0.36^{b} \pm 0.03$	$-0.17^{c} \pm 0.02$	$-0.33^{c} \pm 0.02$	$-0.20^{d} \pm 0.01$
20	$-0.65^{c} \pm 0.05$	$-0.30^{de} \pm 0.06$	$-0.60^{e} \pm 0.03$	$-0.59^{d} \pm 0.06$	$-0.49^{g} \pm 0.04$	$-0.41^{d} \pm 0.05$	$-0.38^{g} \pm 0.04$
$\overline{X}$	-0.42^{B}	-0.21^{B}	-0.60^{C}	-0.40^{A}	-0.25^{B}	-0.34^{A}	-0.23^{C}
			HumiAgra				
5	$-0.24^{a} \pm 0.06$	$-0.09^{a} \pm 0.05$	$-0.35^{a} \pm 0.03$	$-0.31^{b} \pm 0.01$	$-0.08^{b} \pm 0.05$	$-0.30^{ab} \pm 0.04$	$-0.12^{bc} \pm 0.01$
10	$-0.30^{b} \pm 0.04$	$-0.16^{b} \pm 0.02$	$-0.56^{d} \pm 0.02$	$-0.45^{c} \pm 0.03$	$-0.24^{d} \pm 0.02$	$-0.44^{e} \pm 0.02$	$-0.17^{c} \pm 0.02$
20	$-0.63^{c} \pm 0.09$	$-0.31^{f} \pm 0.03$	$-0.63^{f} \pm 0.06$	$-0.64^{e} \pm 0.06$	$-0.39^{f} \pm 0.03$	$-0.54^{f} \pm 0.01$	$-0.31^{f} \pm 0.03$
$\overline{X}$	-0.39^{A}	-0.19^{A}	-0.39^{A}	-0.35^{A}	-0.18^{A}	-0.32^{A}	-0.20^{B}

Explanations in the Table 2. Homogeneous groups ($^{a–g}$) were created separately for each enzyme; homogeneous groups for means were calculated for each enzyme ($^{A–C}$).

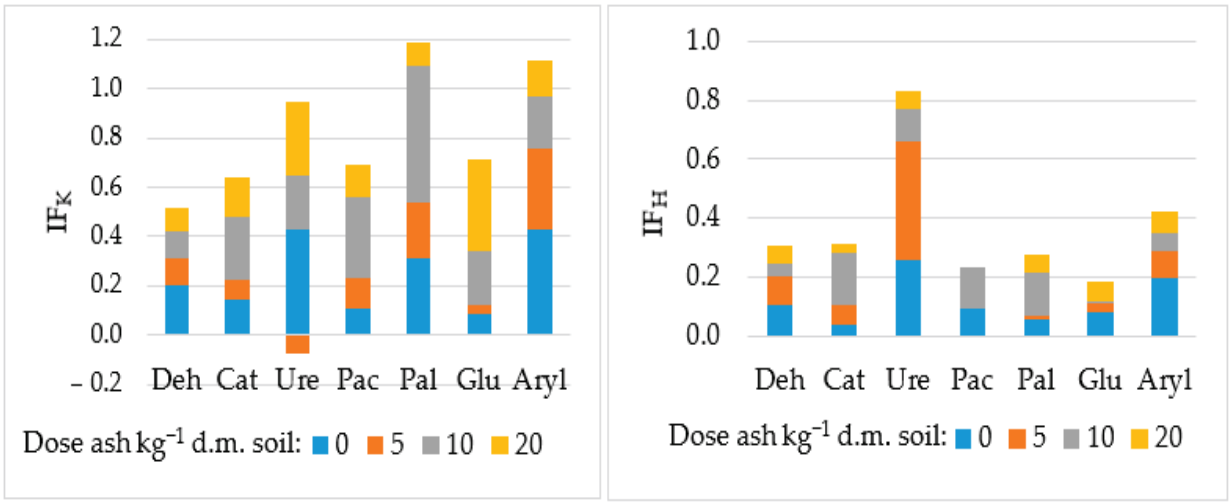

(**a**) (**b**)

Figure 4. Index of the effect of compost [IF_K] (**a**) and HumiAgra [IF_H] (**b**) on the activity of soil enzymes. Explanations as in Table 2.

The IF_K and IF_H values computed for the ash-polluted soil samples pointed to the positive effects of both substances on the activities of dehydrogenases, urease, and arylsulfatase—and, in the case of HumiAgra, also on the activity of β-glucosidase. In turn, soil treatment with ash from *Salix viminalis* contributed to decreased IF_K and IF_H values, indicating a minor pollution-mitigating effect of these organic substances. The lowest value of the IF_K index was noted in the case of urease, which turned out to be the most sensitive enzyme to *Salix viminalis* ash application even at the smallest tested dose, i.e., 5 g kg^{-1} d.m. soil. In the case of the IF_H index, its lowest value was determined for acid phosphatase in the soil polluted with the highest ash dose (20 g kg^{-1} d.m. soil). A comparison of IF_K and IF_H values demonstrated that HumiAgra proved less effective in mitigating the adverse changes caused by the *Salix viminalis* ash than compost.

Soil pollution with an ash dose of 20 g kg^{-1} d.m. soil caused a significant increase in C_{org} content, which was not observed upon soil amendment with the lower ash doses. The highest content of organic carbon was determined in the soil samples fertilized with compost, whereas the values found in the control soil sample and in the samples treated with HumiAgra were similar. The highest tested dose of ash from *Salix viminalis* (20 g kg^{-1} d.m. soil) also increased the total nitrogen content of the soils without and with the addition of compost and HumiAgra. In addition, the N_{Total} content of the soil was significantly affected by the ash dose of 10 g kg^{-1} d.m. soil in the variants with compost addition. Regardless of compost and HumiAgra addition to the soil, its pH increased and its hydrolytic acidity decreased under the influence of *Salix viminalis* ash (Table 6).

Values of these two parameters were correlated with the sum of exchangeable base cations, which was observed to increase upon soil pollution with the ash. Similar observations were made for CEC and BS, whose values increased along with increasing ash doses. The addition of compost and HumiAgra to the soil positively affected its physicochemical properties.

Table 6. The effect of ash from *Salix viminalis* on the chemical and physicochemical properties of soil.

Ash Dose, g kg^{-1} d.m. Soil	Total Organic Carbon (C_{org})	Total Nitrogen (N_{Total})	pH_{KCl}	Hydrolytic Acidity (HAC)	Total Exchangeable Base Cations (EBC)	Total Cation Exchange Capacity of Soil (CEC)	Base Cations Saturation Ratio in Soil (BS)
	g kg^{-1}			mmol$^{(+)}$ kg^{-1} Soil			%
Without Additives							
0	7.87 ^{g} ± 0.18	1.68 ^{d} ± 0.01	4.35 ^{f} ± 0.05	15.71 ^{c} ± 0.04	44.10 ^{k} ± 0.05	59.81 ^{j} ± 0.26	73.73 ^{i} ± 0.31
5	8.10 ^{fg} ± 0.09	1.71 ^{cd} ± 0.02	6.85 ^{d} ± 0.04	5.81 ^{d} ± 0.04	122.00 ^{h} ± 1.00	127.81 ^{g} ± 0.04	95.45 ^{f} ± 0.01
10	8.27 ^{fg} ± 0.15	1.71 ^{cd} ± 0.01	7.00 ^{c} ± 0.03	3.71 ^{f} ± 0.04	123.00 ^{h} ± 0.10	126.71 ^{g} ± 1.04	97.07 ^{d} ± 0.01
20	10.34 ^{b} ± 0.11	1.73 ^{bc} ± 0.02	7.45 ^{b} ± 0.04	2.74 ^{h} ± 0.04	201.10 ^{e} ± 0.50	203.84 ^{e} ± 0.54	98.66 ^{a} ± 0.03
$\overline{X}$	8.64 ^{B}	1.708 ^{A}	6.41 ^{A}	6.99 ^{B}	122.55 ^{C}	129.54 ^{C}	91.23 ^{B}
r	0.94 *	0.923 *	0.80 *	−0.81 *	0.96 *	0.96 *	0.76
Compost							
0	8.57 ^{ef} ± 0.10	1.72 ^{bc} ± 0.02	4.50 ^{e} ± 0.04	17.14 ^{a} ± 0.11	107.00 ^{i} ± 0.05	124.14 ^{h} ± 1.11	86.20 ^{g} ± 0.18
5	9.19 ^{cd} ± 0.13	1.74 ^{bc} ± 0.01	7.05 ^{c} ± 0.05	6.04 ^{d} ± 0.04	197.50 ^{f} ± 0.50	203.54 ^{e} ± 0.14	97.03 ^{d} ± 0.03
10	9.48 ^{c} ± 0.19	1.81 ^{a} ± 0.02	7.50 ^{b} ± 0.03	4.35 ^{e} ± 0.08	229.00 ^{a} ± 1.00	233.35 ^{a} ± 0.92	98.14 ^{c} ± 0.01
20	10.99 ^{a} ± 0.11	1.82 ^{a} ± 0.01	7.80 ^{a} ± 0.03	3.79 ^{f} ± 0.04	220.00 ^{b} ± 0.05	223.79 ^{b} ± 0.04	98.31 ^{bc} ± 0.01
$\overline{X}$	9.56 ^{A}	1.77 ^{A}	6.71 ^{A}	7.83 ^{A}	188.38 ^{A}	196.20 ^{A}	94.92 ^{A}
r	0.99 *	0.91 *	0.81 *	−0.77	0.76	0.76	0.74
HumiAgra							
0	8.06 ^{g} ± 0.08	1.71 ^{cd} ± 0.01	4.45 ^{ef} ± 0.05	16.43 ^{b} ± 0.07	50.30 ^{j} ± 0.05	66.73 ^{i} ± 0.23	75.38 ^{h} ± 0.03
5	8.16 ^{fg} ± 0.13	1.73 ^{bc} ± 0.03	6.85 ^{d} ± 0.05	6.00 ^{d} ± 0.07	136.50 ^{g} ± 0.30	142.50 ^{f} ± 0.38	95.79 ^{e} ± 0.02
10	8.82 ^{de} ± 0.08	1.76 ^{b} ± 0.01	7.05 ^{c} ± 0.05	3.98 ^{f} ± 0.07	204.00 ^{d} ± 0.30	207.985 ^{d} ± 0.08	98.09 ^{c} ± 0.04
20	10.34 ^{b} ± 0.09	1.81 ^{a} ± 0.02	7.55 ^{b} ± 0.05	3.26 ^{g} ± 0.08	215.00 ^{c} ± 0.30	218.26 ^{c} ± 1.26	98.51 ^{ab} ± 0.11
$\overline{X}$	8.85 ^{B}	1.75 ^{A}	6.48 ^{A}	7.42 ^{A}	151.45 ^{B}	158.87 ^{B}	91.94 ^{B}
r	0.97 *	1.00 *	0.82 *	−0.80	0.89 *	0.81 *	0.75

* r—correlation coefficient significant at $p = 0.05$; homogeneous groups ($^{a–k}$) were created separately for each parameter; homogeneous groups for means were calculated for each parameter ($^{A–C}$).

3.3. Correlations between the Analyzed Parameters

The biomass yield of aboveground parts and roots of *Zea mays* L. (Table 7) was positively correlated with the activities of the analyzed soil enzymes and hydrolytic acidity (HAC) of the soil but negatively correlated with soil pH, sum of EBC, CEC, soil saturation with base cations (BS), and content of organic carbon (C_{org}). Activities of all analyzed enzymes were positively correlated with each other and with HAC, as well as negatively correlated (likewise *Zea mays* L. biomass) with soil pH, EBC, CEC, BS, and C_{org} content. Enzymatic activity was not significantly correlated with N_{Total} content of the soil, but a positive correlation was found between contents of C_{org} and N_{Total}, as well between their contents and soil pH, EBC, CEC, and BS.

Table 7. Correlation coefficients between variables.

Variable Factors	R	Deh	Cat	Ure	Pac	Pal	Glu	Aryl	C_{org}	N_{Total}	pH	HAC	EBC	CEC	BS
AP	0.66 *	0.92 *	0.91 *	0.67 *	0.80 *	0.90 *	0.85 *	0.81 *	−0.84 *	−0.14	−0.73 *	0.70 *	−0.56 *	−0.55 *	−0.62 *
R	1.00	0.65 *	0.71 *	0.65 *	0.64 *	0.60 *	0.65 *	0.68 *	−0.52 *	−0.03	−0.57 *	0.59 *	−0.40 *	−0.39 *	−0.51 *
Deh		1.00	0.91 *	0.66 *	0.74 *	0.95 *	0.74 *	0.78 *	−0.89 *	−0.15	−0.65 *	0.62 *	−0.53 *	−0.52 *	−0.52 *
Cat			1.00	0.78 *	0.89 *	0.91 *	0.89 *	0.86 *	−0.82 *	−0.10	−0.79 *	0.78 *	−0.56 *	−0.55 *	−0.70 *
Ure				1.00	0.91 *	0.67 *	0.87 *	0.67 *	−0.54 *	−0.15	−0.77 *	0.81 *	−0.55 *	−0.53 *	−0.69 *
Pac					1.00	0.74 *	0.97 *	0.76 *	−0.68 *	−0.21	−0.93 *	0.94 *	−0.72 *	−0.70 *	−0.87 *
Pal						1.00	0.76 *	0.83 *	−0.79 *	0.01	−0.60 *	0.59 *	−0.41 *	−0.40 *	−0.48 *
Glu							1.00	0.79 *	−0.66 *	−0.15	−0.90 *	0.91 *	−0.67 *	−0.64 *	−0.83 *
Aryl								1.00	−0.58 *	0.09	−0.59 *	0.59 *	−0.42 *	−0.41 *	−0.51 *
C_{org}									1.00	0.49 *	0.72 *	−0.64 *	0.65 *	0.65 *	0.60 *
N_{Total}										1.00	0.41 *	−0.33	0.46 *	0.46 *	0.37 *
pH											1.00	−0.99 *	0.84 *	0.82 *	0.98 *
HAC												1.00	−0.81 *	−0.79 *	−0.98 *
EBC													1.00	0.99 *	0.83 *
CEC														1.00	0.81 *

Explanations in the Tables 2 and 5. * r—coefficient of correlation significant at: $p = 0.05$, $n = 36$.

4. Discussion

4.1. Biomass and Heating Value of Zea mays L. Grown in Soil with the Addition of Ash from Salix viminalis

Soil amendment with *Salix viminalis* ash doses of 5 and 10 g kg^{-1} d.m. did not inhibit either the growth or the development of *Zea mays*, whereas soil pollution with the ash dose of 20 g kg^{-1} d.m. significantly impaired them both. The adverse effect of ash applied at the highest tested dose may be due to its high alkalinity (pH_{KCl} = 12.5) and low nitrogen content (N = 0.38%). Varshney et al. [54] and Cruz et al. [33] have also emphasized that high ash doses applied may cause excessive soil salinity, thereby ultimately contributing to worse conditions for plant growth and root development. However, previous investigations conducted by Liu et al. [1] and Romdhane et al. [31] proved that wood-based ash applied in doses from 20 to 40 g kg^{-1} soil might positively affect *Zea mays* L. biomass. Differences observed for ash effects in the present study and experiments of the aforementioned authors are mainly due to the differences in the chemical composition of the analyzed ashes. In turn, Ondrasek et al. [22] showed that the application of wood-based ash intensified chemical sorption in the rhizosphere, contributing to the enhanced immobilization of elements delivered with fertilizers. In addition, soil treatment with ash may strongly affect its texture, aeration, and water-retention capacity, and by this means determine the dynamics of root growth, leading to multiple potential effects on plant growth [25,26].

The analyzed ash from *Salix viminalis* had no negative impact on the heat of combustion or the heating value of *Zea mays* L., whose values did not change under ash doses applied. This finding indicates the possibility of using biomass from the aboveground parts of this plant for energetic purposes when there is a need for ash management. Also, our previous investigations [55,56] addressing the reclamation of soil contaminated with Cd^{2+}, Co^{2+} and Ni^{2+} demonstrated the usability of *Zea mays* L., *Elymus*, and *Festuca rubra* biomass for energetic purposes. Table 8 below presents the most important results regarding the calorific value compared with the results of other authors and presented in the table.

Table 8. Heating values of *Zea mays* obtained in various studies.

Factor Tested in the Soil	Heating Value MJ kg−1 Air-Dried Plant Matter	Reference
Salix viminalis ash content	15.93–16.50	Our research
Maize variety	7.62–10.79	[57]
Corn grain drying process	13.70–14.94	[6]
Pellets from biomass	15.68	[58]
Cr (VI) content	14.60–15.40	[50]
Maize cultivation	17.51	[59]
Ni^{2+}, Co^{2+}, Cd^{2+} content	14.79–14.97	[55]

An added value of the present study is the finding that the soil amendment with an organic substance (compost and HumiAgra) alleviates the adverse effects of *Salix viminalis* ash dose of 20 g kg^{-1} d.m. soil on *Zea mays* L. biomass. Both published data [60] and our previous research [56] indicate that soil fertilization with compost mitigates the negative impact of inorganic compounds on plant yield. Soil amendment with compost and HumiAgra preparation increased the pool of readily available organic compounds. In addition, compost affects soil properties by enriching it with organic matter susceptible to microbiological degradation. Organic matter mineralization activates its nutrients that are essential to plants. It may also regulate sorption properties of the soil by, e.g., reducing retrogradation of phosphates. In turn, the weaker effect of HumiAgra compared to that of compost may be due to a more diversified chemical composition of the latter [61,62].

4.2. Biochemical and Physicochemical Properties of Soil

Enzymatic activity of soil is one of the key factors driving its fertility [1,63–65]. Soil enzymes mediate soil organic matter degradation and catalyze the main metabolic pro-

cesses of carbon, nitrogen, and phosphorus [66–68]. Microbes secrete intracellular and extracellular enzymes essential for soil nutrient cycling and contribute to soil fertility and health [69–71]. However, works by Pukalchik et al. [32], Smenderovac et al. [72], and Błońska et al. [36] provide conflicting data related to the impact of ash on the biological properties of soil. Smenderovac et al. [72] and Perucci et al. [73] draw attention to the temporary negative impact of ashes on the activity of soil enzymes. In their studies, the activity of alkaline phosphatase and arylsulfatase was inhibited for the first 4 months after the application of wood ash to the soil. This may be due to the greater release of ions into the solution with a higher ash dose. Therefore, in our own research, the negative effect of *Salix viminalis* ash probably increased with the increase in the ash dose. The present study results demonstrated that ash negatively affected the activity of the analyzed soil enzymes. Previous investigations by Pukalchik et al. [32] show also that the application of wood-based ash suppressed the activities of dehydrogenases, acid phosphatase, and β-glucosidase, as well as the activity of fluorescein diacetate (FDA), which pointed to the inhibited microbial activity in the soil. In turn, Perucci et al. [73] and *Smenderovac* et al. [72] demonstrated that the wood-based ash may strongly affect soil texture, aeration, and water retention capacity [74–77], thereby influencing root growth dynamics and consequently leading to plant growth impairment [78,79].

Organic carbon and nitrogen are two of the key elements of soil that inhibit plant growth [1]. In the present study, ash from *Salix viminalis* applied at a dose of 20 g kg^{-1} soil significantly increased the contents of both C_{org} and N_{total} in the soil. Apart from valuable macroelements, the wood-based ash contains heavy metals [12]. Hence, its small doses may meet nutritional demands of plants, but excess doses may exert toxic effects. This was the likely cause of *Zea mays* biomass reduction observed upon soil amendment with the ash dose of 20 g kg^{-1} in the present study. Wood ash has a high density, is porous and fine-grained, and swells in contact with water. These features of ash contribute to the blocking of soil pores, resulting in a modified soil texture and aeration [11,15].

Plant growth and productivity depend primarily on the availability of nutrients and the physicochemical properties of soil, which in turn are determined by the content of exchangeable base cations (EBC) and soil pH [31]. A study conducted by Lucchini et al. [80] demonstrated that wood-based ash improved the physicochemical properties and nutrient availability of soil. The pH value of osier ash used in the present study (pH = 12.5) was similar to that described in previous research [31,35]. The alkaline character of ash analyzed in the present study caused soil pH to increase significantly. The above results are consistent with previous findings reported by Lucchini et al. [80] and Adekayode and Olojugba [81]. Although ash is known for its neutralizing effect on acidic soils, some works did not demonstrate any significant changes in soil pH upon its use [31,82]. The efficacy of acidic soil neutralization is determined by the method of alkalizing fertilizer application, its dose, and its qualities, including its neutralizing value, fraction size, and dissolution rate, as well as by the composition and type of soil [31,35,80].

4.3. Correlations between the Analyzed Parameters

In the case of soils not exposed to the pressure of pollutants, crop yield is usually positively correlated with EBC, soil saturation with bases (BS), CEC, and contents of carbon and nitrogen [83]. In the present study, the soil was exposed to the effect of ash from *Salix viminalis*, and despite increased EBS, BS, and CEC values and also C_{org} content as a result of its application, no positive correlation was observed between the produced *Zea mays* biomass and these parameters. This lack of correlation was probably due to the introduction of not only Ca^{2+}, Mg^{2+}, Na^{+}, and K^{+} ions essential to plants but also excess amounts of heavy metals with ash [24–26,84]. Soil pollution with heavy metals usually upsets its biological properties, which is manifested as adverse effects on plants [85,86] and soil microbiota [87], which ultimately lead to severe disorder in the enzymatic activity of soil [88–91] because heavy metals may cause enzyme denaturation [92,93]. The present

study demonstrated a negative correlation between the activity of seven soil enzymes and basic physicochemical properties of soil changing upon the influence of osier ash.

5. Conclusions

The heating value of *Zea mays* L. remained stable and unmodified by the excess content of ash from *Salix viminalis* in the soil, which makes it a viable energy crop to be grown on soils fertilized with large doses of ash. All the more, it is relatively resistant to adverse ash effects because its biomass was significantly reduced in the present study upon soil pollution with the highest ash dose tested (20 g kg^{-1} d.m. soil). Nevertheless, ash may cause unbeneficial changes in the soil environment, manifested as suppressed enzymatic activity. Although the ash increases soil pH and sorption capacity, these positive effects do not compensate for losses evoked by disorders in the biochemical properties of soil. These adverse effects may, in part, be mitigated by soil fertilization with compost and HumiAgra preparation. The choice of these fertilizers should, however, be driven by their efficacy, with compost shown to surpass HumiAgra in this respect.

Author Contributions: Conceptualization, E.B.-L., J.W. and J.K.; experimental design and methodology, E.B.-L., J.W. and J.K.; investigation, J.W.; statistical analyses, E.B.-L.; writing original draft, E.B.-L.; review and editing, J.W.; supervision, J.K. All authors have read and agreed to the published version of the manuscript.

Funding: This research was funded by the University of Warmia and Mazury in Olsztyn, Faculty of Agriculture and Forestry, Department of Soil Science and Microbiology (grant No. 30.610.006-110), and was financially supported by the Minister of Education and Science under the program entitled "Regional Initiative of Excellence" for the years 2019–2023, project No. 010/RID/2018/19 (amount of funding: PLN 12,000,000).

Data Availability Statement: Data are contained within the article.

Conflicts of Interest: The authors declare no conflict of interest. The funders had no role in the design of the study; in the collection, analyses, or interpretation of data; in the writing of the manuscript; or in the decision to publish the results.

Abbreviations

C	soil without compost and HumiAgra;
K	soil with compost;
H	soil with HumiAgra;
AP	yield of aboveground parts;
R	yield of roots;
Deh	dehydrogenases;
Cat	catalase;
Ure	urease;
Pac	acid phosphatase;
Pal	alkaline phosphatase;
Glu	β-glucosidase;
Aryl	arylsulfatase;
C_{org}	total organic carbon;
N_{total}	total nitrogen;
HAC	hydrolytic acidity;
EBC	total exchangeable base cations;
CEC	total cation exchange capacity of soil;
BS	basic cation saturation ratio in soil.

References

1. Liu, L.; Li, J.; Wu, G.; Shen, H.; Fu, G.; Wang, Y. Combined effects of biochar and chicken manure on maize (*Zea mays* L.) growth, lead uptake and soil enzyme activities under lead stress. *Peer J.* **2021**, *9*, e11754. [CrossRef]
2. Mulyati; Baharuddin, A.B.; Tejowulan, R.S. Improving Maize (*Zea mays* L.) growth and yield by the application of inorganic and organic fertilizers plus. In Proceedings of the IOP Conference Series: Earth and Environmental Science, 3rd International Conference on Bioscience and Biotechnology, Lombok, Indonesia, 12–14 October 2020; IOP Publishing Ltd.: Bristol, UK, 2021; Volume 712, p. 012027. [CrossRef]
3. Holm-Nielsen, J.B.; Al Seadi, T.; Oleskowicz-Popiel, P. The future of anaerobic digestion and biogas utilization. *Bioresour. Technol.* **2008**, *100*, 5478–5484. [CrossRef]
4. Oslaj, M.; Mursec, B.; Vindis, P. Biogas production from maize hybrids. *Biomass Bioenerg.* **2010**, *34*, 1538–1545. [CrossRef]
5. Bubner, B.; Köhler, A.; Zaspel, I.; Zander, M.; Förster, N.; Gloger, J.-C.; Ulrichs, C.; Schneck, V. Breeding of multipurpose willows on the basis of *Salix daphnoides* Vill., *Salix purpurea* L. and *Salix viminalis* L. *Appl. Agric. For. Res.* **2018**, *68*, 53–66. [CrossRef]
6. Maj, G.; Szyszlak-Bargłowicz, J.; Zajac, G.; Słowik, T.; Krzaczek, P.; Piekarski, W. Energy and emission characteristics of biowaste from the corn grain drying process. *Energies* **2019**, *12*, 4383. [CrossRef]
7. Warmbier, K.; Wilczyński, A.; Danecki, L. Properties of one-layer experimental particleboards from willow (*Salix viminalis*) and industrial wood particles. *Eur. J. Wood Prod.* **2013**, *71*, 25–28. [CrossRef]
8. Zhai, F.-F.; Liu, J.-X.; Li, Z.-J.; Mao, J.-M.; Qian, Y.-Q.; Han, L.; Sun, Z.-Y. Assessing genetic diversity and population structure of *Salix viminalis* across Ergun and West Liao basin. *Silva Fenn.* **2017**, *51*, 7001. [CrossRef]
9. Mojiri, A. The potential of corn (*Zea mays*) for phytoremediation of soil contaminated with cadmium and lead. *J. Biol. Environ. Sci.* **2011**, *5*, 17–22.
10. Branquinho, C.; Serrano, H.C.; Pinto, M.J.; Martins-Loução, M.A. Revisiting the plant hyperaccumulation criteria to rare plants and earth abundant elements. *Environ. Pollut.* **2007**, *246*, 437–443. [CrossRef]
11. Johan, P.D.; Ahmed, O.H.; Omar, L.; Hasbullah, N.A. Phosphorus transformation in soils following co-application of charcoal and wood ash. *Agronomy* **2021**, *11*, 2010. [CrossRef]
12. Mandre, M.; Parn, H.; Ots, K. Short-term effects of wood ash on the soil and the lignin concentration and growth of *Pinus sylvestris* L. *For. Ecol. Manag.* **2006**, *223*, 349–357. [CrossRef]
13. Yrjälä, K.; Katainen, R.; Jurgens, G.; Saarela, U.; Saano, A.; Romantschuk, M.; Fritze, H. Wood ash fertilization alters the forest humus *Archea* community. *Soil Biol. Biochem.* **2004**, *36*, 199–201. [CrossRef]
14. Ondrasek, G.; Romic, D.; Rengel, Z. Interactions of humates and chlorides with cadmium drive soil cadmium chemistry and uptake by radish cultivars. *Sci. Total Environ.* **2020**, *720*, 134887. [CrossRef] [PubMed]
15. Jansone, B.; Samariks, V.; Okmanis, M.; Kļaviņa, D.; Lazdiņa, D. Effect of High Concentrations of Wood Ash on Soil Properties and Development of Young Norway Spruce (*Picea abies* (L.) Karst) and Scots Pine (*Pinus sylvestris* L.). *Sustainability* **2020**, *12*, 9479. [CrossRef]
16. Ozolincius, R.; Varnagiryte, I.; Armolaitis, K.; Karltun, E. Initial effects of wood ash fertilization on soil, needle and litterfall chemistry in a Scots pine (*Pinus sylvestris* L.). *Stand Balt. For.* **2005**, *11*, 59–67.
17. Zając, G.; Szyszlak-Bargłowicz, J.; Gołębiowski, W.; Szczepanik, M. Chemical characteristics of biomass. *Energies* **2018**, *11*, 2885. [CrossRef]
18. Tosti, L.; van Zomeren, A.; Pels, J.R.; Dijkstra, J.J.; Comans, R.N.J. Assessment of biomass ash applications in soil and cement mortars. *Chemosphere* **2019**, *223*, 425–437. [CrossRef]
19. Palansooriya, K.N.; Shaheen, S.M.; Chen, S.S.; Tsang, D.C.W.; Hashimoto, Y.; Hou, D.; Bolan, N.S.; Rinklebe, J.; Ok, Y.S. Soil amendments for immobilization of potentially toxic elements in contaminated soils: A critical review. *Environ. Int.* **2020**, *134*, 105046. [CrossRef]
20. Vassilev, S.V.; Baxter, D.; Andersen, L.K.; Vassileva, C.G. An overview of the chemical of biomass ash. *Fuel* **2010**, *89*, 913–933. [CrossRef]
21. Park, J.-H.; Eom, J.-S.; Lee, S.-L.; Hwang, S.-W.; Kim, S.-H.; Kang, S.-W.; Yun, J.-J.; Cho, J.-S.; Lee, Y.-H.; Seo, D.-C. Exploration of the potential capacity of fly ash and bottom ash derived from wood pellet-based thermal power plant for heavy metal removal. *Sci. Total Environ.* **2020**, *740*, 140205. [CrossRef]
22. Ondrasek, G.; Kranjčec, F.; Filipović, L.; Filipović, V.; Bubalo Kovačić, M.; Jelovica Badovinac, I.; Peter, R.; Petravić, M.; Macan, J.; Rengel, Z. Biomass bottom ash & dolomite similarly ameliorate an acidic low-nutrient soil, improve phytonutrition and growth, but increase Cd accumulation in radish. *Sci. Total Environ.* **2021**, *753*, 141902. [CrossRef]
23. Mohamed, S.A.; Ewees, S.A.; Sawsan, A.; Seaf, E.Y.; Dalia, M.S. Improving maize grain yield and its quality grown on a newly reclaimed sandy soil by applying micronutrients, organic manure and biological inoculation. *Res. J. Agric. Biol. Sci.* **2008**, *4*, 537–544.
24. Perkiömäki, J.; Kiikkilä, O.; Moilanen, M.; Issakainen, J.; Tervahauta, A.; Fritze, H. Cadmium-containing wood ash in a pine forest: Effects on humus microflora and cadmium concentrations in mushrooms, berries, and needles. *Can. J. For. Res.* **2003**, *33*, 2443–2451. [CrossRef]
25. Mercl, F.; Tejnecký, V.; Száková, J.; Tlustoš, P. Nutrient dynamics in soil solution and wheat response after biomass ash amendments. *Agron. J.* **2016**, *108*, 2222–2234. [CrossRef]

26. Jagodzinski, L.S.; O'Donoghue, M.T.; Heffernan, L.B.; van Pelt, F.N.; O'Halloran, J.; Jansen, M.A. Wood ash residue causes a mixture of growth promotion and toxicity in Lemna minor. *Sci. Total Environ.* **2018**, *625*, 667–676. [CrossRef] [PubMed]
27. Levula, T.; Saarsalmi, A.; Rantavaara, A. Effects of ash fertilization and prescribed burning on macronutrient, heavy metal, sulphur and 137Cs concentrations in lingonberries (*Vaccinium vitis-idaea*). *For. Ecol. Manag.* **2000**, *126*, 269–279. [CrossRef]
28. Demeyer, A.; Nkana, J.C.V.; Verloo, M.G. Characteristics of wood ash and influence on soil properties and nutrient uptake: An overview. *Bioresour. Technol.* **2001**, *77*, 287–295. [CrossRef] [PubMed]
29. Lundborg, A. Ecological and economical evaluation of biomass ash utilization–the Swedish approach. Ashes and particulate emissions from biomass combustion, Series Thermal Biomass Utilization. *Inst. Chem. Engin. Techn. Univ. Graz.* **1998**, *3*, 29–41.
30. Zimmermann, S.; Frey, B. Soil respiration and microbial properties in an amid forest soil: Effects of wood ash. *Soil Biol. Biochem.* **2002**, *34*, 1727–1737. [CrossRef]
31. Romdhane, L.; Ebinezer, L.B.; Panozzo, A.; Barion, G.; Cortivo, C.D.; Radhouane, L.; Vamerali, T. Effects of soil amendment with wood ash on transpiration, growth, and metal uptake in two contrasting maize (*Zea mays* L.) hybrids to drought tolerance. *Front. Plant Sci.* **2021**, *12*, 661909. [CrossRef]
32. Pukalchik, M.; Mercl, F.; Terekhova, V.; Tlustoš, P. Biochar, wood ash and humic substances mitigating trace elements stress in contaminated sandy loam soil: Evidence from an integrative approach. *Chemosphere* **2018**, *203*, 228–238. [CrossRef]
33. Cruz-Paredes, C.; Frøslev, T.G.; Michelsen, A.; Bang-Andreasen, T.; Hansen, M.; Ingerslev, M.; Skov, S.; Wallander, H.; Kjøller, R. Wood ash application in a managed Norway spruce plantation did not affect ectomycorrhizal diversity or N retention capacity. *Fungal Ecol.* **2019**, *39*, 1–11. [CrossRef]
34. Małek, S.; Ważny, R.; Błońska, E.; Jasik, M.; Lasota, J. Soil fungal diversity and biological activity as indicators of fertilization strategies in a forest ecosystem after spruce disintegration in the Karpaty Mountains. *Sci Total Environ.* **2021**, *751*, 142335. [CrossRef]
35. Nabeela, F.; Murad, W.; Khan, I.; Mian, I.A.; Rehman, H.; Adnan, M. Effect of wood ash application on the morphological, physiological and biochemical parameters of *Brassica napus* L. *Plant Physiol. Biochem.* **2015**, *95*, 15–25. [CrossRef]
36. Błońska, E.; Prażuch, W.; Boroń, P.; Lasota, J. Effects of wood ash on the soil properties and fungal community structure in a beech forest in Poland. *Geoderma Reg.* **2023**, *34*, e00676. [CrossRef]
37. Mundała, P.; Szwalec, A.; Kędzior, R. Accumulation of selected heavy metals in willow shoots (*Salix viminalis* L.) cultivated in the neighbourhood of a coal ash and slag landfill. *Infrastrukt. Ecol. Rural Areas* **2017**, *3*, 1043–1051. [CrossRef]
38. Núñez-Delgado, A.; Quiroga-Lago, F.; Soto-González, B. Runoff characteristics in forest plots before and after wood ash fertilization. *Maderas Cienc. Tecnol.* **2011**, *13*, 267–284. [CrossRef]
39. Someshwar, A.V. Wood and combination wood-fired boiler ash characterization. *J. Environ. Qual.* **1996**, *25*, 962–972. [CrossRef]
40. Öhlinger, R. Dehydrogenase activity with the substrate TTC. In *Methods in Soil Biology*; Schinner, F., Öhlinger, R., Kandeler, E., Margesin, R., Eds.; Springer: Berlin/Heidelberg, Germany, 1996; pp. 241–243.
41. Alef, K.; Nannipieri, P. (Eds.) *Methods in Applied Soil Microbiology and Biochemistry, Enzyme Activities*; Academic: London, UK, 1998; pp. 316–365.
42. Carter, M.R. *Soil Sampling and Methods of Analysis*; Canadian Society of Soil Science; Lewis Publishers: London, UK, 1993.
43. *PN-EN. ISO 18125:2017-07*; Solid Biofuels—Determination of Calorific Value. European Committee for Standardization: Brussels, Belgium, 2010. Available online: https://pkn.pl/pn-en-iso-18125-2017-07 (accessed on 10 October 2023).
44. Kopetz, H.; Jossart, J.; Ragossnig, H.; Metschina, C. *European Biomass Statistics 2007*; European Biomass Association: Brussels, Belgium, 2007.
45. *PN-G-04584*; Oznaczanie Zawartości Siarki Całkowitej i Popiołowej Automatycznymi Analizatorami. Determination of Total Sulphur and Ash Sulphur in Automatic Analyzers. National Standards Body in Poland: Warszaw, Poland, 2001. (In Polish)
46. *ISO 11261*; Soil Quality—Determination of Total Nitrogen—Modified Kjeldahl Method. International Organization for Standardization: Geneva, Switzerland, 1995.
47. Zaborowska, M.; Wyszkowska, J.; Borowik, A.; Kucharski, J. Bisphenol A—A dangerous pollutant distorting the biological properties of soil. *Int. J. Mol. Sci.* **2021**, *22*, 12753. [CrossRef] [PubMed]
48. Borowik, A.; Wyszkowska, J.; Wyszkowski, M. Resistance of aerobic microorganisms and soil enzyme response to soil contamination with Ekodiesel Ultra fuel. *Environ. Sci. Poll. Res.* **2017**, *24*, 24346–24363. [CrossRef] [PubMed]
49. Boros-Lajszner, E.; Wyszkowska, J.; Kucharski, J. Use of zeolite to neutralise nickel in a soil environment. *Environ. Monit. Assess.* **2018**, *190*, 54. [CrossRef]
50. Wyszkowska, J.; Borowik, A.; Zaborowska, M.; Kucharski, J. Sensitivity of *Zea mays* and soil microorganisms to the toxic effect of chromium (VI). *Int. J. Mol. Sci.* **2023**, *24*, 178. [CrossRef]
51. Boros-Lajszner, E.; Wyszkowska, J.; Kucharski, J. Phytoremediation of soil contaminated with nickel, cadmium and cobalt. *Int. J. Phytoremediation* **2021**, *23*, 252–262. [CrossRef]
52. Wyszkowska, J.; Borowik, A.; Zaborowska, M.; Kucharski, J. Calorific value of *Zea mays* biomass derived from soil. *Energies* **2023**, *16*, 3788. [CrossRef]
53. Dell Inc. *Dell Statistica (Data Analysis Software System)*; Version 13.1; Dell Inc.: Tulsa, OK, USA, 2022.
54. Varshney, A.; Dahiya, P.; Sharma, A.; Pandey, R.; Mohan, S. Fly ash application in soil for sustainable agriculture: An Indian overview. *Energ. Ecol. Environ.* **2022**, *7*, 340–357. [CrossRef]

55. Boros-Lajszner, E.; Wyszkowska, J.; Borowik, A.; Kucharski, J. Energetic value of *Elymus elongatus* L. and *Zea mays* L. grown on soil polluted with Ni^{2+}, Co^{2+}, Cd^{2+}, and sensitivity of rhizospheric bacteria to heavy metals. *Energies* **2021**, *14*, 4903. [CrossRef]
56. Wyszkowska, J.; Boros-Lajszner, E.; Kucharski, J. Calorific value of *Festuca rubra* biomass in the phytostabilization of soil contaminated with nickel, cobalt and cadmium which disrupt the microbiological and biochemical properties of soil. *Energies* **2022**, *15*, 3445. [CrossRef]
57. Wojcieszak, D.; Przybył, J.; Czajkowski, Ł.; Majka, J.; Pawłowski, A. Effects of Harvest Maturity on the Chemical and Energetic Properties of Corn Stover Biomass Combustion. *Materials* **2022**, *15*, 2831. [CrossRef]
58. Miranda, M.T.; Sepúlveda, F.J.; Arranz, J.I.; Montero, I.; Rojas, C.V. Analysis of pelletizing from corn cob waste. *J. Environ. Manag.* **2018**, *228*, 303–311. [CrossRef]
59. Jóvér, J.; Antal, K.; Zsembeli, J.; Blaskó, L.; Tamás, J. Assessment of gross calorific value of crop and bio-energy residues. *Res. Agric. Eng.* **2018**, *64*, 121–127. [CrossRef]
60. Gusiatin, Z.M.; Kulikowska, D. Behaviors of heavy metals (Cd, Cu, Ni, Pb and Zn) in soil amended with composts. *Environ. Technol.* **2016**, *37*, 2337–2347. [CrossRef] [PubMed]
61. Mindari, W.; Sasongko, P.E.; Kusuma, Z.; Syekhfani, S.; Ain, N. Efficiency of various sources and doses of humic acid on physical and chemical properties of saline soil and growth and yield of rice. In Proceedings of the AIP Conference Proceedings, 9th International Conference on Global Resource Conservation (ICGRC) and Aji from Ritsumeikan University, Malang City, Indonesia, 7–8 March 2018; AIP Publishing: Melville, NY, USA, 2019; p. 030001. [CrossRef]
62. Tiwari, J.; Ramanathan, A.; Bauddh, K.; Korstad, J. Humic substances: Structure, function and benefits for agroecosystems—A review. *Pedosphere* **2023**, *33*, 237–249. [CrossRef]
63. Baldrian, P. Microbial enzyme-catalyzed processes in soil and their analysis. *Plant Soil Environ.* **2009**, *55*, 370–378. [CrossRef]
64. Ouyang, L.; Tang, Q.; Yu, L.Q.; Zhang, R.D. Effects of amendment of different biochars on soil enzyme activities related to carbon mineralisation. *Soil Res.* **2014**, *52*, 706–716. [CrossRef]
65. Kong, L.; Chu, L.M. Subtropical urban turfs: Carbon and nitrogen pools and the role of enzyme activity. *J. Environ. Sci.* **2018**, *65*, 18–28. [CrossRef]
66. Wallenstein, M.D.; Burns, R.G. Ecology of extracellular enzyme activities and organic matter degradation in soil: A complex community-driven process. In *Methods of Soil Enzymology*; Dick, R.P., Ed.; Soil Science Society of America: Madison, WI, USA, 2011; pp. 35–55. [CrossRef]
67. Stone, M.M.; De Forest, J.L.; Plante, A.F. Changes in extracellular enzyme activity and microbial community structure with soil depth at the Luquillo Critical Zone Observatory. *Soil Biol. Biochem.* **2014**, *75*, 237–247. [CrossRef]
68. Piotrowska-Długosz, A.; Kobierski, M.; Długosz, J. Enzymatic activity and physicochemical properties of soil profiles of luvisols. *Materials* **2021**, *14*, 6364. [CrossRef]
69. Gianfreda, L.; Ruggiero, P. Enzyme activities in soil. In *Nucleic Acids and Proteins in Soil*; Nannipieri, P., Smalla, K., Eds.; Springer: Berlin/Heidelberg, Germany, 2006; pp. 20–25. [CrossRef]
70. Loeppmann, S.; Blagodatskaya, E.; Pausch, J.; Kuzyakov, Y. Enzyme properties down the soil profile—A matter of substrate quality in rhizosphere and detritusphere. *Soil Biol. Biochem.* **2016**, *103*, 274–283. [CrossRef]
71. Mierzwa-Hersztek, M.; Gondek, K.; Baran, A. Effect of poultry litter biochar on soil enzymatic activity, ecotoxicity and plant growth. *Appl. Soil Ecol.* **2016**, *105*, 144–150. [CrossRef]
72. Smenderovac, E.; Emilson, E.; Porter, C.T.; Morris, D.; Hazlett, P.; Diochon, A.; Basiliko, N.; Bélanger, N.; Markham, J.; Rutherford, P.M.; et al. Forest soil biotic communities show few responses to wood ash applications at multiple sites. *Sci. Rep.* **2022**, *12*, 4171. [CrossRef]
73. Perucci, P.; Monaci, E.; Onofri, A.; Vischetti, C.; Casucci, C. Changes in physico-chemical and biochemical parameters of soil following addition of wood ash: A field experiment. *Eur. J. Agron.* **2008**, *28*, 155–161. [CrossRef]
74. Abel, S.; Peters, A.; Trinks, S.; Schonsky, H.; Facklam, M.; Wessolek, G. Impact of biochar and hydrochar addition on water retention and water repellency of sandy soil. *Geoderma* **2013**, *202–203*, 183–191. [CrossRef]
75. Basso, A.S.; Miguez, F.E.; Laird, D.A.; Horton, R.; Westgate, M. Assessing potential of biochar for increasing water-holding capacity of sandy soils. *GCB Bioenergy* **2013**, *5*, 132–143. [CrossRef]
76. Foster, E.J.; Hansen, N.; Wallenstein, M.; Cotrufo, M.F. Biochar and manure amendments impact soil nutrients and microbial enzymatic activities in a semi-arid irrigated maize cropping system. *Agric. Ecosyst. Environ.* **2016**, *233*, 404–414. [CrossRef]
77. Zornoza, R.F.; Moreno-Barriga, J.A.; Acosta, M.A.; Muñoz, A. Faz. Stability, nutrient availability and hydrophobicity of biochars derived from manure, crop residues, and municipal solid waste for their use as soil amendments. *Chemosphere* **2016**, *144*, 122–130. [CrossRef]
78. Borchard, N.; Wolf, A.; Laabs, V.; Aeckersberg, R.; Scherer, H.W.; Moeller, A.W. Physical activation of biochar and its meaning for soil fertility and nutrient leaching—A greenhouse experiment. *Soil Use Manag.* **2012**, *28*, 177–184. [CrossRef]
79. Brantley, K.E.; Savin, M.C.; Brye, K.R.; Longer, D.E. Pine woodchip biochar impact on soil nutrient concentrations and corn yield in a silt loam in the mid-Southern U.S. *Agriculture* **2015**, *5*, 30–47. [CrossRef]
80. Lucchini, P.; Quilliam, R.S.; DeLuca, T.H.; Vamerali, T.; Jones, D.L. Increased bioavailability of metals in two contrasting agricultural soils treated with waste wood-derived biochar and ash. *Environ. Sci. Pollut. Res.* **2014**, *21*, 3230–3240. [CrossRef]

81. Adekayode, F.O.; Olojugba, M.R. The utilization of wood ash as manure to reduce the use of mineral fertilizer for improved performance of maize (*Zea mays* L.) as measured in the chlorophyll content and grain yield. *J. Soil Sci. Environ. Manag.* **2010**, *1*, 40–45. [CrossRef]
82. Arshad, M.A.; Soon, Y.K.; Azooz, R.H.; Lupwayi, N.Z.; Chang, S.X. Soil and crop response to wood ash and lime application in acidic soils. *Agron. J.* **2012**, *104*, 715–721. [CrossRef]
83. Muhammad, I.; Puschenreiter, M.; Wenzel, W.W. Cadmium and Zn availability as affected by pH manipulation and its assessment by soil extraction, DGT and indicator plants. *Bull. Environ. Contam. Toxicol.* **2012**, *416*, 490–500. [CrossRef] [PubMed]
84. Bhattacharya, S.S.; Chattopadhyay, G.N. Increasing bioavailability of phosphorus from fly ash through vermicomposting. *J. Environ. Qual.* **2002**, *31*, 2116–2119. [CrossRef] [PubMed]
85. Rai, V.; Tandon, P.K.; Khatoon, S. Effect of chromium on antioxidant potential of *Catharanthus roseus* varieties and production of their anticancer alkaloids: Vincristine and vinblastine. *Biomed. Res. Int.* **2014**, *2014*, 934182. [CrossRef] [PubMed]
86. Mathur, S.; Kalaji, H.M.; Jajoo, A. Investigation of deleterious effects of chromium phytotoxicity and photosynthesis in wheat plant. *Photosynthetica* **2016**, *54*, 185–192. [CrossRef]
87. Huang, S.; Peng, B.; Yang, Z.; Chai, L.; Zhou, L. Chromium accumulation, microorganism population and enzyme activities in soils around chromium-containing slag heap of steel alloy factory. *Trans. Nonferrous Met. Soc. China* **2009**, *19*, 241–248. [CrossRef]
88. Boerner, R.E.J.; Brinkman, J.A. Fire frequency and soil enzyme activity in southern Ohio aok-hickory forests. *Appl. Soil Ecol.* **2003**, *23*, 137–146. [CrossRef]
89. Peng, B.; Huang, S.H.; Yang, Z.H.; Chai, L.Y.; Xu, Y.Z.; Su, C.Q. Inhibitory effect of Cr(VI) on activities of soil enzymes. *J. Cent. South. Univ. Technol.* **2009**, *16*, 594–598. [CrossRef]
90. Wu, G.; Kanga, H.; Zhang, X.; Shao, H.; Chu, L.; Ruand, C. A critical review on the bio-removal of hazardous heavy metals from contaminated soils: Issues, progress, eco-environmental concerns and opportunities. *J. Hazard. Mater.* **2010**, *174*, 1–8. [CrossRef]
91. Lombard, N.; Prestat, E.; van Elsas, J.D.; Simonet, P. Soil-specific limitations for access and analysis of soil microbial communities by metagenomics. *FEMS Microbiol. Ecol.* **2011**, *78*, 31–49. [CrossRef]
92. Belyaeva, O.N.; Haynes, R.J.; Birukova, O.A. Barley yield and soil microbial and enzyme activities as affected by contamination of two soils with lead, zinc or copper. *Biol. Fertil. Soils* **2005**, *41*, 85–94. [CrossRef]
93. Pérez-Guzmán, L.; Lower, B.H.; Dick, R.P. Corn and hardwood biochars affected soil microbial community and enzyme activities. *Agrosyst. Geosci. Environ.* **2020**, *3*, e20082. [CrossRef]

energies

MDPI

Article

Life Cycle Assessment of Energy Production from Solid Waste Valorization and Wastewater Purification: A Case Study of Meat Processing Industry

Christos Boukouvalas *, Tryfon Kekes, Vasiliki Oikonomopoulou and Magdalini Krokida

Laboratory of Process Analysis and Design, School of Chemical Engineering, National Technical University of Athens, Iroon Polytechneiou 9, 15780 Athens, Greece; tryfonaskks@yahoo.com (T.K.); vasiaoik@central.ntua.gr (V.O.); mkrok@chemeng.ntua.gr (M.K.)
* Correspondence: bouk@chemeng.ntua.gr; Tel.: +30-2107722358

Abstract: The meat processing industry is a very energy-intensive and water-demanding industry that produces large amounts of solid and aqueous wastes. Therefore, methods for the effective treatment of the produced wastes have been studied in order to treat and reuse water within the industry and valorize the solid wastes for the production of energy and value-added products. The primary aim of this work is to evaluate the overall sustainability of energy produced from solid waste valorization and wastewater treatment in the meat processing industry via Life Cycle Assessment (LCA). For this purpose, the total environmental impact of a typical meat industry that utilizes conventional waste management methods (Scenario A) was evaluated and compared with two different industries with appropriate waste treatment/valorization processes. In the first studied valorization scenario (Scenario B), waste management is conducted using anaerobic digestion, composting, membrane bioreactors, and ultraviolet (UV) treatment, whereas in the second studied valorization scenario (Scenario C), aeration treatment, chlorination, and hydrothermal carbonization (HTC) are the selected treatment techniques. As expected, it is evident from this LCA study, that both Scenarios B and C exhibited a significantly improved environmental footprint in all studied indicators compared with Scenario A, with the reduction in certain environmental impact categories reaching up to 80%. Between the two studied alternative scenarios, the biggest improvement in the environmental footprint of the meat industry was observed in Scenario C, mainly due to the substantial quantity of the produced thermal energy. According to the results of the present case study, it is evident that the incorporation of appropriate methods in the meat industry can result in the efficient generation of energy and a significant improvement in the environmental footprint contributing to environmental safety and sustainability.

Keywords: Life Cycle Assessment; sustainability; waste valorization; energy production; wastewater treatment; meat processing industry

1. Introduction

The meat processing industry is a continuously developing field that includes the utilization of large quantities of natural resources, such as water and energy [1]. As a result, the meat processing industry is accountable for severe environmental impacts (on air, water, and soil), which are constantly growing due to vast amounts of energy and water consumption, as well as waste production [2]. Moreover, the management and treatment of the produced wastes requires further consumption of energy and raw materials that can further burden the environmental footprint of the specific industry due to the high organic content of both solid wastes and wastewater [2]. However, the nature of the produced wastes provides a plethora of opportunities for treatment and valorization (water recycling and reuse, energy production, material recovery, etc.) [3].

Among several methods for the treatment and valorization of meat processing waste aiming at energy and production water reuse, the ones that have been selected as the most appropriate due to their efficiency in wastewater treatment and renewable energy production via waste valorization are the following: membrane bioreactor, aeration treatment, chlorination, ultraviolet (UV) treatment, anaerobic digestion, hydrothermal carbonization (HTC), and composting. A membrane bioreactor is a state-of-the-art alternative method for wastewater treatment that couples the biological process with membrane filtration. Specifically, it consists of a bioreactor tank, in which the biomass is degraded, followed by membrane filtration for the removal of microorganisms from the treated water [4]. Aeration treatment involves the addition of air into wastewater, thus allowing the biodegradation of organic compounds resulting in water decontamination [5]. UV treatment is an effective method for the disinfection of treated water, in which water is exposed to ultraviolet light resulting in the disinfection of hazardous pathogens, such as bacteria and viruses [6]. Chlorination is a reliable and efficient method used for water disinfection, which possesses the ability to efficiently oxidize a wide spectrum of organic and inorganic compounds as well as to eliminate any microbial hazards [7]. Anaerobic digestion constitutes an anaerobic fermentation process for solid wastes (wet), in which organic matter is efficiently degraded by microorganisms and converted into biogas [8]. Subsequently, the biogas is transferred into a biogas cogeneration (combined heat and transfer—CHP) unit and generates power (renewable) in the form of electricity and heat [9]. One other advantage of anaerobic digestion is derived from the fact that the solid residue of the process (digestate) can be utilized in composting, further increasing the circularity of the solid wastes [10]. Hydrothermal carbonization (HTC) involves the conversion of organic compounds through certain chemicals into structured solid fuels, which can subsequently be utilized for the generation of electricity and thermal energy [11]. The combination of several of the aforementioned methods in the treatment of wastewater and solid wastes produced during meat processing has the potential not only to reduce the total waste of the industry, thus improving the environmental footprint of the sector, but also to reuse the recovered water and produced energy within the industry, increasing to a degree self-sufficiency of natural resources and reducing the operating cost [12].

However, it is necessary to confirm the environmental benefits of the specific methods in comparison to the conventional existing ones. Life Cycle Assessment (LCA) is a verified tool, defined by the International Organization for Standardization (ISO 14040:2006) for assessing the environmental behavior of processes/products/services [13]. LCA takes into consideration the inputs, outputs, and potential environmental effects of a product system across its life cycle, and can pinpoint hot points and recommend improvements in the production process aiming at environmental sustainability [14]. LCA can be performed according to two different principal approaches, the attributional and the consequential methods. The first reports the environmental features of a current state system, while the latter, which is used in the present work, focuses on prognosticating the effect of changes in established procedures [15]. Additionally, the life cycle impact indicators can be quantified by various methods, including ReCiPE, EDIP, and CML, which frequently exhibit different impact categories, classification of inventory, and model characterization [14].

The primary aim of the present study was to evaluate the environmental sustainability of various treatment methods for wastewater and solid wastes utilized in meat processing industries. For this purpose, a conventional meat processing industrial line was first investigated to highlight the environmental impact of the specific sector and the necessity for efficient utilization of the wastes for energy production and wastewater purification. Subsequently, three different scenarios (Scenarios A, B, and C) for the treatment of wastewater and solid wastes were studied, the first consisting of conventional methods and the latter two of innovative ones, aiming at confirming the environmental benefits of the proposed methods for energy production and wastewater purification.

2. Materials and Methods

LCA study was performed following the recommendations proposed by the ISO 14040 recommendations series (14040:2006 and 14044:2006) [16]. ReCiPe 2016 (H, hierarchist) was selected as a method to perform the impact assessment, with its main objective being the transformation of Life Cycle Inventory results into a limited number of environmental impact scores using characterization factors. Finally, GABI ts software (v10.6.2.9, Sphera Solutions GmbH, Echterdingen, Stuttgart, Germany) was used for the calculation of the impact categories [16].

2.1. Goal

The goal of the LCA study was to determine the effect of the implementation of various wastewater and solid waste treatment methods for energy production in the conventional meat processing industry on different environmental impact categories. First, the environmental impact of the conventional meat processing industry was evaluated, using data obtained from existing references. Subsequently, to evaluate the effect of the benefits of incorporating novel methods for waste valorization and wastewater purification, three different scenarios were studied based on the literature, one with conventional treatment methods and the other two with innovative ones.

2.2. . . . and Scope

2.2.1. Product System

The case of the present work was based on the conventional meat processing industry, with the final products being various pork-meat products, including packaged and fresh meat. Figure 1 depicts the production processes and the involved flows. The main processing steps involved in meat processing include the following:

- Slaughter house;
- Scalding and hide removal;
- Evisceration;
- Trimming;
- Refrigeration and chilling;
- Cutting and deboning;
- Processing;
- Packaging of the final products.

The corresponding flows are highlighted in five different colors in order to be better classified. Light and dark red colors indicate the flows connected to steam and solid wastes, respectively. Flows related to condensate and wastewater are depicted in light and dark purple, respectively. Finally, green connects to the final product flows, and the blue color indicates the rest of the flows in the meat processing.

In the first studied scenario (Scenario A) for the wastewater and solid waste treatment (Figure 2), wastewater is transferred to a municipal wastewater treatment plant, and solid wastes are processed in landfilling. This scenario considers that the meat processing industry is not involved in any recycling treatment and/or valorization of its waste for energy production, which constituted the most common practice for several years.

In the second studied scenario (Scenario B), wastewater and solid wastes are treated on-site within the boundaries of the industry (Figure 3). Specifically, wastewater is first screened, processed in a membrane bioreactor, and finally treated with UV radiation. Therefore, the final product will be cleaned water that can be either recycled in the industry (decreasing freshwater consumption) or returned clean to the aquatic environment [4]. Solid wastes are treated in an anaerobic digester, with the resulting biogas (after CO_2 removal to increase the methane content) used for the production of electricity and heat via cogeneration [17]. The produced heat is recirculated to the anaerobic digester, while electricity is sold to the grid as renewable energy (for economic reasons). Finally, the digestate from the anaerobic digestion is transferred to a composting unit.

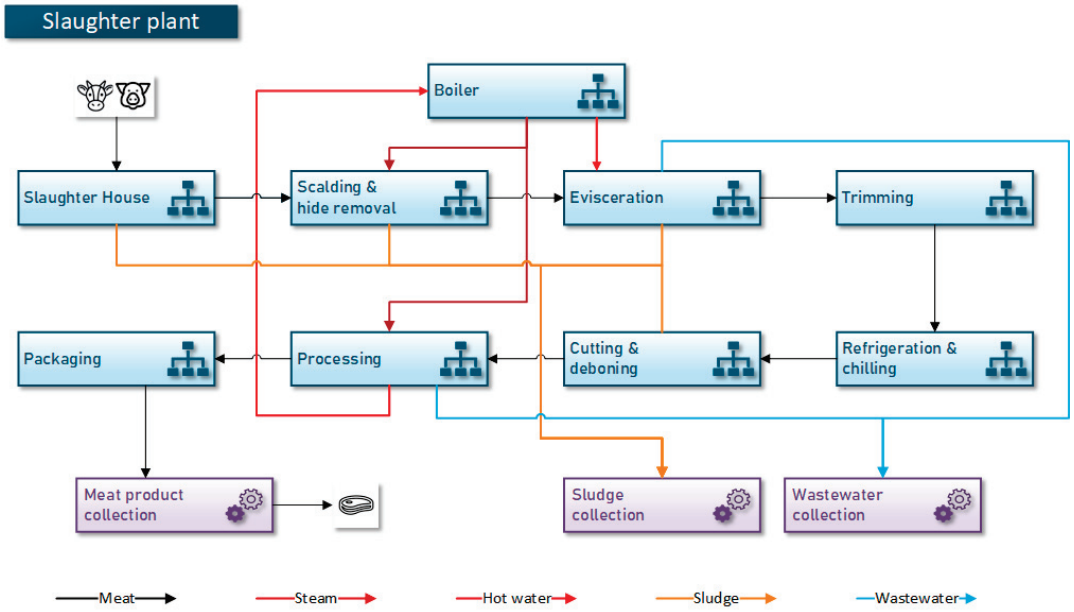

Figure 1. Production process flowcharts and main flows.

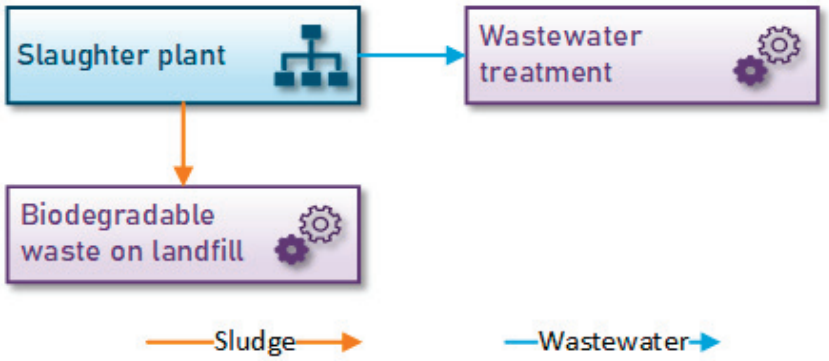

Figure 2. Wastewater and solid waste treatment, and main flows in Scenario A.

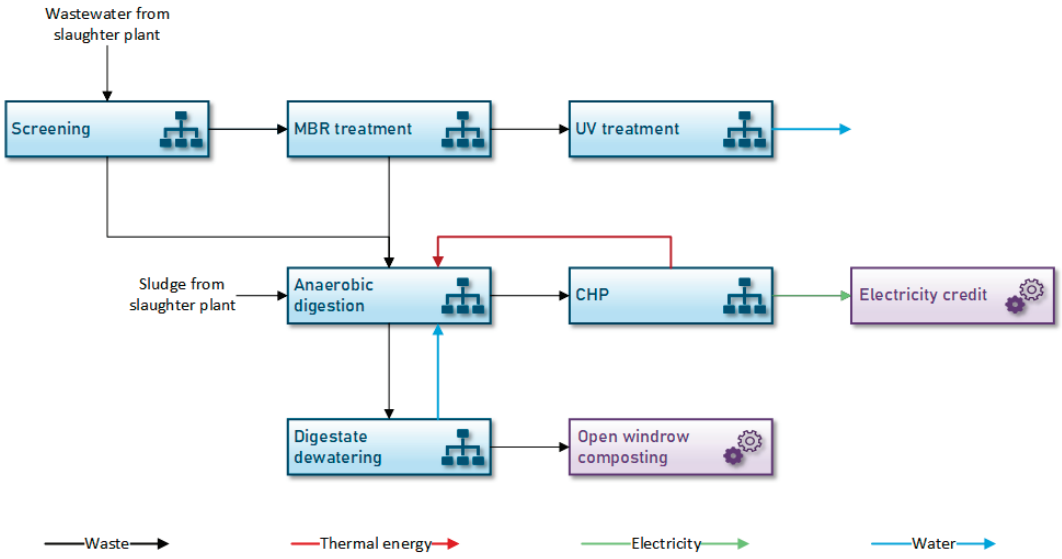

Figure 3. Wastewater and solid waste treatment, and main flows in Scenario B.

In the third studied scenario (Scenario C), wastewater and solid wastes are treated on-site within the boundaries of the industry, similar to the previously analyzed scenario (Figure 4). However, in this studied scenario, different methods were studied for the treatment and valorization of wastewater and solid wastes. More specifically, wastewater is screened as a preliminary treatment to remove large-size solids, which are then processed in landfilling and transferred to an aeration tank. During aeration treatment, air and sodium hypochlorite are transferred into the tank and are mixed with the wastewater, thus enabling the biodegradation of organic compounds. Subsequently, chlorination using sodium hypochlorite as a disinfection agent is utilized in order to eliminate any microbial and chemical hazards, with the final product being clean water that can be safely recycled in the industry or discharged into the aquatic environment [7]. Solid wastes are treated using the hydrothermal carbonization process. At first, the solid wastes are partially dried in order to increase the percentage of solids (circa 92%) and then transferred to an HTC reactor, where a slurry containing solid fuel and hydrolysates is generated, with the latter being removed via filtration and transported to a municipal wastewater treatment plant. Afterward, the obtained solid fuels are completely dried and pelletized. Finally, pellets are blown into a power generator, resulting in the generation of electricity and thermal energy [11]. The generation of thermal energy and electricity in Scenarios B and C is depicted as thermal and electricity credits, respectively. Generally, thermal and electricity credits exhibit an overall positive impact on the environmental footprint of both scenarios due to the fact that energy is produced from waste valorization and not from the conventional burning of fossil fuels. Finally, it must be stated that the wastewater generated within the meat processing industry exhibits high organic content and high concentrations of organic metabolites; thus, the applied methods should be carefully selected to obtain wastewater purification. However, according to the literature, the studied methods in this manuscript have been efficiently applied for the purification of the aforementioned wastewater effluents [18–21].

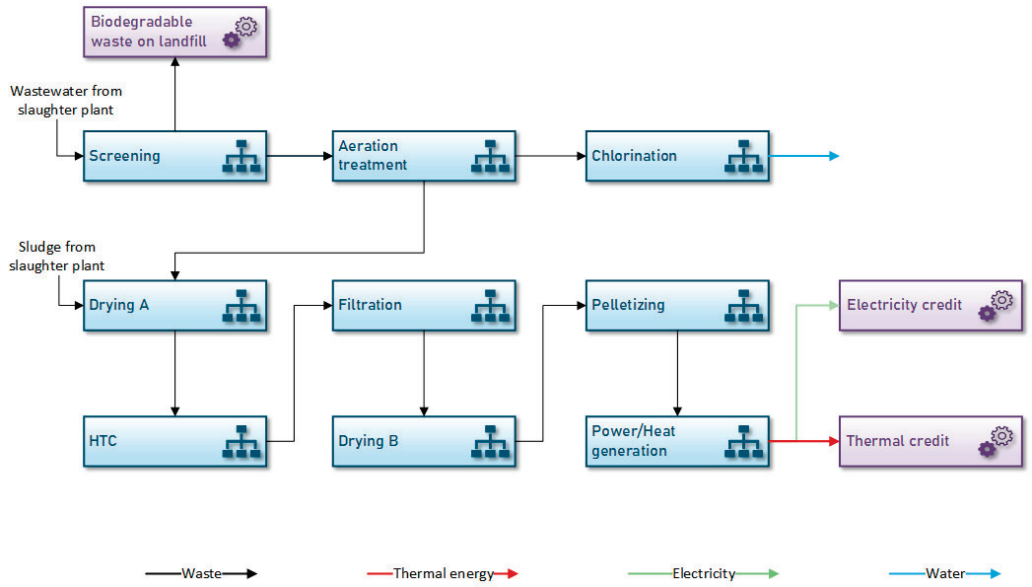

Figure 4. Wastewater and solid waste treatment, and main flows in Scenario C.

2.2.2. Functional Unit

The functional unit selected for the present work was 1 kg/d of produced meat products.

2.2.3. System Boundaries

The system boundaries for the case of the typical meat processing industry that evaluates the environmental footprint of the production of meat products are defined as gate-to-gate. Specifically, the system boundaries include all the production processes from

a slaughter house to packaging. The system boundaries of the two alternative studied scenarios (Scenario B and C) are also defined as gate-to-gate and consist of the production process and the respective wastewater and solid waste treatment. The transportation of the feedstock as well as of the final meat products is not included in the system boundaries.

2.2.4. Data Requirements

The data that were used for this study were obtained from studies accessible in references; the data were also taken from GABI professional and Ecoinvent databases, referring to the geographical area of the European Union 28 (EU-28). All studies and data refer to a period of the last 5 years.

2.2.5. Assumptions and Limitations

Data used in the meat production processes and the three studied scenarios are based on the literature review; thus, they do not represent an accurate recording of an existing situation, possibly leading to a level of uncertainty in the estimation of environmental footprints [22]. However, the main purpose of this study was the confirmation of the environmental benefits of the proposed methods compared with conventional handling of wastewater and solid wastes and, thus, this uncertainty is not expected to influence the results since it affects all the studied scenarios.

2.3. Life Cycle Inventory

Life Cycle Inventory (LCI) connects the processes with quantitative data according to the selected functional unit (1 kg of meat products per day). Table 1 presents the input and output data of every process that is included in the meat processing industry, as shown in Figure 1. As a reference for the collection of the data and the establishment of the inventory, the literature data were used, as listed below; however, appropriate changes were made, and the numbers were verified via communication with the meat processing industry located in the Attica area in Greece. Environmental data were obtained from GABI professional (8007 db version 2022) and Ecoinvent (Ecoinvent 3.8) databases.

Table 1. Life Cycle Inventory (LCI) of the conventional meat processing industry (based on [23] and adjusted to current data via communication with the meat processing industry located in the Attica area).

Process	Input/Output	Flow	Unit	Value
Slaughter house	In	Feedstock	kg	1.53
	In	Electricity	kJ	7.43
	Out	Feedstock	kg	1.47
	Out	Blood (sludge)	kg	0.06
Scalding and hide removal	In	Feedstock	kg	1.47
	In	Steam	kg	0.06
	In	Electricity	kJ	3.62
	Out	Feedstock	kg	1.41
	Out	Hide (sludge)	kg	0.01
	Out	Fur (sludge)	kg	0.05
	Out	Water vapor	kg	0.06
Evisceration	In	Feedstock	kg	1.41
	In	Hot water	kg	1.02
	Out	Carcass	kg	0.94
	Out	Viscera and inedible parts (sludge)	kg	0.34
	Out	Meat prod. 1	kg	0.12
	Out	Wastewater	kg	1.02

Table 1. *Cont.*

Process	Input/Output	Flow	Unit	Value
Trimming	In	Carcass	kg	0.94
	In	Electricity	kJ	2.90
	Out	Carcass	kg	0.90
	Out	Meat prod. 2	kg	0.04
Refrigeration and chilling	In	Carcass	kg	0.90
	In	Electricity	kJ	262.62
	In	Cooling water	kg	16.35
	Out	Carcass	kg	0.62
	Out	Meat prod. 3	kg	0.28
	Out	Cooling water	kg	16.35
Cutting and deboning	In	Carcass	kg	0.62
	In	Electricity	kJ	5.43
	Out	Other meat	kg	0.47
	Out	Meat prod. 4	kg	0.07
	Out	Bones and inedible parts (sludge)	kg	0.08
Processing	In	Other meat	kg	0.47
	In	Steam	kg	0.02
	In	Electricity	kJ	53.97
	In	Fuel (diesel)	kJ	243.42
	In	Water	kg	2.90
	Out	Other meat	kg	0.47
	Out	Condensate	kg	0.02
	Out	Wastewater	kg	2.90
Packaging	In	Other meat	kg	0.47
	In	PP (tray)	kg	0.02
	In	Electricity (packaging)	kJ	102.33
	In	Electricity (tray)	kJ	42.75
	Out	Meat prod. 5	kg	0.49
Boiler	In	Condensate	kg	0.02
	In	Water (deionized)	kg	1.08
	In	Fuel (natural gas)	kJ	721.01
	Out	Steam	kg	0.08
	Out	Hot water	kg	1.02
Total meat products	In	Meat prod. 1	kg	0.12
	In	Meat prod. 2	kg	0.04
	In	Meat prod. 3	kg	0.28
	In	Meat prod. 4	kg	0.07
	In	Meat prod. 5	kg	0.49
	Out	Meat products	kg	1.00

Table 2. Life Cycle Inventory (LCI) of Scenario A.

Process	Input/Output	Flow	Unit	Value
Municipal wastewater treatment	In	Wastewater from evisceration	kg	1.02
		Wastewater from processing	kg	2.90
		Total	kg	3.92
Biodegradable waste on landfill	In	Blood	kg	0.06
		Hide	kg	0.01
		Fur	kg	0.05
		Viscera and inedible parts	kg	0.3
		Bones and inedible parts	kg	0.08
		Total	kg	0.54

Tables 2–4 present the input and output data of every process that is included in the different scenarios, as shown in Figures 2–4.

Table 3. Life Cycle Inventory (LCI) of Scenario B.

Process	Input/Output	Flow	Unit	Value
Screening [24]	In	Wastewater	kg	3.92
	In	Electricity	kJ	0.02
	Out	Solids	kg	0.01
	Out	Wastewater	kg	3.91
Membrane bioreactor [25]	In	Wastewater	kg	3.91
	In	Electricity	kJ	19.70
	Out	Wastewater	kg	3.90
	Out	Sludge	kg	0.01
UV treatment [26]	In	Wastewater	kg	3.90
	In	Electricity	kJ	0.93
	Out	Clean water	kg	3.90
Anaerobic digestion [27]	In	Sludge	kg	0.54
	In	Solid	kg	0.01
	In	Sludge	kg	0.01
	In	Wastewater (recycling)	kg	43.67
	In	Electricity	kJ	176.50
	In	Fuel (diesel)	kJ	2051.07
	In	Heat (CHP)	kJ	1467.09
	Out	Digestate	kg	44.10
	Out	Biogas	kg	0.12
CHP [27]	In	Biogas	kg	0.12
	Out	Heat (CHP)	kJ	1467.09
	Out	Electricity	kJ	1304.08
Digestate thickening [28]	In	Digestate	kg	44.10
	In	Electricity	kJ	79.37
	Out	To compost	kg	0.43
	Out	Wastewater (recycling)	kg	43.67

Table 4. Life Cycle Inventory (LCI) of Scenario C.

Process	Input/Output	Flow	Unit	Value
Screening [24]	In	Wastewater	kg	3.92
	In	Electricity	kJ	0.02
	Out	Solids	kg	0.01
	Out	Wastewater	kg	3.91
Aeration treatment [29]	In	Wastewater	kg	3.91
	In	Electricity	kJ	3.28
	In	Sodium hypochlorite	kg	4.70×10^{-5}
	Out	Wastewater	kg	3.90
	Out	Sludge	kg	0.01
Chlorination [30]	In	Wastewater	kg	3.90
	In	Electricity	kJ	0.87
	In	Sodium hypochlorite (15%)	kg	2.94×10^{-4}
	Out	Clean water	kg	3.90
Drying A [11]	In	Solid wastes	kg	0.54
	In	Sludge	kg	0.01
	In	Heat	kJ	960.00
	Out	Solid wastes	kg	0.24
	Out	Waste vapor	kg	0.31

Table 4. *Cont.*

Process	Input/Output	Flow	Unit	Value
HTC [11]	In	Solid wastes	kg	0.24
	In	Electricity	kJ	336.10
	Out	Slurry	kg	2.35×10^{-1}
	Out	Exhausted gas	kg	0.05×10^{-1}
Filtration [11]	In	Slurry	kg	2.35×10^{-1}
	In	Electricity	kJ	20.30
	Out	Solid fuel	kg	0.97×10^{-1}
	Out	Hydrolysates	kg	1.38×10^{-1}
Drying B [11]	In	Solid fuel	kg	0.97×10^{-1}
	In	Heat	kJ	20.90
	Out	Solid fuel	kg	0.09
	Out	Waste vapor	kg	0.01
Pelletizing [11]	In	Solid fuel	kg	0.09
	In	Electricity	kJ	2.30
	Out	Pelletized fuel	kg	0.09
Pellet power generation [11]	In	Pelletized fuel	kg	0.09
	In	Electricity	kJ	8.16
	Out	Electricity	kJ	389.30
	Out	Thermal energy	kJ	1133.6
	Out	Ash mix	kg	0.45×10^{-3}

3. Results and Discussion

The environmental effects of the typical meat processing industry, along with the environmental effects of each individual process, are presented in Figure 5.

According to the obtained results, the meat processing industry can be classified as an energy-intensive sector that produces large amounts of solid wastes and wastewater and exhibits severe environmental impact on various categories. Generally, the most energy-intensive, water-demanding, and environmentally harmful processes of the studied industry are the processing of meat after the removal of the inedible parts and the boiler, which is necessary for water heating and steam production and can be attributed to the amount of consumed electricity and fossil fuels. More specifically, based on the collected data and taking into account the assumptions and limitations that may lead to a certain level of uncertainty in the studied indices, approximately 0.141 kg CO_2 eq. and 0.001 kg 1,4-DB eq. are produced during the processing of meat per 1 kg of meat products, while freshwater consumption rises up to 0.005 m^3/kg of meat product. The obtained results are similar to those already existing in the literature regarding LCA in meat processing industries. According to a study conducted on pork production in Denmark, climate change was evaluated as equal to 0.1 kg CO_2 eq./kg of pork products [31], while research studying poultry production indicated that 0.16 kg CO_2 eq. are emitted per 1 kg of chicken final products [32]. Furthermore, notable environmental effects were observed for all the other studied indicators, including fossil and metal depletion (circa 0.07 kg oil eq./kg of meat product and 0.0004 kg Cu eq./kg of meat product) and marine ecotoxicity (0.001 kg 1,4-DB eq./kg of meat product). Therefore, in the context of environmental protection, sustainability, and circular economy, it is deemed necessary to incorporate appropriate methods of water purification and waste utilization for energy production within the meat processing industry to improve its environmental footprint. Based on the aforementioned, three different scenarios were selected for this work: the first hypothesizes that the meat processing industry is not directly involved in the treatment and valorization of its waste (Scenario A), while in the latter two scenarios, wastewater and solid wastes are treated on-site within the boundaries of the industry (Scenarios B and C). More specifically, in Scenario B, wastewater is treated using a membrane bioreactor and UV radiation, and solid wastes are valorized for the production of biogas, via anaerobic digestion. Whereas, in Scenario C,

wastewater is subjected to aeration treatment and disinfection with sodium hypochlorite, and the valorization of solid wastes for the generation of electricity and thermal energy is achieved via HTC. Figures 6–8 depict the environmental effects of Scenarios A, B, and C, respectively. In Figures 7 and 8, the total environmental effect of the slaughter plant is not included in order to highlight the effect of each method on water purification and solid waste valorization. The total values are presented in Table 5.

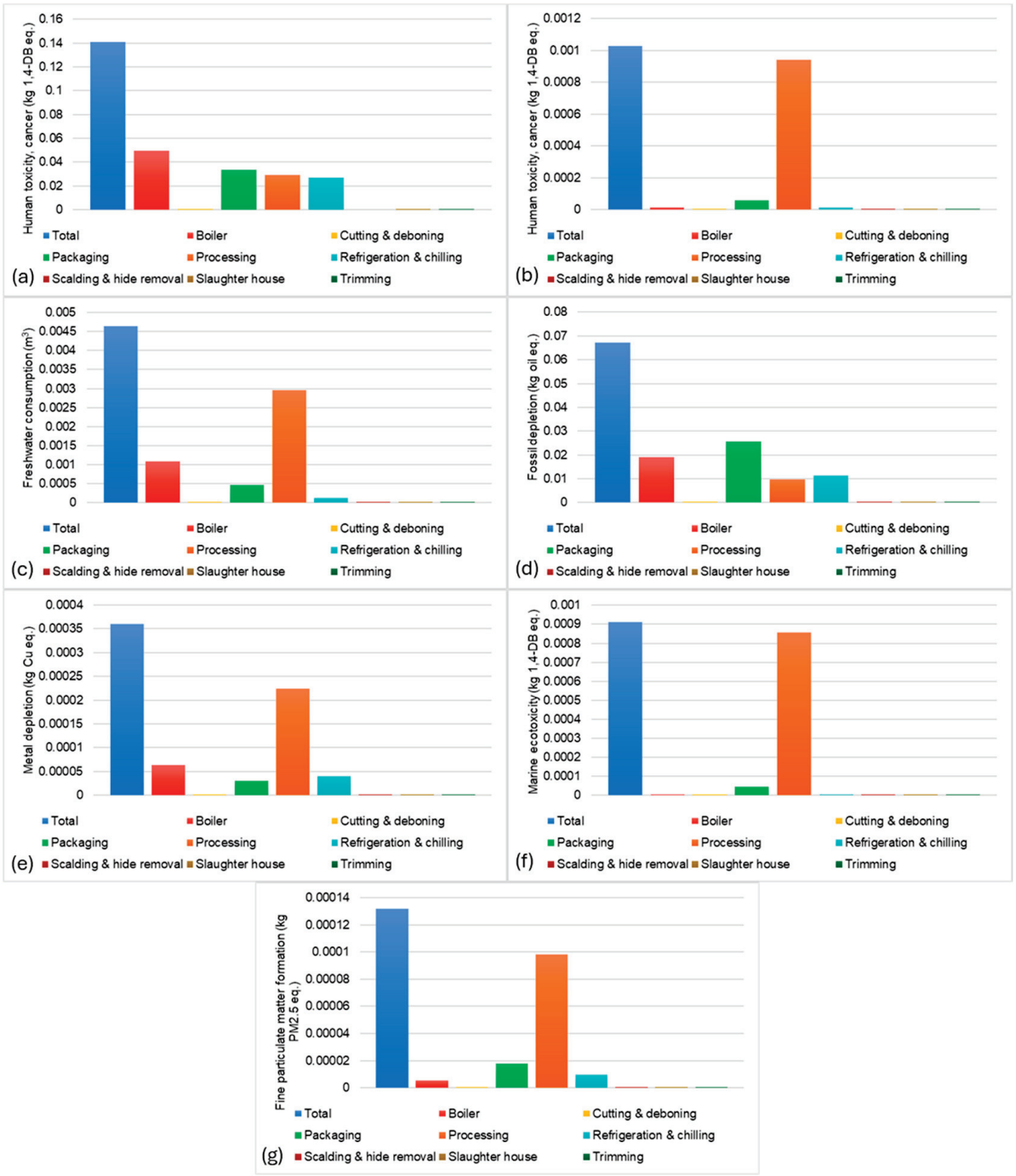

Figure 5. Environmental effects of the meat processing industry on (**a**) climate change (kg CO_2 eq.), (**b**) human toxicity, cancer (kg 1,4−DB eq.), (**c**) freshwater consumption (m^3), (**d**) fossil depletion (kg oil eq.), (**e**) metal depletion (kg Cu eq.), (**f**) marine ecotoxicity (kg 1,4−DB eq.), and (**g**) fine particulate matter formation (kg PM2.5 eq.).

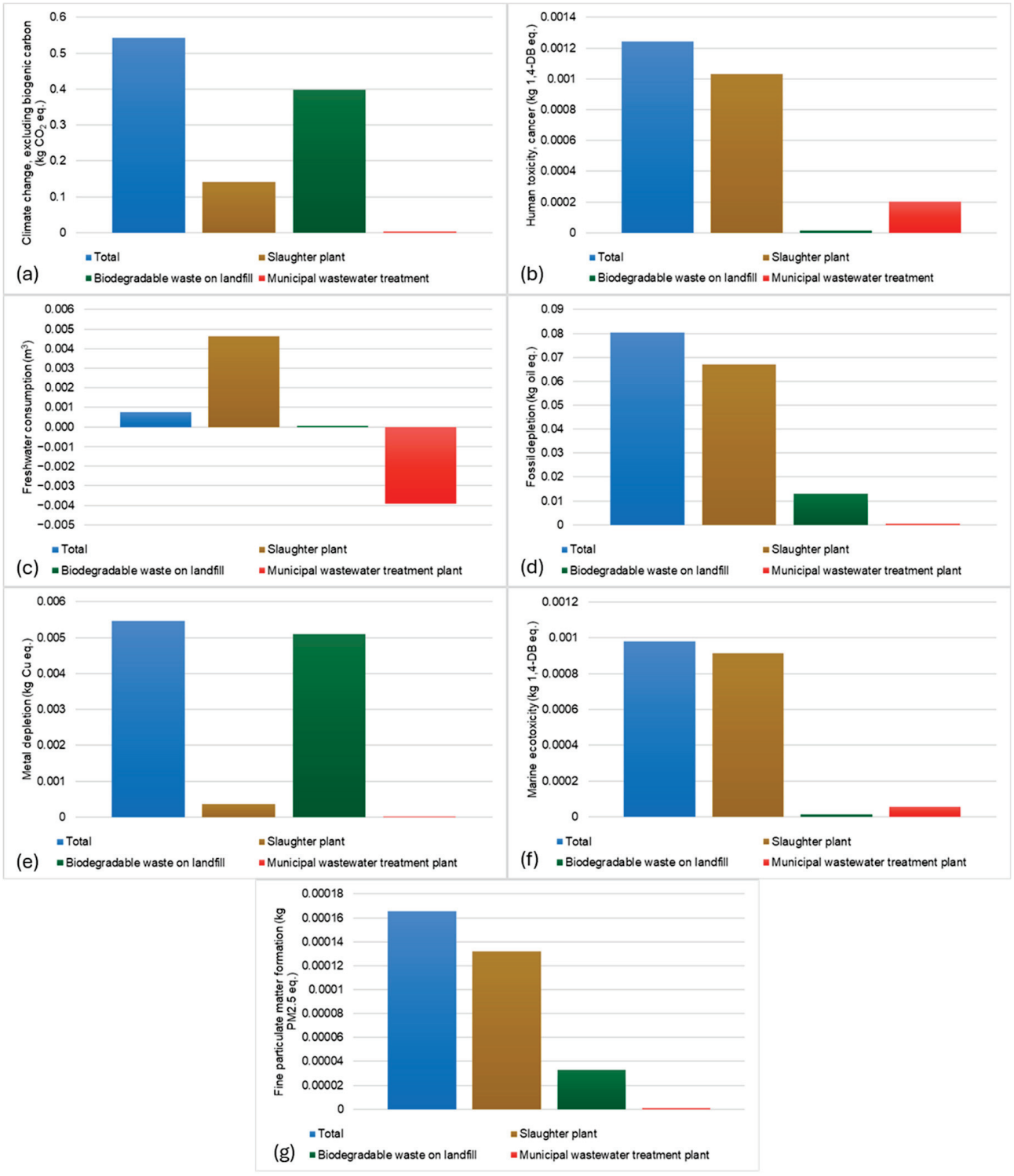

Figure 6. Environmental effects of Scenario A on (**a**) climate change (kg CO_2 eq.), (**b**) human toxicity, cancer (kg 1,4−DB eq.), (**c**) freshwater consumption (m^3), (**d**) fossil depletion (kg oil eq.), (**e**) metal depletion (kg Cu eq.), (**f**) marine ecotoxicity (kg 1,4−DB eq.), and (**g**) fine particulate matter formation (kg PM2.5 eq.).

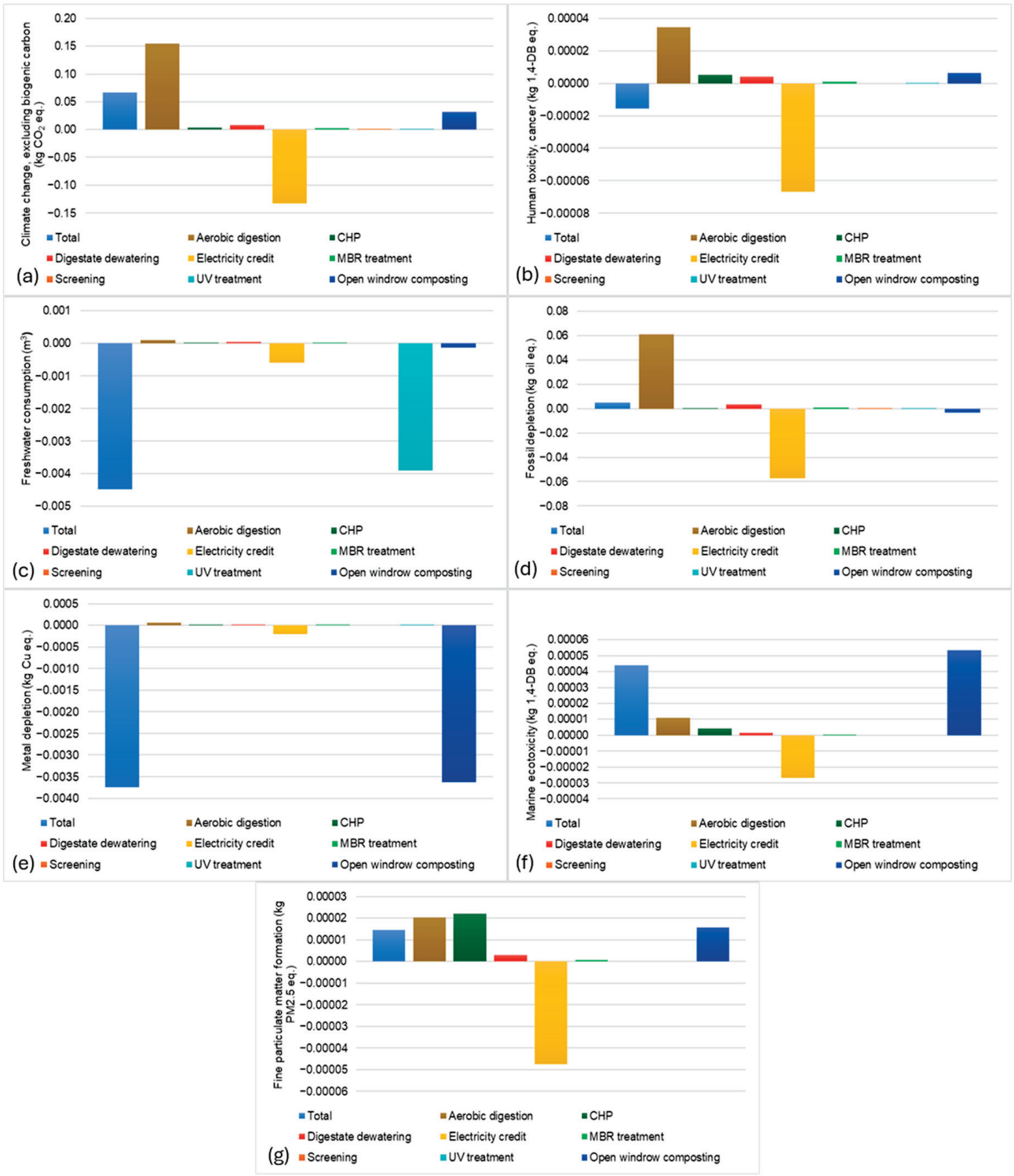

Figure 7. Environmental effects of Scenario B on (**a**) climate change (kg CO_2 eq.), (**b**) human toxicity, cancer (kg 1,4−DB eq.), (**c**) freshwater consumption (m^3), (**d**) fossil depletion (kg oil eq.), (**e**) metal depletion (kg Cu eq.), (**f**) marine ecotoxicity (kg 1,4−DB eq.), and (**g**) fine particulate matter formation (kg PM2.5 eq.).

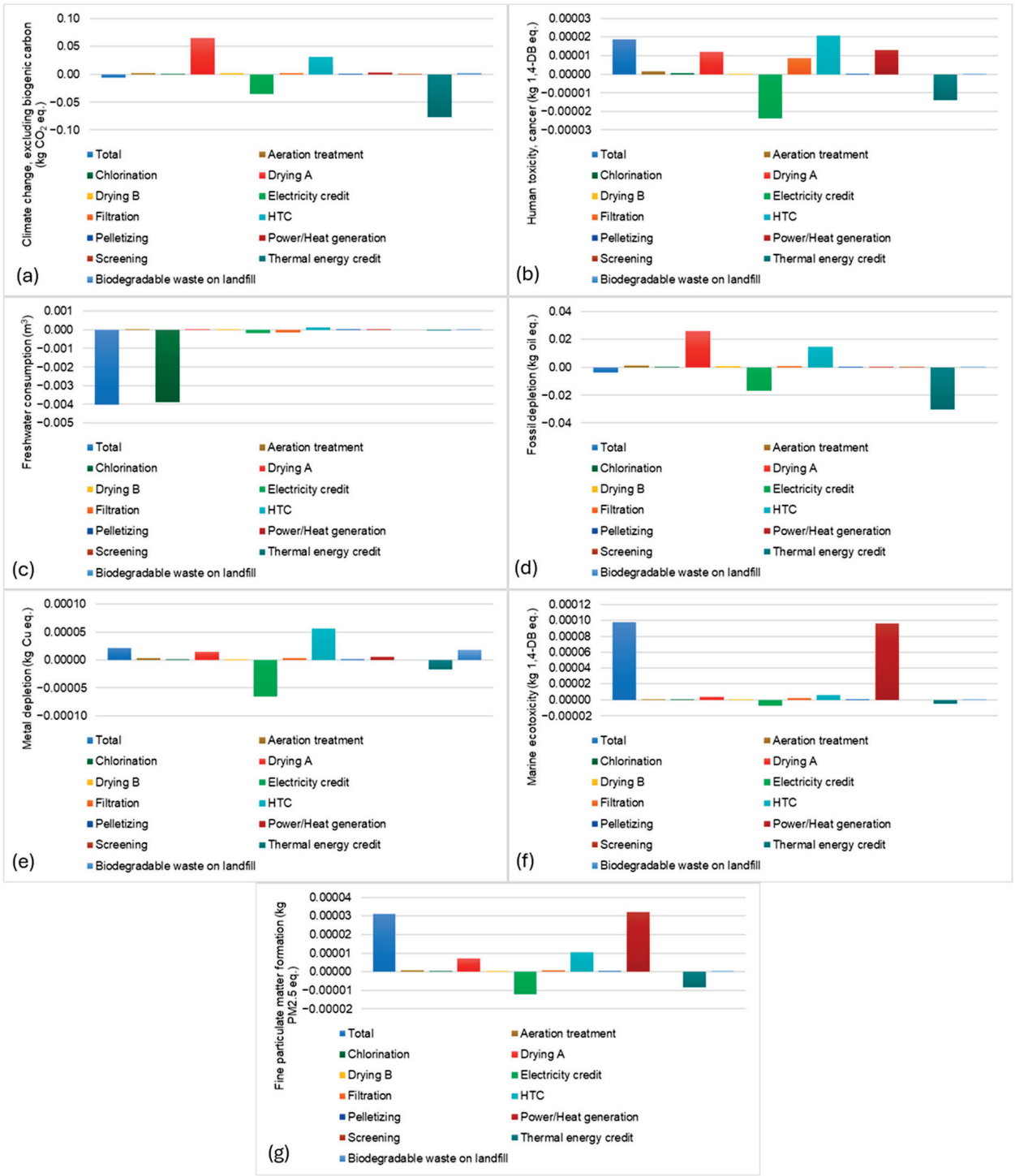

Figure 8. Environmental effects of Scenario C on (**a**) climate change (kg CO_2 eq.), (**b**) human toxicity, cancer (kg 1,4−DB eq.), (**c**) freshwater consumption (m^3), (**d**) fossil depletion (kg oil eq.), (**e**) metal depletion (kg Cu eq.), (**f**) marine ecotoxicity (kg 1,4−DB eq.), and (**g**) fine particulate matter formation (kg PM2.5 eq.).

Based on the attained results of the LCA study of the three distinct scenarios, it can be observed that Scenarios B and C exhibit substantially better environmental footprints compared with Scenario A. The disposal of solid waste on the soil as a landfill, as hypothesized in Scenario A, results in a sharp increase in the emissions of greenhouse gases, measured as climate change and expressed in kg CO_2 eq. Moreover, this specific method of solid waste

handling leads to a further increase in metal and fossil depletion and in fine particulate matter formation. This can be attributed to a necessary possible pretreatment of the solids prior to their disposal and their subsequent treatment in the biodegradation site [33].

Table 5. Comparison of the environmental effects of the three studied scenarios on the studied categories.

Impact Category ($\times 10^{-3}$)	Scenario A	Scenario B	Reduction in Scenario B (%)	Scenario C	Reduction in Scenario C (%)
Climate change (kg CO_2 eq.)	541.30	207.70	61.63	85.41	84.22
Human toxicity, cancer (kg 1,4-DB eq.)	1.24	1.01	18.55	0.69	44.35
Freshwater consumption (m^3)	0.77	0.15	80.52	0.39	49.35
Fossil depletion (kg oil eq.)	80.31	71.81	10.58	41.92	47.80
Metal depletion (kg Cu eq.)	5.46	−3.38	161.90	0.26	95.24
Marine ecotoxicity (kg 1,4-DB eq.)	0.98	0.96	2.04	0.66	32.65
Fine particulate matter formation (kg PM2.5 eq.)	0.17	0.15	11.76	0.11	35.29

On the other hand, the treatment of wastewater and solid wastes in the industry via the implementation of appropriate methods leads to an enhancement in the environmental footprint of the studied case. The efficient purification of wastewater and its safe disposal in the aquatic environment leads to a notable decrease in freshwater consumption in both Scenarios B (screening, MBR, and UV treatment) and C (screening, aeration treatment, and chlorination) [34]. The burden on the environment observed due to anaerobic digestion, depicted in the quantity of GHG emissions and produced kg of 1,4-DB (Figures 7a and 7b, respectively), is successfully compensated by the production of energy and heat via cogeneration (electricity credit), resulting in a positive overall sign of waste treatment in terms of sustainability and environmental safety in Scenario B [35]. However, the generation of large amounts of thermal energy in Scenario C (approximately 1130 kJ/kg of meat products) results in a sharper decrease in the emissions of greenhouse gases compared with Scenario B, as presented in Figures 7a and 8a and Table 6. Finally, it must be noted that the implementation of Scenarios B and C results in negative values for various studied indices (i.e., freshwater consumption for both scenarios, human toxicity for Scenario B, and fossil depletion for Scenario C), thus further validating the positive environmental effect of wastewater treatment and waste valorization. The negative value of freshwater consumption is attributed to the disposal of cleaned water, following the UV treatment, back to the water environment, while the difference in the obtained value of this specific category is due to the transport of the derived hydrolysates, from Scenario C, to a municipal wastewater treatment plant for further treatment. In addition, the negative values of metal depletion for Scenario B, linked with the composting process, are due to the credits from the replacement of conventional fertilizers [36]. A direct comparison of Scenarios A, B, and C is depicted in Figure 9, and the overall reduction in the environmental footprint is presented in Table 5. Moreover, the energy balances (gains and losses of electricity and thermal energy) in the wastewater and solid waste treatment for scenarios B and C are presented in Table 6.

Table 6. Electricity and thermal energy balance in wastewater and solid waste treatment for Scenarios B and C.

Process	Energy Consumed/Generated	Scenario B	Scenario C
Wastewater treatment	Electricity consumed (kJ)	20.65	24.17
	Thermal energy consumed (kJ)	0	0
	Electricity generated (kJ)	0	0
	Thermal energy generated (kJ)	0	0
Solid waste valorization	Electricity consumed (kJ)	255.87	366.86
	Thermal energy consumed (kJ)	3518.16	980.90
	Electricity generated (kJ)	1304.08	389.30
	Thermal energy generated (kJ)	1467.09	1133.60

Table 6. *Cont.*

Process	Energy Consumed/Generated	Scenario B	Scenario C
Energy balance	Electricity (kJ)	1027.56	−1.73
	Thermal energy (kJ)	−2051.07	352.70

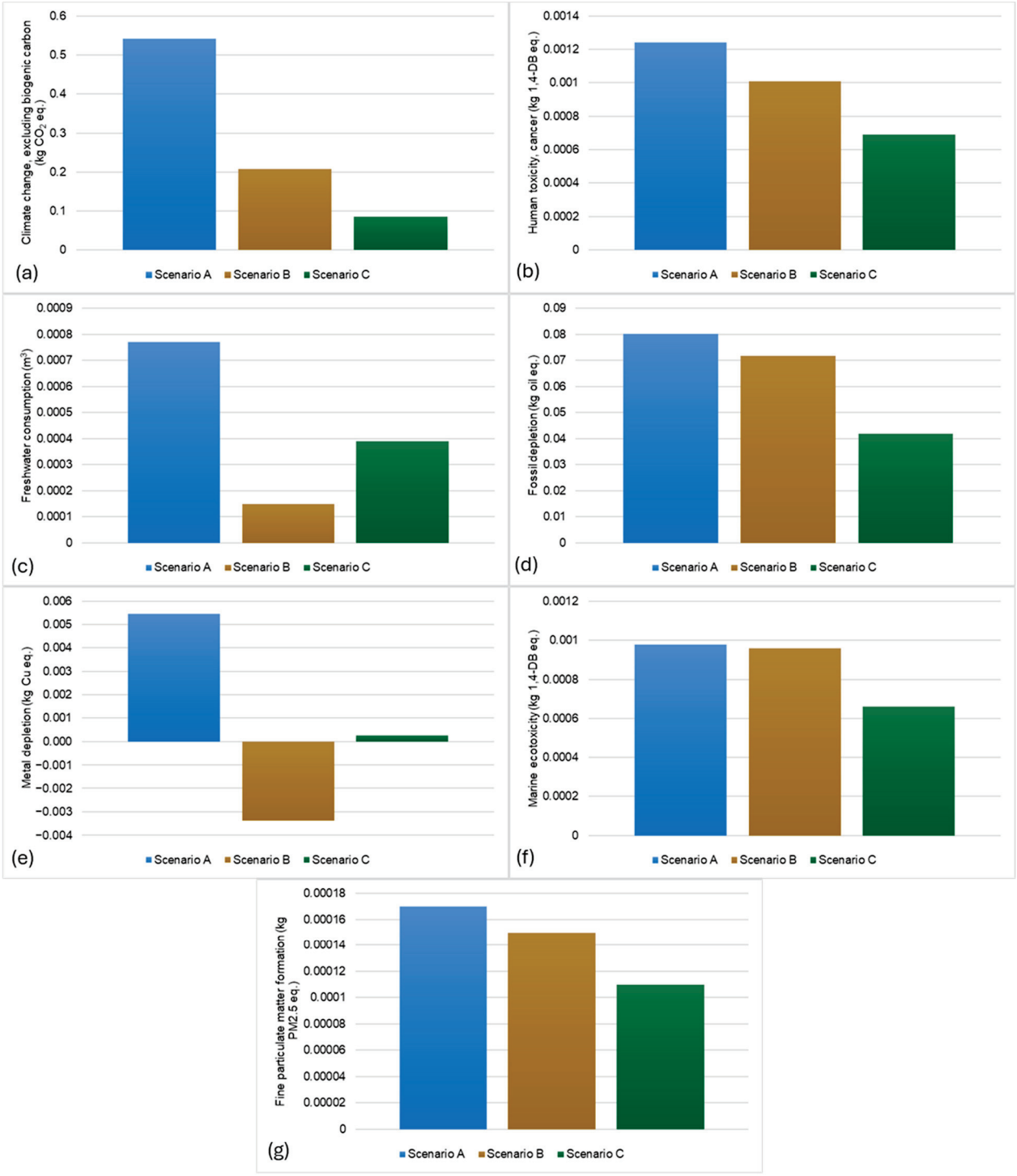

Figure 9. Comparison of the environmental effects of Scenarios A, B and C on (**a**) climate change (kg CO_2 eq.), (**b**) human toxicity, cancer (kg 1,4−DB eq.), (**c**) freshwater consumption (m^3), (**d**) fossil depletion (kg oil eq.), (**e**) metal depletion (kg Cu eq.), (**f**) marine ecotoxicity (kg 1,4−DB eq.), and (**g**) fine particulate matter formation (kg PM2.5 eq.).

The direct comparison of the three studied scenarios highlights the enhancement in the environmental footprint of the meat processing industry in all studied categories, achieved by the utilization of novel methods aiming at wastewater purification and solid waste valorization. The utilization of innovative technologies led to a significant reduction in the amount of produced greenhouse gas, in freshwater consumption, and in metal depletion in both Scenarios B and C. Specifically, the notable decrease in greenhouse gas emissions and freshwater consumption (61.63% and 80.52%, respectively, for Scenario B and 84.22% and 49.35%, respectively, for Scenario C) is a strong indication that sustainability and preservation of the environment and the ecosystems can be achieved via waste utilization and adaptation of innovative and environment-friendly treatment methods. Finally, it must be noted that the valorization of solid wastes and the treatment of wastewater in Scenario B results in a surplus in the balance of electrical energy, due to the cogeneration of biogas, and a deficit in the balance of thermal energy, which can be attributed to the large amounts of thermal energy required in anaerobic digestion. On the other hand, in Scenario C, a surplus of thermal energy is attained due to the burning of pelletized fuels, while the deficit in energy (1.73 kJ) can be considered negligible.

4. Conclusions

Three different scenarios of wastewater and solid waste treatment produced during meat processing were studied in order to evaluate their environmental effects, via LCA analysis. The first scenario consisted of conventional waste treatment techniques, with the solid wastes being disposed of on a landfill and the wastewater transferred to a municipal wastewater treatment plant, while in the latter two, waste treatment technologies aiming at energy production and wastewater purification were used within the industry. In general, the incorporation of waste treatment technologies leads to the generation of substantial quantities of energy and a significant improvement in environmental footprint. Among the studied technologies in Scenario B, anaerobic digestion exhibited the best environmental performance due to the produced electricity and heat during CHP, while the burning of the obtained pelletized fuels in Scenario C resulted in the generation of large amounts of thermal energy. Despite the fact that thermal energy is necessary for the heating of biomass during the anaerobic digestion, this energy is considerably decreased due to the utilization of the thermal energy produced in the CHP, and the observed deficit in electricity in Scenario C is negligible, thus both studied scenarios can be efficiently applied. Furthermore, the purified water from Scenarios B and C is environmentally safe and of high quality, and thus, it can be either reused reducing further the footprint of the industry, or used for other purposes, including aquatic discharge or agricultural purposes. Results derived from the present work suggest that the proposed technologies could be used for moving toward sustainable meat production. Finally, the approach proposed in this work can be broadly extended to numerous other food systems to analyze their environmental footprints, highlight the main areas that require significant improvement, and consequently propose appropriate methodologies for energy production via solid waste valorization and wastewater treatment.

Author Contributions: Conceptualization, T.K., C.B. and V.O.; methodology, C.B.; software, C.B.; validation, T.K., C.B. and V.O.; formal analysis, T.K.; investigation, T.K., C.B. and V.O.; resources, M.K.; data curation, C.B.; writing—original draft preparation, T.K.; writing—review and editing, C.B. and V.O.; visualization, C.B.; supervision, M.K.; project administration, M.K.; funding acquisition, M.K. All authors have read and agreed to the published version of the manuscript.

Funding: This research was funded by the project AccelWater, which has received funding from the European Union's Horizon 2020 research and innovation programme under grant agreement No 958266.

Data Availability Statement: The data presented in this study are available on request from the corresponding author.

Conflicts of Interest: The authors declare no conflicts of interest.

References

1. Baker, P.; Machado, P.; Santos, T.; Sievert, K.; Backholer, K.; Hadjikakou, M.; Russell, C.; Huse, O.; Bell, C.; Scrinis, G.; et al. Ultra-Processed Foods and the Nutrition Transition: Global, Regional and National Trends, Food Systems Transformations and Political Economy Drivers. *Obes. Rev.* **2020**, *21*, e13126. [CrossRef] [PubMed]
2. Djekic, I. Environmental Impact of Meat Industry—Current Status and Future Perspectives. *Procedia Food Sci.* **2015**, *5*, 61–64. [CrossRef]
3. Sayeed, R.; Tiwari, P. Wealth from Meat Industry By-Products and Waste: A Review. In *Sustainable Food Waste Management: Concepts and Innovations*; Thakur, M., Modi, V.K., Khedkar, R., Singh, K., Eds.; Springer: Singapore, 2020; pp. 191–208, ISBN 978-981-15-8967-6.
4. Al-Asheh, S.; Bagheri, M.; Aidan, A. Membrane Bioreactor for Wastewater Treatment: A Review. *Case Stud. Chem. Environ. Eng.* **2021**, *4*, 100109. [CrossRef]
5. Skouteris, G.; Rodriguez-Garcia, G.; Reinecke, S.F.; Hampel, U. The Use of Pure Oxygen for Aeration in Aerobic Wastewater Treatment: A Review of Its Potential and Limitations. *Bioresour. Technol.* **2020**, *312*, 123595. [CrossRef] [PubMed]
6. Wang, J.; Liu, H.; Gao, Y.; Yue, Q.; Gao, B.; Liu, B.; Guo, K.; Xu, X. Pilot-Scale Advanced Treatment of Actual High-Salt Textile Wastewater by a UV/O_3 Pressurization Process: Evaluation of Removal Kinetics and Reverse Osmosis Desalination Process. *Sci. Total Environ.* **2023**, *857*, 159725. [CrossRef] [PubMed]
7. Mazhar, M.A.; Khan, N.A.; Ahmed, S.; Khan, A.H.; Hussain, A.; Rahisuddin; Changani, F.; Yousefi, M.; Ahmadi, S.; Vambol, V. Chlorination Disinfection By-Products in Municipal Drinking Water—A Review. *J. Clean. Prod.* **2020**, *273*, 123159. [CrossRef]
8. Gopal, P.M.; Sivaram, N.M.; Barik, D. Chapter 7—Paper Industry Wastes and Energy Generation from Wastes. In *Energy from Toxic Organic Waste for Heat and Power Generation*; Barik, D., Ed.; Woodhead Publishing: Sawston, UK, 2019; pp. 83–97, ISBN 978-0-08-102528-4.
9. Salman, C.A.; Schwede, S.; Naqvi, M.; Thorin, E.; Yan, J. Synergistic Combination of Pyrolysis, Anaerobic Digestion, and CHP Plants. *Energy Procedia* **2019**, *158*, 1323–1329. [CrossRef]
10. Shi, L.; Simplicio, W.S.; Wu, G.; Hu, Z.; Hu, H.; Zhan, X. Nutrient Recovery from Digestate of Anaerobic Digestion of Livestock Manure: A Review. *Curr. Pollut. Rep.* **2018**, *4*, 74–83. [CrossRef]
11. Unrean, P.; Lai Fui, B.C.; Rianawati, E.; Acda, M. Comparative Techno-Economic Assessment and Environmental Impacts of Rice Husk-to-Fuel Conversion Technologies. *Energy* **2018**, *151*, 581–593. [CrossRef]
12. McCabe, B.K.; Harris, P.; Antille, D.L.; Schmidt, T.; Lee, S.; Hill, A.; Baillie, C. Toward Profitable and Sustainable Bioresource Management in the Australian Red Meat Processing Industry: A Critical Review and Illustrative Case Study. *Crit. Rev. Environ. Sci. Technol.* **2020**, *50*, 2415–2439. [CrossRef]
13. *ISO 14040:2006*; Environmental Management—Life Cycle Assessment—Principles and Framework. International Organization for Standardization: London, UK, 2006.
14. Marathe, K.V.; Chavan, K.R.; Nakhate, P. 8—Life Cycle Assessment (LCA) of PET Bottles. In *Recycling of Polyethylene Terephthalate Bottles*; Thomas, S., Rane, A., Kanny, K., Abitha, V.K., Thomas, M.G., Eds.; William Andrew Publishing: Norwich, UK, 2019; pp. 149–168, ISBN 978-0-12-811361-5.
15. Sandin, G.; Peters, G.M.; Svanstrom, M. LCA Methodology. In *Life Cycle Assessment of Forest Products: Challenges and Solutions*; Springer International Publishing: Cham, Switzerland, 2016; pp. 15–23. ISBN 978-3-319-44027-9.
16. Stramarkou, M.; Boukouvalas, C.; Koskinakis, S.E.; Serifi, O.; Bekiris, V.; Tsamis, C.; Krokida, M. Life Cycle Assessment and Preliminary Cost Evaluation of a Smart Packaging System. *Sustainability* **2022**, *14*, 7080. [CrossRef]
17. Khan, M.U.; Lee, J.T.E.; Bashir, M.A.; Dissanayake, P.D.; Ok, Y.S.; Tong, Y.W.; Shariati, M.A.; Wu, S.; Ahring, B.K. Current Status of Biogas Upgrading for Direct Biomethane Use: A Review. *Renew. Sust. Energ. Rev.* **2021**, *149*, 111343. [CrossRef]
18. Galib, M.; Elbeshbishy, E.; Reid, R.; Hussain, A.; Lee, H.-S. Energy-Positive Food Wastewater Treatment Using an Anaerobic Membrane Bioreactor (AnMBR). *J. Environ. Manag.* **2016**, *182*, 477–485. [CrossRef] [PubMed]
19. Bustillo-Lecompte, C.F.; Mehrvar, M. Slaughterhouse Wastewater Characteristics, Treatment, and Management in the Meat Processing Industry: A Review on Trends and Advances. *J. Environ. Manag.* **2015**, *161*, 287–302. [CrossRef]
20. Irshad, A.; Sureshkumar, S.; Raghunath, B.V.; Rajarajan, G.; Mahesh Kumar, G. Treatment of Waste Water from Meat Industry. In *Integrated Waste Management in India: Status and Future Prospects for Environmental Sustainability*; Prashanthi, M., Sundaram, R., Eds.; Springer International Publishing: Cham, Switzerland, 2016; pp. 251–263. ISBN 978-3-319-27228-3.
21. Abyar, H.; Nowrouzi, M. Highly Efficient Reclamation of Meat-Processing Wastewater by Aerobic Hybrid Membrane Bioreactor-Reverse Osmosis Simulated System: A Comprehensive Economic and Environmental Study. *ACS Sustain. Chem. Eng.* **2020**, *8*, 14207–14216. [CrossRef]
22. Brandao, M.; Heijungs, R.; Cowie, A. On Quantifying Sources of Uncertainty in the Carbon Footprint of Biofuels: Crop/Feedstock, LCA Modelling Approach, Land-Use Change, and GHG Metrics. *Biofuel Res. J.* **2022**, *9*, 1608–1616. [CrossRef]
23. Brown, H.L.; Hamel, B.B.; Hedman, B.A.; Bruce, A. *Hedman Energy Analysis of 108 Industrial Processes*; Fairmont Press: Lilburn, GA, USA, 1987.
24. Huber Technology. Energy-Efficient Mechanical Pre-Treatment. Available online: https://www.huber.de/solutions/centralized-wastewater-treatment/mechanical-pre-treatment.html (accessed on 1 November 2023).
25. Krzeminski, P.; van der Graaf, J.H.J.M.; van Lier, J.B. Specific Energy Consumption of Membrane Bioreactor (MBR) for Sewage Treatment. *Water Sci. Technol.* **2012**, *65*, 380–392. [CrossRef] [PubMed]

26. Schmalwieser, A.W.; Hirschmann, G.; Cabaj, A.; Sommer, R. Method to Determine the Power Efficiency of UV Disinfection Plants and Its Application to Low Pressure Plants for Drinking Water. *Water Supply* **2016**, *17*, 947–957. [CrossRef]
27. Wang, S.; Sahoo, K.; Jena, U.; Dong, H.; Bergman, R.; Runge, T. Life-Cycle Assessment of Treating Slaughterhouse Waste Using Anaerobic Digestion Systems. *J. Clean. Prod.* **2021**, *292*, 126038. [CrossRef]
28. Czekała, W.; Jasiński, T.; Grzelak, M.; Witaszek, K.; Dach, J. Biogas Plant Operation: Digestate as the Valuable Product. *Energies* **2022**, *15*, 8275. [CrossRef]
29. Kamble, S.; Singh, A.; Kazmi, A.; Starkl, M. Environmental and Economic Performance Evaluation of Municipal Wastewater Treatment Plants in India: A Life Cycle Approach. *Water Sci. Technol.* **2019**, *79*, 1102–1112. [CrossRef] [PubMed]
30. Siatou, A.; Manali, A.; Gikas, P. Energy Consumption and Internal Distribution in Activated Sludge Wastewater Treatment Plants of Greece. *Water* **2020**, *12*, 1204. [CrossRef]
31. Dorca-Preda, T.; Mogensen, L.; Kristensen, T.; Knudsen, M.T. Environmental Impact of Danish Pork at Slaughterhouse Gate—A Life Cycle Assessment Following Biological and Technological Changes over a 10-Year Period. *Livest. Sci.* **2021**, *251*, 104622. [CrossRef]
32. Tetteh, H.; Bala, A.; Fullana-i-Palmer, P.; Balcells, M.; Margallo, M.; Aldaco, R.; Puig, R. Carbon Footprint: The Case of Four Chicken Meat Products Sold on the Spanish Market. *Foods* **2022**, *11*, 3712. [CrossRef] [PubMed]
33. Basu, P. Chapter 2—Biomass Characteristics. In *Biomass Gasification and Pyrolysis*; Basu, P., Ed.; Academic Press: Boston, MA, USA, 2010; pp. 27–63. ISBN 978-0-12-374988-8.
34. Raghuvanshi, S.; Bhakar, V.; Sowmya, C.; Sangwan, K.S. Waste Water Treatment Plant Life Cycle Assessment: Treatment Process to Reuse of Water. *Procedia CIRP* **2017**, *61*, 761–766. [CrossRef]
35. Timonen, K.; Sinkko, T.; Luostarinen, S.; Tampio, E.; Joensuu, K. LCA of Anaerobic Digestion: Emission Allocation for Energy and Digestate. *J. Clean. Prod.* **2019**, *235*, 1567–1579. [CrossRef]
36. Mondello, G.; Salomone, R.; Ioppolo, G.; Saija, G.; Sparacia, S.; Lucchetti, M.C. Comparative LCA of Alternative Scenarios for Waste Treatment: The Case of Food Waste Production by the Mass-Retail Sector. *Sustainability* **2017**, *9*, 827. [CrossRef]

energies

MDPI

Article

Possibilities of Utilising Biomass Collected from Road Verges to Produce Biogas and Biodiesel

Robert Czubaszek [1], Agnieszka Wysocka-Czubaszek [1,*], Aneta Sienkiewicz [1], Alicja Piotrowska-Niczyporuk [2], Martin J. Wassen [3] and Andrzej Bajguz [2]

[1] Faculty of Civil Engineering and Environmental Sciences, Bialystok University of Technology, Wiejska 45A Street, 15-351 Bialystok, Poland; r.czubaszek@pb.edu.pl (R.C.); a.sienkiewicz@pb.edu.pl (A.S.)
[2] Department of Biology and Plant Ecology, Faculty of Biology, University of Bialystok, Ciolkowskiego 1J Street, 15-245 Bialystok, Poland; alicjap@uwb.edu.pl (A.P.-N.); abajguz@uwb.edu.pl (A.B.)
[3] Copernicus Institute of Sustainable Development, Faculty of Geosciences, Utrecht University, Princetonlaan 8a, 3584 CB Utrecht, The Netherlands; m.j.wassen@uu.nl
* Correspondence: a.wysocka@pb.edu.pl

Abstract: Grass collected as part of roadside maintenance is conventionally subjected to composting, which has the disadvantage of generating significant CO_2 emissions. Thus, it is crucial to find an alternative method for the utilisation of grass waste. The aim of this study was to determine the specific biogas yield (SBY) from the anaerobic mono-digestion of grass from road verges and to assess the content of Fatty Acid Methyl Esters (FAMEs) in grass in relation to the time of cutting and the preservation method of the studied material. The biochemical biogas potential (BBP) test and the FAMEs content were performed on fresh and ensiled grass collected in spring, summer, and autumn. The highest biogas production was obtained from fresh grass cut in spring (715.05 ± 26.43 NL $kg_{VS}{}^{-1}$), while the minimum SBY was observed for fresh grass cut in summer (540.19 ± 24.32 NL $kg_{VS}{}^{-1}$). The methane (CH_4) content in the biogas ranged between 55.0 ± 2.0% and 60.0 ± 1.0%. The contents of ammonia (NH_3) and hydrogen sulphide (H_2S) in biogas remained below the threshold values for these inhibitors. The highest level of total FAMEs was determined in fresh grass cut in autumn (98.08 ± 19.25 mg $g_{DM}{}^{-1}$), while the lowest level was detected in fresh grass cut in spring (56.37 ± 7.03 mg $g_{DM}{}^{-1}$). C16:0 and C18:0, which are ideal for biofuel production, were present in the largest amount (66.87 ± 15.56 mg $g_{DM}{}^{-1}$) in fresh grass cut in autumn. The ensiling process significantly impacted the content of total FAMEs in spring grass, leading to a reduction in total saturated fatty acids (SFAs) and an increase in total unsaturated fatty acids (USFAs). We conclude that grass biomass collected during the maintenance of road verges is a valuable feedstock for the production of both liquid and gaseous biofuels; however, generating energy from biogas appears to be more efficient than producing biodiesel.

Keywords: biogas; grass; road verges; FAME

1. Introduction

Economic growth, a population that has doubled since 1970, and accelerated material extraction, coupled with an increase in waste, have led to substantial transformations in land use and forest cover. These factors have also induced land degradation, climate change, biodiversity decrease, eutrophication, and pollution of waterways and soils [1]. Cities, which are responsible for generating 80% of the global domestic product [2], are currently undergoing rapid economic growth, resulting in increased rural-to-urban migration [3]. Presently, 55% of the world's population resides in urban areas [4], while in Europe, nearly 75% of the population lives in cities [5]. Many cities grapple with problems such as inadequate infrastructure, traffic congestion [3], energy-inefficient building stock, and air pollution. Nonetheless, in the forthcoming decades, urban areas are expected to be the most profoundly affected by climate change [5]. Conversely, cities are significant contributors

to climate change, emitting 71–76% of global anthropogenic carbon dioxide (CO_2). The realisation of the 11th Sustainable Development Goal (Sustainable Cities and Communities) from Resolution 70/1, adopted by the UN General Assembly on 25 September 2015, titled "Transforming our world: the 2030 Agenda for Sustainable Development", necessitates intelligent urban planning aimed at creating resilient cities [6]. In the European Union (EU), the European Green Deal set a target to transform Europe into a climate-neutral continent by 2050 through a reduction in greenhouse gas (GHG) emissions of at least 55%, compared to 1990 levels. Achieving this goal requires, among other measures, an increase in the share of energy from renewable sources in the EU's energy mix to 40% [7]. The European urban landscape is characterised by small and medium-sized cities, which are expected to play a pivotal role in the development of a sustainable and climate-neutral Europe [5].

Urban green areas, as defined by the Nature Conservation Act of April 2004 [8], encompass areas with technical infrastructure and buildings functionally linked to them, covered with vegetation and serving public functions, particularly including parks; promenades; boulevards; botanical, zoological, and historical gardens; and cemeteries. Urban green areas also include greenery along roads in built-up areas, squares, historic fortifications, buildings, landfills, airports, railway stations, and industrial facilities. Urban green areas are situated within the administrative borders of cities, providing aesthetic, recreational, and health functions [9]. Green areas in urban landscapes enhance air quality, mitigate extreme weather events, and regulate the hydrological cycle [10,11]. Additionally, green spaces in cities effectively alleviate the urban heat island effect [12,13] and play a crucial role in city resilience [14]. Consequently, urban systems with extensive green infrastructure exhibit greater resilience to crises and are more human-friendly [15]. The maintenance of urban green areas is indispensable for their diverse roles in cities, encompassing aesthetic aspects, environmental benefits, stormwater management, urban heat island mitigation, and community cohesion. Maintenance tasks in urban green spaces include trimming, irrigation, fertilisation, and pesticide application [16]. Mowing grass on road verges is conducted to maintain visibility and safety. The cut grass is either left to decay or collected and utilised. However, the maintenance of green areas involves significant labour and machine input, consuming energy resources and resulting in waste generation. Trimming, fertilising, and waste transport consume fossil fuels and emit GHGs into the atmosphere [17]. Despite recent reductions in maintenance workload through improved working plans, decreased trimming frequency, the introduction of wildflowers and meadows, and the self-maintenance of green spaces, large areas, such as sports fields and road verges, are still frequently trimmed. In addition, the policy of urban greenery extension results in increase in both the workload associated with its maintenance and with the amount of biomass produced, which needs to be utilised in a sustainable way [17].

The biobased and circular economy, considered a viable approach for sustainable development, directs societies toward the sequential utilisation of resources, with an emphasis on biomass and bio-waste. The diminishing availability of resources, coupled with an escalating demand for energy and food, underscores the need to optimize the efficient use of biomass and bio-waste. Grass-trimming biomass is commonly subjected to composting, an aerobic process that transforms lignocellulosic waste into a value-added product, namely compost. However, this process is associated with substantial GHG emissions. Furthermore, the utilisation of immature compost may result in water pollution, odour emissions, and adverse effects on plant germination and development [18]. As an alternative, other methods of bio-waste utilisation, such as biogas production, are being explored. The utilisation of green waste for energy generation has the potential to mitigate the elevated fuel consumption and GHG emissions associated with maintaining expanded green spaces within urban areas.

The anaerobic digestion (AD) of grass offers benefits, including waste reduction, decreased GHG emissions, and the generation of renewable energy and valuable fertilizer. However, the biogas potential of grass is relatively low, particularly when compared to biogas production from maize [19]. The specific methane yield (SMY) has been extensively

studied across various wild and cultivated grass species [20–26]. Additionally, co-digestion of grass and other substrates as a strategy to enhance biogas production has been investigated [27,28]. The harvesting date is a critical factor affecting grass SMY, as the lignification process intensifies with advancing maturity, limiting material digestibility [29]. Dragoni et al. [24] noted higher SMY from AD of leaves compared to stems due to their elevated protein content [20].

Another possibility for utilising waste generated during road verges maintenance involves the production of biodiesel. Biodiesel, primarily comprising Fatty Acid Methyl Esters (FAMEs), can be derived from various waste biomasses, including olive pomace oil [30], cooking palm oil [31], beef tallow [32], fish fat [33], chicken fat [34], citrus wax [35], and sewage sludge [36]. Additionally, biodiesel production from spent coffee grounds [37], cherry stone waste [38], and herbal waste [39] represents another feasible approach to resource utilisation. This not only aids in reducing crude oil consumption but also contributes to mitigating GHG emissions and air pollution.

The aim of this study was to determine the potential to obtain material from grass from road verges for the production of liquid biofuels (biodiesel) and to determine the specific biogas yield (SBY) from anaerobic mono-digestion of the studied grass in relation to the time of cutting and the preservation method of the studied material. Since a continuous supply of feedstock is essential for biofuel production, the study was conducted on both fresh and ensiled grass.

2. Materials and Methods

2.1. Substrates and Inoculum

The biogas potential and FAME content were assessed using grass samples harvested from the city of Białystok (53°07′ N, 23°09′ E, 136 m a.s.l.) in the northeastern region of Poland. Białystok, serves as the capital city of the Podlaskie voivodeship, covering an area of 102 km^2, and has a population of 292,000 citizens [40]. The climatic conditions are characterised by an average annual temperature of 7.4 °C and an average annual precipitation of 590 mm, predominantly occurring from May to August [41]. The species composition of the grassed verges was predominantly composed of perennial ryegrass (*Lolium perenne* L.), accompanied by Kentucky bluegrass (*Poa pratensis* L.) and red fescue (*Festuca rubra* L.). Plant material was collected on three occasions in the year 2019: in spring (25 April), summer (31 July), and autumn (7 October). During each collection, the grass was acquired from piles of mown material along the streets, as part of the green area maintenance conducted by an external company employed by the City Hall of Białystok. Following collection, the plant material was promptly transported to the laboratory and homogenised. The moisture content of the fresh material was determined by subjecting it to drying at 105 ± 2 °C until a constant weight was achieved. The material designated for ensiling was allowed to air-dry at room temperature for 24 h. Subsequently, it was cut into lengths of 2–4 cm and ensiled without the addition of any additives for 5–6 weeks. After this period, the moisture content was determined. The chemical composition of both fresh grass and silage is presented in Table 1.

The inoculum for all three biochemical biogas potential (BBP) tests comprised digestate obtained from a mesophilic agricultural biogas plant which was supplied with maize silage supplemented with 10–20% food and agricultural wastes. Prior to the BBP test, the digestate was degassed at a temperature of 38 °C. The chemical properties of the inocula used in all three experiments are presented in Table 2.

Table 1. Chemical composition (mean ± SD, n = 3) of fresh grass and grass silage from three cutting times.

Parameter	Spring		Summer		Autumn	
	Fresh Grass (FG-Sp)	Grass Silage (GS-Sp)	Fresh Grass (FG-Su)	Grass Silage (GS-Su)	Fresh Grass (FG-Au)	Grass Silage (GS-Au)
Total solids (TS), %	38.00 ± 1.35	37.37 ± 0.58	25.83 ± 0.97	29.11 ± 0.37	29.34 ± 0.97	30.33 ± 0.30
Volatile solids (VS), %TS	68.22 ± 7.98	67.93 ± 7.58	84.70 ± 1.32	83.34 ± 2.08	88.83 ± 0.10	87.69 ± 0.08
pH	6.17 ± 0.01	5.44 ± 0.03	5.96 ± 0.04	4.54 ± 0.03	5.97 ± 0.04	4.15 ± 0.02
Total Kieldahl nitrogen (TKN), g kg_{DM}^{-1}	20.76 ± 0.23	22.12 ± 0.63	25.89 ± 0.84	28.39 ± 0.67	27.67 ± 1.12	25.87 ± 0.34
Total phosphorus (TP), g kg_{DM}^{-1}	1.99 ± 0.19	2.32 ± 0.06	3.42 ± 0.26	3.72 ± 0.04	3.06 ± 0.05	3.55 ± 0.12
Potassium (K), g kg_{DM}^{-1}	10.96 ± 1.43	12.97 ± 1.12	23.48 ± 1.36	24.94 ± 0.35	15.00 ± 0.08	18.72 ± 0.46
Sodium (Na), g kg_{DM}^{-1}	3.12 ± 0.48	4.58 ± 0.41	0.85 ± 0.44	0.85 ± 0.10	n.d.	n.d.
Total organic carbon (TOC), g kg_{DM}^{-1}	373.80 ± 18.29	323.49 ± 63.45	371.63 ± 22.42	368.04 ± 8.66	381.87 ± 3.17	421.68 ± 14.38

n.d.—not detected.

Table 2. Chemical composition of inocula (mean ± SD; n = 3) used in three biochemical biogas potential (BBP) tests.

Parameter	Spring	Summer	Autumn
TS, %	4.58 ± 0.00	5.19 ± 0.02	4.76 ± 0.07
VS, %TS	77.41 ± 0.22	78.57 ± 0.21	76.11 ± 0.21
pH	8.11 ± 0.02	7.84 ± 0.05	8.19 ± 0.02
TKN, g kg_{DM}^{-1}	90.83 ± 4.63	90.53 ± 3.18	69.41 ± 1.05
TP, g kg_{DM}^{-1}	8.41 ± 0.14	8.06 ± 0.21	8.81 ± 0.35
K, g kg_{DM}^{-1}	57.12 ± 1.88	49.81 ± 2.06	59.69 ± 1.90
Na, g kg_{DM}^{-1}	7.40 ± 0.29	5.69 ± 0.33	7.20 ± 0.28
TOC, g kg_{DM}^{-1}	433.53 ± 13.49	389.23 ± 6.00	421.53 ± 13.25

2.2. Biochemical Biogas Potential Tests

The BBP test was conducted using wet technology in OxiTop® reactors (WTW, Weilheim, Germany) with a volume of 1 L and a working volume of approximately 300 mL. The reactors were incubated in a thermostatic incubator at 38 ± 1 °C. The substrates and inoculum were added to the reactors in a ratio of 2:1 $VS_{inoculum}$ to $VS_{substrate}$. To maintain anaerobic conditions, the reactors were subjected to a 2 min flush with nitrogen. The BBP tests were performed in triplicate, along with three control reactors filled solely with inoculum and water. Biogas production was monitored at intervals of 240 min based on pressure changes within the reactor, facilitated by the OxiTop®measuring head. The composition of the biogas was analysed using the portable biogas analyzer DP-28BIO (Nanosens, Wysogotowo, Poland) from samples taken with 20 mL gas-tight glass syringes. Biogas composition assessments were conducted daily initially, transitioning to twice a week after the experiment had run for 10 days.

2.3. Transesterification Procedure

Grass samples (1 g) underwent extraction with hexane in the presence of a methanol-potassium hydroxide (KOH) mixture acting as a catalyst with the synthesis process involving the addition of hexane. An analysis using gas chromatography–mass spectrometry in the selected ion monitoring mode (GC-MS/SIM) quantified the presence of up to 31 FAMEs in the grass samples (Table 3). A comprehensive description of the transesterification procedure, i.e., the optimal extraction conditions, is presented in the study by Sienkiewicz et al. [39].

Table 3. Fatty Acid Methyl Esters standards used in the GC-MS analysis of grass samples.

Type of FAME	Systematic Name	The Common Name of FAME	Abbreviation
MUFA	Myristoleic acid methyl ester	Myristoleic acid	C14:1
	cis-10-Pentadecanoic acid methyl ester	Pentadecanoic acid	C15:1
	9-Hexadecenoic acid methyl ester	Palmitoleic acid	C16:1
	cis-10-Heptadecenoic acid methyl ester	Heptadecenoic acid	C17:1
	trans-9-Octadecenoic acid methyl ester (Z)	Elaidic acid	C18:1n9t
	9-Octadecenoic acid methyl ester (E)	Oleic acid	C18:1n9c
	cis-11-Eicosenoic acid methyl ester	Gondoic acid	C20:1
	13-Docosenoic acid methyl ester (Z)	Erucic acid	C22:1n9
	15-Tetracosenoic acid methyl ester (Z)	Nervonic acid	C24:1n9
PUFA	9,12-Octadecadienoic acid methyl ester (E,E)	Linolelaidic acid	C18:2n6t
	9,12-Octadecadienoic acid methyl ester (Z,Z)	Linoleic acid	C18:2n6c
	all-cis-6,9,12-Octadecatrienoic acid	γ-Linolenic acid	C18:3n6
	9,12,15-Octadecatrienoic acid methyl ester (Z,Z,Z)	Linolenic acid	C18:3n3
	cis-11,14-Eicosadienoic acid methyl ester	Eicosadienoic acid	C20:2
	cis-11,14,17-Eicosatrienoic acid methyl ester	Eicosatrienoic acid	C20:3n3
	cis-8,11,14-Eicosatrienoic acid methyl ester	Dihomo-γ-linolenic acid	C20:3n6
	5,8,11,14-Eicosatetraenoic acid methyl ester (all-Z)	Arachidonic acid	C20:4n6
	cis-5,8,11,14,17-Eicosapentaenoic acid methyl ester	Eicosapentaenoic acid	C20:5n3
	cis-13,16-Docasadienoic acid methyl ester	Docosadienoic acid	C22:2n6
	4,7,10,13,16,19-Docosahexaenoic acid methyl ester (all-Z)	Cervonic acid	C22:6n3
SFA	Butyric acid methyl ester	Butyric acid	C4:0
	Hexanoic acid methyl ester	Caproic acid	C6:0
	Octanoic acid methyl ester	Caprylic acid	C8:0
	Decanoic acid methyl ester	Capric acid	C10:0
	Undecanoic acid methyl ester	Undecylic acid	C11:0
	Dodecanoic acid methyl ester	Lauric acid	C12:0
	Tridecanoic acid methyl ester	Tridecylic acid	C13:0
	Tetradecanoic acid methyl ester	Myristic acid	C14:0
	Pentadecanoic acid methyl ester	Pentadecylic acid	C15:0
	Hexadecanoic acid methyl ester	Palmitic acid	C16:0
	Heptadecanoic acid methyl ester	Margaric acid	C17:0
	Octadecanoic acid methyl ester	Stearic acid	C18:0
	Eicosanoic acid methyl ester	Arachidic acid	C20:0
	Heneicosanoic acid methyl ester	Heneicosylic acid	C21:0
	Docosanoic acid methyl ester	Behenic acid	C22:0
	Tricosanoic acid methyl ester	Tricosylic acid	C23:0
	Tetracosanoic acid methyl ester	Lignoceric acid	C24:0

MUFA—monounsaturated fatty acid, PUFA—polyunsaturated fatty acid, SFA—saturated fatty acid.

2.4. Calculations and Statistical Analyses

The BBP test was conducted until the daily biogas production accounted for less than 1% of the total cumulative biogas volume observed over three consecutive days. SBY was calculated in units of NL $kg_{VS}{}^{-1}$ (NL = normal litre, i.e., gas volume corrected to 0 °C and 1.013 bar). The kinetics of biogas production were determined using the modified Gompertz model [42]:

$$G(t) = G_0 \times exp\left\{-exp\left[\frac{R_{max} \times e}{G_0}(\lambda - t) + 1\right]\right\} \quad (1)$$

where

$G(t)$—cumulative biogas production at a specific time t (mL);
G_0—biogas production potential (mL);
R_{max}—maximum daily biogas production rate (mL day^{-1});
λ—duration of lag phase (minimum time to produce biogas) (days);

t—cumulative time taken to achieve biogas production (days);
e—mathematical constant (2.71828).

In addition, based on the plotted curves, the time (days) when 50% (T50) and 95% (T95) of the possible biogas production were reached was determined.

For the calculations of the amount of energy contained in liquid biofuel obtained from grass, the heating value of methyl esters of fatty acids was adopted at 37 MJ kg^{-1} [43]. For the calculations of the avoided carbon dioxide emissions by replacing coal with biogas, emission values of 93.54 kg CO_2 GJ^{-1} [44] and 685 kg CO_2 MWh^{-1} [45] were adopted, respectively, for thermal and electric energy production. In the case of using biodiesel as a substitute for fossil fuel, the diesel oil emission of 74.1 kg CO_2 GJ^{-1} [44] was adopted.

Significant differences in cumulative biogas production, as well as methane (CH_4), hydrogen sulphide (H_2S), and ammonia (NH_3) concentrations in biogas from fresh and ensiled grasses cut in spring, summer, and autumn were assessed with a two-way analysis of variance (ANOVA), using the method of grass preservation and the cutting time as fixed factors. Significant differences in FAMEs between the cutting time of fresh grass and ensiled grass were assessed with a one-way analysis of variance. Differences between means were determined using Tukey's Honest Significant Difference (HSD) test. The homogeneity of variance and normality were checked prior to ANOVA using the Levene and Shapiro–Wilk tests, respectively. Principal Component Analysis (PCA) was performed to build the relationship model between variables. The first seventeen factors were preserved in a biplot for further analysis. The final biplot was created using the two main components (PC1 and PC2), which together explain 61.8% of the total variance. The level of accepted statistical significance was set at $p < 0.05$. All statistical analyses of the data were performed using STATISTICA 13.3 software (TIBCO Software Inc., Palo Alto, CA, USA).

3. Results

3.1. Biogas Production

The cutting time significantly influenced cumulative biogas production ($p < 0.05$). The highest biogas production was obtained from spring-cut grass, yielding 715.05 ± 26.43 NL kg_{VS}^{-1} for fresh grass and 605.44 ± 6.19 NL kg_{VS}^{-1} for grass silage. Conversely, the lowest biogas production was observed with fresh grass cut in summer (540.19 ± 24.32 NL kg_{VS}^{-1}) and grass silage from autumn (547.36 ± 1.20 NL kg_{VS}^{-1}). The ensiling process showed no effect on cumulative biogas production, except in the case of spring cutting, where biogas production from fresh grass exceeded that from ensiled grass (Figure 1).

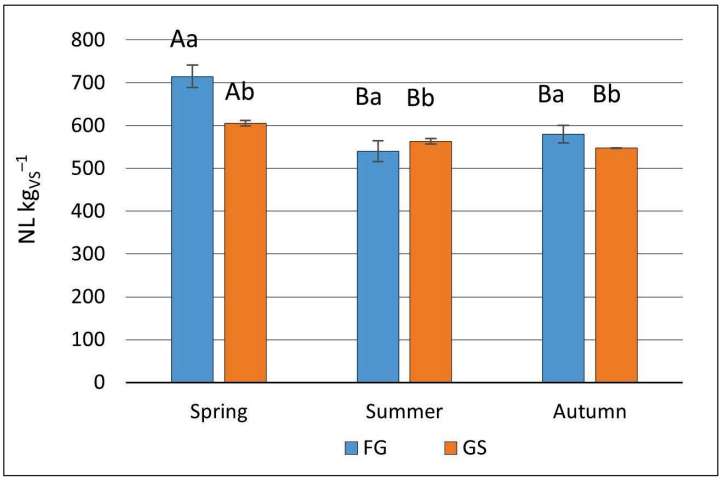

Figure 1. Cumulative biogas production from fresh and ensiled grass cut in spring, summer, and autumn. FG—fresh grass; GS—grass silage. Standard deviations are shown as the vertical bars.

Uppercase letters—significant difference among cutting time; lowercase letters—significant differences between preservation method.

The CH_4 content within the generated biogas, measured at the end of the experiment, displayed the highest values for spring-cut grass, whereas the lowest values were observed for autumn-cut grass (Table 4).

Table 4. Methane (CH_4) concentration (mean ± SD; n = 3) in the produced biogas depending on the method of grass preservation and the cutting time.

Season	Fresh Grass	Grass Silage
	%	
Spring	59.7 ± 0.6 Aa	60.0 ± 1.0 Aa
Summer	58.7 ± 1.2 Aa	58.0 ± 1.0 Aa
Autumn	55.7 ± 1.5 Ba	55.0 ± 2.0 Ba

Uppercase letters—significant difference among cutting time; lowercase letters—significant differences between preservation methods.

The preservation method did not exert any influence on the CH_4 concentration in the biogas. Nevertheless, the preservation method did impact the daily biogas production depending on the cutting time. In spring, the daily biogas production from FG-Sp exhibited higher values in the first 7 days, but subsequently experienced a significant decline by day 9. Concurrently, the daily biogas production from GS-Sp reached its peak on that day. The daily rates from both fresh and ensiled grasses became nearly identical on day 10, gradually decreasing to approximately 5 NL $kg_{VS}{}^{-1}$. In summer, daily biogas production from FG-Su increased rapidly in the first two days, followed by a decline on days 3 and 4, falling notably below the daily rate of biogas production from GS-Su. Subsequently, daily biogas production from FG-Su increased to the same value as daily biogas production from GS-Su and remained similar until the end of the experiment. In autumn, daily biogas production from both fresh and ensiled grasses displayed remarkable similarity to that observed at the beginning of the experiment. A swift increase occurred in the first 2 days, followed by a decrease from day 6 to day 8. After a brief period of heightened production, the daily rate declined and stabilised until the end of the experiment.

Notably, FG-Sp and FG-Au exhibited distinct behaviour compared to FG-Su. Daily biogas production from all three cutting times experienced rapid increases in the first 2 days. For FG-Sp and FG-Au, production remained elevated for the following 6 days. Conversely, daily biogas production from FG-Su, following an initial increase in the first 2 days, significantly decreased on days 3 and 4, dropping below the production from FG-Sp and FG-Au. Subsequently, the daily biogas production increased again, and the values for grasses from all three cutting times became similar. The daily biogas production from ensiled grass exhibited a consistent trend, irrespective of the cutting time (Figure 2). Regardless of the season and grass preservation method, significant biogas production persisted for approximately 14 days, displaying a dynamic course during this period.

Despite discernible fluctuations in the daily patterns of biogas production, the kinetics of biogas generation exhibited consistency across all cutting times and preservation methods. Regardless of the preservation technique employed and the timing of material cutting, the timeframe necessary for grass to achieve 50% of its potential biogas production (T50) varied between 5 and 6 days. The period required for grass to attain 95% of its potential biogas production ranged from 14 to 17 days (Figure 3).

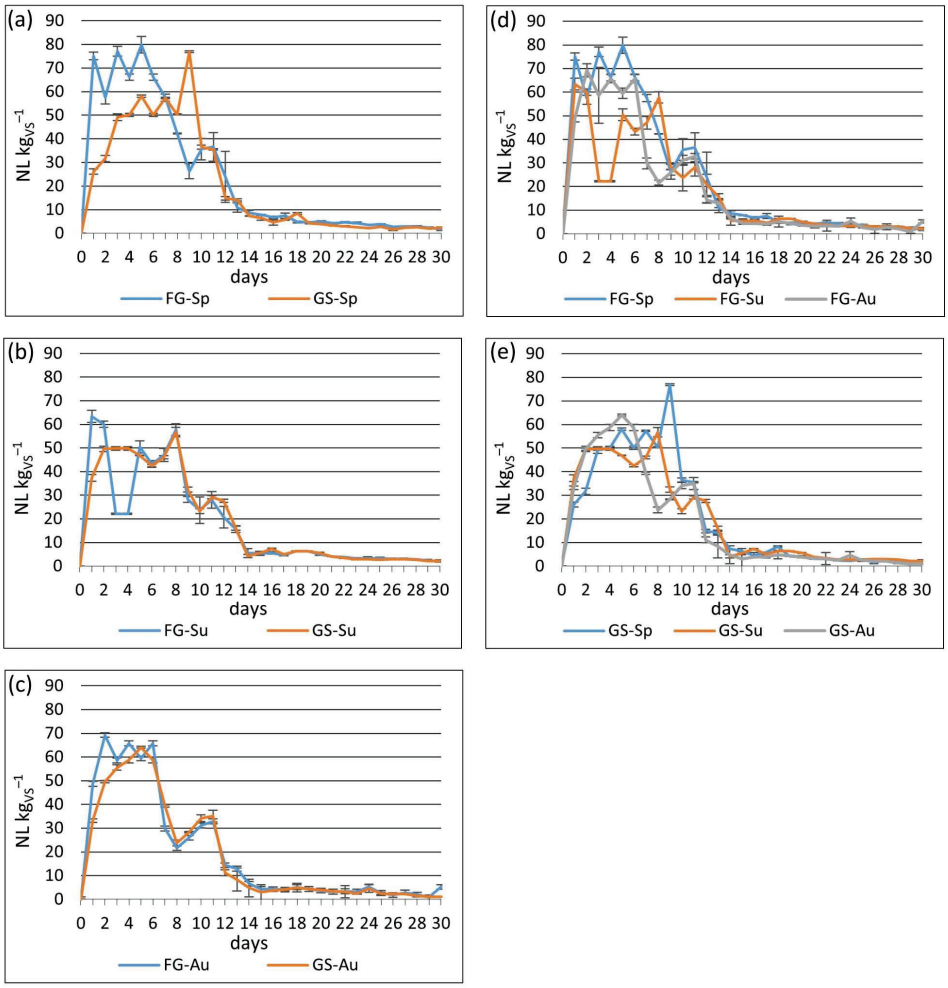

Figure 2. Daily biogas production depending on cutting time: (**a**)—spring, (**b**)—summer, (**c**)—autumn and grass preservation method: (**d**)—fresh grass, (**e**)—grass silage. Standard deviations are shown as vertical bars. FG-Sp—spring fresh grass, GS-Sp—spring grass silage, FG-Su—summer fresh grass, GS-Su—summer grass silage, FG-Au—autumn fresh grass, GS-Au—autumn grass silage.

3.2. Hydrogen Sulphide and Ammonia Concentration in Biogas

The inhibition of the AD process represents a significant impediment in the context of biogas production, wherein inhibitors may be introduced along with the feedstock or generated during distinct stages of process. Quantifying inhibitors, particularly NH_3 and H_2S levels in biogas, is crucial for influencing the conditions of biogas production. In this study, the NH_3 and H_2S contents remained at relatively low levels. Regardless of the cutting time, the H_2S content in the biogas exhibited higher values at the beginning of the experiment, subsequently demonstrating a significant decrease ($p < 0.05$) by the end of the experiment.

The initial H_2S content in biogas derived from spring-cut grass remained consistent at approximately 200 ppm, irrespective of the preservation method, and decreased to values around 100 ppm by the end of the experiment (Figure 4). Significantly higher values ($p < 0.05$) were observed in biogas from summer-cut grass, with an initial H_2S content of 749 ppm in biogas from FG-Su and 666 ppm in biogas from GS-Su. The final values for both fresh and ensiled grass were approximately 200 ppm. Although the highest initial H_2S content was observed in biogas from autumn-cut grass (exceeding 800 ppm), it was not significantly different from that of summer-cut grass. Notably, the final values aligned with those obtained from biogas derived from summer-cut grass. The ensiling process did not exert any significant effect on the H_2S concentration for any cutting time.

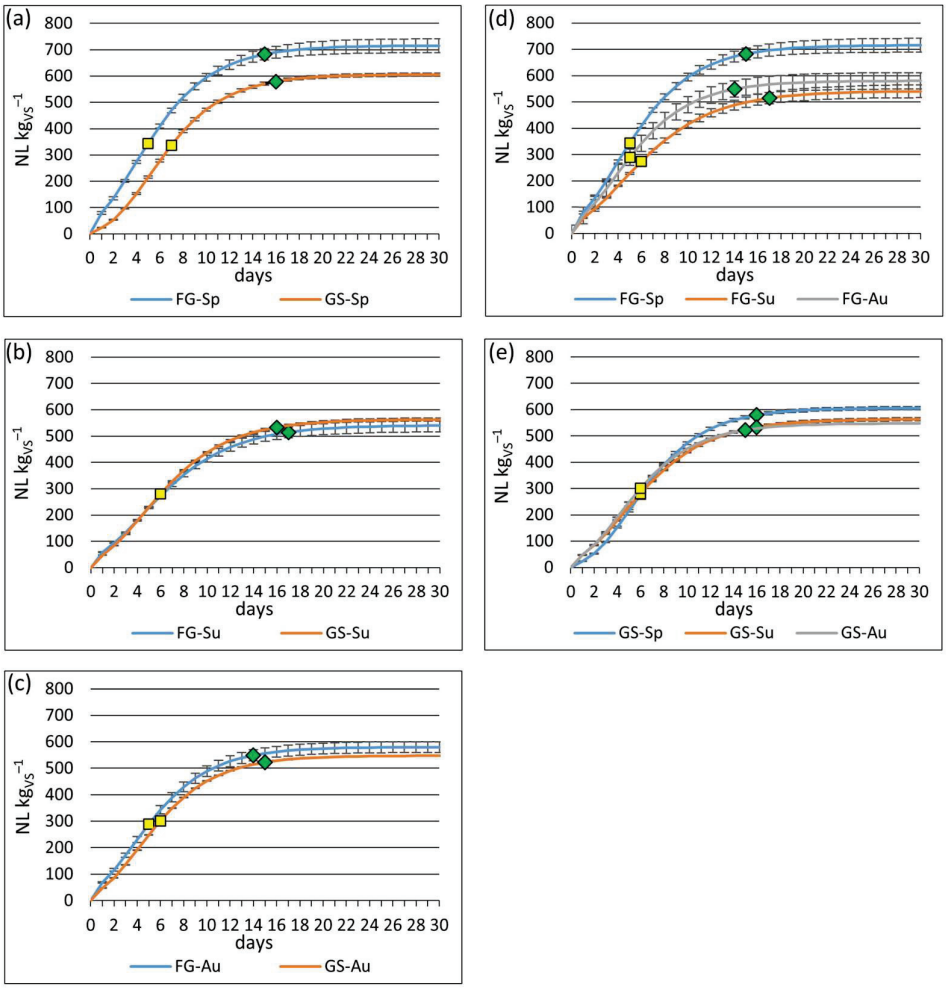

Figure 3. Cumulative biogas production depending on cutting time: (**a**)—spring, (**b**)—summer, (**c**)—autumn and grass preservation method: (**d**)—fresh grass, (**e**)—grass silage. Standard deviations are shown as vertical bars. The yellow squares and green squares represent T50 and T95, respectively. FG-Sp—spring fresh grass, GS-Sp—spring grass silage, FG-Su—summer fresh grass, GS-Su—summer grass silage, FG-Au—autumn fresh grass, GS-Au—autumn grass silage.

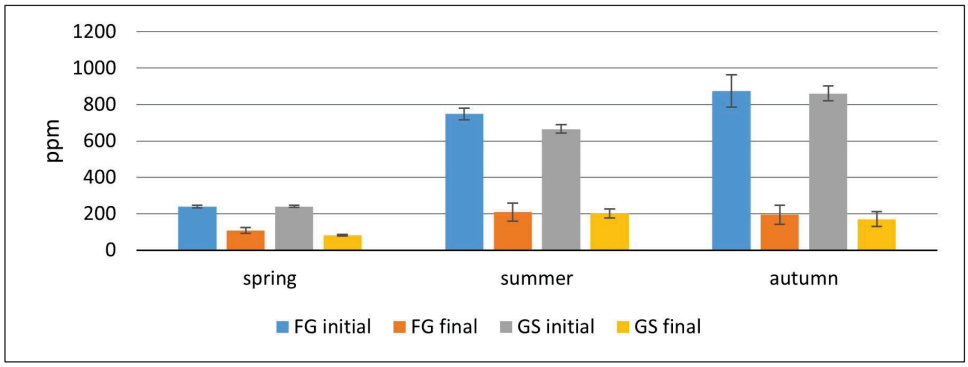

Figure 4. The initial and final concentration of the hydrogen sulphide (H_2S) in biogas produced from fresh and ensiled grass harvested in spring, summer, and autumn. Standard deviations are shown as vertical bars. FG—fresh grass, GS—grass silage.

Biogas derived from spring-cut grass exhibited the lowest initial and final NH_3 concentrations, irrespective of the preservation method. Conversely, significantly higher values were observed in biogas from summer-cut grass ($p < 0.05$), with the highest NH_3 concentra-

tion found in biogas obtained from autumn-cut grass. In the case of biogas from FG-Sp and FG-Su, the disparities between initial and final NH_3 concentrations were not statistically significant. However, for grass silage, these differences were more pronounced. Biogas generated from autumn-cut grass displayed a notably elevated initial NH_3 concentration, which substantially decreased to approximately 100 ppm in the final stage of the experiment (Figure 5). The ensiling process did not affect the NH_3 concentration at any cutting time.

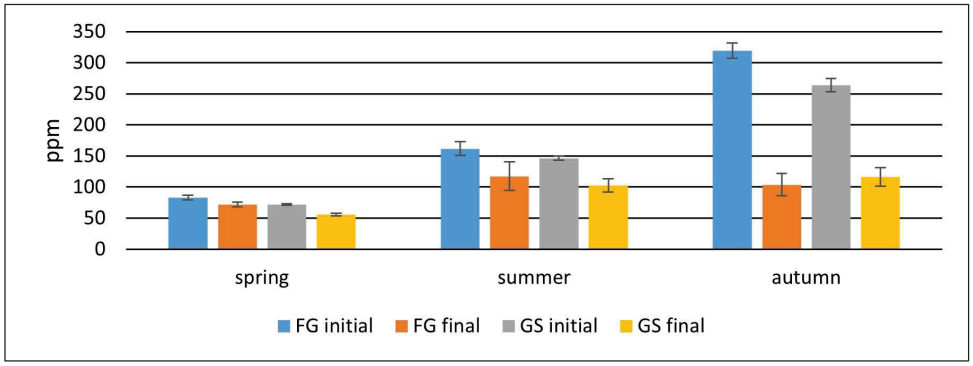

Figure 5. The initial and final concentration of the ammonia (NH_3) in biogas produced from fresh and ensiled grass harvested in spring, summer, and autumn. Standard deviations are shown as vertical bars. FG—fresh grass, GS—grass silage.

3.3. Identity and Composition of the Fatty Acid Methyl Esters

In both fresh and ensiled grass, up to 31 FAMEs were detected (Tables 5–8). The total number of distinct fatty acid types ranged from 29 to 31. FG-Sp and FG-Su exhibited 29 fatty acid types, while GS-Au presented 31 types. In all the analysed grasses, irrespective of the preservation method and cutting time, nine monounsaturated fatty acids (MUFAs) were detected (Table 5). In FG-Sp and FG-Su, seven polyunsaturated fatty acids (PUFAs) (C18:2n6c, C18:3n6, C18:3n3, C20:3n6, C20:4n6, C22:2n6, and C22:6n3) were identified, whereas all eight PUFAs were detected in the remaining studied materials (Table 6). In fresh and ensiled grass cut during spring and summer, 13 saturated fatty acids (SFAs) were detected, while in GS-Au, 14 SFAs were found (Table 7).

Table 5. The content of monounsaturated fatty acids (mean ± SD, n = 3) in fresh grass and ensiled grass cut in spring, summer, and autumn.

MUFA	Spring		Summer		Autumn	
	Fresh Grass	Grass Silage	Fresh Grass	Grass Silage	Fresh Grass	Grass Silage
			$\mu g\ g_{DM}^{-1}$			
C14:1	41.82 ± 3.45 a	53.80 ± 4.52 a	44.19 ± 4.18 ab	40.67 ± 1.68 b	50.47 ± 0.80 b	38.57 ± 4.29 b
C15:1	2029.49 ± 163.04 a	1764.68 ± 144.67 a	3045.15 ± 275.50 b	2299.93 ± 158.04 b	3220.13 ± 208.92 b	2183.10 ± 108.36 b
C16:1	49.70 ± 1.39 a	30.42 ± 0.57 a	84.55 ± 1.49 b	34.94 ± 4.22 a	64.25 ± 0.14 c	58.53 ± 6.70 b
C17:1	31.42 ± 5.62 a	17.15 ± 1.98 a	26.88 ± 3.12 a	14.35 ± 0.76 a	58.71 ± 10.77 b	10.87 ± 0.12 b
C18:1n9t	1057.18 ± 17.57 a	1658.08 ± 43.13 a	2440.22 ± 157.08 b	1731.72 ± 210.57 a	2218.06 ± 414.44 b	1724.16 ± 29.90 a
C18:1n9c	1654.50 ± 27.35 a	2579.70 ± 63.36 a	3792.84 ± 204.24 b	2690.75 ± 323.81 a	3566.10 ± 780.84 b	2636.25 ± 30.26 a
C20:1	2565.06 ± 39.92 a	3676.00 ± 181.32 a	5030.33 ± 703.53 b	5479.67 ± 42.68 b	4280.08 ± 369.89 b	3958.95 ± 300.64 a
C22:1n9	52.43 ± 3.62 a	71.55 ± 6.76 a	18.52 ± 3.55 a	510.70 ± 4.03 b	661.11 ± 27.51 b	328.91 ± 22.32 c
C24:1n9	73.41 ± 3.44 a	78.83 ± 5.58 a	35.92 ± 7.35 b	36.88 ± 2.86 b	24.69 ± 1.25 b	34.15 ± 1.01 b

Lowercase letters indicate statistical differences at $p < 0.05$ between fresh grasses from three cuttings and between grass silages from three cuttings.

Table 6. The content of polyunsaturated fatty acids (mean ± SD, n = 3) in fresh grass and ensiled grass cut in spring, summer and autumn.

PUFA	Spring		Summer		Autumn	
	Fresh Grass	Grass Silage	Fresh Grass	Grass Silage	Fresh Grass	Grass Silage
	μg g_{DM}^{-1}					
C18:2n6c	1604.74 ± 215.64 a	1519.43 ± 22.02 a	3783.55 ± 336.06 b	2916.66 ± 172.87 b	4252.92 ± 596.37 b	3915.85 ± 121.42 c
C18:3n6	2069.96 ± 195.12 a	2801.27 ± 498.34 ab	3583.26 ± 571.10 b	3456.37 ± 307.91 a	3340.06 ± 481.85 b	2155.99 ± 93.15 b
C18:3n3	143.42 ± 19.80 a	206.38 ± 34.91 ab	263.44 ± 35.08 b	246.26 ± 20.88 a	231.67 ± 39.95 b	149.52 ± 6.79 b
C20:2	n.d.	0.63 ± 0.05 a	n.d.	1.41 ± 0.02 a	8.76 ± 1.11 b	12.98 ± 0.74 b
C20:3n6	3.84 ± 0.27 a	3.95 ± 0.17 a	3.93 ± 0.40 a	3.41 ± 0.07 a	4.75 ± 0.44 b	7.57 ± 1.44 b
C20:4n6	20.95 ± 1.25 a	24.98 ± 5.00 a	38.31 ± 1.77 b	31.51 ± 1.35 a	39.94 ± 3.55 b	40.75 ± 2.96 b
C22:2n6	12.04 ± 0.15 a	19.44 ± 1.06 a	53.73 ± 3.90 b	190.18 ± 30.42 b	37.27 ± 1.73 c	198.09 ± 4.22 b
C22:6n3	10.36 ± 1.78 a	9.25 ± 1.72 a	9.24 ± 0.34 a	7.47 ± 0.25 a	9.70 ± 0.74 a	9.21 ± 0.41 a

Lowercase letters indicate statistical differences at $p < 0.05$ between fresh grasses from three cuttings and between grass silages from three cuttings; n.d.—not detected.

Table 7. The content of saturated fatty acid (mean ± SD, n = 3) in fresh grass and ensiled grass cut in spring, summer, and autumn.

SFA	Spring		Summer		Autumn	
	Fresh Grass	Grass Silage	Fresh Grass	Grass Silage	Fresh Grass	Grass Silage
	μg g_{DM}^{-1}					
C10:0	n.d.	n.d.	n.d.	n.d.	n.d.	0.32 ± 0.01 b
C11:0	31.34 ± 6.38 a	43.31 ± 2.35 a	34.77 ± 0.94 a	33.35 ± 0.46 b	51.33 ± 7.43 b	31.89 ± 1.30 b
C12:0	62.68 ± 12.75 a	86.62 ± 4.70 a	69.54 ± 1.89 a	66.70 ± 0.91 b	102.67 ± 14.85 b	63.78 ± 2.60 b
C13:0	65.16 ± 6.59 a	5.44 ± 0.60 a	65.58 ± 1.35 a	62.17 ± 1.30 b	94.17 ± 10.98 b	59.28 ± 3.81 b
C14:0	134.66 ± 11.09 a	145.14 ± 1.47 a	176.30 ± 5.20 b	146.79 ± 10.05 a	348.10 ± 24.81 c	276.05 ± 15.66 b
C15:0	53.13 ± 1.75 a	125.41 ± 6.48 a	162.95 ± 15.90 b	146.74 ± 9.34 b	77.43 ± 13.80 a	5.31 ± 0.75 c
C16:0	38,624.38 ± 5439.91 a	37,817.45 ± 2401.71 a	60,815.76 ± 5207.88 ab	50,256.54 ± 4253.57 b	66,870.67 ± 15,557.59 b	48,455.37 ± 3459.92 b
C17:0	163.78 ± 3.87 a	58.62 ± 2.19 a	55.62 ± 5.00 b	208.80 ± 34.00 b	327.25 ± 12.89 c	222.97 ± 20.59 b
C18:0	5055.66 ± 766.19 a	5204.94 ± 504.84 a	5834.18 ± 761.21 a	4569.61 ± 772.48 a	6832.39 ± 577.13 a	4503.25 ± 151.92 a
C20:0	81.52 ± 11.13 a	78.98 ± 0.51 a	188.72 ± 18.00 b	157.65 ± 6.95 b	204.37 ± 8.86 b	198.35 ± 7.36 c
C21:0	18.33 ± 3.67 a	13.80 ± 1.64 a	25.68 ± 1.43 b	27.28 ± 0.49 b	36.72 ± 2.59 c	28.97 ± 2.47 b
C22:0	153.02 ± 28.65 a	196.22 ± 14.34 ab	207.79 ± 37.37 a	180.38 ± 30.72 a	312.34 ± 16.73 b	242.77 ± 2.54 b
C23:0	300.20 ± 20.28 a	37.05 ± 0.35 a	112.45 ± 8.92 b	249.52 ± 33.01 b	338.56 ± 50.69 a	99.17 ± 10.95 c
C24:0	204.25 ± 22.52 a	86.78 ± 1.14 a	23.62 ± 0.41 b	15.93 ± 1.68 a	416.86 ± 9.74 c	329.87 ± 55.04 b

Lowercase letters indicate statistical differences at $p < 0.05$ between fresh grasses from three cuttings and between grass silages from three cuttings, n.d.—not detected.

Table 8. Sum of mean FAMEs content ± SD in fresh grass and ensiled grass cut in spring, summer, and autumn, both with and without distinction for MUFAs, PUFAs, and SFAs.

Material	Σ MUFAs ± SD	Σ PUFAs ± SD	Σ SFAs ± SD	Σ FAMEs ± SD
	μg g_{DM}^{-1}			
Spring				
Fresh grass	7555.01 ± 265.40	3865.31 ± 434.01	44,948.11 ± 6334.78	56,368.43 ± 7034.19
Grass silage	9930.21 ± 451.89	4585.33 ± 563.27	43,899.76 ± 2942.32	58,415.30 ± 3957.48
Summer				
Fresh grass	14,518.60 ± 1360.04	7735.46 ± 948.65	67,772.96 ± 6065.50	90,027.02 ± 8374.19
Grass silage	12,839.61 ± 748.65	6853.27 ± 533.77	56,121.46 ± 5154.96	75,814.34 ± 6437.38
Autumn				
Fresh grass	14,143.60 ± 1814.56	7925.07 ± 1125.74	76,012.86 ± 16,308.09	98,081.53 ± 19,248.39
Grass silage	10,973.49 ± 503.60	6489.96 ± 231.13	54,517.35 ± 3734.92	71,980.80 ± 4469.65

The compositional analysis of the studied material revealed that the amount of SFA methyl esters (74.02–79.74%) exceeded that of unsaturated fatty acids (MUFAs and PUFAs) (Figure 6). The highest share of SFAs was identified in FG-Sp (79.74%), whereas the lowest SFA amount was observed in GS-Su (74.02%). The analysed grasses also exhibited distinct shares of MUFAs and PUFAs. The highest share of MUFAs was noted in GS-Sp (17%), while the lowest was observed in FG-Sp (13.4%). The highest share of PUFAs was noted in GS-Su (9.04%) and the lowest PUFAs were observed in FG-Sp (6.86%). The dominant

FAMEs included C16:0 fatty acid, as well as C18:0, C18:1n9t/c, C18:2n6c, and C18:3n6 (Tables 5–8), all of which are suitable for biofuel production. FG-Au exhibited the highest content of C16:0, C18:0, and C18:2n6c, while FG-Su had the highest concentrations of C18:1n9t/c and C18:3n6. Other FAMEs, such as C10:0, C11:0, C13:0, C14:1, C16:1, C17:1, C20:2, C20:3n6, C20:4n6, C21:0, C22:6n3, and C24:1n9, had a minimal impact on FAMEs composition, indicated by low content (i.e., less than about 100 μg g_{DM}^{-1}, Tables 5–8).

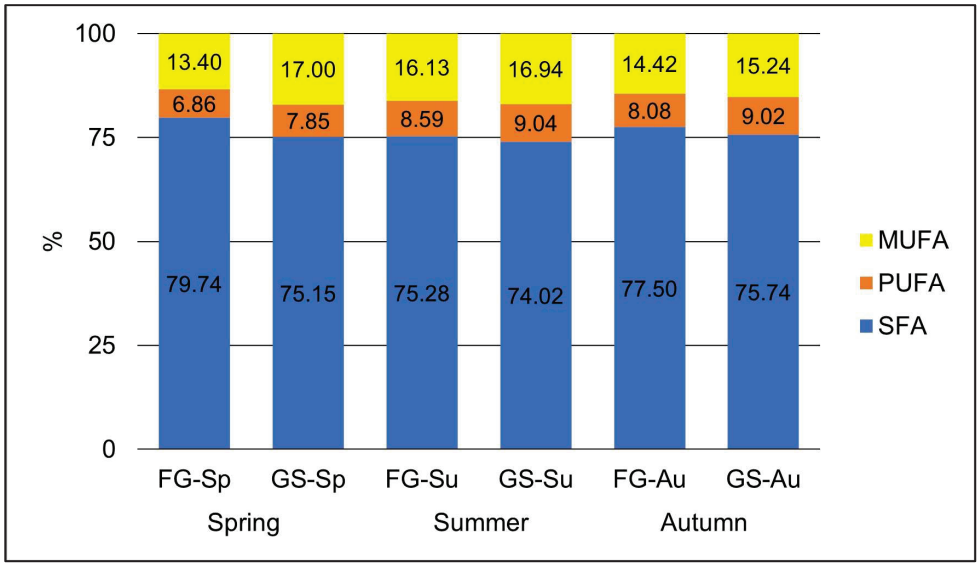

Figure 6. FAMEs composition of fresh grass and ensiled grass harvested in spring, summer and autumn. FG-Sp—spring fresh grass, GS-Sp—spring grass silage, FG-Su—summer fresh grass, GS-Su—summer grass silage, FG-Au—autumn fresh grass, GS-Au—autumn grass silage.

The highest concentration of total FAMEs was determined in FG-Au and FG-Su (98.08 and 90.03 mg g_{DM}^{-1}, respectively, Table 8). C16:0 and C18:0 were found in the largest amounts (66.87 and 6.83 mg g_{DM}^{-1}, respectively) in FG-Au (Table 7). This is noteworthy, as these compounds are ideal for biofuel production. The lowest concentration of total FAMEs was detected in FG-Sp (56.37 mg g_{DM}^{-1}) and GS-Sp (58.42 mg g_{DM}^{-1}) (Table 8).

Principal Component Analysis facilitated the categorisation of the tested samples, maintaining a significant degree of explained variance. During this analysis, the variable count was condensed to two principal components (designated as PC1 and PC2), intimating that the initial dataset of 31 FAMEs is correlated and reducible (Figure 7). All variables, with the exception of C15:0, C22:6n3, and C24:1n9, presented positive loadings, ranging from 0.0479 (C14:1) to 0.9376 (C18:2n6c), in association with the first component. Contrastingly, C15:0 and C24:1n9 were associated with positive loadings (0.9232 and 0.0937, respectively), whereas C22:6n3 exhibited a negative loading (–0.1667) with the second component.

A comparison of case positions on the graph, considering component forms and factor loadings, revealed distinct characteristics among them. Specifically, Case 1, exhibiting positive coordinate values on the first axis, was identified as having a higher content of plant hormones, excluding C15:0, C22:6n3, and C24:1n9, according to the relevant factor loadings. Conversely, Case 2, with positive coordinate values for the second axis, was associated with higher C15:0, and C24:1n9 contents, based on the factor loadings with the second axis. In contrast, Case 3, showing a negative coordinate value on the second axis, was characterised by a lower C22:6n3 content, based on its factor loading with the second axis (Figure 7).

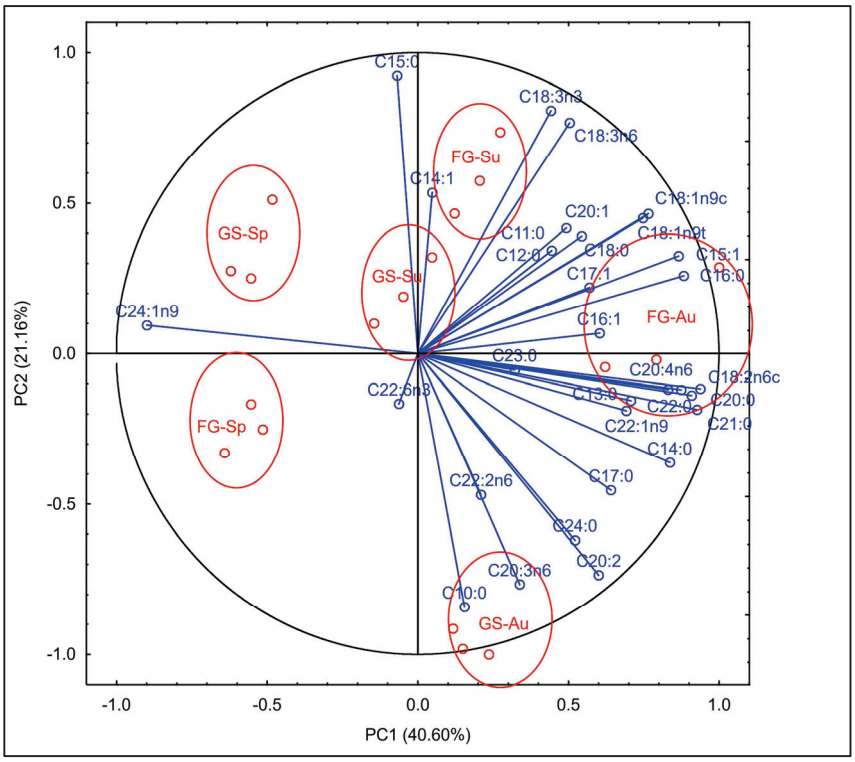

Figure 7. Biplot of FAMEs content in grass samples, showing the first two principal components (PC1 and PC2) of the PCA model that together explain 61.8% of the total variance, i.e., 40.60% and 21.16% for PC1 and PC2, respectively. Blue biplot vectors indicate the strength and direction of factor loading for all analysed fatty acids. FG-Sp—spring fresh grass, GS-Sp—spring grass silage, FG-Su—summer fresh grass, GS-Su—summer grass silage, FG-Au—autumn fresh grass, GS-Au—autumn grass silage.

3.4. Energy Balance and CO_2 Reduction

In the assessment of the energy potential from the utilisation of grass from road verges, slightly higher quantities can be generated from fresh grass in comparison to grass silage (Table 9). This observed correlation is consistently reflected in the energy content of the liquid biofuel generated from the investigated grass. Notably, in the case of spring-cut grass, the energy content in biodiesel derived from ensiled grass slightly surpasses the value calculated for fresh grass. Comparing both examined biofuels produced from grass, it becomes evident that biogas production yields an approximately twofold increase in energy output.

Table 9. Energy production in a biogas plant based on grass from road verges and energy contained in the produced biodiesel.

Cutting Time	Energy from Biogas						Energy in Biodiesel	
	Fresh Grass			Grass Silage			Fresh Grass	Grass Silage
	Electricity	Heat	Total	Electricity	Heat	Total	GJ t_{DM}^{-1}	
	kWh t_{DM}^{-1}	GJ t_{DM}^{-1}	GJ t_{DM}^{-1}	kWh t_{DM}^{-1}	GJ t_{DM}^{-1}	GJ t_{DM}^{-1}		
Spring	923	2.90	6.22	782	2.50	5.32	2.09	2.16
Summer	852	2.70	5.77	863	2.70	5.81	3.33	2.81
Autumn	910	2.90	6.18	837	2.60	5.61	3.63	2.66
Mean	**895**	**2.83**	**6.06**	**827**	**2.60**	**5.58**	**3.02**	**2.54**

A highly important aspect in favour of biofuel production is the mitigation of CO_2 emissions into the atmosphere generated during the combustion of fossil fuels. The comparison of biogas and biodiesel produced from the analysed biomass revealed that the avoided CO_2 emissions for biogas are approximately four times greater than those for

biodiesel. Assuming an average grass yield of 4 t_{DM} ha^{-1} and adopting avoided emission values averaging 840 and 200 kg CO_2 $t_{DM}{}^{-1}$ for biogas and biodiesel, respectively (Table 9), the calculated values for these biofuels amount to 3360 and 800 kg CO_2 ha^{-1}.

4. Discussion

In this study, the biogas production from both grass and grass silage ranged from 540.19 ± 24.32 NL $kg_{VS}{}^{-1}$ to 715.05 ± 26.43 NL $kg_{VS}{}^{-1}$, exhibiting similarity to biogas yields from typical feedstock like farm manures or maize silage [46]. These values slightly surpassed the range provided by Rajendran et al. [46], who reported SBY for grass between 280 NL $kg_{VS}{}^{-1}$ and 550 NL $kg_{VS}{}^{-1}$. However, Żurek and Martyniak [47] documented a biogas yield from silage of three species of perennial grasses within the range of 485–612 NL $kg_{VS}{}^{-1}$.

In the present study, both biogas yield and CH_4 concentration were influenced by the cutting time. Despite being statistically significant, the differences were relatively minor. Several authors [20,21,24,26,48] have reported lower SMY from grass harvested later in the vegetation season. According to Korres et al. [49], cutting time significantly impacts biogas production due to alterations in the proportion of cell wall components, namely cellulose, hemicellulose, and lignin, with increasing lignin content. Lignin, being the most recalcitrant, limits the biodegradability of grass and grass silage during the AD process [29,48]. Moreover, the CH_4 content in biogas from late-season-mown grass decreases due to reductions in crude protein and crude fat contents [50] and an increase in the stem-to-leaves ratio [49], given that stems produce lesser CH_4 amounts [24]. The lignin content in the studied grass increased in summer and remained similar in autumn, influencing the biogas yield and CH_4 content [51]. The marginal differences in biogas yield and CH_4 content may be attributed to frequent mowing conducted multiple times a year, shortening the physiological vegetation age of grasses and reducing lignification, as suggested by Triolo et al. [48] and Piepenschneider et al. [23].

Continuous feedstock supply is imperative for sustained biogas production, while the biomass can be harvested only during the growing season. Consequently, ensiling becomes essential to avoid feedstock shortages throughout the year [52]. In this study, ensiling had minimal adverse effects on biogas yield and no impact on the CH_4 concentration in biogas. Results on the impact of ensiling on CH_4 potential present contradictory findings. Cui et al. [53] reported a higher SMY from ensiled wilted maize stover, while Feng et al. [54] found that ensiling, although an appropriate storage method for *Festuca arundinacea*, had no positive effect on CH_4 yield. Similar conclusions were drawn by Hillion et al. [55], who reported that co-ensiling was effective for storing highly fermentable fresh waste, but CH_4 potential remained unaffected during storage. Menardo et al. [56] demonstrated that although ensiling improved the CH_4 production rate initially, it did not affect the cumulative CH_4 production of corn stalks. Conversely, Liu et al. [57] observed a higher CH_4 yield from ensiled giant reed compared to fresh material. Sun et al. [58] reported that ensiling material with relatively high biodigestibility did not significantly increase CH_4 yield, while in the case of raw materials with relatively low biodigestibility values, it could enhance CH_4 production. In practical terms, the total CH_4 yield is crucial for the economic efficiency of biogas plants, and thus, studies on the effects of ensiling on biogas production should consider the trade-off between storage loss and CH_4 enhancement [58]. Hermann et al. [59] reported that ensiling showed little effect on CH_4 yield considering the increase in CH_4 concentration, with a mutual decrease in dry matter content during the storage. Teixeira Franco et al. [60] suggested that ensiling may increase CH_4 potential only under specific conditions, accounting for storage losses.

In addition to CH_4 and CO_2, biogas encompasses nitrogen (N_2), hydrogen (H_2), carbon monoxide (CO), oxygen (O_2), H_2S, and NH_3. The latter two compounds, released during the digestion of feedstock, may exhibit inhibitory effects on biogas production. The H_2S content in biogas is contingent upon the feedstock and AD technology, fluctuating between 2 and 12,000 ppm [61–63]. Elevated concentrations of H_2S result from the decomposition of

sulphur-containing compounds, such as amino acids, sulphoxides, sulphonic acids, and the biological reduction of sulphates in the feedstock [64].

The presence of H_2S not only hampers the AD process by denaturing proteins in microorganisms responsible for feedstock digestion, but also leads to the formation of a corrosive condensate with water in biogas, causing damage to combined heat and power (CHP) units and installations [65,66]. The toxicity of sulphur oxides (SOx) released into the atmosphere [65,67] and the corrosion of installations or engine damage in biogas plants compel operators to eliminate H_2S from biogas. However, the threshold value is contingent not only on the safety of the biogas installation but also on its subsequent applications. In biogas used in microturbines, the threshold value is high (70,000 ppm); in CHP units, the acceptable range is between 100 and 500 ppm [67,68], and biogas upgraded to biomethane should contain 4–10 ppm [69].

In this study, the initial H_2S concentrations for summer- and autumn-cut grass exceeded the threshold values for CHP units, whereas the H_2S concentration in biogas from spring-cut grass remained very low, even at the beginning of the experiment. Similar disparities in H_2S concentration, influenced by cutting time, were reported by Chumenti et al. [25], who observed a significantly higher H_2S content in biogas produced from summer-cut grass compared to biogas from spring-cut grass. Chumenti et al. [70] also reported significant differences in H_2S concentrations in biogas produced from fresh and ensiled grass, contradicting the results of this study. Studies by Żurek and Martyniak [47] indicated relatively low H_2S concentrations in biogas from perennial grasses, ranging from 272 to 298 ppm.

Another studied inhibitor is produced during the AD process. NH_4^+ is released through the degradation of nitrogen-rich compounds, primarily proteins, urea, and nucleic acids [64,71–73]. This compound is not degraded under anaerobic conditions and is in equilibrium with NH_3, whose concentration is influenced by pH and temperature. A decrease in pH may lead to an increase in NH_3 concentration, adversely affecting the community structure of archaea, which is responsible for CH_4 production, and consequently reducing CH_4 yield [74]. Inhibition of archaea leads to an increase in Volatile Fatty Acids (VFA) and a reduction in pH value [75]. Threshold values for NH_3 concentration range from 80 to 400 ppm [76]; however, the toxicity limits in the literature vary significantly, ranging from 60 to 14,000 ppm [64,77]. In this study, even the highest NH_3 value was lower than the threshold value and decreased significantly by the end of the experiment.

The compositional analysis of grass identified predominant FAMEs such as C16:0, C18:0, C18:1n9t/c, C18:2n6c, and C18:3n6, which are considered suitable for fuel production. Synthesised biodiesel, as reported in the literature, demonstrated the highest yield when derived from waste cooking oil (80.6%), followed by a mix of waste cooking oil and animal fats (79.3%). Characterisation of the produced biodiesel revealed the presence of various FAMEs components, with oleic acid (C18:1n9c), palmitic acid (C16:0), and linoleic acid (C18:2n6c) identified as major constituents [78]. Spectroscopic studies assessing the quality of FAMEs obtained from waste cooking oil confirmed their compliance with the European Standard EN 14214:2006 requirements [79]. FAMEs extracted from spent coffee grounds exhibited a composition composed of C16:0 (41.7%) and C18:0 (48.2%), rendering these extracts suitable for conversion into biodiesel. Furthermore, the residual solid fraction resulting from lignin and FAME extraction underwent AD under mesophilic conditions, yielding CH_4 at a rate of 360 NL $kg_{VS}{}^{-1}$ [37]. The FAME composition derived from cherry stone waste indicated a notable unsaturated to saturated fatty acid ratio [38]. Similarly, herbal waste exhibited higher amounts of unsaturated FAMEs compared to saturated ones, with linoleic acid identified as the major polyunsaturated FAME and palmitic acid as the major saturated FAME [39].

The comparative analysis of the compositional profiles between the examined grass samples and other waste materials, such as municipal sewage sludge [80], revealed analogous distributions of FAMEs. Palmitic acid (C16:0) emerged as the predominant saturated fatty acid, constituting 37.5%, followed by stearic acid (C18:0) at 12.0%. Oleic acid (C18:1n9c)

dominated the unsaturated fatty acids, accounting for 29.0%, while linoleic acid (C18:2n6c) represented 6.2% of the total FAMEs. Similarly, in lipids extracted from primary sludge, Villalobos-Delgado et al. [81] identified palmitic acid (C16:0) as the major saturated fatty acid (42–58%), trailed by stearic acid (C18:0) at 18.3–24.5%, and oleic (C18:1n9c) and linoleic (C18:2n6c) acids at 9.5–22.3%.

The concentration of total FAMEs in the grass samples varied from 98.08 mg $g_{DM}{}^{-1}$ in FG-Au to 56.37 mg $g_{DM}{}^{-1}$ in FG-Sp. Notably, the C16:0 fatty acid ranged from 37.82 to 66.87 mg $g_{DM}{}^{-1}$, and C18:0 from 4.50 to 6.83 mg $g_{DM}{}^{-1}$, constituting the most abundant components. These specific FAMEs are considered ideal for biofuel production. In comparison, integrated processes for food waste yielded 248.21 g of FAMEs per 1 kg [82]. Similarly, high lipid concentrations (248 mg $g_{DM}{}^{-1}$) were observed in *Chlorella vulgaris* [83], highlighting the advantage of microalgae biomass production from waste in a more spatially efficient manner than other crop types. In herbal waste, the highest total FAMEs concentration was observed in rye bran (35.79 mg $g_{DM}{}^{-1}$), herbal tea (11.69 mg $g_{DM}{}^{-1}$), and chicory (8.78 mg $g_{DM}{}^{-1}$), with the majority of herbal waste (62.5%) falling within the total FAMEs content range of 1.42 to 5.02 mg $g_{DM}{}^{-1}$ [39].

The lipid content in temperate grasses is relatively low and tends to decrease as the plant matures [84]. The highest concentration of total FAMEs was observed in fresh grass samples collected in autumn and summer, with values of 98.08 mg $g_{DM}{}^{-1}$ and 90.03 mg $g_{DM}{}^{-1}$, respectively. Whetsell and Rayburn [85] highlighted that vegetative growth and leafiness significantly influence the Fatty Acid (FA) content in grasses, emphasising the negative impact of summer months, specifically May, June, and July, on total FA content. Furthermore, the total FA content exhibited a stronger correlation with linolenic acid (C18:3) than with linoleic acid (C18:2), with lower correlations observed between linoleic acid (C18:2) and linolenic acid (C18:3) content. Concentrations of linoleic acid (C18:2), linolenic acid (C18:3), and total FAs were higher during the summer compared to spring growth [86]. Consistent with these findings, the present study reported the lowest concentration of total FAMEs in FS-Sp (56.37 mg $g_{DM}{}^{-1}$) and GS-Sp (58.42 mg $g_{DM}{}^{-1}$). Intriguingly, GS-Sp exhibited a higher content of these compounds than FG-Sp.

The ensiling process significantly influenced the content of total FAMEs in spring grass, resulting in a reduction in total saturated fatty acids and an increase in total unsaturated fatty acids. These results are in good agreement with the findings of Khan et al. [87], who attributed variations in plant maturity at harvest as the primary explanation for the variability in FA content, highlighting higher contents of C18:3n3 in silages from young grass. Notably, the FAMEs content in grass silage from summer and autumn was lower than in fresh grass from these cutting times. The highest concentration of total FAMEs in ensiled grass (75.81 mg $g_{DM}{}^{-1}$) was detected in samples from summer, closely related to the dry matter content in the analysed samples.

Biodiesel production from waste oils presents challenges, including elevated Free Fatty Acids (FFA) during transesterification. The presence of FFA and water leads to the formation of glycerol (propane-1,2,3-triol) as a by-product and reduces methyl ester levels [88]. The amount of glycerol is contingent on the conversion methods, as well as the type of alcohol and catalyst employed [89]. A substantial portion (70–95%) of the total biodiesel production cost is associated with raw materials [90]. Utilising waste materials, such as waste cooking oil, can significantly reduce production costs, with the cost of obtaining waste cooking oil being 2.5 to 3.5 times lower than that of edible vegetable oils [91]. Osman et al. [92] have explored computational and machine learning techniques, biodiesel characteristics, transesterification processes, waste materials, and policies encouraging biodiesel production from waste. Consequently, the studied grasses represent a potential source for biodiesel production. However, further investigations into their properties are needed.

Although the studied grass exhibits potential for application in both biodiesel and biogas production, its limited availability results in a low energy yield per hectare [51]. Hence, grass waste from the maintenance of road verges should not be viewed as the

primary substrate for the production of liquid or gaseous biofuels. Instead, it should be considered a supplementary feedstock, to be used alongside other resources that are available in quantities sufficient for the operations of biofuel plants. The findings underscore the potential for alternative utilisation of biowaste, thereby prompting consideration for future policy adjustments in urban waste management strategies, integrating energy generation in alignment with the principles of circular economy.

5. Conclusions

The results of this study confirmed the suitability of grass biomass collected during road verges maintenance of for the production of both liquid and gaseous biofuels. Considering the total energy content of the produced biofuels, the biogas production proved to be more efficient than biodiesel production. An additional aspect favouring this direction of utilising the analysed substrates is the potential for both electricity and heat production. On the other hand, the fact that grass from road verges is also suitable for biodiesel production makes it a versatile feedstock for various types of biofuels. However, it should be noted that the analysed type of biomass, due to its properties, is often a challenging feedstock and cannot be considered as the primary substrate for biogas production. The conducted research, nevertheless, demonstrated that its application should not negatively impact the methanogenic fermentation process. Regarding the produced biodiesel, additional studies are necessary to demonstrate its actual suitability as a transportation fuel.

Author Contributions: Conceptualisation, R.C., A.W.-C. and A.S.; methodology, R.C., A.W.-C., A.S., A.P.-N. and A.B.; formal analysis, R.C., A.W.-C., A.S., A.P.-N. and A.B.; investigation, R.C., A.W.-C., A.S., A.P.-N. and A.B.; writing—original draft preparation, R.C., A.W.-C. and A.S.; writing—review and editing, R.C., A.W.-C., A.S., A.P.-N., M.J.W. and A.B.; visualisation, R.C. and A.S. All authors have read and agreed to the published version of the manuscript.

Funding: This work was financially supported by the Ministry of Science and Higher Education as part of the project WZ/WB-IIŚ/3/2023 and this work was funded by the Ministry of Science and Higher Education as part of the subsidies to maintain research potential awarded to the Faculty of Biology of the University of Bialystok (SWB-3).

Data Availability Statement: Data are contained within the article.

Conflicts of Interest: The authors declare no conflicts of interest. The funders had no role in the design of the study; in the collection, analyses, or interpretation of data; in the writing of the manuscript; or in the decision to publish the results.

References

1. United Nations Environment Programme. *Global Material Flows and Resource Productivity: Assessment Report for the UNEP International Resource Panel*, 1st ed.; United Nations Environment Programme: Paris, France, 2016.
2. World Economic Forum. *BiodiverCities by 2030: Transforming Cities' Relationship with Nature*, 1st ed.; World Economic Forum: Cologny/Geneva, Switzerland, 2022.
3. United Nations Environment Programme. Sustainable Cities. Available online: http://www.unep.org/regions/asia-and-pacific/regional-initiatives/supporting-resource-efficiency/sustainable-cities (accessed on 6 May 2023).
4. United Nations, Department of Economic and Social Affairs, Population Division. *World Urbanization Prospects 2018: Highlights (ST/ESA/SER.A/421)*, 1st ed.; United Nations: New York, NY, USA, 2019.
5. European Environmental Agency. Urban Sustainability. Available online: https://www.eea.europa.eu/en/topics/in-depth/urban-sustainability (accessed on 6 May 2023).
6. United Nations General Assembly. *A/RES/70/1 Transforming Our World: The 2030 Agenda for Sustainable Development*; United Nations General Assembly: New York, NY, USA, 2015.
7. European Commission. *The European Green Deal. Communication from the Commission to the European Parliament, the European Council, the Council, the European Economic and Social Committee and the Committee of the Regions. COM(2019) 640 Final*; European Commision: Brussels, Belgium, 2019.
8. Journal of Laws 2004 No. 92/880 Nature Conservation Act of April 2004 (In Polish). Available online: https://isap.sejm.gov.pl/isap.nsf/download.xsp/WDU20040920880/U/D20040880Lj.pdf (accessed on 6 May 2023).
9. Khoshtaria, T.K.; Chachava, N.T. The Planning of Urban Green Areas and Its Protective Importance in Resort Cities (Case of Georgian Resorts). *Ann. Agrar. Sci.* **2017**, *15*, 217–223. [CrossRef]

10. Bai, T.; Mayer, A.L.; Shuster, W.D.; Tian, G. The Hydrologic Role of Urban Green Space in Mitigating Flooding (Luohe, China). *Sustainability* **2018**, *10*, 3584. [CrossRef]
11. Pascal, M.; Laaidi, K.; Beaudeau, P. Relevance of green, shaded environments in the prevention of adverse effects on health from heat and air pollution in urban areas. *Sante Publique* **2019**, *S1*, 197–205. [CrossRef]
12. Wang, W.; Liu, K.; Tang, R.; Wang, S. Remote Sensing Image-Based Analysis of the Urban Heat Island Effect in Shenzhen, China. *Phys. Chem. Earth Parts A/B/C* **2019**, *110*, 168–175. [CrossRef]
13. Kumar, P.; Debele, S.E.; Khalili, S.; Halios, C.H.; Sahani, J.; Aghamohammadi, N.; Andrade, M.D.F.; Athanassiadou, M.; Bhui, K.; Calvillo, N.; et al. Urban Heat Mitigation by Green and Blue Infrastructure: Drivers, Effectiveness, and Future Needs. *Innovation* **2024**, *5*, 100588. [CrossRef] [PubMed]
14. Starczewski, T.; Rogatka, K.; Kukulska-Kozieł, A.; Noszczyk, T.; Cegielska, K. Urban Green Resilience: Experience from Post-Industrial Cities in Poland. *Geosci. Front.* **2023**, *14*, 101560. [CrossRef]
15. Caprotti, F.; Springer, C.; Harmer, N. 'Eco' For Whom? Envisioning Eco-Urbanism in the Sino-Singapore Tianjin Eco-City, China. *Int. J. Urban Reg. Res.* **2015**, *39*, 495–517. [CrossRef]
16. Hitchmough, J.; Fieldhouse, K. *Plant User Handbook: A Guide to Effective Specifying*, 1st ed.; Wiley-Blackwell: Oxford, UK; Malden, MA, USA; Carlton, VIC, Australia, 2003.
17. Li, N.; Liu, Y. Sustainable Design in Urban Green Space. In *Sustainability in Urban Planning and Design*; Almusaed, A., Almssad, A., Truong-Hong, L., Eds.; IntechOpen: London, UK, 2020.
18. Ansari, S.A.; Shakeel, A.; Sawarkar, R.; Maddalwar, S.; Khan, D.; Singh, L. Additive Facilitated Co-Composting of Lignocellulosic Biomass Waste, Approach towards Minimizing Greenhouse Gas Emissions: An up to Date Review. *Environ. Res.* **2023**, *224*, 115529. [CrossRef] [PubMed]
19. Bedoić, R.; Čuček, L.; Ćosić, B.; Krajnc, D.; Smoljanić, G.; Kravanja, Z.; Ljubas, D.; Pukšec, T.; Duić, N. Green Biomass to Biogas–A Study on Anaerobic Digestion of Residue Grass. *J. Clean. Prod.* **2019**, *213*, 700–709. [CrossRef]
20. Seppälä, M.; Paavola, T.; Lehtomäki, A.; Rintala, J. Biogas Production from Boreal Herbaceous Grasses–Specific Methane Yield and Methane Yield per Hectare. *Bioresour. Technol.* **2009**, *100*, 2952–2958. [CrossRef]
21. McEniry, J.; O'Kiely, P. Anaerobic Methane Production from Five Common Grassland Species at Sequential Stages of Maturity. *Bioresour. Technol.* **2013**, *127*, 143–150. [CrossRef] [PubMed]
22. Cadavid-Rodríguez, L.S.; Bolaños-Valencia, I.V. Grass from Public Green Spaces an Alternative Source of Renewable Energy in Tropical Countries. *Rev. ION* **2016**, *29*, 109–116. [CrossRef]
23. Piepenschneider, M.; Bühle, L.; Hensgen, F.; Wachendorf, M. Energy Recovery from Grass of Urban Roadside Verges by Anaerobic Digestion and Combustion after Pre-Processing. *Biomass Bioenerg.* **2016**, *85*, 278–287. [CrossRef]
24. Dragoni, F.; Giannini, V.; Ragaglini, G.; Bonari, E.; Silvestri, N. Effect of Harvest Time and Frequency on Biomass Quality and Biomethane Potential of Common Reed (Phragmites Australis) Under Paludiculture Conditions. *Bioenerg. Res.* **2017**, *10*, 1066–1078. [CrossRef]
25. Chiumenti, A.; Boscaro, D.; Da Borso, F.; Sartori, L.; Pezzuolo, A. Biogas from Fresh Spring and Summer Grass: Effect of the Harvesting Period. *Energies* **2018**, *11*, 1466. [CrossRef]
26. Roj-Rojewski, S.; Wysocka-Czubaszek, A.; Czubaszek, R.; Kamocki, A.; Banaszuk, P. Anaerobic Digestion of Wetland Biomass from Conservation Management for Biogas Production. *Biomass Bioenerg.* **2019**, *122*, 126–132. [CrossRef]
27. De Moor, S.; Velghe, F.; Wierinck, I.; Michels, E.; Ryckaert, B.; De Vocht, A.; Verbeke, W.; Meers, E. Feasibility of Grass Co-Digestion in an Agricultural Digester, Influence on Process Parameters and Residue Composition. *Bioresour. Technol.* **2013**, *150*, 187–194. [CrossRef]
28. Poulsen, T.G.; Adelard, L. Improving Biogas Quality and Methane Yield via Co-Digestion of Agricultural and Urban Biomass Wastes. *Waste. Manag.* **2016**, *54*, 118–125. [CrossRef] [PubMed]
29. Prochnow, A.; Heiermann, M.; Plöchl, M.; Linke, B.; Idler, C.; Amon, T.; Hobbs, P.J. Bioenergy from Permanent Grassland–A Review: 1. *Biogas. Bioresour. Technol.* **2009**, *100*, 4931–4944. [CrossRef]
30. Alvarez Serafini, M.S.; Tonetto, G.M. Production of Fatty Acid Methyl Esters from an Olive Oil Industry Waste. *Braz. J. Chem. Eng.* **2019**, *36*, 285–297. [CrossRef]
31. Olutoye, M.A.; Hameed, B.H. A Highly Active Clay-Based Catalyst for the Synthesis of Fatty Acid Methyl Ester from Waste Cooking Palm Oil. *Appl. Catal. A General* **2013**, *450*, 57–62. [CrossRef]
32. García-Morales, R.; Zúñiga-Moreno, A.; Verónico-Sánchez, F.J.; Domenzain-González, J.; Pérez-López, H.I.; Bouchot, C.; Elizalde-Solis, O. Fatty Acid Methyl Esters from Waste Beef Tallow Using Supercritical Methanol Transesterification. *Fuel* **2022**, *313*, 122706. [CrossRef]
33. Golmakani, M.-T.; Moosavi-Nasab, M.; Raayatpisheh, M.; Dehghani, Z. Fatty Acid Methyl Ester Production from Rainbow Trout Waste Oil Using Microwave-Assisted Transesterification. *Process Biochem.* **2024**, *139*, 33–43. [CrossRef]
34. Dube, A.S. Synthesis of Chicken Fat Methyl Ester. *IJRASET* **2018**, *6*, 2223–2227. [CrossRef]
35. Cruz, A.G.; Mtz-Enríquez, A.I.; Díaz-Jiménez, L.; Ramos-González, R.; Valdés, J.A.A.; Flores, M.E.C.; Martínez, J.L.H.; Ilyina, A. Production of Fatty Acid Methyl Esters and Bioactive Compounds from Citrus Wax. *Waste Manag.* **2020**, *102*, 48–55. [CrossRef]
36. Magalhães-Ghiotto, G.A.V.; Marcucci, S.M.P.; Trevisan, E.; Arroyo, P.A. Extraction and Characterization of the Lipids from Domestic Sewage Sludge and in Situ Synthesis of Methyl Esters. *Environ. Prog. Sustain. Energy* **2023**, *42*, e14027. [CrossRef]

37. Lee, M.; Yang, M.; Choi, S.; Shin, J.; Park, C.; Cho, S.-K.; Kim, Y.M. Sequential Production of Lignin, Fatty Acid Methyl Esters and Biogas from Spent Coffee Grounds via an Integrated Physicochemical and Biological Process. *Energies* **2019**, *12*, 2360. [CrossRef]
38. Kniepkamp, K.; Errico, M.; Yu, M.; Roda-Serrat, M.C.; Eilers, J.-G.; Wark, M.; van Haren, R. Lipid Extraction of High-Moisture Sour Cherry (Prunus Cerasus L.) Stones by Supercritical Carbon Dioxide. *J. Chem. Technol. Biotechnol.* **2024**, *99*, 810–819. [CrossRef]
39. Sienkiewicz, A.; Piotrowska-Niczyporuk, A.; Bajguz, A. Fatty Acid Methyl Esters from the Herbal Industry Wastes as a Potential Feedstock for Biodiesel Production. *Energies* **2020**, *13*, 3702. [CrossRef]
40. Statistical Office in Białystok. Available online: https://bialystok.stat.gov.pl/en/ (accessed on 20 February 2024).
41. Górniak, A. *Climate of the Podlaskie Voivodeship in the Time of Global Warming (In Polish)*, 1st ed.; Wydawnictwo Uniwersytetu w Białymstoku: Białystok, Poland, 2021.
42. Wang, K.; Yun, S.; Xing, T.; Li, B.; Abbas, Y.; Liu, X. Binary and Ternary Trace Elements to Enhance Anaerobic Digestion of Cattle Manure: Focusing on Kinetic Models for Biogas Production and Digestate Utilization. *Bioresour. Technol.* **2021**, *323*, 124571. [CrossRef]
43. Journal of Laws 2020. Regulation of the Minister of Climate of July 11, 2020 on the Calorific Value of Individual Biocomponents and Liquid Fuels (In Polish). Available online: https://isap.sejm.gov.pl/isap.nsf/download.xsp/WDU20200001278/O/D20201278.pdf (accessed on 8 September 2023).
44. The National Centre for Emissions Management. *Emission Factors for CO2, SO2, NOx and Total Particulate Matter for Electrical Energy on the Basis of Information in National Database on Emissions of Greenhouse Gases and Other Substances for 2020 (In Polish)*; The National Centre for Emissions Management: Warsaw, Poland, 2020.
45. The National Centre for Emissions Management. *Calorific Values (CO) and CO2 Emission Factors (EC) in 2019 to Be Reported under the Emission Trading Scheme for 2022*; The National Centre for Emissions Management: Warsaw, Poland, 2021.
46. Rajendran, K.; Aslanzadeh, S.; Taherzadeh, M.J. Household Biogas Digesters—A Review. *Energies* **2012**, *5*, 2911–2942. [CrossRef]
47. Żurek, G.; Martyniak, M. The Biogas Potential of Selected Perennial Grasses from Genus Bromus. *Biul. IHAR* **2020**, *289*, 3–10. [CrossRef]
48. Triolo, J.M.; Pedersen, L.; Qu, H.; Sommer, S.G. Biochemical Methane Potential and Anaerobic Biodegradability of Non-Herbaceous and Herbaceous Phytomass in Biogas Production. *Bioresour. Technol.* **2012**, *125*, 226–232. [CrossRef] [PubMed]
49. Korres, N.E.; Thamsiriroj, T.; Smyth, B.M.; Nizami, A.S.; Singh, A.; Murphy, J.D. Grass Biomethane for Agriculture and Energy. In *Genetics, Biofuels and Local Farming Systems*; Lichtfouse, E., Ed.; Sustainable Agriculture Reviews; Springer: Dordrecht, The Netherlands, 2011; pp. 5–49. ISBN 978-94-007-1521-9.
50. Weiland, P. Biomass Digestion in Agriculture: A Successful Pathway for the Energy Production and Waste Treatment in Germany. *Eng. Life Sci.* **2006**, *6*, 302–309. [CrossRef]
51. Czubaszek, R.; Wysocka-Czubaszek, A.; Banaszuk, P.; Zając, G.; Wassen, M.J. Grass from Road Verges as a Substrate for Biogas Production. *Energies* **2023**, *16*, 4488. [CrossRef]
52. Nizami, A.-S.; Korres, N.E.; Murphy, J.D. Review of the Integrated Process for the Production of Grass Biomethane. *Environ. Sci. Technol.* **2009**, *43*, 8496–8508. [CrossRef] [PubMed]
53. Cui, X.; Sun, H.; Sobhi, M.; Ju, X.; Guo, J.; Dong, R. Butyric Acid Fermentation during Ensiling of Wilted Maize Stover for Efficient Methane Production. *ACS Sustainable Chem. Eng.* **2020**, *8*, 6713–6721. [CrossRef]
54. Feng, L.; Kristensen, E.F.; Moset, V.; Ward, A.J.; Møller, H.B. Ensiling of Tall Fescue for Biogas Production: Effect of Storage Time, Additives and Mechanical Pretreatment. *Energy Sustain. Dev.* **2018**, *47*, 143–148. [CrossRef]
55. Hillion, M.-L.; Moscoviz, R.; Trably, E.; Leblanc, Y.; Bernet, N.; Torrijos, M.; Escudié, R. Co-Ensiling as a New Technique for Long-Term Storage of Agro-Industrial Waste with Low Sugar Content Prior to Anaerobic Digestion. *Waste Manag.* **2018**, *71*, 147–155. [CrossRef]
56. Menardo, S.; Balsari, P.; Tabacco, E.; Borreani, G. Effect of Conservation Time and the Addition of Lactic Acid Bacteria on the Biogas and Methane Production of Corn Stalk Silage. *Bioenerg. Res.* **2015**, *8*, 1810–1823. [CrossRef]
57. Liu, S.; Ge, X.; Liew, L.N.; Liu, Z.; Li, Y. Effect of Urea Addition on Giant Reed Ensilage and Subsequent Methane Production by Anaerobic Digestion. *Bioresour. Technol.* **2015**, *192*, 682–688. [CrossRef] [PubMed]
58. Sun, H.; Cui, X.; Li, R.; Guo, J.; Dong, R. Ensiling Process for Efficient Biogas Production from Lignocellulosic Substrates: Methods, Mechanisms, and Measures. *Bioresour. Technol.* **2021**, *342*, 125928. [CrossRef]
59. Herrmann, C.; Heiermann, M.; Idler, C. Effects of Ensiling, Silage Additives and Storage Period on Methane Formation of Biogas Crops. *Bioresour. Technol.* **2011**, *102*, 5153–5161. [CrossRef] [PubMed]
60. Teixeira Franco, R.; Buffière, P.; Bayard, R. Ensiling for Biogas Production: Critical Parameters. *A Review. Biomass Bioenerg.* **2016**, *94*, 94–104. [CrossRef]
61. Fortuny, M.; Baeza, J.A.; Gamisans, X.; Casas, C.; Lafuente, J.; Deshusses, M.A.; Gabriel, D. Biological Sweetening of Energy Gases Mimics in Biotrickling Filters. *Chemosphere* **2008**, *71*, 10–17. [CrossRef] [PubMed]
62. Mamun, M.R.A.; Torii, S. Removal of Hydrogen Sulfide (H_2S) from Biogas Using Zero-Valent Iron. *J. Clean Energy Technol.* **2015**, *3*, 428–432. [CrossRef]
63. Calbry-Muzyka, A.; Madi, H.; Rüsch-Pfund, F.; Gandiglio, M.; Biollaz, S. Biogas Composition from Agricultural Sources and Organic Fraction of Municipal Solid Waste. *Renew. Energy* **2022**, *181*, 1000–1007. [CrossRef]
64. Chen, Y.; Cheng, J.J.; Creamer, K.S. Inhibition of Anaerobic Digestion Process: A Review. *Bioresour. Technol.* **2008**, *99*, 4044–4064. [CrossRef] [PubMed]

65. Żarczyński, A.; Rosiak, K.; Anielak, P.; Wolf, W. Practical Methods of Cleaning Biogas from Hydrogen Sulphide. Part 1. Application of Solid Sorbents. *Acta Innov.* **2014**, *12*, 24–34.
66. Czatzkowska, M.; Harnisz, M.; Korzeniewska, E.; Koniuszewska, I. Inhibitors of the Methane Fermentation Process with Particular Emphasis on the Microbiological Aspect: A Review. *Energy. Sci. Eng.* **2020**, *8*, 1880–1897. [CrossRef]
67. Aita, B.C.; Mayer, F.D.; Muratt, D.T.; Brondani, M.; Pujol, S.B.; Denardi, L.B.; Hoffmann, R.; da Silveira, D.D. Biofiltration of H_2S-Rich Biogas Using Acidithiobacillus Thiooxidans. *Clean. Technol. Environ. Policy* **2016**, *18*, 689–703. [CrossRef]
68. Moreno-Andrade, I.; Moreno, G.; Quijano, G. Theoretical Framework for the Estimation of H_2S Concentration in Biogas Produced from Complex Sulfur-Rich Substrates. *Environ. Sci. Pollut. Res.* **2020**, *27*, 15959–15966. [CrossRef] [PubMed]
69. Jung, H.; Kim, D.; Choi, H.; Lee, C. A Review of Technologies for In-Situ Sulfide Control in Anaerobic Digestion. *Renew. Sust. Energ. Rev.* **2022**, *157*, 112068. [CrossRef]
70. Chiumenti, A.; Pezzuolo, A.; Boscaro, D.; da Borso, F. Exploitation of Mowed Grass from Green Areas by Means of Anaerobic Digestion: Effects of Grass Conservation Methods (Drying and Ensiling) on Biogas and Biomethane Yield. *Energies* **2019**, *12*, 3244. [CrossRef]
71. Rajagopal, R.; Massé, D.I.; Singh, G. A Critical Review on Inhibition of Anaerobic Digestion Process by Excess Ammonia. *Bioresour. Technol.* **2013**, *143*, 632–641. [CrossRef]
72. Westerholm, M.; Moestedt, J.; Schnürer, A. Biogas Production through Syntrophic Acetate Oxidation and Deliberate Operating Strategies for Improved Digester Performance. *Appl. Energy* **2016**, *179*, 124–135. [CrossRef]
73. Tian, H.; Fotidis, I.A.; Kissas, K.; Angelidaki, I. Effect of Different Ammonia Sources on Aceticlastic and Hydrogenotrophic Methanogens. *Bioresour. Technol.* **2018**, *250*, 390–397. [CrossRef]
74. Yang, Z.; Wang, W.; He, Y.; Zhang, R.; Liu, G. Effect of Ammonia on Methane Production, Methanogenesis Pathway, Microbial Community and Reactor Performance under Mesophilic and Thermophilic Conditions. *Renew. Energy* **2018**, *125*, 915–925. [CrossRef]
75. Kalamaras, S.D.; Vitoulis, G.; Christou, M.L.; Sfetsas, T.; Tziakas, S.; Fragos, V.; Samaras, P.; Kotsopoulos, T.A. The Effect of Ammonia Toxicity on Methane Production of a Full-Scale Biogas Plant—An Estimation Method. *Energies* **2021**, *14*, 5031. [CrossRef]
76. Theuerl, S.; Klang, J.; Prochnow, A. Process Disturbances in Agricultural Biogas Production—Causes, Mechanisms and Effects on the Biogas Microbiome: A Review. *Energies* **2019**, *12*, 365. [CrossRef]
77. Krakat, N.; Demirel, B.; Anjum, R.; Dietz, D. Methods of Ammonia Removal in Anaerobic Digestion: A Review. *Water Sci. Technol.* **2017**, *76*, 1925–1938. [CrossRef] [PubMed]
78. Al-Mawaali, S.; Al-Balushi, K.; Souissi, Y. Sustainable Biodiesel Production from Waste Cooking Oil and Waste Animal Fats. In Proceedings of the 8th World Congress on Civil, Structural, and Environmental Engineering, Lisbon, Portugal, 29−31 March 2023.
79. Matwijczuk, A.; Zając, G.; Karcz, D.; Chruściel, E.; Matwijczuk, A.; Kachel-Jakubowska, M.; Łapczyńska-Kordon, B.; Gagoś, M. Spectroscopic Studies of the Quality of WCO (Waste Cooking Oil) Fatty Acid Methyl Esters. *BIO Web Conf.* **2018**, *10*, 02019. [CrossRef]
80. Demirbas, A.; Bamufleh, H.; Gaber, G.; Al-Sasi, B.O. Biodiesel Production from Lipids of Municipal Sewage Sludge by Direct Methanol Transesterification. *Energy Sources A REcovery Util. Environ. Eff.* **2017**, *39*, 800–805. [CrossRef]
81. Villalobos-Delgado, F.d.J.; Reynel-Avila, H.E.; Mendoza-Castillo, D.I.; Bonilla-Petriciolet, A. Lipid Extraction in the Primary Sludge Generated from Urban Wastewater Treatment: Characteristics and Seasonal Composition Analysis. *Water Sci. Technol.* **2023**, *87*, 2930–2943. [CrossRef]
82. Patel, A.; Hrůzová, K.; Rova, U.; Christakopoulos, P.; Matsakas, L. Sustainable Biorefinery Concept for Biofuel Production through Holistic Volarization of Food Waste. *Bioresour. Technol.* **2019**, *294*, 122247. [CrossRef] [PubMed]
83. López-Pacheco, I.Y.; Ayala-Moreno, V.G.; Mejia-Melara, C.A.; Rodríguez-Rodríguez, J.; Cuellar-Bermudez, S.P.; González-González, R.B.; Coronado-Apodaca, K.G.; Farfan-Cabrera, L.I.; González-Meza, G.M.; Iqbal, H.M.N.; et al. Growth Behavior, Biomass Composition and Fatty Acid Methyl Esters (FAMEs) Production Potential of *Chlamydomonas reinhardtii*, and *Chlorella vulgaris* Cultures. *Mar. Drugs.* **2023**, *21*, 450. [CrossRef] [PubMed]
84. Frame, J.; Laidlaw, A.S. *Improved Grassland Management*, 2nd ed.; The Crowood Press: Ramsbury, UK, 2011.
85. Whetsell, M.; Rayburn, E. Variation in Fatty Acids Concentration in Grasses, Legumes, and Forbs in the Allegheny Plateau. *Agronomy* **2022**, *12*, 1693. [CrossRef]
86. Boufaïed, H.; Chouinard, P.Y.; Tremblay, G.F.; Petit, H.V.; Michaud, R.; Bélanger, G. Fatty Acids in Forages. II. In Vitro Ruminal Biohydrogenation of Linolenic and Linoleic Acids from Timothy. *Can. J. Anim. Sci.* **2003**, *83*, 513–522. [CrossRef]
87. Khan, N.A.; Cone, J.W.; Fievez, V.; Hendriks, W.H. Causes of Variation in Fatty Acid Content and Composition in Grass and Maize Silages. *Anim. Feed Sci. Technol.* **2012**, *174*, 36–45. [CrossRef]
88. Monika; Banga, S.; Pathak, V.V. Biodiesel Production from Waste Cooking Oil: A Comprehensive Review on the Application of Heterogenous Catalysts. *Energy Nexus* **2023**, *10*, 100209. [CrossRef]
89. Pitt, F.D.; Domingos, A.M.; Barros, A.A.C. Purification of Residual Glycerol Recovered from Biodiesel Production. *S. Afr. J. Chem. Eng.* **2019**, *29*, 42–51. [CrossRef]
90. Ahmia, A.C.; Danane, F.; Bessah, R.; Boumesbah, I. Raw Material for Biodiesel Production. Valorization of Used Edible Oil. *J. Ren. Energ.* **2023**, *17*, 335–343. [CrossRef]

91. Rehan, M.; Gardy, J.; Demirbas, A.; Rashid, U.; Budzianowski, W.M.; Pant, D.; Nizami, A.S. Waste to Biodiesel: A Preliminary Assessment for Saudi Arabia. *Bioresour. Technol.* **2018**, *250*, 17–25. [CrossRef]
92. Osman, A.I.; Nasr, M.; Farghali, M.; Rashwan, A.K.; Abdelkader, A.; Al-Muhtaseb, A.H.; Ihara, I.; Rooney, D.W. Optimizing Biodiesel Production from Waste with Computational Chemistry, Machine Learning and Policy Insights: A Review. *Environ. Chem. Lett.* **2024**, *22*, 1–67. [CrossRef]

energies

MDPI

Review

Animal Manure as an Alternative Bioenergy Resource in Rural Sub-Saharan Africa: Present Insights, Challenges, and Prospects for Future Advancements

Timothy Sibanda [1,*,†] and Jean Damascene Uzabakiriho [2,†]

[1] School of Molecular and Cell Biology, Faculty of Science, University of the Witwatersrand, Johannesburg 2050, South Africa
[2] Department of Biochemistry, Microbiology and Biotechnology, Faculty of Agriculture, Engineering and Natural Sciences, University of Namibia, Windhoek 13301, Namibia; juzabakiriho@unam.na
* Correspondence: timothy.sibanda@wits.ac.za
† These authors contributed equally to this work.

Abstract: Energy availability is a pivotal driver in fostering sustainable socio-economic development. However, sub-Saharan Africa (SSA) grapples with paradoxes headlined by abundant energy resources but with the world's lowest access to clean energy index per capita. Faced with a lack of access to clean energy sources like electricity, rural areas in the majority of SSA countries almost exclusively depend on biomass-fuels, mostly fuelwood, leading to heightened respiratory health risks as well as environmental degradation and accelerated climate change. As an alternative, this review investigates the potential of animal manure as a sustainable energy resource for rural SSA households, emphasising its utilisation as a feedstock for biogas production using anaerobic digestor technology. Results show that despite the abundance of literature that reports on successes in lab-scale bioreactor optimisation, as well as successes in the initial rollout of biogas biodigester technology in SSA with the help of international collaborators, the actual uptake of biogas bioreactor technology by rural communities remains low, while installed bioreactors are experiencing high failure rates. Resultantly, rural SSA still lags significantly behind in the adoption of sustainable clean energy systems in comparison to rural communities in other regions. Among some of the hurdles identified as driving low technology assimilation are onerous policy requirements, low-level government involvement, high bioreactor-instalment costs, the lack of training and awareness, and water scarcity. Prospects for success lie in innovative technologies like the low-cost portable FlexiBiogas system and private–public partnerships, as well as flexible energy policy frameworks. Bridging the knowledge-implementation gap requires a holistic approach considering cultural, technological, and policy aspects.

Keywords: energy poverty; biogas; animal manure; sub-Saharan Africa; greenhouse gas emissions; climate change

1. Introduction

Energy availability is the cog that drives sustainable socio-economic development [1,2]. However, the status of energy availability in sub-Saharan Africa has more than its fair share of paradoxes. Three facts that stand out are as follows: (i) the population of sub-Saharan Africa constitutes about 15% of the world's population [1,3]; (ii) the region is rich in energy resources and yet remains poor in energy supply, accounting for only 4.3% of the global energy demand [3]; and (iii) the region has the lowest level of access to electricity worldwide, with 75% of the global population without access to electricity residing in this region [1]. Presently, sub-Sharan African economies are overly dependent on fossil fuels such as oil, coal, and gas to power the various industries that are central to their economic growth [4]. Despite this over-reliance on fossil fuels, however, Africa and the sub-Saharan African region still contribute only approximately 2% of the aggregate global

greenhouse gas emissions while the world's more developed economies like the USA, Australia, Germany, and China are responsible for the bulk of the emissions [5].

With greenhouse gas emissions being linked to worsening climate change, the evidence of which includes increasingly drier and hotter climatic conditions in some parts of the world while others experience unprecedented floods, wildfires, rising seas levels, among other changes, the discourse among developed countries is rapidly gravitating towards clean energy usage to mitigate the damaging effects of climate change [6,7]. However, less developed economies in the sub-Saharan Africa region will find it cheaper in the foreseeable future to consume readily available fossil energy sources despite their harmful effects to the environment [4]. At the household level, 76–80% of urban populations in the sub-Saharan African region have access to electricity for cooking and heating, while almost the same percentage (70%) of rural populations rely on unsustainable biomass sources, especially fuelwood [8,9], exposing them to respiratory health complications due to polluted indoor environments in addition to environmental degradation due to deforestation [10,11]. The persistently high demand for wood fuel in rural sub-Saharan African households is unsustainable as it directly threatens forests resources, thereby accelerating desertification, which inadvertently increases the region's carbon footprint and contributes to global warming [12]. In any case, The United Nations, through its non-binding Agenda 21, as well as the Kyoto Protocol, strongly advocate for the development of sustainable, climate-friendly renewable energy systems, particularly in the face of the imminent depletion of fossil fuels [13]. Hence, the need for appropriate investment in small-scale biogas technologies to achieve a self-sufficient paradigm shift from traditional to sustainable and climate-friendly modern bioenergy to deliver a range of benefits to rural households [14–16]. In this context, manure ought to be considered as a valuable resource, given its potential for anaerobic digestion, which stands out as a promising avenue for its sustainable management. The use of animal manure for energy generation, and in particular as feedstock for anaerobic digestor technology, has received extensive coverage in both the research and review literature globally as well as in the sub-Saharan Africa (SSA) context. The vast majority of this research, however, is focussed on anaerobic digestor-process improvement [17], in particular on feedstock choices for increased biogas output [18–20], bioreactor design and diagnosis of bioreactor failures [21], impacts of private–public partnerships on biogas technology development [22], and socio-economic barriers to technology adoption [23,24]. In so doing, lab-scale successes and achievements are often misconstrued for on-the-ground implementation success whereas, in practicality, there is a disconnect between research and implementation [25]. There is still a dearth of information with regard to the practicality of using animal manure as a clean energy source in rural SSA.

This review, therefore, plugs this gap by providing an in-depth analysis of animal manure as an alternative, sustainable energy source for energy-poverty-stricken rural sub-Saharan Africa (SSA). Emphasis is placed on current knowledge and the use of animal manure as an energy source, opportunities for growth, and the associated limitations, as well as on prospects for future advancements in rural settings. The focus on rural areas was informed by the fact that more people live in rural areas compared to urban areas in sub-Saharan African countries [8,26], in addition to the fact that, due to high poverty levels, energy poverty is felt more in rural areas than in urban areas. Consequently, there are high rates of deforestation in rural areas as residents harvest forest resources to meet their daily energy requirements.

2. Animal Manure as an Alternative Source of Energy in Rural SSA

Renewable energy resources continue to hog the spotlight in climate change debates due to their low carbon footprints [5]. Currently, these include solar, wind, hydroelectric, and biomass resources, which are soon to be joined by green hydrogen. Biomass, and animal manure specifically, is a centuries-old source of renewable energy, which can either be directly burned to produce heat energy (akin to coal or wood fuel) [7] or can be fed

into an anaerobic biodigester to produce combustible gas called biogas [27]. However, the direct burning of dung pellets for heating and cooking has the disadvantage of producing smoke that pollutes indoor air and leads to chronic respiratory and eye infections, the same problem as occurs from burning fuelwood [28]. Besides the production of poisonous gases like carbon monoxide, sulphur dioxide, and nitrogen oxide, when directly burned as pellets, cow dung has a low heating value ranging from 10 to 17 MJ/kg, depending on its moisture content [7]. Anaerobic digestion, however, converts the biomass into energy-rich biogas, which is ultimately used as a clean renewable energy source for domestic cooking, heating, and lighting [13]. An added advantage is the production of bio-digestate, which is a nutrient-rich slurry that farmers can then apply to their fields as organic fertiliser to increase agricultural productivity. Furthermore, according to ref. [29], the application of digestate facilitates the settling of phosphorous and metals such as copper and zinc, consequently diminishing their discharge into surface waters preventing eutrophication or algal bloom. Within the anaerobic digester, the principal components undergoing alteration are carbon and nitrogen that result in an 85% reduction in biological-oxygen demand [30].

The development of anaerobic digester technology for biogas production presents a plausible avenue to ameliorate energy poverty, which is partly responsible for slow economic development in SSA countries [31]. What makes animal manure particularly ideal as a feedstock for biogas production is its high moisture and volatile-solids content [12]. In addition, animal manure also contains a diverse assemblage of microorganisms, some of which play significant roles during the anaerobic digestion process. For example, the microbial profile of cow dung consists of different bacterial species, including *Bacillus* spp., *Corynebacterium* spp., *Lactobacillus* spp., *Citrobacter koseri*, *Enterobacter aerogenes*, *Escherichia coli*, *Klebsiella oxytoca*, *Klebsiella pneumoniae*, *Kluyvera* spp., *Morgarella morganii*, *Pasteurella* spp., *Providencia alcaligenes*, *Providencia stuartii*, and *Pseudomonas* spp., as well as protozoa and yeast (*Saccharomyces* and *Candida*), lignocellulolytic fungi, and archaea [32–34]. As a potential replacement for fossil fuels, biogas is produced when animal manure is subjected to anaerobic digestion by methanogenic bacteria, generating biogas whose composition varies from 45 to 70% for methane gas (biomethane) and 25–40% for carbon dioxide, as well as containing some trace gases, including hydrogen sulphide (<10 ppm), nitrogen (<3 ppm), and hydrogen (<1 ppm), depending on the animal source of the manure [12] This follows a four-stage process starting with hydrolysis, followed by acid-genesis and acetogenesis that are induced by a specific consortia of bacteria, with the final step of methanogenesis undertaken by a consortia of methanogenic archaea, as detailed in the extant literature [2,13,27,31,35], and as shown in Figure 1 below.

A study by [2] reports that in a supervised anaerobic digestion, cow dung and poultry litter can produce biogas yields of 0.034 and 0.03 m^3/kg, respectively, with methane concentrations of 60% and 62%, respectively. Biogas with such methane compositions is not only comparable to fossil fuel derived natural gas that is 75–98% methane [2,13] but is also classified as good-grade gas since biogas burns more effectively when its methane component is greater than 50% [31]. In terms of heating value, [36] report that the heating value of pure methane (natural gas) is 8900 kcal/m^3 whereas the heating value of unpurified biomass-based biogas is in the range of 4800 to 6700 kcal/m^3, with a cooking efficiency of approximately 55% on a small scale. Furthermore, research shows that the energy value of 1 m^3 of biogas is between 2000 and 4000 kcal, which can meet the cooking needs of a family of 4 to 5 people for 3 h, with about 3 m^3 of biogas needed to cater for the family's cooking needs per day [36]. Regarding anaerobic digester performances, ref. [2] notes that the cause of irregular and inconsistent biodigester performance is usually a lack of supervision, which often results in digester underfeeding, improper water mixing, and irregular feeding, which all reduce yields significantly. With adequate training and consistent use, however, people reliant on digesters for biogas production should be able to solve these problems.

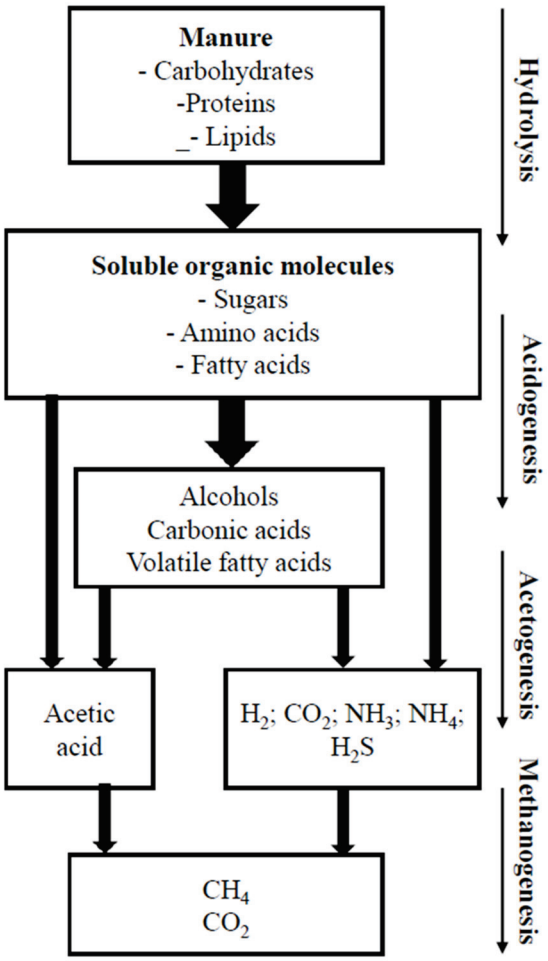

Figure 1. Stages in the anaerobic digestion process for the production of biogas from animal manure.

2.1. Present State of Knowledge and Use of Animal Manure for Energy in Rural SSA

The present understanding and use of manure for energy in rural SSA reveals a nuanced landscape shaped by historical practices, international collaborations, and regional variations [37,38]. The use of animal manure as feedstock for the generation of biogas using fixed-dome and floating-drum digesters has been practiced in sub-Saharan Africa since the 1950s [28], howbeit on a scale too small to tilt the scales towards economic development [37]. In Kenya, for example, biogas was introduced in 1948, with the first biodigester being built in that country in 1957 by the company Tunnel Engineering Ltd. [37, 39]. Other early pacesetters are South Africa, where biogas digesters were set up in the 1950s, and Tanzania that began in 1975, while the most recent newcomer to the technology is South Sudan, where the first biogas digester was installed in 2001 [40]. To date, and through public–private partnerships, anaerobic digester technology for biogas production has been rolled out in different rural areas of Kenya, mostly using cow dung as the main feedstock [39]. An organisation called the Netherlands Development Organisation, founded in the Netherlands in 1965, provides technical assistance to the Africa Biogas Partnership Programme (ABPP) supporting national programs on domestic biogas in several sub-Saharan African countries, including Ethiopia, Kenya, Tanzania, Uganda, and Burkina Faso [9,39]. This has seen over 18,000 biodigesters being installed across Kenya since 2009 [39]. In addition to ABPP, another organisation, the International Fund for Agricultural Development (IFAD), which is funded by the UK Department for International Development, has been assessing the potential of renewable energy technologies like biogas in conjunction with a Keyan company, Biogas International Limited (BIL), since 2012 [28]. IFAD has also facilitated south–south cooperation between Kenyan engineers and the

Indian Institute for Technology, providing a platform for scaling up the biogas technology in Kenya and beyond [28]. The African landscape is characterised by three different size types of biogas digesters which include the household digester plant whose gas production capacity is designed to meet all the cooking and 2–4 h of lighting needs of a family; the institutional/community digester plant that is typically shared by neighbours, and the large-scale plant that is designed to supply gas to closed communities [40]. Rural areas are typically serviced by either family plants or institutional plants, depending on population distribution. Historically, the fixed-dome bioreactor has been favoured over other designs like the floating-drum bioreactor due to its perceived durability and low maintenance costs [40].

In terms of biogas technology uptake, countries in southern Africa have been slow compared to countries in western, central, and eastern Africa, which embraced international collaborations to build public–private partnerships as support structures in setting up national domestic biogas programmes that have supported the increased uptake of the technology compared to countries in southern Africa. While statistics is scarce, ref. [41] show that, as of 2005, several southern African countries like South Africa, Swaziland, Zimbabwe, and Botswana had approximately 100 medium/small-scale digesters (100 m^3) each, Burundi (central Africa) had more than 279 digesters, and Tanzania and Kenya (eastern Africa) had more than 1000 and 500 digesters, respectively. While a lot might have changed since 2005, data in Table 1 show that it is the central and east African countries like Rwanda, Tanzania, Kenya, Uganda, Ethiopia, Cameroon, Benin, and Burkina Faso that have increased the uptake of biogas technology, even going as far as increasing the number of trained technicians for both installation and maintenance of biodigesters, with solid plans for expansion [37]. Contrastingly, not much development has been realised in southern sub-Saharan Africa outside of South Africa, where significant progress is being made [42].

Table 1. Distribution of biogas digester facilities in some SSA countries.

Country	No. Installed	Capacity (m^3)	Operational (%)	Reference
Zambia	60	4–80		[23]
Zimbabwe	711	50–200	15	[43,44]
Ethiopia	15,738–18,534	Various	40	[24,45,46]
Cameroon	164 *	Various		[46]
Burkina Faso	10,310	Various		[46]
Botswana	15	Various		[46]
Kenya	13,000–18,560	Various	30	[24,46,47]
Senegal	875	Various		[46]
Tanzania	12,000	Various		[48]
Uganda	8000	Various		[47]
Nepal †	431,629	various	90	[49]

* Data relates only to domestic-level bioreactors. † Nepal is included for benchmarking purposes.

In terms of digester feedstock/substrate, while animal manure is the main type used in sub-Saharan Africa, ref. [41] points to a combination of food waste and human excreta, rice husks, and banana and plantain peels as well as groundnuts as among some of the unconventional substrate types used in pilot studies in Nigeria. The use of human excreta for biogas generation in rural communities is likely to be met with stiff resistance rooted in cultural beliefs and there may not be any food waste at all due to food insufficiency in these settings. However, while there is hope for a change in human perception and cultural beliefs, what is more concerning is that the available literature points to a mismatch between laboratory-scale manure-to-biogas research and actual biogas rollout in sub-Saharan Africa. The scholarly literature is concerned mostly with optimising anaerobic digestor conditions for optimal biogas output but offers little insight about the actual use of animal manure for energy generation. In the majority of cases where anaerobic digester technology has been rolled out, refs. [23,25] point to a high failure rate where biogas plants lie unused due to,

among other factors; a lack of state investment in biogas research, difficulty in accessing biogas technology within some national contexts, a lack of supportive policy frameworks in some countries, low institutional capacity to implement national biogas programmes, prohibitive regulatory barriers, insufficient feedstock, the constant cost of maintenance, a lack of training for potential biogas owners, and climate unpredictability that leads to water shortages and ultimately anaerobic digestor failure.

Differences in biogas adoption rates between Asia (using Nepal as an example of a developing Asian country) and SSA are influenced by, among other things, the cheaper cost of building materials in Nepal (Asia) as compared to SSA, the higher numbers of livestock and hence available feedstock in Nepal compared to SSA, differences in the availability of loans for biogas infrastructure installation in Nepal compared to SSA countries outside of South Africa, and the relative maturity of biogas promotion schemes in Nepal, where it was first introduced in 1992 as the Biogas Support Program, compared to SSA where the first scheme was introduced in Rwanda in 2007 [24,49]. Intriguingly, there were already 11,919 installed biogas plants in Nepal by the year 1992 when the support scheme was introduced. Again, unlike in SSA where most national governments are struggling, at the policy level, to steer development of the biogas sector, Nepal has managed to institutionalise the biogas industry through a line agency called the Alternative Energy Promotion Centre (AEPC), which was set up under the Ministry of Science and Technology in 1996 to promote renewable energy projects in that country [49]. The AEPC was set up with a clear mandate to "form and organise policies on the distribution and implementation of RETs to boost rural people's living conditions through clean energy supply and protection of the local environment from deterioration" [49]. This made it easier for Nepal to receive international funding to support its biogas industry, resulting in an over 90% success rate compared to a 40% maximum success rate among SSA countries. Nepal lies in an earthquake prone area, and in 2015, 16,721 biogas plants were earthquake damaged. However, by the year 2018 the Nepalese government had already repaired 43.8% of the damaged plants [49]. Comparatively, Zimbabwe currently has 68 non-functional digesters, 26 abandoned digesters, 3 collapsed digesters, and 7 digesters that never have worked since being commissioned (Table 2). SSA governments therefore still have a lot to learn from successful examples like Nepal if they are to turn around the fortunes of the once hyped but underdeveloped biogas industry.

Table 2. Status survey of Zimbabwe's biodigester infrastructure from 1980 to 2012.

Year of Construction (Phases)	No. Collapsed	No. Functional	No. Non-Functional	No. Yet to Be Fed	No. Abandoned	No. Never Worked	No. under Construction
1980–1990	0	2	21	0	7	2	2
1991–2000	0	6	17	0	6	3	0
2001–2010	3	5	30	2	13	2	2
2011–2012	0	1	0	0	0	0	2
Total	3	14	68	2	26	7	6

Source: [44].

2.2. Opportunities and Challenges

Biogas has the potential to supply a more sustainable source of energy than solid biomass like wood fuels in rural households in sub-Saharan Africa [50]. The biggest opportunity for the development of biogas technology in rural sub-Sharan Africa is the vast availability of biomass, particularly animal manure [51]. This is because the main economic activity in rural sub-Saharan Africa is farming, with cattle and small stock rearing playing a significant role in sustaining those local economies [52]. Furthermore, farmers tend to house their livestock in kraals during the night, making it easier to accumulate significant amounts of manure in a short period of time [51]. For example, ref. [53] estimate that the livestock population in Ethiopia is about 150 million, with an estimated 42 million

tonnes of dry-weight dung per year, 84% of which is produced by cattle alone. In another example, a study by ref. [54] in rural Vhembe District in the Limpopo Province of South Africa estimated the following animal populations: 1,050,685 cows with an estimated 12 kg of manure per animal per day, equivalent to an estimated 0.2 Nm^3 of methane per day; 373,037 pigs (5 kg/animal, 3.6 Nm^3 methane); 1,542,903 chickens (0.08 kg/animal, 0.35 Nm^3 methane); 253,139 sheep (6 kg/animal, 0.053 Nm^3 methane), and 1,147,987 goats with an estimated 6 kg manure output per animal and an estimated equivalent of 0.367 Nm^3 of methane per day. Assuming these numbers to be representative of approximate animal populations in all of South Africa's provinces, they represent huge renewable energy resources that have the capacity to confine South Africa's energy deficiency to history if utilised for biogas generation. Conversely, these statistics also show the amount of environmental damage that is currently ensuing because of the unmanaged animal manure, with statistics indicating that every 1 kg of cow dung can release about 60 L of gas emissions into the atmosphere, the largest component of which is methane gas [36]. However, adopting the biogas technology hinges upon various factors, including environmental, economic, technical, and social factors [55]. It is imperative to scrutinise seasonal and geographical variation in the composition of specific of manures [14]. These considerations will profoundly determine the technical and economic feasibility of accessing manure. The availability of manure is linked to the organisational structure of animal husbandry, displaying regional differences [14].

In addition to the ready availability of animal manure, farmers who rear mixed stock also get different kinds of manure that can be mixed for optimum biogas production. In a supervised anaerobic digestion experiment, ref. [34] reported that mixing cow and pig dung with water at a ratio of 3:2:5 resulted in a 10% increase in methane production. In yet another study, ref. [35] established that mono-digestion of either chicken or goat manure alone resulted in lower biomethane production compared to co-digestion of chicken and goat manure, attributing that to the balance of micro- and macronutrients that favour microbial metabolism and pH regulation in a co-digestion set-up. Meanwhile, use of a single type of feedstock may result in poor biogas yields if the feedstock used is either recalcitrant to digestion or has a low carbon to nitrogen (C:N) ratio [13]. Other advantages of resorting to biogas as an alternative source of energy include the fact that the production of biogas does not need external application of energy (besides the feedstock), and that it is a simple and low-cost technology that is easy to set up [13]. In view of the rugged terrain characteristics of many rural settings, low population density, as well as the often-irregular patterns of household distribution, the cheaper and technically viable option is to decentralise the energy distribution system by setting up small-scale anaerobic digesters household by household [38]. It is estimated that the cost opportunity for a unit of biogas energy over a digester's 15 to 20-year life span is bound to be lower than either a unit of solar energy or the cost of extending a conventional electric grid [56]. Furthermore, estimates report that, with a supply of around 25 kg of animal manure per day, biogas equivalent to 2 L of kerosine can be produced a day, which is enough to meet the energy cooking needs of a family of six [36]. Perhaps the standout advantages of converting animal manure into biogas are that (i) the biodigester facility can be located anywhere where sufficient biomass feedstock is available, making it particularly suitable for rural areas where farming is the main economic activity; (ii) power generation is not time-bound and can be generated when and where needed, as long as sufficient biomass feedstock is available; and (iii) the generation of gas or electricity or both in a rural setting promotes industrialisation of such communities [27]. Additionally, unlike solar energy, biogas can be easily stored without the need for batteries [9]. Also, although the primary recognized applications of digestate are as a soil supplement through land application and as a biofertiliser, within the realm of a bio-based economy the digestate can also be used for various other value-added products such as algae cultivation and biosorbent production [57]. These advancements underscore the need for a shift towards leveraging animal manure as a valuable resource not only for bioenergy production but also for promoting sustainable development as well

as mitigating environmental impacts associated with waste disposal. Therefore, livestock manure management under a biorefinery approach seems a fitting solution for future sustainable development that meets the demands of a circular bioeconomy.

However, despite the enormous potential that biogas has of transforming the fortunes of citizens in rural SSA, the biggest hurdle to the adoption of this technology is that it is seen as too complicated and expensive [56]. The claim is not without merit, because the initial investment costs, especially the costs of either buying a prefabricated biodigester or the materials needed for constructing a biodigester, are usually too steep for poor rural households to foot in a single payment [37]. The traditional brick dome biodigesters (Figure 2), while reliable and durable, generally require expertise to construct, in addition to the high cost of the materials required [26].

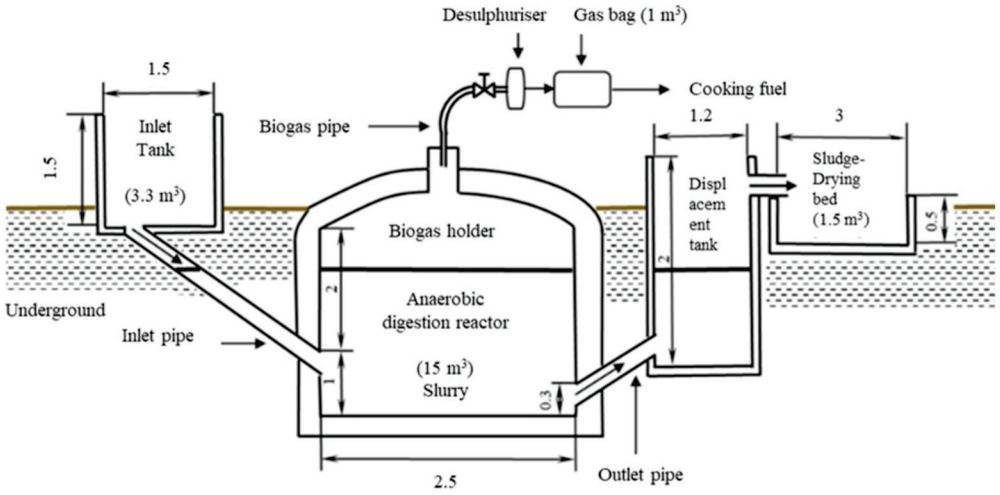

Figure 2. Schematic diagram of a fixed-dome biogas digester with dimensions measured in meters [58].

Biogas technology does, however, become cheaper in the medium to long-term when taking into consideration the health benefits, the lower time and/or cost spent on firewood collection/purchase, as well as the lower time spent on cooking. There is a need for an integrative strategy aimed at ensuring the full participation and technology buy-in of the target rural communities. Currently, the major limitation to the rollout of biogas technology in sub-Saharan Africa is that, while most national governments in the region mention the word 'biomass' in their renewable energy policy documents, most lack concise implementation timelines and methodologies and thus the rate of transformation of policy into reality on the ground remains low [59–62]. By contrast, in China, for example, renewable energy policies have been used to support the installation of household scale digesters in rural areas, which now account for 70% of China's installed biogas capacity [63]. The technology buy-in of rural communities should be coupled with information dissemination about the potential of animal manure in not only easing energy poverty but also eradicating the health risks associated with indoor house pollution emanating from the use of wood fuel, supporting conservation of forests, and supporting employment creation as well as a general advancement in the quality of life. Admittedly, this will require decentralisation and devolution of powers from national-level to community-level leadership structures. Also, apart from local utilisation, biogas cannot be easily liquified and bottled for sale or export unless it is further enriched to increase its C:N ratio, which can present huge technical challenges. Another potentially limiting factor in the production of biogas from animal manure is the availability of water. Water is needed for both animal consumption as well as for feeding into the anaerobic digesters [50]. However, because of climate change, sub-Saharan Africa is one of the regions hardest hit by recurring droughts and above-average temperature increases, which is negatively impacting on animal husbandry and, potentially,

biogas production. The success of AD systems is intimately tied to water-to-manure ratio, making water an unarguably critical factor for optimal microbial activity and sustainable biogas production [38,64]. Inadequate water provision can induce AD-process instability, reduced gas production, and extended retention times, thereby affecting the economic viability of biogas projects [65–67]. Furthermore, fluctuations in moisture content within the feedstock can alter the microbial community composition, potentially fostering the growth of acid-forming bacteria and the subsequent deterioration of the overall biogas quality [67,68].

Addressing these intricate microbial dynamics in the wake of a water-scarcity framework is essential for optimising AD performance in SSA. Consequently, water availability for biogas production requires an effective multifaceted approach encompassing technological innovation and policy intervention [37,38]. Prospective mitigation strategies would aim at bolstering water accessibility, advocating for sustainable water management practices, and ensuring the resilience of AD systems in the face of climate variability [15,38,50]. According to [50] 60% of 700 biodigesters in Ethiopia were non-operational due to lack of water. Hence, dry savannas and desert environments require careful consideration for the functioning of biogas particularly in dry seasons [38] considering that, already, 40% of the SSA population is faced with water shortages even for drinking and cooking. To mitigate against water scarcity, induced limitations on biogas production, ref. [50] have suggested a combination of water harvesting techniques, including rainwater harvesting and storage, domestic water recycling and aquaculture. While water harvesting may ensure water availability for digesters particularly during the rainy season, thereby ensuring continuous production of biogas, it may not be easy to harvest enough water to last through both the wet and dry seasons, with the usual situation likely to be compounded by droughts. On the other hand, drawing water is already a daily chore in resource-poor settings of SSA, and the practice is made more difficult by the excessive distances travelled to fetch water for domestic use [37,38,50,69], which makes it an almost impossible supposition for poor villagers to be fetching water for biogas digesters. In another study, however, ref. [38] suggest, based on laboratory-scale biodigester experiments, a redesign of digesters to incorporate larger inlet and outlet pipes to enable use of undiluted fresh dung, which proved to produce more methane per mass of substrate compared to the currently adopted 1:1 substrate to water ratio. With further research, this approach has the potential to increase the success of anaerobic digester technology in resource-poor, drought-ravaged settings. What may be a limitation, though, is the requirement for fresh dung, which may require that livestock be penned every night to ensure substrate availability.

Holistically, however, governmental support through conducive policies and regulatory frameworks is crucial for overcoming water availability challenges in AD projects. Governments could plug this gap by investing more in water resource management, such as in the construction of dams as well as the construction of wind turbines for underground water extraction. This will not only make AD technology technically more viable but will also go a long way toward improving the quality of life owing to constant water availability. Also, governments, as custodians of policy, need to promote the adoption of biogas technology by removing policy red-tape and providing an enabling environment for public–private partnerships, which are critical for unveiling financial support for initial investments, as well as integrating water management considerations into broader energy and agricultural policies [13,37,50]. The establishment of clear guidelines for water use in AD systems, along with the enforcement of standards, can create an enabling environment for sustainable biogas production [38,50]. Collaborative efforts between governments, international organisations, and private stakeholders are essential for developing comprehensive policies that address water-scarcity challenges holistically [37,38,64].

2.3. Prospects for Future Advancements

The anaerobic digestion technology for biogas production still has room for expansion through a combination of relatively inexpensive policy initiatives and the development

of new technology combinations [56]. For example, the over-reliance on fixed-dome and floating-drum digesters has contributed to the low adaptation of biogas technology in sub-Saharan Africa due to the need for large quantities of bricks, concrete, and steel, resulting in steep initial costs for poor rural households. However, there are alternative biogas technologies like the FlexiBiogas system (developed by the Kenyan Company Biogas International Limited (BIL), (Nairobi, Kenya)) which is portable and expandable, has a shorter retention time, can be transported easily and at lower cost, and does not require skilled technicians for installation, making it suitable for use in rural communities where fuelwood consumption is highest [28]. Additionally, the FlexiBiogas system can produce biogas using different kinds of feedstock such as kitchen waste, animal manure, and agricultural residue, and with dung from just one or two cows in an integrated farming system, the system can produce approximately 1.2 m^3 of biogas daily in addition to the benefits of by-products like biofertiliser, making it suitable for uptake by poor rural households [28]. Research also suggests that the use of mixed animal manure–crop residue–grass feedstocks in anaerobic digestor technology not only results in significantly increased biogas output as compared to the mono-digestion of cow dung but also goes a long way toward augmenting the otherwise insufficient manure-based feedstock [70]. Considering that rural economies are agro based, the harvesting of crop residues after a farming season will not only help in preserving them as feedstock for biogas production but will also help as cattle feed during the winter when pastures are depleted, which will help farmers to curb cattle loses. These initiatives, if adopted, may translate into more efficient anaerobic digester systems and reduce the high failure rates currently being experienced. To reduce the costs of fixed-dome anaerobic digestor systems, construction materials should be sourced locally. For instance, groups of families could form brick-laying cooperatives that would ensure that they have enough bricks for bioreactor construction as well as for sale, which could augment their income. To increase the competitiveness of anaerobic digestor systems, and to sway the preference of rural people from a firewood-based energy economy to sustainable waste-to-energy systems such as biogas, there is need for a thorough assessment of biogas technologies from both economic and environmental perspectives to better understand the trade-offs between biogas yields and the costs associated with installation and maintenance of bioreactor systems.

Another of the available low-cost biogas digester technologies is the low-cost polyethylene tube digester (Figures 3 and 4) that was developed by GTZ/EnDev project in Bolivia, which has been applied in Bolivia, Peru, Ecuador, Colombia, Centro America, and Mexico since 2010 [71]. According to [71], this kind of biogas digester costs between 93 Euro and 148 Euro as of 2010 (USD 100.94–USD 160.63, January 2024 exchange rate), and it could produce enough biogas for cooking and lighting for 4–5 h after charging it with 20 kg of cow dung or any animal dung plus 60 L of water. Furthermore, the author states that installation of this digester takes at most a day, including time spent on excavating the trench.

As technology improves, the cost of biodigesters should keep decreasing so that even poor rural households can afford them. Both the FlexiBiogas system as well as the polyethylene tube digesters are low costs initiatives, with the former having a slight advantage over the latter in that no excavation is needed for the biogas digester. Additionally, the FlexiBiogas system uses less water than the polyethene biogas digester, making it more suitable for sub-Saharan Africa where the climate is getting drier due to climate change.

Policy-wise, governments should promote public–private partnerships and incentives-based bioenergy policies that are adequately supported by action plans as well as monitoring and evaluation strategies [53]. For instance, the South African renewable energy masterplan is anchored by four pillars, one of which reads, "Building local capabilities in terms of skills and technological innovation, to enable the rollout of renewable energy and storage technologies and associated industrial development" [42]. If sub-Saharan African governments must be true to the aim of turning around the energy situation in their rural areas and to adopting carbon neutral clean energy systems, then skills development must

be aggressively pursued as it is one of the cogs that drive the transformation of policy into practice.

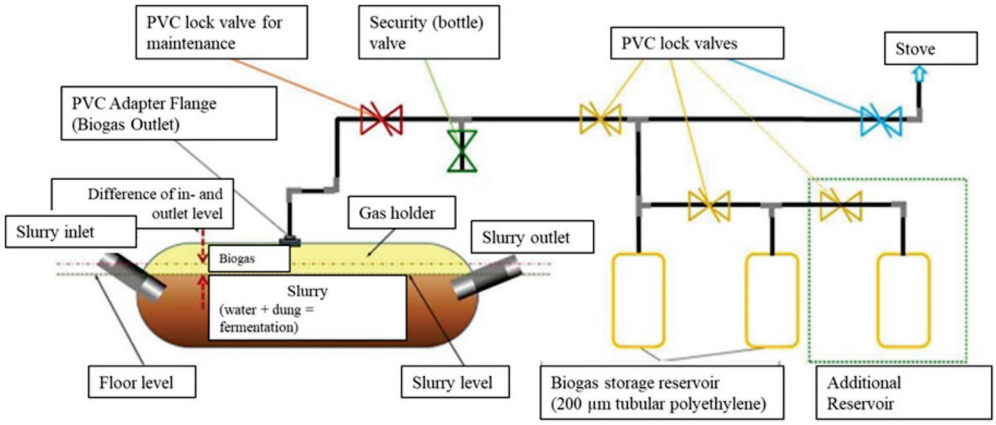

Figure 3. Schematic diagram of a low-cost polyethylene tube biogas digester, complete with biogas supply lines [71].

Figure 4. Open and closed trench for a tube digester in the Bolivian Altiplano [71].

To increase the uptake and feasibility of the anaerobic biogas digester technology in rural areas, research should also be directed at enhancing biogas output. To that end, several research studies have been conducted to assess the effectiveness of applying 'accelerators' to the anaerobic digestion tanks/bags in increasing biogas output. The study by [72] found that supplementation of a manure slurry with 2% by weight (wt%) of metal-oxide (iron oxides (30–45%)—including magnetite (Fe_3O_4) and hematite (Fe_2O_3), carbon (char or coke fines, 8–20%), and other metal (Na, Mg, K, Al, etc.) oxides)-rich bag-filter-gas dust from an iron processing plant resulted in a 51.3% increase in methane yield as compared to the control digester. They attributed the increase to the improved electron-transport capacity of the anaerobic digester, resulting in increased redox potentials. These observations of Wang et al. corroborate the findings of an earlier study by [73] who observed increased biogas production as well as shortened digestion periods when the substrate was supplemented with iron (Fe) salts, including $Fe_2(SO_4)_3$, $Fe(NO_3)_3$, $FeCl_3$, and $FeCl_2$. The use of iron filings to maximise biogas production from cow dung was corroborated by [74], who observed that supplementing a cow dung and jatropha-fruit-exocarp mixture with 10 g of iron fillings resulted in the production of 586 mL of biogas/day from a 1000 mL slurry as compared to 77 mL of biogas from 1000 mL of cow dung alone. However, while the results were positive for iron fillings, iron oxides, and/or iron salts, a study by [75] revealed that using zinc oxide nanoparticles as feed additives in an anaerobic digester reduced methane production by at least 84.55% owing to a reduction in the abundances of functional bacteria in the families

Ruminococcaceae and *Lachnospiraceae*, as well as a massive 96.82% reduction of bacteria in the *Methanothermobacter* genus leading to poor fermentation and methanogenesis, respectively. In yet another promising study, however, ref. [76] observed that adding carbon materials as additives in anaerobic digesters significantly increased biogas yield by as much as 30–70%, an observation that they attributed to increased methanogenesis because of the conductive properties of carbon that facilitate direct interspecies electron transfer between fermenting bacteria and methanogens. While these research studies point to more efficient anaerobic digester systems that can result in more biogas being produced from the same amount of substrate compared to non-supplemented digesters, they may not be suitable for recommendation to poor rural households since this may become an additional cost to them. That said, further research needs to be performed into how to improve anaerobic digester efficiency while bearing in mind poor-resource settings.

3. Conclusions

The scrutiny of animal manure as an alternative bioenergy resource in rural sub-Saharan Africa reveals a multifaceted tableau of insights, opportunities, challenges, and an auspicious outlook. While animal manure can be directly burned to produce heat energy, this not only leads to inefficient utilisation of the resource but also results in indoor air pollution leading to a plethora of respiratory health complications. The cleaner and more efficient option, therefore, is to use animal manure as feedstock for the generation of biogas using anaerobic digester (AD) technology. Theoretically, the sub-Saharan Africa region has adequate livestock to produce enough manure to feed biogas digesters for the generation of clean energy. Pragmatically, however, the uptake of AD technology in sub-Saharan Africa is very low compared to developing nations of Asia, and therefore the existence of renewable resources has not been fully exploited for the betterment of people's livelihoods in this region. While international collaborators have helped to kick-start AD technology in SSA, this initiative has not been met with commensurate policy frameworks, and this combined with a lack of skilled technicians, lack of funding, inefficient feedstock utilisation, season drought leading to lack of water, and the inability to repair damaged biogas infrastructure among other factors has resulted in a near collapse of the African Biogas Initiative. Additionally, research-level successes have not been translated into on-field practice. There is a need to close the gap between research-level knowledge and practical, on-field implementation that requires implementation of facilitative rather than prohibitive policies, investment in technical training, and the raising of awareness of the benefits of biogas, especially among rural communities, in order to tap into the transformative capacity of animal manure as a clean bioenergy resource for sustainable energy development.

Author Contributions: Conceptualisation, T.S. and J.D.U.; writing—original draft preparation, T.S. and J.D.U.; writing—review and editing, T.S. and J.D.U. All authors have read and agreed to the published version of the manuscript.

Funding: This research received no external funding.

Acknowledgments: The authors acknowledge their respective institutions for their time spent working on this article.

Conflicts of Interest: The authors declare no conflicts of interest.

References

1. Tomala, J.; Mierzejewski, M.; Urbaniec, M.; Martinez, S. Towards Sustainable Energy Development in Sub-Saharan Africa: Challenges and Opportunities. *Energies* **2021**, *14*, 6037. [CrossRef]
2. Rahman, K.M.; Harder, M.K.; Woodard, R. Energy Yield Potentials from the Anaerobic Digestion of Common Animal Manure in Bangladesh. *Energy Environ.* **2018**, *29*, 1338–1353. [CrossRef]
3. Copinschi, P. Energy and the Economy in Sub-Saharan Africa. In *The Palgrave Handbook of International Energy Economics*; Springer: Berlin/Heidelberg, Germany, 2022.

4. Hanif, I. Impact of Economic Growth, Nonrenewable and Renewable Energy Consumption, and Urbanization on Carbon Emissions in Sub-Saharan Africa. *Environ. Sci. Pollut. Res.* **2018**, *25*, 15057–15067. [CrossRef] [PubMed]
5. Bekun, F.V.; Alola, A.A. Determinants of Renewable Energy Consumption in Agrarian Sub-Sahara African Economies. *Energy Ecol. Environ.* **2022**, *7*, 227–235. [CrossRef]
6. Lawal, A.I. Determinants of Renewable Energy Consumption in Africa: Evidence from System GMM. *Energies* **2023**, *16*, 2136. [CrossRef]
7. Szymajda, A.; Łaska, G.; Joka, M. Assessment of Cow Dung Pellets as a Renewable Solid Fuel in Direct Combustion Technologies. *Energies* **2021**, *14*, 1192. [CrossRef]
8. Tucho, G.T.; Nonhebel, S. Bio-Wastes as an Alternative Household Cooking Energy Source in Ethiopia. *Energies* **2015**, *8*, 9565–9583. [CrossRef]
9. Wardle, J.M.; Fischer, A.; Tesfaye, Y.; Smith, J. Seasonal Variability of Resources: The Unexplored Adversary of Biogas Use in Rural Ethiopia. *Curr. Res. Environ. Sustain.* **2021**, *3*, 100072. [CrossRef] [PubMed]
10. Michoud, B.; Hafner, M. Energy Access in Sub-Saharan Africa: General Context. In *Financing Clean Energy Access in Sub-Saharan Africa*; Springer: Berlin/Heidelberg, Germany, 2021; pp. 7–26.
11. Dovie, D.B.K.; Witkowski, E.T.F.; Shackleton, C.M. The Fuelwood Crisis in Southern Africa-Relating Fuelwood Use to Livelihoods in a Rural Village. *GeoJournal* **2004**, *60*, 123–133. [CrossRef]
12. Washaya, S.; Washaya, D.D. Benefits, Concerns and Prospects of Using Goat Manure in Sub-Saharan Africa. *Pastoralism* **2023**, *13*, 28. [CrossRef]
13. Mmusi, K.; Mudiwa, J.; Rakgati, E.; Vishwanathan, V. Biogas a Sustainable Source of Clean Energy in Sub Saharan Africa: Challenges and Opportunities. *J. Appl. Mater. Sci. Eng. Res.* **2021**, *5*, 7–12.
14. Liebetrau, J.; O'Shea, R.; Wellisch, M.; Lyng, K.-A.; Bochmann, G.; McCab, B.K.; Harris, P.W.; Lukehurst, C.; Kornatz, P.; Murphy, J.D. *Potential and Utilization of Manure to Generate Biogas in Seven Countries*; International Energy Agency: Paris, France, 2021.
15. Mensah, T.N.O.; Oyewo, A.S.; Breyer, C. The Role of Biomass in Sub-Saharan Africa's Fully Renewable Power Sector—The Case of Ghana. *Renew. Energy* **2021**, *173*, 297–317. [CrossRef]
16. Bedi, A.S.; Pellegrini, L.; Tasciotti, L. The Effects of Rwanda's Biogas Program on Energy Expenditure and Fuel Use. *World Dev.* **2015**, *67*, 461–474. [CrossRef]
17. Gadirli, G.; Pilarska, A.A.; Dach, J.; Pilarski, K.; Kolasa-Więcek, A.; Borowiak, K. Fundamentals, Operation and Global Prospects for the Development of Biogas Plants—A Review. *Energies* **2024**, *17*, 568. [CrossRef]
18. Biodun, M.B.; Fayomi, O.S.I.; Okeniyi, J.O. The Possibility of Biogas Production in Nigeria from Organic Waste Material: A Review. *IOP Conf. Ser. Mater. Sci. Eng.* **2021**, *1107*, 012166. [CrossRef]
19. Tolessa, A.; Zantsi, S.; Louw, T.M.; Greyling, J.C.; Goosen, N.J. Estimation of Biomass Feedstock Availability for Anaerobic Digestion in Smallholder Farming Systems in South Africa. *Biomass Bioenergy* **2020**, *142*, 105798. [CrossRef]
20. Kunatsa, T.; Xia, X. Co-Digestion of Water Hyacinth, Municipal Solid Waste and Cow Dung: A Methane Optimised Biogas–Liquid Petroleum Gas Hybrid System. *Appl. Energy* **2021**, *304*, 117716. [CrossRef]
21. Mulinda, C.; Hu, Q.; Pan, K. Dissemination and Problems of African Biogas Technology. *Energy Power Eng.* **2013**, *5*, 506–512. [CrossRef]
22. Mohammed, A.S.; Atnaw, S.M.; Desta, M. The Biogas Technology Development in Ethiopia: The Status, and the Role of Private Sectors, Academic Institutions, and Research Centers. In *Lecture Notes in Energy*; Springer Science and Business Media Deutschland GmbH: Berlin/Heidelberg, Germany, 2023; Volume 92, pp. 227–243.
23. Shane, A.; Gheewala, S.H.; Kasali, G. Potential, Barriers and Prospects of Biogas Production in Zambia. *J. Sustain. Energy Environ.* **2015**, *6*, 21–27.
24. Mwirigi, J.; Balana, B.B.; Mugisha, J.; Walekhwa, P.; Melamu, R.; Nakami, S.; Makenzi, P. Socio-Economic Hurdles to Widespread Adoption of Small-Scale Biogas Digesters in Sub-Saharan Africa: A Review. *Biomass Bioenergy* **2014**, *70*, 17–25. [CrossRef]
25. Kalina, M.; Ogwang, J.Ò.; Tilley, E. From Potential to Practice: Rethinking Africa's Biogas Revolution. *Humanit. Soc. Sci. Commun.* **2022**, *9*, 374. [CrossRef]
26. ESMAP. *The Power of Dung: Lessons Learned from On-Farm Biodigester Programs in Africa*; World Bank: Washington, DC, USA, 2019.
27. Manala, C.; Madyira, D.; Mbohwa, C.; Shuma, R. Summary-View: Biomass Anaerobic Respiration Technology in South Africa. In Proceedings of the 7th International Conference on Appropriate Technology, Victoria Falls, Zimbabwe, 23–26 November 2016; pp. 27–41.
28. Rota, A.; Sehgal, K. *FlexiBiogas—A Climate Change Adaptation and Mitigation Technology*; IFAD Rural: Rome, Italy, 2014.
29. Onwosi, C.O.; Ozoegwu, C.G.; Nwagu, T.N.; Nwobodo, T.N.; Eke, I.E.; Igbokwe, V.C.; Ugwuoji, E.T.; Ugwuodo, C.J. Cattle Manure as a Sustainable Bioenergy Source: Prospects and Environmental Impacts of Its Utilization as a Major Feedstock in Nigeria. *Bioresour. Technol. Rep.* **2022**, *19*, 101151. [CrossRef]
30. Nayal, F.S.; Mammadov, A.; Ciliz, N. Environmental Assessment of Energy Generation from Agricultural and Farm Waste through Anaerobic Digestion. *J. Environ. Manag.* **2016**, *184*, 389–399. [CrossRef] [PubMed]
31. Akhator, P.; Musa, B. Anaerobic Co-Digestion of Food Waste and Cow Dung in a Pilot Fixed-Dome Bio-Digester for Biogas Production. *Int. J. Eng. Sci. Appl.* **2022**, *6*, 56–64.

32. Liang, J.; Zhang, R.; Chang, J.; Chen, L.; Nabi, M.; Zhang, H.; Zhang, G.; Zhang, P. Rumen Microbes, Enzymes, Metabolisms, and Application in Lignocellulosic Waste Conversion—A Comprehensive Review. *Biotechnol. Adv.* **2024**, *71*, 108308. [CrossRef] [PubMed]
33. Liang, J.; Fang, W.; Wang, Q.; Zubair, M.; Zhang, G.; Ma, W.; Cai, Y.; Zhang, P. Metagenomic Analysis of Community, Enzymes and Metabolic Pathways during Corn Straw Fermentation with Rumen Microorganisms for Volatile Fatty Acid Production. *Bioresour. Technol.* **2021**, *342*, 126004. [CrossRef]
34. Gupta, K.K.; Aneja, K.R.; Rana, D. Current Status of Cow Dung as a Bioresource for Sustainable Development. *Bioresour. Bioprocess.* **2016**, *3*, 28. [CrossRef]
35. Nkosi, S.M.; Lupuleza, I.; Sithole, S.N.; Zelda, Z.R.; Matheri, A.N. Renewable Energy Potential of Anaerobic Mono-and Co-Digestion of Chicken Manure, Goat Manure, Potato Peels and Maize Pap in South Africa. *S. Afr. J. Sci.* **2021**, *117*, 1–8. [CrossRef] [PubMed]
36. Ratminingsih; Jumadi, J. A Study on the Potential of Cow Dung Waste as an Environmentally Friendly Alternative Energy Source. *Adv. Soc. Sci. Educ. Humanit. Res.* **2021**, *528*, 76–80.
37. Smith, J.; Balana, B.B.; Black, H.; von Blottnitz, H.; Casson, E.; Glenk, K.; Langan, S.; Matthews, R.; Mugisha, J.; Smith, P.; et al. The Potential of Small-Scale Biogas Digesters to Alleviate Poverty and Improve Long Term Sustainability of Ecosystem Services in Sub-Saharan Africa. In Proceeding of the 1st World Sustainability Forum, Online, 13–15 September 2021; Volume 5, pp. 2911–2942.
38. Wardle, J.; Dionisi, D.; Smith, J.; Wardle, J.; Smith, J. Investigating the Challenges of Biogas Provision in Water Limited Environments through Laboratory Scale Biodigesters. *Int. J. Sustain. Energy* **2023**, *42*, 829–844. [CrossRef]
39. Libaisi, J.; Njenga, M. Biogas as a Smart Investment for Women's Empowerment and Livelihood Enhancement. In *Recovering Bioenergy in Sub-Saharan Africa: Gender Dimensions, Lessons and Challenges*; CGIAR: Bogor Barat, Indonesia, 2020; pp. 33–38.
40. Amigun, B.; Von Blottnitz, H. Capacity-Cost and Location-Cost Analyses for Biogas Plants in Africa. *Resour. Conserv. Recycl.* **2010**, *55*, 63–73. [CrossRef]
41. Dahunsi, O.S.; Shoyombo, A.; Fagbiele, O. Biofuel Development in Sub-Saharan Africa. In *Anaerobic Digestion*; IntechOpen: London, UK, 2019; pp. 1–13.
42. NDP. *South African Renewable Energy Masterplan (SAREM): An Industrial and Inclusive Development Plan for the Renewable Energy and Storage Value Chains by 2030*; WDB: Pretoria, South Africa, 2023.
43. Kaifa, J.; Parawira, W. A Study of the Current State of Biogas Production in Zimbabwe: Lessons for Southern Africa. *Biotechnol. Microbiol.* **2019**, *13*, 60–68. [CrossRef]
44. Kajau, G.; Madyira, D.M. Analysis of the Zimbabwe Biodigester Status. In Proceedings of the Procedia Manufacturing; Elsevier B.V.: Amsterdam, The Netherlands, 2019; Volume 35, pp. 561–566.
45. Tesfay, A.H.; Hailu, M.H.; A Gebrerufael, F.; Adaramola, M.S. Implementation and Status of Biogas Technology in Ethiopia- Case of Tigray Region. *Momona Ethiop. J. Sci.* **2021**, *12*, 257–273. [CrossRef]
46. Surroop, D.; Bundhoo, Z.M.A.; Raghoo, P. Waste to Energy through Biogas to Improve Energy Security and to Transform Africa's Energy Landscape. *Curr. Opin. Green. Sustain. Chem.* **2019**, *18*, 79–83. [CrossRef]
47. Mukeshimana, M.C.; Zhao, Z.Y.; Ahmad, M.; Irfan, M. Analysis on Barriers to Biogas Dissemination in Rwanda: AHP Approach. *Renew. Energy* **2021**, *163*, 1127–1137. [CrossRef]
48. Hewitt, J.; Holden, M.; Robinson, B.L.; Jewitt, S.; Clifford, M.J. Not Quite Cooking on Gas: Understanding Biogas Plant Failure and Abandonment in Northern Tanzania. *Renew. Sustain. Energy Rev.* **2022**, *165*, 112600. [CrossRef]
49. Lohani, S.P.; Dhungana, B.; Horn, H.; Khatiwada, D. Small-Scale Biogas Technology and Clean Cooking Fuel: Assessing the Potential and Links with SDGs in Low-Income Countries—A Case Study of Nepal. *Sustain. Energy Technol. Assess.* **2021**, *46*, 101301. [CrossRef]
50. Bansal, V.; Tumwesige, V.; Smith, J.U. Water for Small-Scale Biogas Digesters in Sub-Saharan Africa. *GCB Bioenergy* **2017**, *9*, 339–357. [CrossRef]
51. Ndambi, O.A.; Pelster, D.E.; Owino, J.O.; de Buisonjé, F.; Vellinga, T. Manure Management Practices and Policies in Sub-Saharan Africa: Implications on Manure Quality as a Fertilizer. *Front. Sustain. Food Syst.* **2019**, *3*, 29. [CrossRef]
52. Graham, M.W.; Butterbach-Bahl, K.; du Toit, C.J.L.; Korir, D.; Leitner, S.; Merbold, L.; Mwape, A.; Ndung'u, P.W.; Pelster, D.E.; Rufino, M.C.; et al. Research Progress on Greenhouse Gas Emissions from Livestock in Sub-Saharan Africa Falls Short of National Inventory Ambitions. *Front. Soil Sci.* **2022**, *2*, 927452. [CrossRef]
53. Benti, N.E.; Gurmesa, G.S.; Argaw, T.; Aneseyee, A.B.; Gunta, S.; Kassahun, G.B.; Aga, G.S.; Asfaw, A.A. The Current Status, Challenges and Prospects of Using Biomass Energy in Ethiopia. *Biotechnol. Biofuels* **2021**, *14*, 209. [CrossRef]
54. Rasimphi, T.E.; Tinarwo, D. Relevance of Biogas Technology to Vhembe District of the Limpopo Province in South Africa. *Biotechnol. Rep.* **2020**, *25*, e00412. [CrossRef] [PubMed]
55. Wang, Y.; Ghimire, S.; Wang, J.; Dong, R.; Li, Q. Alternative Management Systems of Beef Cattle Manure for Reducing Nitrogen Loadings: A Case-Study Approach. *Animals* **2021**, *11*, 574. [CrossRef]
56. Brown, V.J. Biogas a Bright Idea for Africa. *Environ. Health Perspect.* **2006**, *114*, A300–A303. [CrossRef] [PubMed]
57. Singh, P.K.; Mohanty, P.; Mishra, S.; Adhya, T.K. Food Waste Valorisation for Biogas-Based Bioenergy Production in Circular Bioeconomy: Opportunities, Challenges, and Future Developments. *Front. Energy Res.* **2022**, *10*, 903775. [CrossRef]

58. Hanum, F.; Nagahata, M.; Nindhia, T.G.T.; Kamahara, H.; Atsuta, Y.; Daimon, H. Evaluation of a Small-Scale Anaerobic Digestion System for a Cattle Farm under an Integrated Agriculture System in Indonesia with Relation to the Status of Anaerobic Digestion System in Japan. *Sustainability* **2023**, *15*, 3833. [CrossRef]
59. *GoZ Ministry of Energy and Power Development National Renewable Energy Policy*; Ministry of Energy, Republic of Zimbabwe: Harare, Zimbabwe, 2019; pp. 1–58.
60. NEP. *The-National-Energy-Policy-2019*; The Ministry of Energy: Lusaka, Zambia, 2019; pp. 1–58.
61. CPP. *Cameroon Country Priority Plan and Diagnostic of the Electricity Sector*; Government of the Republic of Cameroon: Younde, Cameroon, 2021; pp. 1–54.
62. GovNamibia. *Government of the Republic of Namibia Renewable Energy Policy*; Ministry of Mines and Energy: Windhoek, Namibia, 2017; pp. 1–64.
63. IEA. *Outlook for Biogas and Biomethane: Prospects for Organic Growth*; International Energy Agency: Paris, France, 2020; pp. 1–93.
64. Rupf, G.V.; Bahri, P.A.; De Boer, K.; McHenry, M.P. Barriers and Opportunities of Biogas Dissemination in Sub-Saharan Africa and Lessons Learned from Rwanda, Tanzania, China, India, and Nepal. *Renew. Sustain. Energy Rev.* **2015**, *52*, 468–476. [CrossRef]
65. Afzal, I.; Shinwari, Z.K.; Sikandar, S.; Shahzad, S. Plant Beneficial Endophytic Bacteria: Mechanisms, Diversity, Host Range and Genetic Determinants. *Microbiol. Res.* **2019**, *221*, 36–49. [CrossRef]
66. Bhatt, A.H.; Tao, L. Economic Perspectives of Biogas Production via Anaerobic Digestion. *Bioengineering* **2020**, *7*, 74. [CrossRef]
67. Borgström, Y. *Pretreatment Technologies to Increase the Methane Yields by Anaerobic Digestion in Relation to Cost Efficiency of Substrate Transportation. Master of Science*; Linkoping Institute of Technology: Linkoping, Sweden, 2011.
68. Klocker, D. Impact of Intermediate and End-Products of Anaerobic Digestion on Sludge Filterability: Understanding Fouling in AnMBRs. Master's Thesis, Delft University of Technology, Delft, The Netherlands, 2017.
69. Mengistu, M.G.; Simane, B.; Eshete, G.; Workneh, T.S. Factors Affecting Households' Decisions in Biogas Technology Adoption, the Case of Ofla and Mecha Districts, Northern Ethiopia. *Renew. Energy* **2016**, *93*, 215–227. [CrossRef]
70. Robin, T.; Ehimen, E. Exploring the Potential Role of Decentralised Biogas Plants in Meeting Energy Needs in Sub-Saharan African Countries: A Techno-Economic Systems Analysis. *Sustain. Energy Res.* **2024**, *11*, 8. [CrossRef]
71. Lüer, M. Installation Manual for Low-Cost Polyethylene Tube Digesters. Available online: https://energypedia.info/images/1/19/Low_cost_polyethylene_tube_installation.pdf (accessed on 3 April 2024).
72. Wang, K.; Yun, S.; Ke, T.; An, J.; Abbas, Y.; Liu, X.; Zou, M.; Liu, L.; Liu, J. Use of Bag-Filter Gas Dust in Anaerobic Digestion of Cattle Manure for Boosting the Methane Yield and Digestate Utilization. *Bioresour. Technol.* **2022**, *348*, 126729. [CrossRef] [PubMed]
73. Yun, S.; Zhang, C.; Wang, Y.; Zhu, J.; Huang, X.; Du, T.; Li, X.; Wei, Y. Synergistic Effects of Fe Salts and Composite Additives on Anaerobic Digestion of Dairy Manure. *Int. Biodeterior. Biodegrad.* **2019**, *136*, 82–90. [CrossRef]
74. Adekunle, A.S.; Ibitoye, S.E.; Omoniyi, P.O.; Jilantikiri, L.J.; Sam-Obu, C.V.; Yahaya, T.; Mohammad, B.G.; Olusegun, H.D. Production and Testing of Biogas Using Cow Dung, Jatropha and Iron Filins. *J. Bioresour. Bioprod.* **2019**, *4*, 143–148. [CrossRef]
75. Qi, L.; Liu, X.; Miao, Y.; Chatzisymeon, E.; Yang, P.; Lu, H.; Pang, L. Response of Cattle Manure Anaerobic Digestion to Zinc Oxide Nanoparticles: Methane Production, Microbial Community, and Functions. *J. Environ. Chem. Eng.* **2021**, *9*, 106704. [CrossRef]
76. Yun, S.; Fang, W.; Du, T.; Hu, X.; Huang, X.; Li, X.; Zhang, C.; Lund, P.D. Use of Bio-Based Carbon Materials for Improving Biogas Yield and Digestate Stability. *Energy* **2018**, *164*, 898–909. [CrossRef]

energies

MDPI

Article

The Impact of Aluminosilicate Additives upon the Chlorine Distribution and Melting Behavior of Poultry Litter Ash

Izabella Maj [1], Kamil Niesporek [1], Krzysztof Matus [2,*], Francesco Miccio [3], Mauro Mazzocchi [3] and Paweł Łój [4]

[1] Department of Power Engineering and Turbomachinery, Faculty of Energy and Environmental Engineering, Silesian University of Technology, 44-100 Gliwice, Poland; izabella.maj@polsl.pl (I.M.); kamil.niesporek@polsl.pl (K.N.)
[2] Materials Research Laboratory, Faculty of Mechanical Engineering, Silesian University of Technology, 44-100 Gliwice, Poland
[3] Institute of Science, Technology and Sustainability for Ceramics, Italian National Research Council, via Granarolo 64, 84018 Faenza, Italy; francesco.miccio@cnr.it (F.M.); mauro.mazzocchi@issmc.cnr.it (M.M.)
[4] Department of Fundamentals of Machinery Design, Faculty of Mechanical Engineering, Silesian University of Technology, 44-100 Gliwice, Poland; pawel.loj@polsl.pl
* Correspondence: krzysztof.matus@polsl.pl

Abstract: The use of poultry litter (PL) as a sustainable fuel is gaining more attention due to its wide availability and carbon neutrality. However, this type of feedstock is rich in ash and typically contains a high concentration of chlorine (Cl) and alkali elements (Na, K). Therefore, it is likely to cause unwanted issues during combustion and co-combustion, such as chlorine-induced corrosion, ash deposition, and bed agglomeration. In this study, for the first time, the influence of aluminosilicate additives on the above problems of poultry litter was investigated. Three aluminosilicate minerals are under consideration: kaolin, halloysite, and bentonite. Their influence on the chemical composition and meting tendencies of two poultry litter ashes are determined. The investigated ashes, PL1 and PL2, are characterized by different chlorine contents of 6.38% and 0.42%, respectively. The results show that in the case of the chlorine-rich PL1 ash, the additives reduced the chlorine content by up to 45%, resulting in a 3.93% of chlorine in the case of halloysite, 3.48% in the case of kaolin, and 4.25% in the case of bentonite. The additives also positively influenced the shrinkage starting temperature and the deformation temperature of the PL1 ash.

Keywords: biomass; poultry litter; combustion; ash; chlorine corrosion; kaolin; halloysite; bentonite

1. Introduction

A sustainable energy policy based on low- or no-emission energy sources is crucial for meeting climate commitments. Reducing greenhouse gas emissions from fossil fuel combustion is important to limit the greenhouse effect, and therefore, alternative energy sources such as biomass are gaining interest. This is supported by the fact that in 2022, biomass energy production represented 6% of the world's energy demand, comprising 55% of renewable energy generation [1]. Biomass is a versatile energy carrier, which can undergo various conversion processes, such as combustion, pyrolysis, gasification, or hydrothermal carbonization [2–5].

One of the poorly recognized biomass types is poultry litter (PL). It contains mostly animal manure and bedding material, such as straw or sawdust. The number of poultry farms in Europe is growing due to the high local demand for meat and eggs, together with an increase in the export of these products. According to the data [6], 1.4 billion tonnes of manure from farmed animals were produced annually in EU countries and the UK in the period of 2016–2019.

Poultry litter is traditionally used either directly as fertilizer on agricultural land or composted. As a result, this leads to uncontrolled emissions of methane and ammonia,

lowering local air quality [7]. It also contaminates groundwater with pathogens, antibiotic resistance genes (ARGs), and hormones, as well as other pollutants [8].

Therefore, the issue of animal litter utilization has become vital, and its combustion has been established as one of the most desired disposal paths [9,10]. Consequently, this issue has caught the attention of the European Parliament. According to the regulations of the European Parliament and the Council (EU 2017/1262), the combustion of poultry litter on farm premises is allowed [11]. This fact has already been reflected in a growing number of studies concerning poultry litter combustion, such as the study [12] where the combustion of chicken litter along with a 10% addition of straw or wood is claimed to provide self-sufficiency in heating a poultry farm. In addition to the direct combustion of animal-origin biomass, co-combustion with coal or pyrolysis is also proposed in numerous studies [13–15].

Although biomass combustion technology has been well-known and has accompanied humanity since its beginnings, from a technological point of view, it presents us with a series of challenges and issues. Current power boilers were primarily designed for the combustion of conventional fuels such as coal, which have significantly different physical and chemical properties than biomass. Coal, unlike biomass, typically contains low amounts of volatiles and a high sulfur content [16]. Consequently, the most critical factor for the appearance of boiler corrosion in coal combustion is considered to be the temperature of the sulfuric acid dew point [17,18]. On the other hand, in the case of biomass, which is typically low in sulfur, the main issues with its thermal processing arise from its high content of elements such as potassium, sodium, and chlorine [19,20]. Their presence leads to the formation of chlorides and oxides of alkali metals in the ash, promoting ash agglomeration, and slagging [21–26]. Alkali metal chlorides such as NaCl and KCl, with low melting temperatures, are the main compounds responsible for the high-temperature corrosion of boiler heating elements in biomass combustion [19,20,27,28]. They not only contribute to an increased oxidation rate but also lead to the loss of the protective oxide layer, and the formation of cracks and subsurface corrosion mechanisms [19,27,29]. The corrosion process particularly affects alloys based on the formation of protective chromium-rich oxides. Due to active oxidation, the protective layer degrades [21,30,31]. Additionally, besides corrosion, ash deposition on heating surfaces reduces boiler efficiency. To mitigate corrosion problems in biomass-fired power plants, the working steam temperature is typically kept below 540 °C, resulting in a lower efficiency of electricity generation [19,32].

Tackling slagging and ash agglomeration is crucial for the operation of biomass-fired boilers. Therefore, to predict the risk of ash agglomeration and slagging, authors of numerous studies [33,34] recommend relying on ash fusion temperatures (AFT). In general, the higher these temperatures, the lower the risk of ash slagging.

Although relying on AFT can assist in assessing the risk of ash slagging and agglomeration, it does not constitute a solution for these issues. To limit ash deposition, agglomeration, and corrosion processes during biomass combustion, various fuel additives are applied to influence reactions within the combustion zone. These additives are expected to impact the ash's composition, particularly by reducing its chlorine content, and consequently elevate its melting temperatures. Currently, there is significant research interest in additives based on aluminosilicates, with an emphasis on kaolin [24,28,35–39].

Nevertheless, the impact of aluminosilicates other than kaolin remains poorly investigated. Furthermore, the available literature is solely focused on the applications of additives in the combustion of plant-origin biomass and, according to the authors' knowledge, the influence of aluminosilicate additives on animal litter ash has not been tested yet. Therefore, the presented research covers a knowledge gap and provides novel information, that may increase interest in animal-origin biomass utilization. The work aims to determine the influence of three aluminosilicate additives: kaolin, halloysite, and bentonite on the ash properties of two types of poultry litter collected from European poultry farms. The influence of the equal doses of additives on the ashes' characteristics is determined with laboratory characterization, as a first step before the implementation of the process,

taking into account the ashes' chemical composition, chlorine content, melting tendencies, phase composition as well as microstructural characteristics. The presented research can contribute to the increase in the interest in animal waste thermal conversion, therefore increasing the share of renewable energy in the global energy market and strengthening energy production in rural areas.

2. Materials and Methods

2.1. Poultry Litter

Two types of poultry litter, PL1 and PL2, were subjected to investigation in this study. The samples were collected from poultry farms located in central Europe. The samples were air-dried in laboratory conditions at an ambient temperature and milled in a vibrating mill. The samples were characterized in terms of proximate analysis: moisture content via the thermogravimetric method, ash content according to PN-EN ISO 18122:2015 [40], higher heating value (HHV) and lower heating value (LHV) according to PN-EN ISO 18125:2017 [41], as well as an elemental (ultimate) analysis of carbon (C), hydrogen (H), and nitrogen (N) contents according to PN-EN ISO 16948:2015-07 [42], sulfur (S) and chlorine (Cl) contents according to PN-EN ISO 16994:2016-10 [43].

According to the proximate analysis presented in Table 1, sample PL1 is characterized by an ash content of 15.8% (a.r.), an HHV of 16.93 MJ/kg (d.b.), and an LHV of 15.89 MJ/kg (d.b.). Sample PL2 is characterized by a significantly higher ash content of 48.9% (a.r.), which is reflected in lower values of the HHV and LHV, reaching 11.79 and 10.96 MJ/kg (d.b.), respectively.

Table 1. Proximate analysis of the investigated samples (a.r.—as received, d.b.—dry basis).

Sample	Moisture	Ash	Higher Heating Value		Lower Heating Value	
	$M^{a.r.}$	$A^{d.b.}$	$HHV^{d.b.}$	$HHV^{a.r.}$	$LHV^{d.b.}$	$LHV^{a.r.}$
	%	%	MJ/kg	MJ/kg	MJ/kg	MJ/kg
PL1	6.8	15.8	16.93	15.78	15.89	14.81
PL2	8.7	48.9	11.79	10.76	10.96	9.79

According to the elemental analysis presented in Table 2, both the PL1 and PL2 samples contain nitrogen at a relatively high level of 1.53% and 2.60%, respectively. They are characterized by various sulfur contents, 0.09% in sample PL1 and 0.36 in sample PL2, while the chlorine contents are similar, being 0.56% in sample PL1 and 0.47% in sample PL2.

Table 2. Elemental (ultimate) analysis of the investigated samples (dry basis) together with their Cl/S molar ratios.

Sample	C	H	N	S	Cl	Cl/S
	%	%	%	%	%	-
PL1	43.8	4.74	1.53	0.09	0.56	5.64
PL2	30.3	3.85	2.60	0.36	0.47	1.18

The investigated fuels significantly differ in their Cl/S molar ratios, which are calculated as 5.64 for PL1 and 1.18 for PL2. The Cl/S ratio is of great importance due to sulfate formation, a reaction of sulfur with alkali chlorides, resulting in alkali sulfates [44,45]. Sulfur in flue gas mainly exists as SO_2 and to a lesser extent as SO_3 [44]. The equilibrium and reaction rate equations describing this are as follows:

$$SO_2(g) + 1/2O_2(g) \leftrightarrow SO_3(g) \quad (1)$$

Alkali chlorides have a high ability to react with both SO_3 and SO_2 according to the following reactions (2)–(6) [44,46]:

$$SO_3(g) + 2ACl(g) + H_2O(g) \rightarrow A_2SO_4(s) + 2HCl(g) \quad (2)$$

$$ACl + H_2O \rightarrow AOH + HCl \quad (3)$$

$$AOH + SO_2 \rightarrow AHSO_3 \quad (4)$$

$$AHSO_3 + 1/2O_2 \rightarrow AHSO_4 \quad (5)$$

$$AHSO_4 + ACl \rightarrow A_2SO_4 + HCL \quad (6)$$

where A = Na or K.

Therefore, a high sulfur and sulfate content in fuel is expected to reduce the chlorine content in its ash deposits [47,48], thereby limiting the rate of ash deposition and corrosion [47,48].

2.2. Fuel Additives

In this work, three commonly occurring, natural aluminosilicate minerals were selected to serve as fuel additives: kaolin, halloysite, and bentonite. The additives are materials of the clay category whose characteristics and applications were elaborated in detail in [49]. The scanning electron microscope (SEM) pictures of halloysite, kaolin, and bentonite used in this investigation are presented in Figures 1–3.

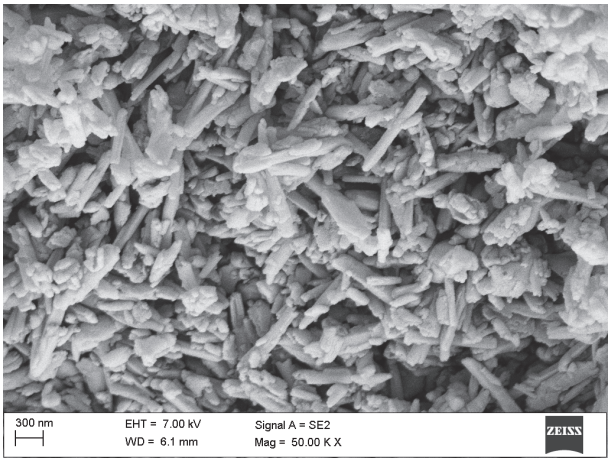

Figure 1. Scanning electron microscope (SEM) image of halloysite [49].

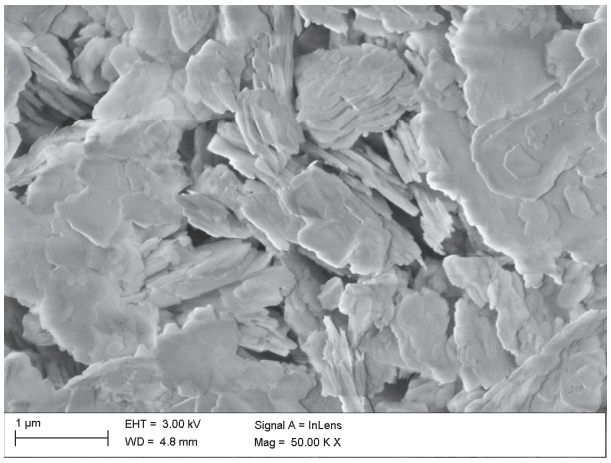

Figure 2. Scanning electron microscope (SEM) image of kaolin [49].

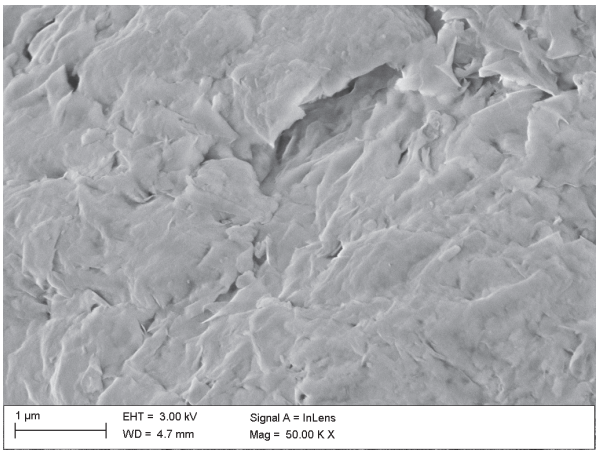

Figure 3. Scanning electron microscope (SEM) image of bentonite [49].

The presented structural analysis of halloysite samples revealed the presence of halloysite nanoplates (HNPs) and halloysite nanotubes (HNTs), while kaolin is a layered silicate mineral that features a predominantly plated structure. Bentonite is a clay consisting mostly of montmorillonite, which, similarly to kaolin, features a plated structure.

Aluminosilicate clays have been considered to be fuel additives due to their favorable characteristics: their easy and safe application, high specific surface area, high porosity, and consequently, high reactivity [50,51]. Studies do not reveal any negative impact of aluminosilicates on the combustion process, such as limitations in their efficiency or generation of pollutants [52,53]. Industrial-application aluminosilicate minerals are chemically stable powders, which results in their convenient application and transportation. Kaolin, halloysite, and bentonite are widely available and do not necessitate costly handling before application. [54].

The application of the aluminosilicate clay powder to the combustion process leads to bonding alkalis in compounds with high melting points, while chlorine is released into flue gas as hydrogen chloride (HCl) [29,55]. According to reactions (7) and (8), aluminosilicates undergo a reaction with potassium chloride (KCl), a compound with a melting point of 770 °C, resulting in the formation of kalsilite ($KAlSiO_4$) and leucite ($KAlSi_2O_6$) with melting points of above 1600 °C and 1500 °C, respectively. Aluminosilicates are proven to react with other potassium compounds: potassium sulfate (K_2SO_4) and potassium carbonate (K_2CO_3) according to reactions (9) and (10). In addition to reactions (7)–(10), the bonding of alkalis can be a multi-staged process, starting at a temperature range below the combustion zone, via the adsorption of the alkali metals on the aluminosilicates' surface [56].

$$Al_2O_3{\cdot}2SiO_2(s) + 2\,KCl(g) + H_2O(g) \rightarrow 2\,KAlSiO_4(s,l) + 2HCl(g) \quad (7)$$

$$Al_2O_3{\cdot}2SiO_2(s) + 2SiO_2(s) + 2\,KCl(g) + H_2O(g) \rightarrow 2\,KAlSi_2O_6(s,l) + 2HCl(g) \quad (8)$$

$$Al_2Si_2O_5(OH)_4(s) + K_2SO_4(g) \rightarrow 2\,KAlSiO_4(s,l) + 2H_2O(g) + SO_3(g) \quad (9)$$

$$Al_2Si_2O_5(OH)_4(s) + K_2CO_3(g) \rightarrow 2\,KAlSiO_4(s,l) + 2H_2O(g) + CO_2(g) \quad (10)$$

The presence of aluminosilicates in the combustion zone leads to the mitigation of unwanted issues connected to the presence of alkalis and chlorine, bed agglomeration in fluidized beds, ash deposition, slagging and fouling on boiler heating surfaces, but also chlorine-induced corrosion by limiting the concentration of chlorine in the ash deposits.

2.3. Ash Preparation and Analyses

The examined poultry litter samples underwent incineration in an air atmosphere in an electric furnace within a consistent temperature zone of 550 °C. The following ash samples were prepared: pure PL1, PL1 with halloysite, PL1 with kaolin, PL1 with bentonite, pure PL2, PL2 with halloysite, PL2 with kaolin, and PL2 with bentonite.

The stoichiometric ratio of the additive can be calculated based on the chlorine content in the fuel, as performed in [35]. With this method, the stoichiometric ratio of the additive (SR) can be calculated according to Equation (11).

$$SR = \frac{M_{Additive}}{M_{Cl_2}} = \frac{258.14\ g}{70.9\ g} = 3.64 \quad (11)$$

This method overlooks several factors including the sulfation of alkali metals, the impurities present in the additives, the incomplete homogenization of the fuel-additive mixture, and the losses of the additives during combustion. Additionally, potential discrepancies may arise for fuels with higher chlorine contents compared to alkali metals, a scenario uncommon in plant-derived biomass but relevant in animal-derived feedstock.

For PL1, whose chlorine content equals 0.56%, the SR is calculated as 2.04%, and for PL2, whose chlorine content equals 0.47%, the SR is 1.71%. Although recommended stoichiometric doses are approximately 2%, based on the authors' previous studies with coal and biomass, the dosage for each additive was increased to 8% of the fuel mass for several reasons, mainly the elevated ash content in the poultry litter, its heterogeneity, and the presence of impurities in the additive. Such properties of poultry litter may cause unfavorable reaction conditions, resulting in the need for over-stoichiometric additive doses.

According to the research presented in the literature, aluminosilicates are usually applied to fuels in doses of 1–15%. In the research [57], biomass pellets produced with kaolin are investigated, and the stoichiometric amount was boosted by 10% to guarantee the effective integration of kaolin into the pellets. As a result, an additive level spanning from 0.6% to 2.3% was applied. However, the research concluded that kaolin's influence on combustion was negligible, largely due to its low levels of additive incorporation. In another study [58], higher additive ratios, of up to 15%, were investigated during the combustion of agricultural biomass. In this case, a swift formation of K–Al/Fe silicates was observed, with the trend rapidly increasing at an additive ratio of up to 12% and gradually rising between 12% and 15%. The application of kaolin to olive cake and wood in a dose of 5% was investigated in [28] and a rise in the initial deformation temperatures was observed.

In the presented research, the ashes obtained by the incineration of poultry litter with and without additives were subjected to elemental analysis, ash fusion temperatures (AFTs) determination, microstructural characterization, and X-ray diffraction (XRD) phase analysis.

The ashes' chemical composition was determined using inductively coupled Plasma-optical emission spectrometry (ICP-OES).

Ash fusion temperatures were determined under oxidizing conditions through the microscope-photographic method according to standard ISO 21404:2020-08 [59]. This process involved identifying and recording the shrinkage starting temperature (SST), deformation temperature (DT), hemisphere temperature (HT), and flow temperature (FT). The maximum testing temperature was 1500 °C.

The structure and morphology of the powders were examined using a high-resolution scanning electron microscope (HRSEM). The examinations were conducted using a Supra 35 scanning electron microscope from Zeiss (Jena, Germany) with an accelerating voltage of 20 kV and magnifications ranging from 100× to 50,000×, equipped with an X-ray detector with energy dispersion (EDS), model EDX UltraDry from Thermo Scientific™ (Waltham, MA, USA). The powders intended for the study were coated with a layer of gold approximately 15 nm thick to dissipate the electric charge.

X-ray powder diffractometry analyses were performed on fine powders in PMMA sample holders minimizing orientation effects. A Bruker D8 Advance (Bruker Co., Billerica, MA, USA) diffractometer with a high-speed SSD Lynxeye detector was used (Theta-Theta Bragg-Brentano geometry configuration and $CuKa_1$ radiation), with a 5–80 2-q range; step: 0.02 deg/s; time: 0.5 s (≈1.5 min equivalent time).

3. Results and Discussion

3.1. Influence of Additives on Chlorine Distribution in Ash

The elemental compositions of the investigated ashes are displayed in Table 3. The chlorine contents have been recalculated taking into account the dilution of ashes with additives (Cl^{rec}).

Table 3. Elemental compositions of the ashes (dry basis).

Sample	Cl	$Cl^{rec.}$	SO_3	K_2O	SiO_2	Fe_2O_3	Al_2O_3	Mn_3O_4	TiO_2	CaO	MgO	P_2O_5	Na_2O	BaO	SrO
PL1	6.38	6.38	1.37	11.2	59.20	2.60	3.51	0.12	0.25	6.53	2.20	5.02	0.68	0.03	0.02
PL1 halloysite	3.42	3.93	1.04	8.40	56.20	6.95	8.57	0.21	1.07	5.45	1.94	4.19	0.68	0.05	0.02
PL1 kaolin	2.97	3.48	0.98	8.53	58.90	2.34	12.30	0.09	0.37	5.41	1.83	4.06	0.58	0.03	0.02
PL1 bentonite	3.74	4.25	1.10	8.55	58.90	2.65	7.00	0.11	0.23	5.63	2.41	4.06	4.55	0.04	0.02
PL2	0.42	0.42	1.30	6.10	65.90	1.90	4.80	0.08	0.26	5.30	1.70	5.20	0.80	0.03	0.01
PL2 halloysite	0.30	0.46	1.20	6.90	60.70	5.20	8.00	0.17	0.87	5.30	1.60	3.90	0.75	0.05	0.02
PL2 kaolin	0.22	0.38	1.10	6.40	66.60	1.70	8.90	0.07	0.31	5.00	1.50	4.20	0.61	0.03	0.01
PL2 bentonite	0.33	0.49	1.00	6.80	65.30	1.90	6.20	0.08	0.21	5.90	1.80	3.40	1.26	0.05	0.02

As presented in Section 2.1, a higher sulfur content in the fuel can contribute to reducing the chlorine content in the ashes. This analogy is illustrated by the analysis of Figure 4. Fuel PL1 with a high Cl/S ratio shows significant chlorine content in the ash—above 6%. Fuel PL2, with a similar chlorine content but a significantly higher sulfur content, has a much lower Cl/S ratio, which results in a much lower chlorine content in the ash, not exceeding 0.5%.

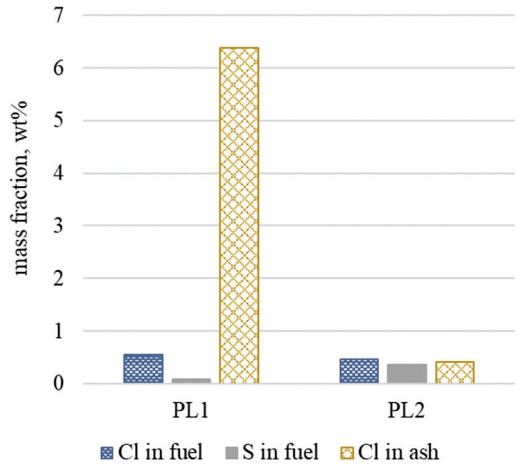

Figure 4. Chlorine and sulfur contents in the fuel samples together with the chlorine content in the ash (dry basis).

The influence of additives on the chlorine content in ashes is presented in Figures 5 and 6. For the PL1 ash, whose initial chlorine concentration in ash is extremely high, it has been visibly reduced as a result of the additives' presence. Chlorine content reductions of 38.46%, 45.51%, and 33.44% are observed in the cases of halloysite, kaolin, and bentonite additions, respectively, being the net of the ash dilution effect due to the additive. The release of chlorine into the gaseous phase took place as a result of the alumina-silication of potassium chlorides. The chlorine is expected to be released in the form of HCl according to Equations (7) and (8).

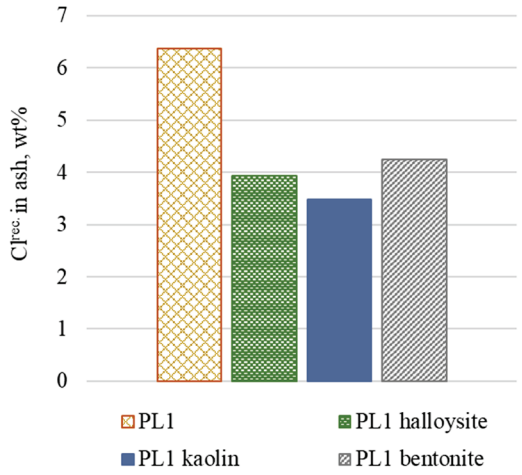

Figure 5. Recalculated chlorine contents in PL1 ashes.

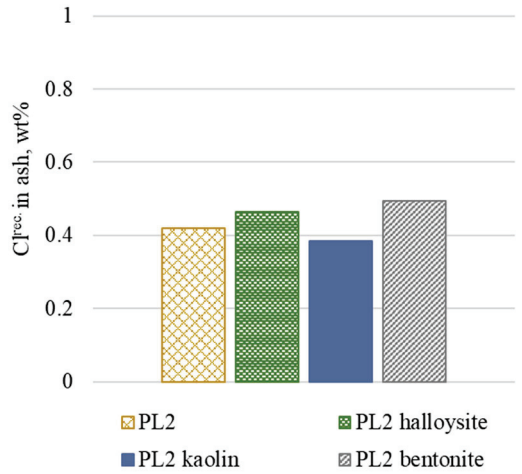

Figure 6. Recalculated chlorine contents in PL2 ashes.

For the PL2 ash, whose initial chlorine concentration is significantly lower, the influence of additives is not clear. In the case of kaolin, a reduction of 8.67% is observed, whereas bentonite and halloysite have no positive effect. Two factors are likely to cause the absence of a clear chlorine reduction. First is the high ash content in PL2 (48.9%), which results in the dilution of the reagents, causing unfavorable conditions for the reactions to occur. Second is the already low chlorine content in the PL2 ash (0.42%), which is a result of the chlorine sulfation reactions taking place during the incineration phase.

3.2. Influence of Additives on Ash Fusion Temperatures

The shrinkage starting temperature (SST), deformation temperature (DT), hemisphere temperature (HT), and flow temperature (FT) of the investigated samples are presented in Table 4 as well as Figures 7 and 8.

Table 4. Ash fusion temperatures of the investigated samples.

Sample	SST	DT	HT	FT
PL1	1040	1170	1330	1370
PL1 halloysite	1130	1210	1280	1300
PL1 kaolin	1100	1270	1330	1380
PL1 bentonite	1150	1220	1300	1350
PL2	1140	1240	1390	1490
PL2 halloysite	1160	1240	1310	1380
PL2 kaolin	1170	1270	1340	1420
PL2 bentonite	1150	1260	1380	1470

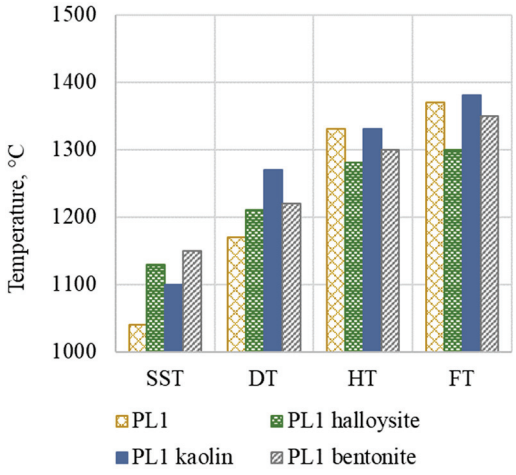

Figure 7. Ash fusion temperatures of the PL1 ashes.

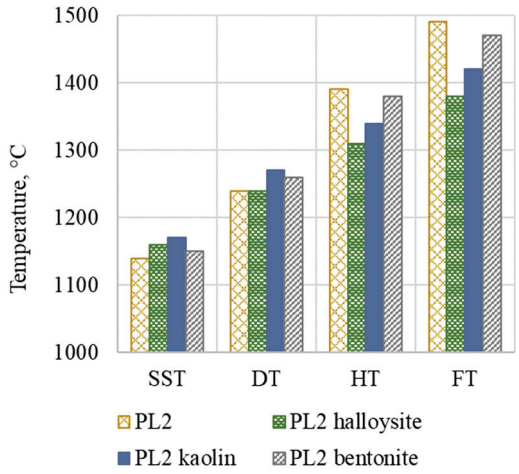

Figure 8. Ash fusion temperatures of the PL2 ashes.

For the PL1 ash, whose shrinkage starting temperature and deformation temperature values are lower than those of the PL2 ash, the presence of additives elevates them. However, the performance of additives in the case of the PL2 ash is not clear, but, what needs to be emphasized is that the SST and DT temperatures of PL2 are already high and comparable to those of coal. No positive change in the hemisphere temperatures and flow temperatures of both the PL1 and PL2 ashes can be observed. These tendencies are in line with other research on the influence of aluminosilicate additives on the AFT of various fuels, where, in the case of low-melting biomass ashes, the clear positive influence was observed by Sobieraj et al. [35], but no clear positive influence was determined in the case of the coal ashes with AFT temperatures exceeding 1100 °C tested by Wang et al. [60].

Therefore, it can be concluded that the performance of additives is particularly effective in the conversion of fuels with low melting temperatures.

3.3. Influence of Additives on Ash Morphology

Figure 9 depicts the PL1 ash with additions of halloysite, kaolin, and bentonite. In comparison, the PL2 ashes appear to be more heterogeneous and irregular, with partially idiomorphic crystalline particles, small platelets, and minute granules in clusters (Figure 10a).

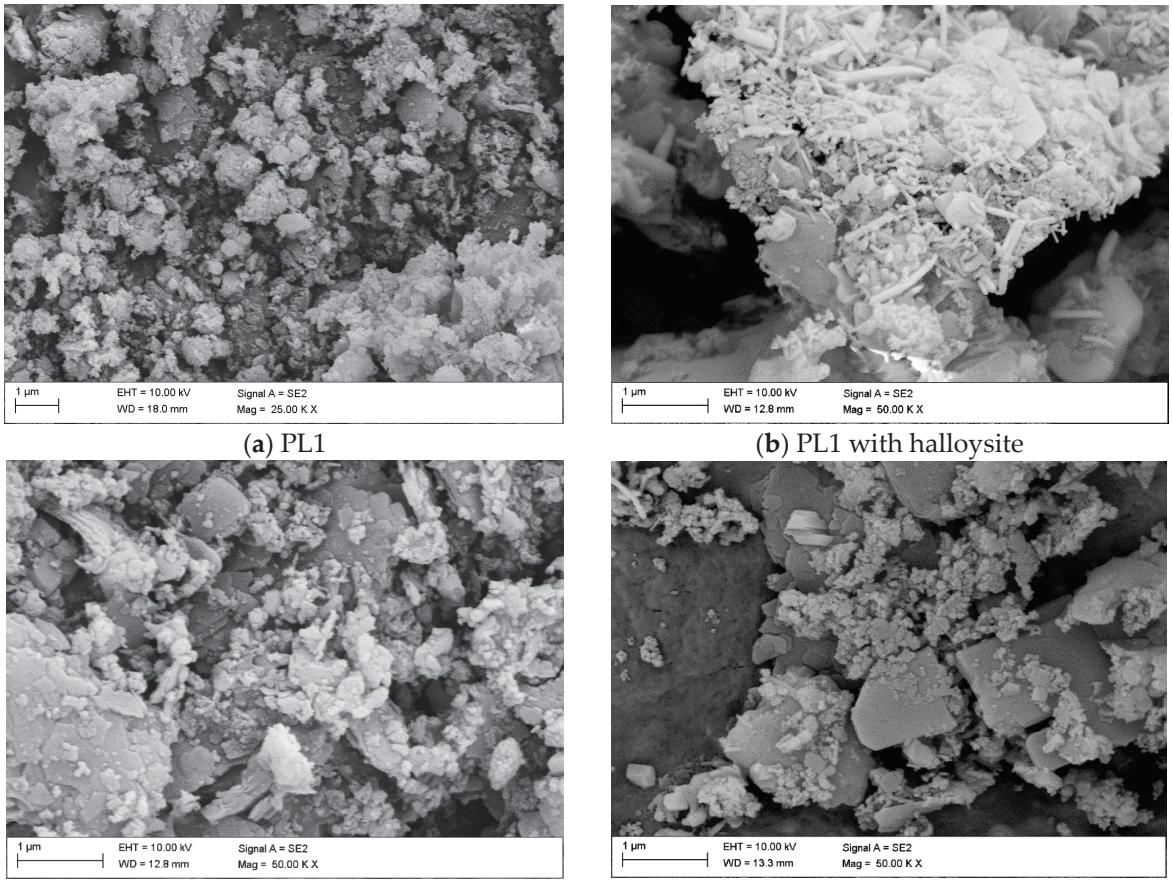

(**a**) PL1 (**b**) PL1 with halloysite

(**c**) PL1 with kaolin (**d**) PL1 with bentonite

Figure 9. SEM pictures of the PL1 ashes without additives (**a**), with halloysite (**b**), with kaolin (**c**), and with bentonite (**d**).

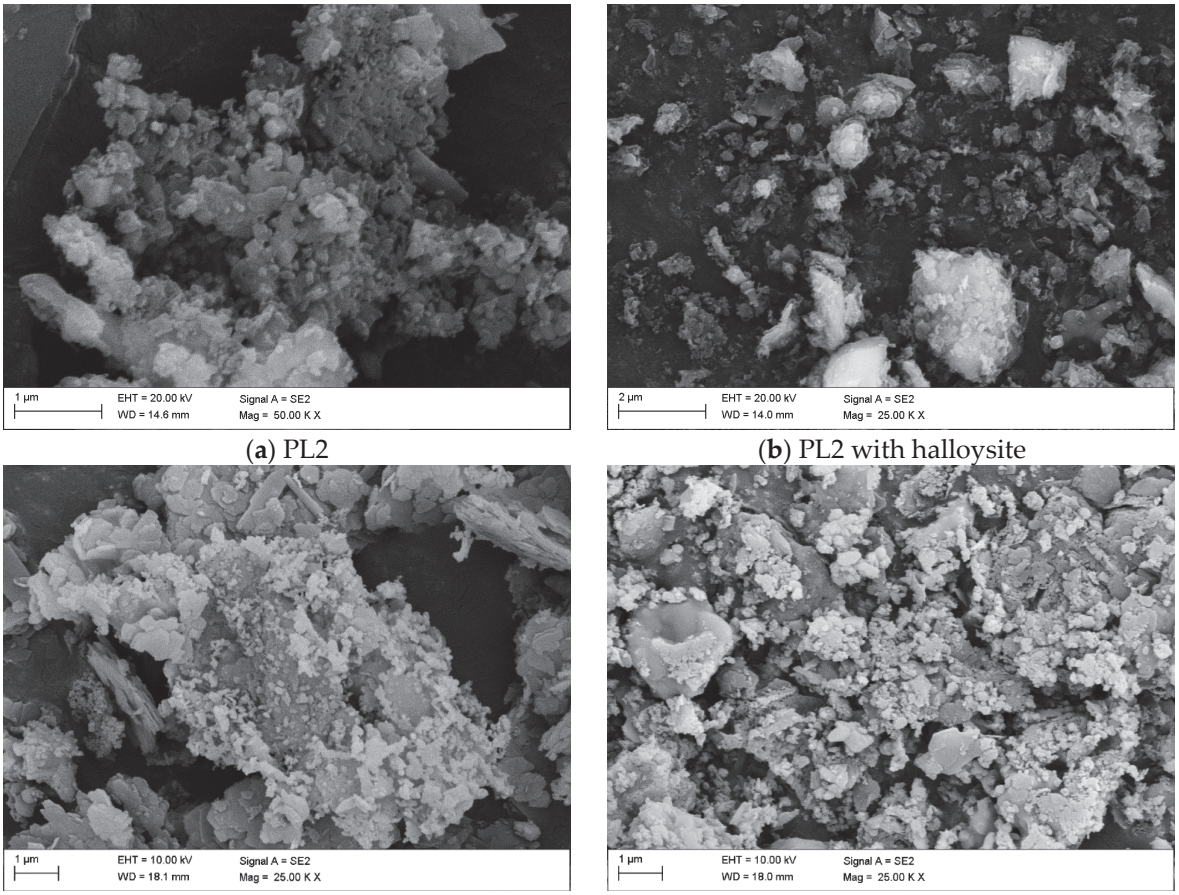

(**a**) PL2 (**b**) PL2 with halloysite

(**c**) PL2 with kaolin (**d**) PL2 with bentonite

Figure 10. SEM pictures of the PL2 ashes without additives (**a**), with halloysite (**b**), with kaolin (**c**), and with bentonite (**d**).

In the case of the halloysite addition (Figure 9b), a significant presence of the typical tubular crystals is observed primarily on the surface of the ash agglomerates, where the halloysite has adhered. Also, bentonite seems to allow a certain adhesion of particles and agglomerates onto the platelets of PL1 ash (Figure 9c).

In opposition to this, in Figure 10b, the interaction between PL2 ash and halloysite seems to be scarce probably due to the predominant ash amount in the ash-additive blending.

The electrical status of the clay surfaces interacting with one of the ash particles should also be taken into account: the possibility of the presence (or not) of such weak interactions may be effective in obtaining a homogeneous distribution especially when the added clay is in a smaller amount vs. that of the ash and when particular crystals' morphologies (e.g., for halloysite and its tubular crystalline shape) may be a distinctive characteristic.

Kaolin platelets, kaolin sheets, and even packed sheets with adhered ash particles are present for both PL1 and PL2 (Figures 9c and 10c), leading to a rather homogeneous distribution of the two materials. Kaolin seems to yield better results in terms of reciprocal distribution and homogeneity.

Concerning the PL1 with bentonite particles, mixtures seem to be less effective, showing a clear distinction between the two separate fractions (Figure 9d). A noticeable difference in the better blending of bentonite with the PL2 ash can be noted in Figure 10d, again attributable to the larger ash content of PL2. In this micrograph, the ash particles seem to surround and lay stuck on the bentonite platelets.

The performance of aluminosilicate additives in the ash deposits may be more visible in a higher temperature range, as presented in the work by Hardy et al. [61]. After

the thermal conversion at 1000 °C, the effectiveness of the chlorine removal produced by kaolin, halloysite, and bentonite was significantly elevated compared that to 600 °C. However, the temperature of 950–1000 °C is claimed to be the highest favorable due to the unwanted high-temperature transformation of aluminosilicates [29]. The porosity of aluminosilicate particles decreases at higher temperatures, thereby limiting the pore diffusion of gaseous alkali chlorides into the particles. What is more, in a temperature above 950 °C, meta-kaolinite dissociates into amorphous silica and alumina-silica spinel, which transfer converts into pseudomullite at 1000 °C and both alumina silica spinel and pseudomullite have low potential to react with KCl [62,63].

3.4. Influence of Additives on Phase Composition

The X-ray diffraction (XRD) patterns of the investigated samples are presented in Figures 11 and 12 together with the main detected phases listed in Table 5.

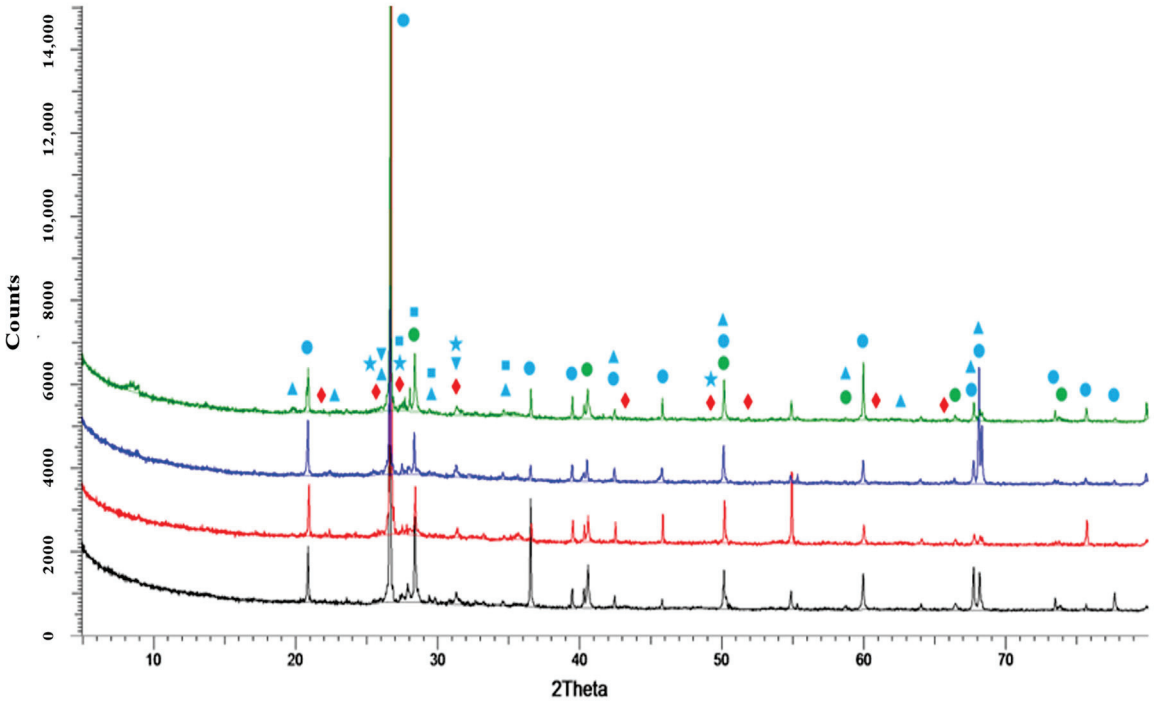

Figure 11. X-ray diffraction patterns of samples PL1 (black), PL1 with halloysite (red), PL1 with kaolin (blue), and PL1 with bentonite (green).

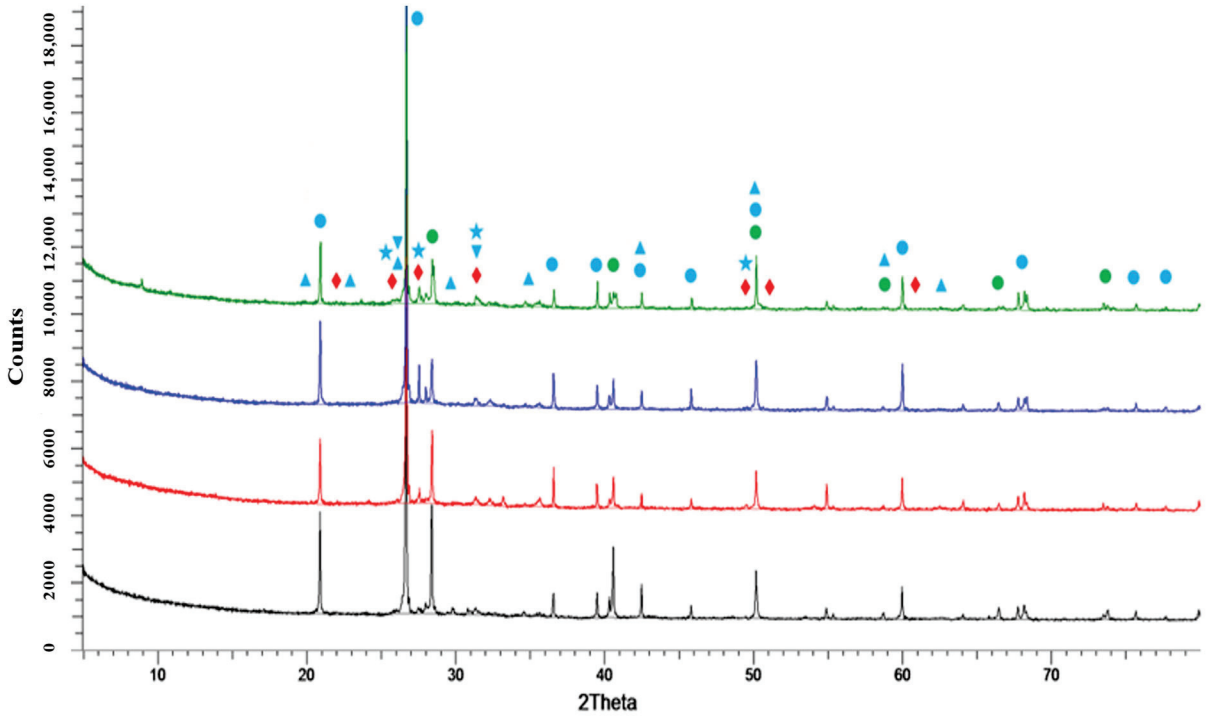

Figure 12. X-ray diffraction patterns of samples PL2 (black), PL2 with halloysite (red), PL2 with kaolin (blue), and PL2 with bentonite (green).

Table 5. The selected main phases detected via X-ray diffraction together with their symbols.

Symbol	Phase
●	SiO_2 Quartz; Quartz low
●	KCl
♦	Ca-Phosphates (TCMP, Mg-Whitlockite; Cl-Hydroxylapatite)
▲	$KAlSiO_4$
▼	$KAlSi_2O_6$
★	$KAlSi_3O_8$

The main detected phase in all samples is quartz, which corresponds to the oxide analysis presented in Table 3 as well as what is typical for animal-origin waste [64,65]. Phases containing calcium and aluminum are also detected as feldspar, phosphates, and zeolites, which may indicate the possible use of the investigated ashes in the circular economy, for example, for the synthesis of zeolites [66]. Chlorine is present mainly as potassium chloride (KCl), which is typical for biomass fuels [67]. The presence of KCl is higher in the samples without additives, for both PL1 and PL2 fuels (green dots). In the fuels with additives, the peaks of $KAlSiO_4$, $KAlSi_2O_6$, and $KAlSi_3O_8$ are detected (blue triangles and stars), which is a sign of the reactions between additives and potassium compounds, likely indicating that KCl was dissociated, liberating chlorine in the gas phase.

Also, the presence of some secondary/scarce crystalline phases as metaphosphates and sulfates, and those as mica-like and chain silicates (likely coming from additive phyllosilicates), may indicate the disruption of previous structures (added clay minerals + biomasses) and the rearrangement of new ones.

These latter rearrangements, of course, may be allocating the potassium ions coming from chlorides melting or yielding other crystalline species typical of thermal treatments of biomasses. Those crystalline arrangements are able to coordinate and host the K^+ ion in

silicate lattices, in between layered structures, in channeled radicals, or by anionic radicals, which could be favored in the range of reached temperatures listed in Table 4. Overall, the XRD analysis would confirm the interaction between ashes and additives.

4. Conclusions

High-temperature corrosion, ash agglomeration, and the slagging of heating surfaces are ash-related problems causing significant concerns in boilers burning or co-burning biomass fuels. When utilizing high-chlorine feedstocks, such as poultry litter, these issues may be particularly severe, and thus, effective methods for their mitigation must be adopted.

In the presented research, for the first time, the influence of kaolin, halloysite, and bentonite on poultry litter ashes has been investigated, taking into account their chlorine distributions and melting tendencies. For chlorine-rich PL1 ash, the chlorine content reductions of 38.46%, 45.51%, and 33.44% are observed as a result of the performance of halloysite, kaolin, and bentonite, respectively. The initial chlorine concentration in the PL1 sample was reduced from 6.38% to 3.93% in the case of halloysite, to 3.48% in the case of kaolin, and to 4.25% in the case of bentonite.

Furthermore, the presence of additives elevates the shrinkage starting temperature and the deformation temperature of PL1 ash, which is expected to make it less prone to agglomeration and slagging. The shrinkage starting temperature and the deformation temperature of PL1 ash were increased from 1040 up to 1150 °C (bentonite) and from 1170 up to 1270 °C (kaolin), respectively.

No clear effect was observed for the PL2 ash, which was rich in ash and low in chlorine, and its ash fusion temperatures were already high. The elevated ash content together with its heterogeneity may cause unfavorable reaction conditions, resulting in the poor performance of additives.

The performance of additives is particularly effective in the conversion of fuels with low melting tendencies and lower ash contents. The presented research covers a knowledge gap and is a preliminary step before the process's implementation, which will be continued with the same approach, taking into account the optimization of the additives' dose as well as various combustion parameters. The first step will be carried out at a laboratory scale, taking into account various doses of the additives and different combustion temperatures. Further investigation on a semi-industrial scale will also include emission measurements with a focus on chlorine's fate and NO_x. Selecting the right dose of fuel additives not only matters for reducing high temperature corrosion effectively but also significantly impacts economic aspects. Previous studies have often overlooked this important aspect. Therefore, in future research, the focus will be on recognizing the influence of individual additives on the economic aspects of the process.

The thermal conversion of poultry litter may be a crucial part of sustainable energy production, especially in rural areas and developing countries, as this type of feedstock is available locally in big quantities. The combustion of poultry litter may provide self-sufficiency in the heating for poultry farms, reducing the consumption of fossil fuels.

Author Contributions: Conceptualization, I.M.; methodology, I.M. and K.M.; software, K.M. and M.M.; validation, I.M., K.N., F.M., M.M. and K.M.; formal analysis, I.M., F.M., M.M., K.N. and K.M.; investigation, I.M., K.N., K.M. and M.M.; resources, I.M., K.M. and P.Ł.; data curation, I.M., K.N., K.M., F.M. and M.M.; writing—original draft preparation, I.M., K.N., F.M., K.M., M.M. and P.Ł.; writing—review and editing, I.M., K.N., K.M., F.M. and M.M.; visualization, I.M., M.M. and K.N.; supervision, I.M.; project administration, I.M.; funding acquisition, I.M. All authors have read and agreed to the published version of the manuscript.

Funding: This research was supported by the National Science Centre, Poland, grant number 2021/43/D/ST8/02609 "The influence of aluminosilicate additives on high-temperature corrosion and ash properties of animal-origin biomass". This research was also partly funded under the National Recovery and Resilience Plan (NRRP), Mission 04 Component 2 Investment 1.5—NextGenerationEU, Call for tender n. 3277 dated 30 December 2021.

Data Availability Statement: The original contributions presented in the study are included in the article, further inquiries can be directed to the corresponding author.

Acknowledgments: This research was funded in the vast majority by the National Science Centre, Poland 2021/43/D/ST8/02609. For the purpose of open access, the author has applied a CC-BY public copyright license to any author accepted manuscript (AAM) version arising from this submission.

Conflicts of Interest: The authors declare no conflicts of interest. The funders had no role in the design of the study; in the collection, analyses, or interpretation of data; in the writing of the manuscript; or in the decision to publish the results.

References

1. Bioenergy—IEA. Available online: https://www.iea.org/energy-system/renewables/bioenergy (accessed on 4 October 2023).
2. Zhao, P.; Yu, S.; Li, Q.; Zhang, Y.; Zhou, H. Understanding Heavy Metal in the Conversion of Biomass Model Component: Migration and Transformation Characteristics of Cu during Hydrothermal Carbonization of Cellulose. *Energy* **2024**, *293*, 130700. [CrossRef]
3. Yu, S.; Yang, X.; Zhou, H.; Tan, Z.; Cong, K.; Zhang, Y.; Li, Q. Thermal and Kinetic Behaviors during Co-Pyrolysis of Microcrystalline Cellulose and Styrene–Butadiene–Styrene Triblock Copolymer. *Processes* **2021**, *9*, 1335. [CrossRef]
4. Yu, S.; He, J.; Zhang, Z.; Sun, Z.; Xie, M.; Xu, Y.; Bie, X.; Li, Q.; Zhang, Y.; Sevilla, M.; et al. Towards Negative Emissions: Hydrothermal Carbonization of Biomass for Sustainable Carbon Materials. *Adv. Mater.* **2024**, e2307412. [CrossRef] [PubMed]
5. Ibitoye, S.E.; Mahamood, R.M.; Jen, T.-C.; Loha, C.; Akinlabi, E.T. An Overview of Biomass Solid Fuels: Biomass Sources, Processing Methods, and Morphological and Microstructural Properties. *J. Bioresour. Bioprod.* **2023**, *8*, 333–360. [CrossRef]
6. Köninger, J.; Lugato, E.; Panagos, P.; Kochupillai, M.; Orgiazzi, A.; Briones, M.J.I. Manure Management and Soil Biodiversity: Towards More Sustainable Food Systems in the EU. *Agric. Syst.* **2021**, *194*, 103251. [CrossRef]
7. Whitely, N.; Ozao, R.; Artiaga, R.; Cao, Y.; Pan, W.P. Multi-Utilization of Chicken Litter as Biomass Source. Part I. Combustion. *Energy Fuels* **2006**, *20*, 2660–2665. [CrossRef]
8. Hubbard, L.E.; Givens, C.E.; Griffin, D.W.; Iwanowicz, L.R.; Meyer, M.T.; Kolpin, D.W. Poultry Litter as Potential Source of Pathogens and Other Contaminants in Groundwater and Surface Water Proximal to Large-Scale Confined Poultry Feeding Operations. *Sci. Total Environ.* **2020**, *735*, 139459. [CrossRef] [PubMed]
9. Tańczuk, M.; Junga, R.; Kolasa-Więcek, A.; Niemiec, P. Assessment of the Energy Potential of Chicken Manure in Poland. *Energies* **2019**, *12*, 1244. [CrossRef]
10. Kelleher, B.P.; Leahy, J.J.; Henihan, A.M.; O'Dwyer, T.F.; Sutton, D.; Leahy, M.J. Advances in Poultry Litter Disposal Technology—A Review. *Bioresour. Technol.* **2002**, *83*, 27–36. [CrossRef]
11. Commission Regulation (EU) 2017/1262—Of 12 July 2017—Amending Regulation (EU) No 142/2011 as Regards the Use of Manure of Farmed Animals as a Fuel in Combustion Plants. Available online: https://eur-lex.europa.eu/legal-content/EN/TXT/?uri=uriserv:OJ.L_.2017.182.01.0034.01.ENG (accessed on 10 February 2024).
12. Turzyński, T.; Kluska, J.; Kardaś, D. Study on Chicken Manure Combustion and Heat Production in Terms of Thermal Self-Sufficiency of a Poultry Farm. *Renew. Energy* **2022**, *191*, 84–91. [CrossRef]
13. Pachón Gómez, E.M.; Domínguez, R.E.; López, D.A.; Téllez, J.F.; Marino, M.D.; Almada, N.; Gange, J.M.; Moyano, E.L. Chicken Litter: A Waste or a Source of Chemicals? Fast Pyrolysis and Hydrothermal Conversion as Alternatives in the Valorisation of Poultry Waste. *J. Anal. Appl. Pyrolysis* **2023**, *169*, 105796. [CrossRef]
14. Li, S.; Wu, A.; Deng, S.; Pan, W. Effect of Co-Combustion of Chicken Litter and Coal on Emissions in a Laboratory-Scale Fluidized Bed Combustor. *Fuel Process. Technol.* **2008**, *89*, 7–12. [CrossRef]
15. Simbolon, L.M.; Pandey, D.S.; Horvat, A.; Kwapinska, M.; Leahy, J.J.; Tassou, S.A. Investigation of Chicken Litter Conversion into Useful Energy Resources by Using Low Temperature Pyrolysis. *Energy Procedia* **2019**, *161*, 47–56. [CrossRef]
16. Vainio, E.; Kinnunen, H.; Laurén, T.; Brink, A.; Yrjas, P.; DeMartini, N.; Hupa, M. Low-Temperature Corrosion in Co-Combustion of Biomass and Solid Recovered Fuels. *Fuel* **2016**, *184*, 957–965. [CrossRef]
17. Ruozzi, A.; Vainio, E.; Kinnunen, H.; Hupa, L. Cold-End Corrosion in Biomass Combustion—Role of Calcium Chloride in the Deposit. *Fuel* **2023**, *349*, 128344. [CrossRef]
18. Vainio, E.; Vänskä, K.; Laurén, T.; Yrjas, P.; Coda Zabetta, E.; Hupa, M.; Hupa, L. Impact of Boiler Load and Limestone Addition on SO3 and Corrosive Cold-End Deposits in a Coal-Fired CFB Boiler. *Fuel* **2021**, *304*, 121313. [CrossRef]
19. Nielsen, H.P.; Frandsen, F.J.; Dam-Johansen, K.; Baxter, L.L. The Implications of Chlorine-Associated Corrosion on the Operation of Biomass-Fired Boilers. *Prog. Energy Combust. Sci.* **2000**, *26*, 283–298. [CrossRef]
20. Nielsen, H.P.; Baxter, L.L.; Sclippab, G.; Morey, C.; Frandsen, F.J.; Dam-Johansen, K. Deposition of Potassium Salts on Heat Transfer Surfaces in Straw-Fired Boilers: A Pilot-Scale Study. *Fuel* **2000**, *79*, 131–139. [CrossRef]
21. Karuana, F.; Prismantoko, A.; Suhendra, N.; Darmawan, A.; Hariana, H.; Darmadi, D.B.; Akhsin Muflikhun, M. Investigation of Austenitic Stainless Steel Corrosion Resistance against Ash Deposits from Co-Combustion Coal and Biomass Waste. *Eng. Fail. Anal.* **2023**, *150*, 107368. [CrossRef]

22. Król, D.; Motyl, P.; Poskrobko, S. Chlorine Corrosion in a Low-Power Boiler Fired with Agricultural Biomass. *Energies* **2022**, *15*, 382. [CrossRef]
23. Ovčačíková, H.; Velička, M.; Vlček, J.; Topinková, M.; Klárová, M.; Burda, J. Corrosive Effect of Wood Ash Produced by Biomass Combustion on Refractory Materials in a Binary Al–Si System. *Materials* **2022**, *15*, 5796. [CrossRef]
24. Steenari, B.M.; Lindqvist, O. High-Temperature Reactions of Straw Ash and the Anti-Sintering Additives Kaolin and Dolomite. *Biomass Bioenergy* **1998**, *14*, 67–76. [CrossRef]
25. Gruber, T.; Schulze, K.; Scharler, R.; Obernberger, I. Investigation of the Corrosion Behaviour of 13CrMo4–5 for Biomass Fired Boilers with Coupled Online Corrosion and Deposit Probe Measurements. *Fuel* **2015**, *144*, 15–24. [CrossRef]
26. Wang, H.; Zhou, T.; Tan, X.; Hu, N.; Wang, Y.; Yang, H.; Zhang, M. Experimental Study on the Sintering Characteristics of Biomass Ash. *Fuel* **2024**, *356*, 129586. [CrossRef]
27. Mlonka-Mędrala, A.; Magdziarz, A.; Kalemba-Rec, I.; Nowak, W. The Influence of Potassium-Rich Biomass Ashes on Steel Corrosion above 550 °C. *Energy Convers. Manag.* **2019**, *187*, 15–28. [CrossRef]
28. Roberts, L.J.; Mason, P.E.; Jones, J.M.; Gale, W.F.; Williams, A.; Hunt, A.; Ashman, J. The Impact of Aluminosilicate-Based Additives upon the Sintering and Melting Behaviour of Biomass Ash. *Biomass Bioenergy* **2019**, *127*, 105284. [CrossRef]
29. Niu, Y.; Tan, H.; Hui, S. Ash-Related Issues during Biomass Combustion: Alkali-Induced Slagging, Silicate Melt-Induced Slagging (Ash Fusion), Agglomeration, Corrosion, Ash Utilization, and Related Countermeasures. *Prog. Energy Combust. Sci.* **2016**, *52*, 1–61. [CrossRef]
30. Grabke, H.J.; Reese, E.; Spiegel, M. The Effects of Chlorides, Hydrogen Chloride, and Sulfur Dioxide in the Oxidation of Steels below Deposits. *Corros. Sci.* **1995**, *37*, 1023–1043. [CrossRef]
31. Wu, D.L.; Dahl, K.V.; Christiansen, T.L.; Montgomery, M.; Hald, J. Corrosion Behaviour of Ni and Nickel Aluminide Coatings Exposed in a Biomass Fired Power Plant for Two Years. *Surf. Coat. Technol.* **2019**, *362*, 355–365. [CrossRef]
32. Okoro, S.C.; Montgomery, M.; Frandsen, F.J.; Pantleon, K. Influence of Preoxidation on High Temperature Corrosion of a Ni-Based Alloy under Conditions Relevant to Biomass Firing. *Surf. Coat. Technol.* **2017**, *319*, 76–87. [CrossRef]
33. Garcia-Maraver, A.; Mata-Sanchez, J.; Carpio, M.; Perez-Jimenez, J.A. Critical Review of Predictive Coefficients for Biomass Ash Deposition Tendency. *J. Energy Inst.* **2017**, *90*, 214–228. [CrossRef]
34. Lachman, J.; Baláš, M.; Lisý, M.; Lisá, H.; Milčák, P.; Elbl, P. An Overview of Slagging and Fouling Indicators and Their Applicability to Biomass Fuels. *Fuel Process. Technol.* **2021**, *217*, 106804. [CrossRef]
35. Sobieraj, J.; Gądek, W.; Jagodzińska, K.; Kalisz, S. Investigations of Optimal Additive Dose for Cl-Rich Biomasses. *Renew. Energy* **2021**, *163*, 2008–2017. [CrossRef]
36. Hariana, H.; Ghazidin, H.; Darmawan, A.; Hilmawan, E.; Prabowo; Aziz, M. Effect of Additives in Increasing Ash Fusion Temperature during Co-Firing of Coal and Palm Oil Waste Biomass. *Bioresour. Technol. Rep.* **2023**, *23*, 101531. [CrossRef]
37. Morris, J.D.; Daood, S.S.; Nimmo, W. The Use of Kaolin and Dolomite Bed Additives as an Agglomeration Mitigation Method for Wheat Straw and Miscanthus Biomass Fuels in a Pilot-Scale Fluidized Bed Combustor. *Renew. Energy* **2022**, *196*, 749–762. [CrossRef]
38. Wang, L.; Hustad, J.E.; Skreiberg, Ø.; Skjevrak, G.; Grønli, M. A Critical Review on Additives to Reduce Ash Related Operation Problems in Biomass Combustion Applications. *Energy Procedia* **2012**, *20*, 20–29. [CrossRef]
39. Míguez, J.L.; Porteiro, J.; Behrendt, F.; Blanco, D.; Patiño, D.; Dieguez-Alonso, A. Review of the Use of Additives to Mitigate Operational Problems Associated with the Combustion of Biomass with High Content in Ash-Forming Species. *Renew. Sustain. Energy Rev.* **2021**, *141*, 110502. [CrossRef]
40. *PN-EN ISO 18122:2015*; Solid Biofuels: Determination of Ash Content. International Organization for Standardization: Geneva, Switzerland, 2015.
41. *PN-EN ISO 18125:2017*; Solid Biofuels: Determination of Calorific Value. International Organization for Standardization: Geneva, Switzerland, 2017.
42. *PN-EN ISO 16948:2015*; Solid Biofuels: Determination of Total Content of Carbon, Hydrogen and Nitrogen. International Organization for Standardization: Geneva, Switzerland, 2015.
43. *PN-EN ISO 16994:2016*; Solid Biofuels: Determination of Total Content of Sulfur and Chlorine. International Organization for Standardization: Geneva, Switzerland, 2016.
44. Andersson, S.; Blomqvist, E.W.; Bäfver, L.; Jones, F.; Davidsson, K.; Froitzheim, J.; Karlsson, M.; Larsson, E.; Liske, J. Sulfur Recirculation for Increased Electricity Production in Waste-to-Energy Plants. *Waste Manag.* **2014**, *34*, 67–78. [CrossRef]
45. Aho, M.; Ferrer, E. Importance of Coal Ash Composition in Protecting the Boiler against Chlorine Deposition during Combustion of Chlorine-Rich Biomass. *Fuel* **2005**, *84*, 201–212. [CrossRef]
46. Glarborg, P.; Marshall, P. Mechanism and Modeling of the Formation of Gaseous Alkali Sulfates. *Combust. Flame* **2005**, *141*, 22–39. [CrossRef]
47. Skrifvars, B.J.; Laurén, T.; Hupa, M.; Korbee, R.; Ljung, P. Ash Behaviour in a Pulverized Wood Fired Boiler—A Case Study. *Fuel* **2004**, *83*, 1371–1379. [CrossRef]
48. Theis, M.; Skrifvars, B.J.; Zevenhoven, M.; Hupa, M.; Tran, H. Fouling Tendency of Ash Resulting from Burning Mixtures of Biofuels. Part 2: Deposit Chemistry. *Fuel* **2006**, *85*, 1992–2001. [CrossRef]
49. Maj, I.; Matus, K. Aluminosilicate Clay Minerals: Kaolin, Bentonite, and Halloysite as Fuel Additives for Thermal Conversion of Biomass and Waste. *Energies* **2023**, *16*, 4359. [CrossRef]

50. Murray, H.H. Applied Clay Mineralogy Today and Tomorrow. *Clay Miner.* **1999**, *34*, 39–49. [CrossRef]
51. Bergaya, F.; Lagaly, G. Chapter 1 General Introduction: Clays, Clay Minerals, and Clay Science. In *Handbook of Clay Science*; Bergaya, F., Theng, B.K.G., Lagaly, G., Eds.; Elsevier: Amsterdam, The Netherlands, 2006; Volume 1, pp. 1–18.
52. Wejkowski, R.; Kalisz, S.; Tymoszuk, M.; Ciukaj, S.; Maj, I. Full-Scale Investigation of Dry Sorbent Injection for NOx Emission Control and Mercury Retention. *Energies* **2021**, *14*, 7787. [CrossRef]
53. Kalisz, S.; Ciukaj, S.; Mroczek, K.; Tymoszuk, M.; Wejkowski, R.; Pronobis, M.; Kubiczek, H. Full-Scale Study on Halloysite Fireside Additive in 230 t/h Pulverized Coal Utility Boiler. *Energy* **2015**, *92*, 33–39. [CrossRef]
54. Nickovic, S.; Vukovic, A.; Vujadinovic, M.; Djurdjevic, V.; Pejanovic, G. Technical Note: High-Resolution Mineralogical Database of Dust-Productive Soils for Atmospheric Dust Modeling. *Atmos. Chem. Phys.* **2012**, *12*, 845–855. [CrossRef]
55. Punjak, W.A.; Shadman, F. Aluminosilicate Sorbents for Control of Alkali Vapors during Coal Combustion and Gasification. *Energy Fuels* **1988**, *2*, 845–855. [CrossRef]
56. Zhang, Z.; Liu, J.; Yang, Y.; Shen, F.; Zhang, Z. Theoretical Investigation of Sodium Capture Mechanism on Kaolinite Surfaces. *Fuel* **2018**, *234*, 318–325. [CrossRef]
57. Kuptz, D.; Kuchler, C.; Rist, E.; Eickenscheidt, T.; Mack, R.; Schön, C.; Drösler, M.; Hartmann, H. Combustion Behaviour and Slagging Tendencies of Pure, Blended and Kaolin Additivated Biomass Pellets from Fen Paludicultures in Two Small-Scale Boilers < 30 KW. *Biomass Bioenergy* **2022**, *164*, 106532. [CrossRef]
58. Li, F.; Wang, X.; Zhao, C.; Li, Y.; Guo, M.; Fan, H.; Guo, Q.; Fang, Y. Influence of Additives on Potassium Retention Behaviors during Straw Combustion: A Mechanism Study. *Bioresour. Technol.* **2020**, *299*, 122515. [CrossRef]
59. *PN-EN ISO 21404:2020*; Solid Biofuels: Determination of Ash Melting Behaviour. International Organization for Standardization: Geneva, Switzerland, 2020.
60. Wang, Y.; Li, L.; An, Q.; Tan, H.; Li, P.; Peng, J. Effect of Different Additives on Ash Fusion Characteristic and Mineral Phase Transformation of Iron-Rich Zhundong Coal. *Fuel* **2022**, *307*, 121841. [CrossRef]
61. Hardy, T.; Kordylewski, W.; Mościcki, K. Use of Aluminosilicate Sorbents for Control of KCl Vapors in Biomass Combustion Gases. *J. Power Technol.* **2013**, *93*, 37–43.
62. Wang, L.; Becidan, M.; Skreiberg, Ø. Sintering Behavior of Agricultural Residues Ashes and Effects of Additives. *Energy Fuels* **2012**, *26*, 5917–5929. [CrossRef]
63. Zheng, Y.; Jensen, P.A.; Jensen, A.D. A Kinetic Study of Gaseous Potassium Capture by Coal Minerals in a High Temperature Fixed-Bed Reactor. *Fuel* **2008**, *87*, 3304–3312. [CrossRef]
64. Maj, I. Significance and Challenges of Poultry Litter and Cattle Manure as Sustainable Fuels: A Review. *Energies* **2022**, *15*, 8981. [CrossRef]
65. Font-Palma, C. Methods for the Treatment of Cattle Manure—A Review. *C* **2019**, *5*, 27. [CrossRef]
66. Belviso, C. State-of-the-Art Applications of Fly Ash from Coal and Biomass: A Focus on Zeolite Synthesis Processes and Issues. *Prog. Energy Combust. Sci.* **2018**, *65*, 109–135. [CrossRef]
67. Mlonka-Mędrala, A.; Gołombek, K.; Buk, P.; Cieślik, E.; Nowak, W. The Influence of KCl on Biomass Ash Melting Behaviour and High-Temperature Corrosion of Low-Alloy Steel. *Energy* **2019**, *188*, 116062. [CrossRef]

energies

MDPI

Article

Assessing Energy Potential and Chemical Composition of Food Waste Thermodynamic Conversion Products: A Literature Review

Andreja Škorjanc, Darko Goričanec and Danijela Urbancl *

Faculty of Chemistry and Chemical Engineering, University of Maribor, Smetanova 17, 2000 Maribor, Slovenia; andreja.skorjanc@student.um.si (A.Š.); darko.goricanec@um.si (D.G.)
* Correspondence: danijela.urbancl@um.si

Abstract: This study examines the considerable volume of food waste generated annually in Slovenia, which amounted to over 143,000 tons in 2020. The analysis shows that 40% of food waste consists of edible parts, highlighting the potential for reduction through increased consumer awareness and attitudes towards food consumption. The study shows that the consumption phase contributes the most to waste food (46%), followed by primary production (25%) and processing/manufacture (24%). The study addresses various thermodynamic processes, in particular, thermal conversion methods, such as torrefaction pyrolysis and hydrothermal carbonization, which optimize energy potential by reducing the atomic ratio (H/C) and (O/C), thereby increasing calorific value and facilitating the production of solid fuels. The main results show the effectiveness of torrefaction, pyrolysis and hydrothermal carbonization (HTC) in increasing the energy potential of food waste.

Keywords: energy; thermodynamic conversions; pyrolysis; torrefaction; hydrothermal carbonization; food waste; energy potential; chemical composition

1. Introduction

Increasing demand for electricity and limited fossil fuel resources are driving the growing importance of and the search for new, environmentally friendly energy sources [1]. One possible way to obtain such fuel resources is the processing of waste from the agricultural and food industry, which accounts for more than 95% of total waste biomass, which can be utilized in a biogas plant, composting plant, incineration or combustion. However, the main problems with biomass use are its transport and storage, high moisture content, low calorific value, low density and heterogeneous structure. In addition, biomass has hydrophilic properties and is prone to rapid decomposition, creating conditions for the growth and decay of microorganisms. To overcome these properties, fresh biomass (consisting of polymers, carbohydrates, including cellulose and hemicellulose, lignin, lipids, proteins and organic acids) needs to be mechanically, thermally and chemically pretreated [2]. This study is limited to thermomechanical transformations, including pyrolysis, torrefaction, hydrothermal carbonization and gasification.

The focus in many EU and other developed countries is to reduce food waste through effective source separation. Food waste management can be achieved in a variety of ways, including biological technologies and thermochemical processes. Thermochemical conversion is a viable option for the management of MSW in addition to biological processes. Thermochemical processes, such as gasification, incineration, liquefaction, pyrolysis, torrefaction and hydrothermal carbonization (HTC), are likely to be more beneficial for the valorization of FW than anaerobic digestion (AD). However, most of these processes usually require a pre-treatment of the feedstock and a gas cleaning system to avoid emissions such as NOx, SOx, particulate matter and heavy metals. Among these processes, HTC has become a cost-effective method for the thermochemical processing of high moisture

biomass, which includes food waste, to produce a product with interesting properties as a biofuel [3].

In recent times, numerous researchers have studied hydrothermal carbonization. For instance, Khoo et al. [4] investigated the effects of temperature and residence time on the physical and chemical properties of the resulting products. From the research, it was found that the carbon yield significantly decreased with increasing temperature. However, this method increased the heating value compared to raw biomass [4].

Food waste, according to this definition, includes edible and inedible parts. The inedible part of food is the part of the food that was never intended for human consumption and is more difficult to avoid, e.g., peels, skins, bones, seeds and shells. The current definition of food waste does not include food waste destined for processing into animal feed, food for charitable purposes, paper tissues collected as bio-waste and packaging that is thrown away with the food waste. In the analysis itself, the authors use different measurement methods, which makes it even more difficult to compare the results, as the studies are very limited [5]. Another definition of FW is defined as food and inedible parts of food returned from the food supply chain that require recovery or disposal [6].

In addition, the fluctuation range of harvests must be considered, so the data must be measured over several consecutive years. Direct measurement of food waste by researchers who are experts in this field is cited in the literature as a sufficiently reliable method [7]. There are studies in the literature that, based on various sources, provide estimates of the amount of food wasted at the EU level. After reviewing the studies at the EU and global level, the results for the EU range between 158 and 298 kg/year/capita. These estimates are due to differences in the different studies, system limitations, objectives and methods [8].

The proximate and ultimate analyses of torrefied biomass are optimized during the torrefaction process to enable the production of powdered biochar with high calorific value and low moisture content [9]. Lu et al. investigated that it is possible to obtain more energy from carbonaceous char as solid fuel than from the gases produced during anaerobic digestion [10].

HTC has great potential for the future conversion of food waste, transforming it from a lengthy process into a simple and rapid one. In a short time, it converts heterogeneous and wet biomass (with water content ranging approximately between 50% and 95%) into sterile and storable char [11].

The chemical and physical composition varies depending on the type of food waste. These differences pose a major challenge to the adoption of existing international standards for the disposal, recycling and assessment of food waste. There is also a general consensus in the literature that current technologies for food waste recycling need to be further improved to be economically viable. Various studies have highlighted the importance of improving downstream bioprocesses, leading to the creation of an integrated biogas plant for the treatment of food waste. The study highlighted the benefits of converting food waste into energy [12].

The objective of this paper is to address the composition of food waste and to study its role in biorefineries to identify nutrient synergies and their use in thermal conversion processes. The novelty of this study represents the fact that there is no research on different types of waste food for the presented thermochemical process future work.

2. Sources and Types of Food Waste

According to EU data, the total amount of food thrown away in 2021 was more than 58 million tons. Household food waste accounted for around 31 million tons of fresh weight or 54% of the total. Figures for Europe show that over 88 million tons of food is wasted each year from primary production to consumption, at a very high cost of an estimated €143 billion. In addition, 72% of food waste is generated by households and 17 million tons by the processing sector. In terms of food groups, the highest percentage of loss is in roots, tubers and oilseeds (25%), with fruit and vegetables accounting for around 22%, meat and livestock products accounting for 12%, and cereals and pulses at 9%. Recent

studies have shown that fruit and vegetables are the two food groups that generate the most waste in Europe. In line with these recommendations, food waste from different sectors of the agri-food industry (vegetables, fruit, beverages, meat and seafood products, etc.) is a promising and cost-effective source of functional or bioactive compounds. Excess food products are also used in nutraceuticals and pharmaceuticals or converted into animal feed products [13].

In some studies, apple pomace has been selected as the primary food by-product. As a major waste product of the apple processing industry, they have great potential for use in the biotechnology industry and also due to their large volume. A total of 0.7 million tons of apple pomace is produced annually in the EU. Another area is the growing consumption of meat, which is increasing, while the demand for lower quality products such as blood, offal or certain muscles is decreasing. According to EU figures, 2 million tons of animal blood are produced in the EU every year. Brewing industry residues are also an important source of waste in the EU, with European breweries producing around 4 million tons of waste brewing grains per year [14].

Food and kitchen waste are available all over the world. The individual process valorization of these foodstuffs requires the proper identification and classification of residues and raw materials. A qualitative and characteristic classification of foodstuffs can be useful, i.e., by group of individual foodstuffs; these are fruit and vegetables, starchy foods, meat, fish and other foodstuffs, such as raw and cooked food, salads, bread and also desserts [15].

Food waste can originate from plants or animals and is generated by different parts of the food supply chain (Table 1) [16].

Different categories have been proposed depending on the causes of waste: old and unprocessed food due to poor logistics, over-processed food due to poor evaluation, and inadequate food handling and waste due to oversized portions. Studies look at the average composition of household, institutional and catering waste and show that these residues have a pH ranging from 4.2 to 6.7 and 52–88% water. In particular, the high water content can lead to nutrient loss during dehydration and can lead to a reduction in calorific value. Fractions rich in polysaccharides are thus a good source of carbon for bioconversion processes [15].

A shared waste collection facility was likely to be the most cost-effective. It would be designed to process different waste streams from the food industry, households and other different sectors [17].

On the other hand, food waste is a sustainable source of energy despite disposal problems and environmental impacts. Food waste from markets has attracted a lot of attention because of its rich organic composition. It has an energy value that can be converted into value-added products, such as materials, biochemicals, enzymes and biofuels. Biofuel production by various methods such as intermediate pyrolysis, fast pyrolysis, hydrothermal liquefaction or gasification and subsequent Fischer–Tropsch synthesis are the main thermochemical methods for the conversion of biomass into liquid hydrocarbons. Thermocatalytic reforming (TCR) is the next new technology, which is a combination of intermediate pyrolysis and post-catalytic reforming. This process involves intermediate pyrolysis in which thermal heating and decomposition of the biomass takes place in the complete absence of oxygen with intermediate heating rates and solid retention times (in minutes). The next step is reforming, which takes place at elevated temperatures in the absence of oxygen, with appropriate physical and chemical properties. The recovery of this type of waste thus depends on the type of pre-treatment and the extent of recycling [18].

Table 1. The types and sources of individual food wastes generated in different parts of the food supply chain.

Source	Plant Sources	Animal Resources
Primary production	- Unharvested crops. - Crops left in the field after harvest. - Harvested unsold crops. - Fruit and vegetables in the process of decomposition. - Crops damaged by machinery or other improper handling. - Loss of food due to improper storage. - Worse crop quality (weather conditions, cultivation method)	- Discarded fish. - Loss of food due to inadequate storage. - Dead animals during breeding. - Loss of milk due to animal disease.
Processing and manufacturing	- Causes in the processing (inefficiency, pollution, etc.). - Inedible part of food (wrappers, seeds, bones, fruit peelings, etc.). - Low utilization of by-products. - Few manufacturing defects (food recalls) - Inedible parts of food (created when separating the edible part of food during processing). - Food damaged due to inadequate packaging.	
Retail and marketing	- Food spoiled due to inadequate refrigeration/storage equipment. - Food with an expired shelf life. - Unsold food. - Damaged packaging. - Food withdrawn and recalled due to health risk, inadequate quality or inadequate labelling.	
Final preparation and consumption	- Improper food storage. - Too large portions or purchased quantities. - Expiration dates of edible food. - Not enough meal preparation planning. - Unattractive to consumers. - Inedible part of food (bones, fruit pits and peels, etc.).	

Food waste consists of lipids, hemicellulose, cellulose, starch, lignin and protein, which make up 82–96% of the total volatile compounds. They are similar to other carbonaceous solid wastes used in bioenergy production (in woody biomass and agricultural and general municipal solid wastes). They are relatively much richer in lipids (saturated fats) and proteins. This makes them particularly attractive for processing into biofuels and chemicals. On the other hand, lipids can be inhibitory during methane (CH4)-producing processes (e.g., anaerobic digestion) as they increase the methanation time. Protein is also a large proportion of food waste and is associated with a proportion of meat and dairy products together with lipids. Most food waste contains a high water content (on average 80 % by weight). The high water content makes food waste susceptible to biodegradation and poses a major problem for long-term storage. For this reason, reducing the water content, which should normally be below 10%, is an essential pre-treatment step. Pyrolysis and gasification reduce the energy input during treatment and thus avoid negative impacts. The value of the O/C ratio indicates the degree of polarity, and the H/C atomic ratio indicates the degree of aromaticity and stability of the samples. Summarizing the results from different studies, it could be concluded that the carbon content of food waste ranges from 40.0 to 60.0%, hydrogen from 5.0 to 13.0%, nitrogen from 1.5 to 6.0% and oxygen content is defined in a wider range from 17.0 to 41.0%. According to some reports, high oxygen content in individual food samples may result in a high proportion of liquid in pyrolysis, while on

the other hand, low oxygen content is desirable as the reduction of oxygen compounds improves the stability of the bio-oil [12].

Evidence from various studies suggests that elevated HHV in food waste is usually characterized by a high proportion of meat and dairy products in a given sample (HHV of meat > 25.2 MJ/kg) [19].

As mentioned earlier, animal products are rich in protein and fat, while fruit, vegetables and cereals are higher in carbohydrates. Given the elemental composition of proteins, fats and carbohydrates, there is a large amount of carbon present, which makes discarded food easily biodegradable [20].

3. Materials and Methods

Pyrolysis, gasification, liquefaction, carbonization and torrefaction are common thermochemical processes for converting biomass from food waste to produce liquid, solid and gaseous products. The effect of these processes depends on the oxygen supply and the reaction temperature. Almost all biomasses can be burned if their calorific value is high enough, which can reduce the consumption of fossil fuels [21].

A number of countries have targeted legislation and regulations for solid waste management, but implementation varies widely. The most common food waste treatment methods in use today are anaerobic digestion, composting, incineration, fast pyrolysis, gasification, hydrothermal carbonization and hydrothermal liquefaction (Figure 1) [22].

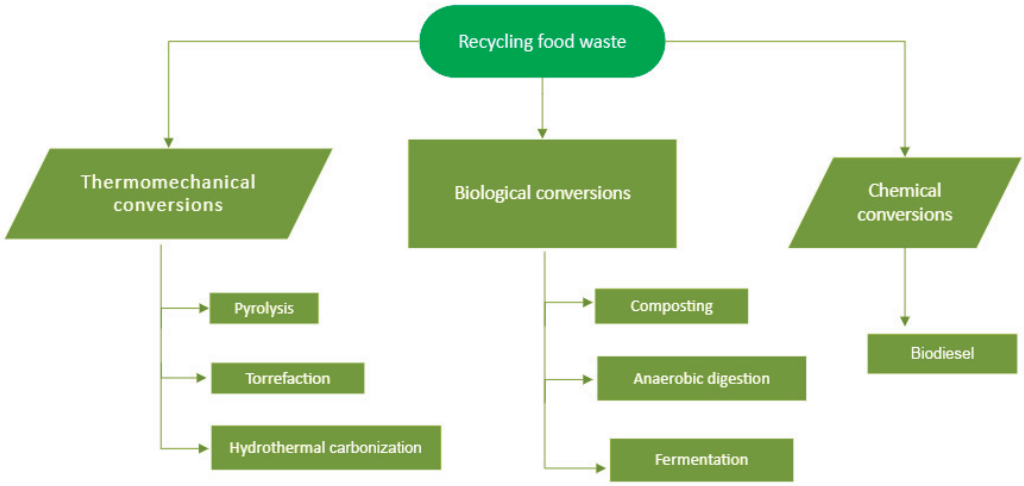

Figure 1. Typical food waste recovery technologies.

3.1. The Methods for Thermochemical Conversion

3.1.1. Torrefaction

Torrefaction (also known as low-temperature pyrolysis) is one of the most efficient processes for treating biomass. The process is carried out between 200 °C and 300 °C in a neutral atmosphere, at atmospheric pressure and with a residence time of up to 90 min. The absence of oxygen inhibits the combustion process and accelerates the thermal decomposition of the torrefied biomass [2].

The final result of the torrefied biomass is influenced by the temperature, duration and flow rate of the carrier gas, particle size, composition and presence of catalyst, etc. [21].

The resulting biochar typically has much better physical and chemical properties than raw biomass; it has a higher calorific value, higher energy and mass density, improved hydrophobicity and better friability, giving it similar properties to coal [23].

Torrefaction causes the breakdown of hemicellulose and the dehydration of cellulose and lignin [24]. Studies have shown that the oxygen–carbon ratio is reduced, and the energy value is increased [2].

The process is particularly suitable for treating food waste with high moisture content and subject to biodegradation. One of the disadvantages of torrefaction is the presence of dioxins (by-products of incineration in various industrial processes) and dioxin-like contaminants in the charred end product [25].

As the moisture content of the biomass is significantly reduced during the torrefaction process, the moisture content of the final product is about 1 to 3% [2].

Hydrogen is also an important energy source in biomass combustion, but it is usually present in biomass in the form of CH or OH bonds. The oxygen contained in biomass is useful in combustion, but a higher oxygen content reduces the calorific value of the biomass. It is important that the torrefaction process achieves a calorific value close to that of coal (25–35 MJ kg^{-1}). Recently, torrefaction has been used as an efficient method of biomass pre-treatment for the production of bio-oil from pyrolysis [21].

3.1.2. Pyrolysis

Pyrolysis produces energy from waste biomass in the form of solid and liquid biochar and synthetic gas [26]. This thermal decomposition process takes place in the absence of oxygen. The chemical reactions are complex and consist of several steps. The process takes place in a pyrolysis reactor in two stages. The first stage produces a liquid, solid char and gas, and the second stage produces a liquid bio-oil. In the absence of a condenser, all the feedstock is thermally decomposed into gases, which are then used in the combustion chamber to provide heat [27].

The pyrolysis process is carried out at high temperatures, ranging from 300 to 1000 °C. The operating conditions have a strong influence on the resulting products, as fast pyrolysis uses finely ground feedstock, which gives high bio-oil yields. In slow pyrolysis, however, the bio-oil content is much lower. The operating parameters can be varied to obtain the desired range of products, which depends on the feedstock selected [26].

3.1.3. Gasification

The gasification process usually takes place in a temperature range between 600 °C and 1200 °C. Gasification is usually divided into gasification, steam gasification and supercritical water gasification, depending on the reaction environment. Gasification of biomass is an oxygen-deficient thermal process in which the feedstock is converted into a gaseous product, where the main products are H2 and CO. The improved properties of biomass are higher calorific value and lower volatile content [21].

Gasification is a thermochemical partial oxidation process that takes place at high temperatures. During the gasification process, the solid feedstock is transformed into a gaseous fuel. The composition of the resulting gases depends strongly on the type of feedstock, but the product produced is mainly composed of methane, carbon monoxide and hydrogen [28].

3.1.4. Hydrothermal Carbonization

Hydrothermal carbonization is the process of converting selected biomass into energy- and carbon-rich charcoal. It involves hydrolysis, polymerization, dehydration and carbonization processes taking place at moderate temperatures between 180 and 260 °C and pressures between 35 and 55 bar. As food waste contains moisture, it is used as an organic solvent at higher temperatures and pressures when exposed to HTC due to its reduced dielectric constant. Such exposure of food waste is not economically feasible in the above processes due to the intense evaporation of the moisture present [29].

The hydrothermally produced solid product can be used as a fuel, adsorbent or catalyst, while the use of the liquid product is limited. The main constituents of the hydrothermally produced gaseous product are carbon dioxide and trace hydrocarbons [30].

The HTC process reduces the ratio of hydrophilic to hydrophobic substances, converting organic feedstocks into hydrocarbon-rich solids. Studies have confirmed that the use of HTC in conjunction with a mechanical water removal process is more energy efficient

than using a conventional thermal drying process to control water content. The use of a combination of HTC and pyrolysis is a promising method to reduce the high energy efficiencies associated with water evaporation [31].

3.2. Technologies Depending on FW Type

In Table 2, several technological options for processing food waste are listed. The selected technology should be simple and capable of handling the heterogeneous nature and moisture content of food waste. It must allow for relatively short treatment times, on-site separation and separation at transfer stations to continuously reduce the volume of waste and thus the need to transport it to landfill [22].

Table 2. Characteristics of technological processes for treating food waste from a technical and economic perspective [22].

Technology	Characteristic	Processing Cycle	The Results
Incineration	- Large quantities required. - Necessary mixing for uniform quality.	- Large amounts of different heterogeneous biomasses, including food waste.	- Heat for steam production and heating. - Ash. - Heavy metals.
Fast pyrolysis	- Fast processing. - Pre-treatment of drying the raw material to a moisture content of 10–15% is required.	- Some food waste is unsuitable because it contains moisture.	- 60–75% of liquid product. - 15–20% biochar. - 10–20% non-condensable gases.
Gasification	- Pre-treatment of drying the raw material to a moisture content of 10 to 20% is required. - Waste must be carbonized. - Part of the waste is not suitable for gasification.	- Pre-drying process is required.	- Synthetic gas.
Hydrothermal Carbonization (HTC)	- Waste can be wet. - Acetone is required for extraction. - Crushing into a mixture.	- Short processing cycles.	- 49–75% of the carbon present is retained in the charcoal. - 20–37% in the liquid phase. - 2–11% in the gaseous phase.
Hydrothermal liquefaction (HTL) Torrefaction	- Water and inexpensive catalyst are required. - There is no sensitivity to wet waste. - A portion of food waste in municipal waste, due to its high moisture content, is not suitable for torrefaction	- It processes heterogeneous wet waste. - Needs to be crushed into a relatively homogeneous mixture. - Very rapid processing cycles.	- By-products include the liquid phase (approximately 85% of the hydrolysate)—mixed solid phases (approximately 15% as dry weight). - Produces solid fuels with high energy content and improved combustion properties.

4. Results and Discussion

To summarize the data from the Statistical Office of the Republic of Slovenia (SURS), over 143,000 tons of food waste was generated in Slovenia in 2020. The amount of food waste is increasing annually and has increased by an average of 3% per year in the period from 2013 to 2021. According to SURS estimates, 40% of food waste consists of edible parts, which could be significantly reduced with appropriate consumer awareness and the right attitude towards food. The remaining part consisted of peels, skins, seeds, etc., which are considered inedible parts of food waste. Although the average annual amount of food wasted by Slovenians is lower than the European average, a comparison between 2017 and 2020 shows an increase in the amount of food wasted and thrown away per capita, from 64 kg to 68 kg [16].

The amount of food waste produced at different stages of the food supply chain is shown in Figure 2 [32].

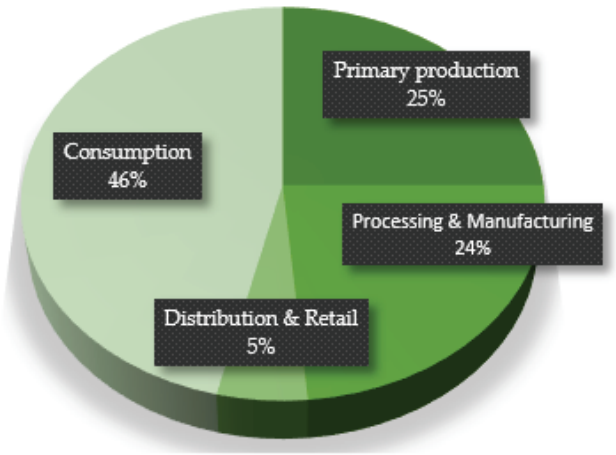

Figure 2. The amount of food waste produced at different stages of the food supply chain.

Unlike biochemical conversion, in which the substrates are slowly broken down during anaerobic metabolism, thermal conversion is an energy-intensive way of obtaining energy from biomass. During thermal conversion, the high heating values of the biomass and processes such as dehydration, deoxygenation and dihydroxylation are determined. The calorific values of biomass are crucial for the selection of biomass for energy production and the assessment of its potential for economic feasibility. The thermal values of biomass samples can be determined by computational models or direct measurements [33].

Table 3 shows the approximate and final values of selected biomass produced from different types of food waste, both dry and ash-free values, and a summary of the calorific contents for each biomass.

High-moisture food waste has a low calorific value. The low calorific value is also due to the high elemental oxygen-to-carbon (O/C) ratio. The high HHV of animal-based food waste is probably due to the higher hydrogen-to-carbon (H/C) ratio. During combustion itself, combustible gases are released, which are associated with a large amount of energy. A number of studies have reported that most of the calorific values of food waste were not only below a combustible index of 23 MJ/kg but also higher than a combustible index of 14.5 MJ/kg. This points to the fact that most types of food waste cannot be considered as alternative renewable fuels without pre-treatment. These chemical components are present in hydrolyzed form in liquid food waste. The chemical and elemental composition (carbon-C, hydrogen-H, oxygen-O, sulphur-S, nitrogen-N, etc.) of food waste and charcoal makes it possible to determine the quality of the fuel or charcoal produced from food waste. Lignin-rich food waste is desirable for the production of highly efficient solid fuels because of its high thermal stability in comparison with cellulose and hemicellulose. The lower the

atomic O/C ratio, the higher the calorific value of the solid fuel produced. All food wastes with a low fuel ratio are less reactive unless pre-treatment is carried out [29].

Table 4 shows the values of elemental composition in biochar obtained from different biomass sources through the processes of torrefaction and hydrothermal carbonization, and it emphasizes the lack of research in the field of torrefaction.

Table 3. Approximate and final values of selected biomass derived from different types of food waste, dry and ash-free, and a summary of the calorific values for each biomass.

Biomass	C	N	O	H	S	Ash Content	VM %	FC %	HHV (MJ/kg)	O/C	H/C
Animal-based [33]	[30]										
Egg	23.49	3.03	7.65	23.11	1.02	62.50	18.90	18.60	10.09	1.24	1.17
Fish	44.42	7.41	28.67	7.90	1.25	10.35	75.56	14.09	15.20	0.49	2.12
Meat (Beef fat—processing)	70.95	0.70	16.90	11.01	-	0.44	99.50	0.06	36.64	0.11	1.16
Manure and whey	28.2	1.7	20.3	3.6	0.5	45.7	-	-	15.9	0.54	1.53
Plant-based [33]	[30,34]										
Pumpkin	48.85	3.50	39.33	6.67	-	1.65	92.32	6.03	19.12	0.60	1.63
Potatoes	42.20	2.15	48.05	5.84	-	1.76	93.39	4.85	14.12	0.86	1.65
Carrot	42.45	2.17	47.63	5.55	-	2.19	81.86	15.95	13.88	0.84	1.56
Grape pomace (GP)	44.14	1.27	41.91	6.18	-	6.50	76.22	17.28	-	0.79	1.68
Garlic	42.96	1.08	37.40	5.49	0.88	12.20	67.64	20.17	15.83	0.65	1.52
Peanut	59.27	3.30	22.39	8.18	-	6.86	93.95	0.81	27.77	0.29	1.64
Apple chip pomace (ACP)	47.94	1.96	40.90	6.66	0.07	2.47	81.65	15.88	-	0.64	1.66
Rice husk	46.26	1.36	45.92	6.46	-	11.80	73.50	14.70	16.20	0.74	1.67
Corn stalk	45.67	0.31	47.60	6.42	-	2.59	87.19	2.59	17.65	0.78	1.68
Wheat straw	51.25	0.63	42.81	5.18	0.13	3.70	80.00	7.80	17.10	0.63	1.21
Empty fruit bunces	48.30 45.53	1.00	43.70	6.66	0.34	3.00	82.21	10.41	19.45	0.68	1.65
Olive pulp-including kernels	51.91	1.65	40.45	5.99	-	3.10	75.20	21.80	21.70	0.58	1.38
Coconut husk	50.05	0.41	43.63	5.80	0.10	3.40	61.80	34.80	19.10	0.66	1.39
Banana peel	47.50	1.00	45.50	7.03	-	8.30	-	-	9.19	0.71	1.77
Energy crops	40.30	2.1	24.0	4.6	0.3	28.7	-	-	16.4	0.44	1.37
Vegetable, garden and fruit waste	29.50	2.0	21.4	3.0	0.3	43.8	-	-	14.9	0.54	1.22

Table 4. A comparison between torrefaction and hydrothermal carbonization of certain food waste, including their chemical composition and energy value.

	Torrefaction [24,34]									Hydrothermal Carbonization [12,33–35]								
Biomass (Animal- and Plant-Based)	C	N	O	H	S	Ash	HHV (MJ/kg)	O/C	H/C	C	N	O	H	S	Ash	HHV (MJ/kg)	O/C	H/C
Manure and whey	-	-	-	-	-	-	-	-	-	35.5	-	13.6	3.8	-	-	14.5	0.28	1.28
Chicken	-	-	-	-	-	-	-	-	-	66.1	6.46	16.22	9.9	0.3	1.02	32.97	0.18	1.8
Grape pomace [35]	-	-	-	-	-	-	-	-	-	61.46	1.72	29.97	5.16	-	1.69	-	0.36	1.01
Apple chip pomace	-	-	-	-	-	-	-	-	-	62.10	2.26	27.86	6.94	0.07	0.77	-	0.34	1.34
Rice husk	55.82	0.91	-	-	0.02	21.24	-	-	-	49.26	0.68	43.57	6.48	-	12.10	16.50	0.66	1.57
Corn fiber	-	-	-	-	-	-	-	-	-	49.25	0.25	44.28	6.21	-	0.53	19.47	0.67	1.15
Wheat straw	-	-	-	-	-	-	-	-	-	53.02	0.63	40.88	5.36	0.11	1.30	19.30	0.57	1.21
Empty fruit bunces	47.07	1.35	42.24	4.95	0.11	-	-	0.67	1.26	54.30	1.02	38.29	4.14	0.24	4.16	22.07	0.53	0.91
Olive pulp-including kernels	51.8	0.1	41.5	6.1	0.02	0.5	19.6	0.60	1.41	61.16	1.68	30.63	6.53	-	4.80	24.30	0.37	1.28
Coconut husk	-	-	-	-	-	-	-	-	-	59.52	0.50	34.17	5.71	0.10	0.30	23.90	0.43	1.15
Energy crops	-	-	-	-	-	-	-	-	-	41.2	-	21.9	3.9	-	-	23.1		
Raw vegetables, fruits and peels [12]	55.86	3.15	10.93	5.15	-	24.91	23.83	0.15	1.10	-	-	-	-	-	-	-	0.52	1.41

Elemental composition analysis, which includes hydrogen (H), carbon (C), nitrogen (N), sulphur (S) and oxygen (O), has a central role to play in assessing the properties of biomass and coal and allows for an accurate material balance and determination of calorific value. This analysis can be performed individually or in combination to obtain

comprehensive results, with C, H, N and S expressed on a dry basis. In particular, the hydrogen content affects the amount of heat of combustion and, conversely, the C content. Although oxygen promotes combustion, it reduces the calorific value due to its diluting effect on carbon. Elemental analyses of biomass generally show a higher proportion of O and C, followed by H, N and S, although the proportions vary depending on the type of biomass [33].

In the process of torrefaction of biomass, the decrease in the O/C ratio is due to the increased lignin content, which has a lower O/C ratio than cellulose and hemicellulose. This shift reduces the oxygen content, enriches elemental carbon and consequently increases the calorific value. In addition, the H/C ratio decreases due to the release of volatile compounds, but this is attenuated by the increasing lignin content at higher torrefaction temperatures, which affects the balance between hydrogen and carbon. Although torrefaction increases calorific value due to the lower O/C and H/C ratios, it also results in weight loss, which offsets some of the calorific benefits gained, especially at higher temperatures. Therefore, torrefied biomass has a higher carbon content and lower oxygen content compared to raw biomass, which has a positive effect on the O/C ratio and calorific value (Table 4).

Based on the measured values of biomass products, it is evident that food waste with high moisture content and high O/C ratio has a low heating value (HHV). The understanding of the HHV of fuels and substrates is determined on the basis of the atomic ratios of O/C and H/C. The high heating value of animal waste biomass is most likely due to the higher H/C ratio, as combustion releases a large amount of gases [33]. Food waste with a low fuel ratio is less reactive unless preprocessing is used.

Waste containing meat with a higher carbon content (70.95%) had a higher calorific value (36.46%), which is in line with the claim that high-carbon biomass has a high calorific value. The predominantly low HHV values of the different biomass food wastes are consequently attributed to the high oxygen levels, which do not promote combustion but have a negative effect on the conversion of biomass to liquid fuel. Pyrolysis as a biomass conversion process lowers the atomic H/C and O/C ratios, increases the heating value and thus achieves better solid fuel production [36].

As shown in Table 2, several technological options are available for the treatment of food waste. When selecting a technology for the treatment of food waste, a number of aspects need to be carefully considered. The technology selected must be simple and able to cope with the heterogeneity of food waste and its moisture content. It must generate materials or products with energy value that can be used for further applications. In addition, it must allow relatively short recovery cycles [22].

Compared to other municipal waste fractions, food waste is characterized by its high moisture content and poses a challenge for efficient incineration or conversion processes. A high moisture content, especially in fruit and vegetables, can lead to the release of dioxins when incinerated together with organic substances. This moisture content significantly lowers the heating value of food waste and thus reduces its energy quality. The varying characteristics of different food waste sources, compounded by limitations such as small sample sizes and inconsistent categorization, underscore the need for comprehensive analysis to refine energy models. The moisture content of food waste ranges from 1.59% to 74%, exceeding the variability of coal. The complex chemical composition of food waste, including lignin, cellulose, hemicellulose and extractive substances, varies between solid and liquid forms, which affects the assessment of energy potential. The high cellulose content, which mainly comes from plant and fruit parts, underlines the potential of food waste for energy conversion. HTC for charcoal production depends on process parameters such as pressure, temperature and the ratio of biomass to water, with temperature having the greatest impact on product yield. Higher temperatures favor liquid and gaseous products over solid carbonaceous charcoal, as shown in Table 4 [30].

In studies on the HTC of food waste, temperature plays a decisive role in changing the quantities of volatile substances. Elevated temperatures reduce the volatiles and increase

the amount of fixed carbon and ash, resulting in a higher carbon content in the carbonaceous coal. As mentioned above, the effect of temperature varies depending on the type of food waste due to its different chemical composition and thermal stability. Optimal temperature selection is critical to maximize the carbon content depending on the intended use, as found in various studies [30].

In addition, hydrodynamic cavitation (HC) technology has shown distinct advantages in simplicity and cost-effectiveness at different stages, including water treatment, lignocellulosic biomass pre-treatment, food processing and emulsification [37].

Torrefaction, a thermal pre-treatment process carried out at 200–300 °C in an inert atmosphere, improves the properties of biomass by increasing energy density, improving ignition properties and reducing moisture content. It increases the ratio of carbon to oxygen (C/O) and carbon to hydrogen (C/H), improving combustion efficiency and biomass storage. While the energy yield exceeds the mass yield due to the loss of volatile compounds, torrefaction significantly densifies the biomass and increases its energy content. During this process, the removal of oxygen produces gaseous compounds containing carbon, oxygen and hydrogen, which are crucial for reducing heat content and enabling the conversion of biomass into a solid fuel like coal. In addition to carbonization, torrefaction offers a way to produce solid fuels for heat and power generation, which underlines its importance for energy production [38].

Torrefaction is like pyrolysis and carbonization. The essential difference between pyrolysis, carbonization and torrefaction lies in their production objectives. The main objective of pyrolysis is to maximize liquid production while minimizing char yield. In carbonization, the objective is to increase the fixed carbon content and reduce the hydrocarbon content of the solid product, while in torrefaction, the objective is to increase the solid biochar content with specific atomic ratios (O/C) and (H/C) [36]. For electricity generation, torrefied biomass is used either alone or in combination with coal, which reduces the need for large quantities of coal. Different tests were performed to determine the moisture content (MC), ash content (ash), volatile matter content (VM) and fixed carbon content (FC) of different biomasses. These tests provide a basis for comparing how raw or torrefied biomass performs compared to coal in energy production. The volatile matter content of raw biomass before torrefaction is typically high, ranging from 70 to 88% by weight, while the fixed carbon content is low, ranging from 10 to 21% by weight. After torrefaction, the composition of VM (and MC) in the biomass decreases, resulting in an increase in the FC composition. The VM content of torrefied biomass is approximately 40 to 85 wt.%, while the FC content is 13 to 45 wt.%. Some authors use the FC/VM ratio to analyze the degree of torrefaction of biomass. The value of the atomic ratio increases with increasing torrefaction temperature as the FC content increases, while the VM content decreases after torrefaction. Based on the values investigated above, raw biomass has an FC/VM ratio of 0.14 to 0.24, while torrefied biomass has an FC/VM ratio of 0.33 to 0.53 [38].

Chen et al. reported on the volatile matter (VM) content in raw biomass before torrefaction. Research results showed that VM content is typically high, ranging between 70 and 88 mass%, while its fixed carbon (FC) content is usually low, ranging between 10 and 21 mass%. After torrefaction, the composition of VM (and moisture content, MC) in biomass decreases, resulting in an increase in the FC composition. The volatile matter content in torrefied biomass is approximately in the range of 40 to 85 mass%, while the FC content ranges between 13 and 45 mass% [39].

Nhuchhen and Basu, along with some other researchers, utilized the FC/VM ratio for the analysis of torrefaction extent in biomass. The ratio should increase with the increase in torrefaction temperature since the FC content increases, while the VM content decreases after torrefaction [40].

5. Conclusions

Considering the prevailing energy crisis and escalating pollution, there is an urgent need for research efforts aimed at promoting cleaner production through the exploration of

environmentally sustainable energy sources. Central to this endeavor is the compelling challenge posed by excessive food waste, a prominent global problem facing humanity. This paper presents the results of investigations exploring various thermodynamic processes to convert food waste into valuable products with significant energy potential, representing a remarkable advance in the field. Careful research and analysis have shown that food waste, especially that with a relatively high moisture content, has a relatively low energy value, typically around 14 MJ/kg. Consequently, most food waste cannot be used as a renewable fuel source without pre-treatment by pyrolysis, torrefaction or hydrothermal carbonization.

According to Ipiales et al., hydrochar as a solid product contains approximately 40–90% of the initial carbon from the raw material and includes energy values ranging from 15–30 MJ/kg [41].

All processes, pyrolysis, torrefaction and hydrothermal carbonization are recognized techniques used to optimize the energy potential of food waste by reducing the atomic H/C and O/C ratios, thereby increasing the calorific value and enabling better solid fuel production. The post-pyrolysis results show significant differences in the yield of the different food waste categories, with meat/fat having the lowest yield (3.4%) and egg waste having the highest char value (50.52%). This indicates that biomass with a low char yield can be converted into gasses or bio-oils after pyrolysis. In addition, oily wastes prove to be particularly suitable for pyrolysis as they have a high energy yield and minimal operating costs associated with carbon management.

An advantage of torrefaction is that it allows for precise measurement of biomass weight loss during the process [42].

The concept of fuel ratio, expressed as the predefined ratio of carbon to volatile matter (FC/VM), is proving to be a key benchmark for evaluating the fuel potential of food waste and offers insights into its suitability as a substitute for charcoal or coal. The effectiveness of hydrothermal carbonization (HTC) as a transformative technology for food waste conversion is underappreciated as it demonstrates its versatility in processing plant and animal waste into products like biofuels. HTC is proving to be a viable way to produce solid fuels from wet and low-grade biomass, complemented by pyrolysis, which excels in the production of bio-synthetic fuels from high-energy biomass. Torrefaction, which takes place by controlled heating in a non-oxidative atmosphere at 200 to 300 °C, is characterized by its ability to remove moisture and volatile compounds to produce an energy-rich fuel.

A review of the recent literature indicates that torrefaction is a highly promising technique for enhancing the efficiency of biomass for energy utilization. Despite numerous studies conducted, there still remains a wealth of information on torrefaction that is not adequately identified and researched in detail [42].

As mentioned in the introduction, the novelty of this study lies in the fact that there is a lack of research on different types of food waste for the presented thermodynamic process. Our future work will focus on exploring this area further.

In summary, the results and research of this study highlight the promising potential of thermodynamic processes such as pyrolysis, torrefaction and hydrothermal carbonization in converting food waste into valuable energy sources.

Author Contributions: Conceptualization, methodology, validation, investigation, formal analysis, writing—original draft: A.Š.; formal analysis, writing—review and editing, supervision: D.G.; writing—review and editing, supervision: D.U. All authors have read and agreed to the published version of the manuscript.

Funding: This research received no external funding.

Data Availability Statement: The original contributions presented in the study are included in the article, further inquiries can be directed to the corresponding author.

Conflicts of Interest: The authors declare no conflicts of interest.

References

1. Zou, C.; Zhao, Q.; Zhang, G.; Xiong, B. Energy Revolution: From a Fossil Energy Era to a New Energy Era. *Nat. Gas Ind. B* **2016**, *3*, 1–11. [CrossRef]
2. Dyjakon, A.; Noszczyk, T.; Smędzik, M. The Influence of Torrefaction Temperature on Hydrophobic Properties of Waste Biomass from Food Processing. *Energies* **2019**, *12*, 4609. [CrossRef]
3. Sarrion, A.; Medina-Martos, E.; Iribarren, D.; Diaz, E.; Mohedano, A.F.; Dufour, J. Life Cycle Assessment of a Novel Strategy Based on Hydrothermal Carbonization for Nutrient and Energy Recovery from Food Waste. *Sci. Total Environ.* **2023**, *878*, 163104. [CrossRef] [PubMed]
4. Khoo, C.G.; Lam, M.K.; Mohamed, A.R.; Lee, K.T. Hydrochar Production from High-Ash Low-Lipid Microalgal Biomass via Hydrothermal Carbonization Effects of Operational Parameters and Products Characterization. *Environ. Res.* **2020**, *188*, 109828. [CrossRef] [PubMed]
5. EIP-AGRI Focus Group. *Reducing Food Loss on the Farm: Final Report*; EIP AGRI Agriculture and Inovation: Brussels, Belgium, 2020.
6. Definitional Framework for Food Waste—Full Report. FUSIONS Report Available in (2014). Available online: https://www.eu-fusions.org/index.php/publications (accessed on 23 February 2024).
7. Bajzelj, B.; McManus, W.; Parry, A. *Food Waste in Primary Production in the UK*; WARP: Nevada, CA, USA, 2019. [CrossRef]
8. Caldeira, C.; De Laurentiis, V.; Corrado, S.; Van Holsteijn, F.; Sala, S. Quantification of Food Waste per Product Group along the Food Supply Chain in the European Union: A Mass Flow Analysis. *Resour. Conserv. Recycl.* **2019**, *149*, 479–488. [CrossRef] [PubMed]
9. Sithole, T.; Pahla, G.; Mashifana, T.; Mamvura, T.; Dragoi, E.-N.; Saravanan, A.; Sadeghifar, H. A Review of the Combined Torrefaction and Densification Technology as a Source of Renewable Energy. *Alex. Eng. J.* **2023**, *82*, 330–341. [CrossRef]
10. Lu, X.; Jordan, B.; Berge, N.D. Thermal Conversion of Municipal Solid Waste via Hydrothermal Carbonization: Comparison of Carbonization Products from Current Waste Management Tehniques. *Waste Manag.* **2012**, *32*, 1353–1365. [CrossRef] [PubMed]
11. Tradler, S.B.; Mayr, S.; Himmelsbach, M.; Priewasser, R.; Baumgartner, W.; Stadler, A.T. Hydrothermal Carbonization as an All-Inclusive Process for Food-Waste Conversion. *Bioresour. Technol. Rep.* **2018**, *2*, 77–83. [CrossRef]
12. Pour, F.H.; Makkawi, Y.T. A Review of Post-Consumption Food Waste Management and Its Potentials for Biofuel Production. *Energy Rep.* **2021**, *7*, 7759–7784. [CrossRef]
13. Socas-Rodríguez, B.; Álvarez-Rivera, G.; Valdés, A.; Ibáñez, E.; Cifuentes, A. Food By-Products and Food Wastes: Are They Safe Enough for Their Valorization? *Trends Food Sci. Technol.* **2021**, *114*, 133–147. [CrossRef]
14. Scherhaufer, S.; Davis, J.; Metcalfe, P.; Gollnow, S.; Colin, F.; De Menna, F.; Vittuari, M.; Östergren, K. Environmental Assessment of the Valorisation and Recycling of Selected Food Production Side Flows. *Resour. Conserv. Recycl.* **2020**, *161*, 104921. [CrossRef]
15. Esteban-Lustres, R.; Torres, M.D.; Piñeiro, B.; Enjamio, C.; Domínguez, H. Intensification and Biorefinery Approaches for the Valorization of Kitchen Wastes—A Review. *Bioresour. Technol.* **2022**, *360*, 127652. [CrossRef]
16. Črnivec, I.G.O.; Korošec, M.; Maček, K.; Rac, I.; Juvančič, L.; Poklar Ulrih, N. *Analiza Stanja in Vzrokov Nastajanja Odpadne Hrane v Sloveniji: Z Vlogami Ključnih Akterjev v Sloveniji v Shemi Poročanja Distribucije Presežkov Hrane*; Biotehniška Fakulteta: Ljubljana, Slovenia, 2021.
17. Engelberth, A.S. Evaluating Economic Potential of Food Waste Valorization: Onward to a Diverse Feedstock Biorefinery. *Curr. Opin. Green Sustain. Chem.* **2020**, *26*, 100385. [CrossRef]
18. Ouadi, M.; Bashir, M.A.; Speranza, L.G.; Jahangiri, H.; Hornung, A. Food and Market Waste–A Pathway to Sustainable Fuels and Waste Valorization. *Energy Fuels* **2019**, *33*, 9843–9850. [CrossRef]
19. Jo, J.-H.; Kim, S.-S.; Shim, J.-W.; Lee, Y.-E.; Yoo, Y.-S. Pyrolysis Characteristics and Kinetics of Food Wastes. *Energies* **2017**, *10*, 1191. [CrossRef]
20. Jouhara, H.; Ahmad, D.; Czajczyńska, D.; Ghazal, H.; Anguilano, L.; Reynolds, A.; Rutkowski, P.; Krzyżyńska, R.; Katsou, E.; Simons, S.; et al. Experimental Investigation on the Chemical Characterisation of Pyrolytic Products of Discarded Food at Temperatures up to 300 °C. *Therm. Sci. Eng. Prog.* **2018**, *5*, 579–588. [CrossRef]
21. Chen, W.-H.; Lin, B.-J.; Lin, Y.-Y.; Chu, Y.-S.; Ubando, A.T.; Show, P.L.; Ong, H.C.; Chang, J.-S.; Ho, S.-H.; Culaba, A.B.; et al. Progress in Biomass Torrefaction: Principles, Applications and Challenges. *Prog. Energy Combust. Sci.* **2021**, *82*, 100887. [CrossRef]
22. Brilovich Mosseri, M.; Duenyas, A.; Cohen, E.M.A.; Vitkin, E.; Steinbruch, E.; Epstein, M.; Kribus, A.; Gozin, M.; Golberg, A. Hydrothermal Liquefaction of Representative to Israel Food Waste Model. *Energy Convers. Manag. X* **2023**, *20*, 100475. [CrossRef]
23. Ong, H.C.; Yu, K.L.; Chen, W.-H.; Pillejera, M.K.; Bi, X.; Tran, K.-Q.; Pétrissans, A.; Pétrissans, M. Variation of Lignocellulosic Biomass Structure from Torrefaction: A Critical Review. *Renew. Sustain. Energy Rev.* **2021**, *152*, 111698. [CrossRef]
24. Chen, L.; Chen, X.; Zhao, Y.; Xie, X.; Yang, S.; Hua, D.; Wang, C.; Li, T. Effect of Torrefaction on the Physiochemical Characteristics and Pyrolysis of the Corn Stalk. *Polymers* **2023**, *15*, 4069. [CrossRef]
25. Matsakas, L.; Gao, Q.; Jansson, S.; Rova, U.; Christakopoulos, P. Green Conversion of Municipal Solid Wastes into Fuels and Chemicals. *Electron. J. Biotechnol.* **2017**, *26*, 69–83. [CrossRef]
26. Jouhara, H.; Ahmad, D.; Van Den Boogaert, I.; Katsou, E.; Simons, S.; Spencer, N. Pyrolysis of Domestic Based Feedstock at Temperatures up to 300 °C. *Therm. Sci. Eng. Prog.* **2018**, *5*, 117–143. [CrossRef]
27. Widiyannita, A.M.; Cahyono, R.B.; Budiman, A.; Sutijan; Akiyama, T. *Study of Pyrolysis of Ulin Wood Residues*; AIP Publishing: New York, NY USA, 2016; p. 050004.

28. Jouhara, H.; Nannou, T.K.; Anguilano, L.; Ghazal, H.; Spencer, N. Heat Pipe Based Municipal Waste Treatment Unit for Home Energy Recovery. *Energy* **2017**, *139*, 1210–1230. [CrossRef]
29. Mendoza Martinez, C.L.; Sermyagina, E.; Saari, J.; Silva De Jesus, M.; Cardoso, M.; Matheus De Almeida, G.; Vakkilainen, E. Hydrothermal Carbonization of Lignocellulosic Agro-Forest Based Biomass Residues. *Biomass Bioenergy* **2021**, *147*, 106004. [CrossRef]
30. Khan, M.A.; Hameed, B.H.; Siddiqui, M.R.; Alothman, Z.A.; Alsohaimi, I.H. Hydrothermal Conversion of Food Waste to Carbonaceous Solid Fuel—A Review of Recent Developments. *Foods* **2022**, *11*, 4036. [CrossRef] [PubMed]
31. Shi, Z.; Liu, S.; Wang, S.; Niedzwiecki, L.; Baranowski, M.; Czerep, M.; Tang, C.; Kawi, S.; Wang, C.-H.; Jiang, J.; et al. Hydrothermal Carbonization Coupled with Pyrolysis: An Innovative Approach to Digestate Management. *Green Energy Resour.* **2023**, *1*, 100034. [CrossRef]
32. Lopez, J.S.; Caldeira, C.; De Laurentiis, V.; Sala, S. *Brief on Food Waste in the European Union*; The European Commission's Knowledge Centre for Bioeconomy: Brussels, Belgium, 2020.
33. Ugwu, S.N.; Enweremadu, C.C. Ranking of Energy Potentials of Agro-Industrial Wastes: Bioconversion and Thermo-Conversion Approach. *Energy Rep.* **2020**, *6*, 2794–2802. [CrossRef]
34. Ganesapillai, M.; Mehta, R.; Tiwari, A.; Sinha, A.; Bakshi, H.S.; Chellappa, V.; Drewnowski, J. Waste to Energy: A Review of Biochar Production with Emphasis on Mathematical Modelling and Its Applications. *Heliyon* **2023**, *9*, e14873. [CrossRef] [PubMed]
35. Zhang, B.; Heidari, M.; Regmi, B.; Salaudeen, S.; Arku, P.; Thimmannagari, M.; Dutta, A. Hydrothermal Carbonization of Fruit Wastes: A Promising Technique for Generating Hydrochar. *Energies* **2018**, *11*, 2022. [CrossRef]
36. Braz, C.E.; Crnkovic, P. Physical Chemical Characterization of Biomass Samples for Application in Pyrolysis Process. *Chem. Eng. Trans.* **2014**, *37*, 523–528. [CrossRef]
37. Xia, G.; You, W.; Manickam, S.; Yoon, J.Y.; Xuan, X.; Sun, X. Numerical Simulation of Cavitation-Vortex Interaction Mechanism in an Advanced Rotational Hydrodynamic Cavitation Reactor. *Ultrason. Sonochem.* **2024**, *105*, 106849. [CrossRef] [PubMed]
38. Mamvura, T.A.; Danha, G. Biomass Torrefaction as an Emerging Technology to Aid in Energy Production. *Heliyon* **2020**, *6*, e03531. [CrossRef] [PubMed]
39. Chen, W.H.; Cheng, W.Y.; Lu, K.M.; Huang, Y.P. An Evalution on Improvement of Pulverized Biomass Property for Solid Fuel through Torrefaction. *Appl. Energy* **2011**, *88*, 3636–3644. [CrossRef]
40. Nhuchhen, D.R.; Basu, P. Experimental Investigation of Mildly Pressurized Torrefaction in Air and Nitrogen. *Energy Fuels* **2014**, *28*, 3110–3121. [CrossRef]
41. Ipiales, R.P.; de La Rubia, M.A.; Diaz, E.; Mohedano, A.F.; Rodriguez, J.J. Integration of Hydrothermal Carbonization and Anaerobic Digestion for Energy Recovery of Biomass Waste: An Overview. *Energy Fuels* **2021**, *35*, 17032–17050. [CrossRef]
42. Chen, W.-H.; Kuo, P.-C. A Study on Torrefaction of Various Biomass Materials and Its Impact of Lignocellulosic Structure Simulated by a Thermogravimetry. *Energy* **2010**, *35*, 2580–2586. [CrossRef]

energies

MDPI

Article

The Trade-Off between Combustion and Partial Oxidation during Chemical Looping Conversion of Methane

Francesco Miccio [1,*], Mauro Mazzocchi [1], Mattia Boscherini [2], Alba Storione [2], Matteo Minelli [2] and Ferruccio Doghieri [2]

[1] Institute of Science, Technology and Sustainability for Ceramics (ISSMC), National Research Council of Italy, Via Granarolo 64, 48018 Faenza, Italy; issmc@issmc.cnr.it

[2] Department of Civil, Chemical, Environmental and Materials Engineering (DICAM), Alma Mater Studiorum, University of Bologna, Via U. Terracini 28, 40131 Bologna, Italy; mattia.boscherini3@unibo.it (M.B.); alba.storione2@unibo.it (A.S.); matteo.minelli@unibo.it (M.M.); ferruccio.doghieri@unibo.it (F.D.)

* Correspondence: francesco.miccio@cnr.it

Abstract: The chemical looping reforming and combustion of methane have attracted increasing interest as processes for clean energy and syngas production, with potential to reduce carbon dioxide emissions. Previous literature on the development of oxygen carriers evidenced the effects that oxygen availability exerts on the selectivity of the oxidation reaction. In the present paper, we evaluate the performance of chromite sand (Chro), cerium dioxide (CeO_2), and mixed cerium–copper oxide (Ce–Cu) as oxygen carriers for either reforming or combustion according to their oxygen availability. The oxides are tested in 2 to 5 min reduction intervals in a CH_4/N_2 mixture (5, 10 and 20% vol.) followed by regeneration in O_2/N_2 (3, 5, or 21% vol.), with redox cycles conducted either at 850 °C or 950 °C. The obtained rank of selectivity towards complete CH_4 combustion is Ce–Cu > CeO_2 > Chro. Another relevant finding is the role of the degree of carrier conversion in promoting partial or total oxidation. In particular, the selectivity towards CO_2 markedly decreases at increasing carrier conversion, disclosing new strategies for process design and optimization by controlling the carrier conversion degree.

Keywords: chemical looping; combustion; reforming; methane; oxygen carrier

1. Introduction

Chemical looping combustion is an emerging technology allowing for the inherent separation of CO_2 in flue gases [1,2].

It is accomplished by using a suitable oxygen carrier, usually a metal oxide with multiple oxidation states (e.g., FeO_x, MnO_x, NiO_x), and it has the important advantage of limiting NO_x formation thanks to the flameless behavior and well controlled process temperature [3]. Chemical looping can also be effectively used for the reforming and partial oxidation of methane, with high selectivity toward H_2 and CO depending on the nature of the carrier [4]. Cu and Ni oxides generally favor complete oxidation, while cerium oxide is more suitable for partial oxidation to CO. In addition to selectivity, other crucial issues to consider for oxide selection in chemical looping operation are coke deposition and carrier lifetime, in particular, for fluidized bed systems, where attrition phenomena are more relevant [2]. Furthermore, the safety and disposal of the spent carrier are also fundamental aspects that need to be explored. In this respect, the use of Ni compounds is decreasing due to concerns about their toxicity [5].

The trade-off between combustion and partial oxidation is somehow connected to the prompt availability of oxygen-rich sites in the microstructure of the carrier. In the case of cerium dioxide, for example, it has been repeatedly observed that while the production of carbon monoxide is overall favored compared to combustion, carbon dioxide can be nonetheless formed at the start of the reaction due to the high availability of surface

oxygen species [6,7]. The availability of surface oxygen, related to the energy barrier for oxygen vacancy formation, the amount of total oxygen available for exchange (oxygen carrying capacity), the morphology and the surface chemistry, particularly oxygen vacancy concentration, all greatly affect the selectivity of oxidation [8]. For example, it has been suggested that the mechanism of methane oxidation on cerium dioxide changes as surface oxygen is depleted, with the activation of methane occurring preferentially on oxygen anions at the start of reaction, while on more reduced surfaces activation occurs also on oxygen vacancy sites [9]. Oxygen vacancies have also been observed to play a critical role in determining selectivity for reforming over combustion for iron oxygen carriers [10], with increased vacancy concentration favoring the partial oxidation of methane and lowering the energy barrier for C–H bond cleavage. In the present paper, we further investigate this shift in selectivity, which needs to be carefully evaluated to properly design the chemical looping process.

Natural chromite sand, made of a mixture of chromium and iron oxide mixed with other species such as alumina, silica, and others, is commonly used in metallurgy as foundry sand and as a source of chromium [11,12]. It has been previously investigated, as a catalyst, for use in fluidized bed combustion for CO abatement providing limited advantages [13], whilst copper-modified chromite proved more effective [14]. Its potential application as an oxygen carrier has, to the author's knowledge, so far not been investigated at depth in the literature. However, due to its inclusion of high concentrations of oxidation active iron oxide species (especially in low-grade chromite sands) and its high melting point, these materials may deserve further investigation. Copper oxide is a well-known catalyst for low-temperature combustion as well as for the decomposition of methane [15], but it is not commonly used for reforming processes. The use of CeO_2 for reforming processes has been investigated via several aspects, in particular the redox kinetics and carbon deposition at different temperatures and residence times [7,16,17]. Chemical looping combustion with CuO or CeO_2 has also been tested in fluidized bed apparatus [18–20], providing good results in terms of the material's lifetime, mechanical resistance, and regeneration efficiency.

The aim of the present research is to understand the potential use and the chemical behavior of different natural and synthetic oxygen carriers under changing operating conditions, moving from chemical looping combustion to partial methane oxidation. The influence of equivalence factor, temperature and conversion time is reported and discussed to provide further insights into the design of the process and the materials.

2. Materials and Methods

2.1. Materials

Three types of oxygen carriers have been selected: natural chromite sand (Cromitec 400, hereafter defined Chro), CeO_2 and CeO_2/CuO (samples named Ce–Cu) granules.

Commercial powders of CeO_2 (PIKEM, Wilnecote, UK) and CuO (Merck, Darmstadt, Germany) have been uniaxially pressed around 90 MPa, obtaining 20 mm diameter pellets subsequently crushed and sieved to 0.60–0.84 mm and thermally treated for 20 min in air at 900 °C.

For all the prepared materials O_2 capacity was computed based on reducible species content. The main properties of the carriers are reported in Table 1.

Cerium–copper carrier exhibits the highest O_2 capacity value while chromite has the lowest, the oxygen capacity being related to FeO alone; therefore, this excludes the possibility that Cr_2O_3 can be reduced at the process temperature.

Samples of the carriers have been characterized by electronic microscopy FE-SEM (Zeiss SIGMA, Carl Zeiss Microscopy GmbH, Jena, Germany, D) and X-ray powder diffractometry (XRD) using a Bruker D8 Advance (Bruker–Karlsruhe, Karlsruhe, Germany, D) diffractometer.

Table 1. Properties of oxygen carriers.

	Chro	CeO_2	Ce–Cu
Size (mm)	0.20–0.40	0.60–0.84	0.60–0.84
Density (kg/m^3)	4170	7220	6930
O_2 capacity (mmol/g)	0.90	1.45	2.98
Major phases			
CeO_2, wt. %	-	>99	68
CuO, wt. %	-	-	32
Cr_2O_3, wt. %	47	-	-
FeO, wt. %	26	-	-
Al_2O_3, wt. %	15	-	-
MgO, wt. %	10	-	-
SiO_2, wt. %	1	-	-

2.2. Experimental Apparatus

The schematic of the experimental rig used for chemical looping tests is shown in Figure 1. The reactor is a 10 mm ID quartz tube equipped with a ceramic distributor in the bottom. The reactor is installed inside an electric furnace (Carbolite 1200, Carbolite LTD, Hope Valley, UK). Bronkhorst mass-flowmeters are used to supply gas streams from compressed gas bottles (O_2, N_2, CH_4). A Pollutek GAS-3100P continuous gas analyzer (Pollutek Gas Analysis, Lubbeek, Belgium) has been employed for O_2, CO, CO_2, CH_4 and H_2 detection.

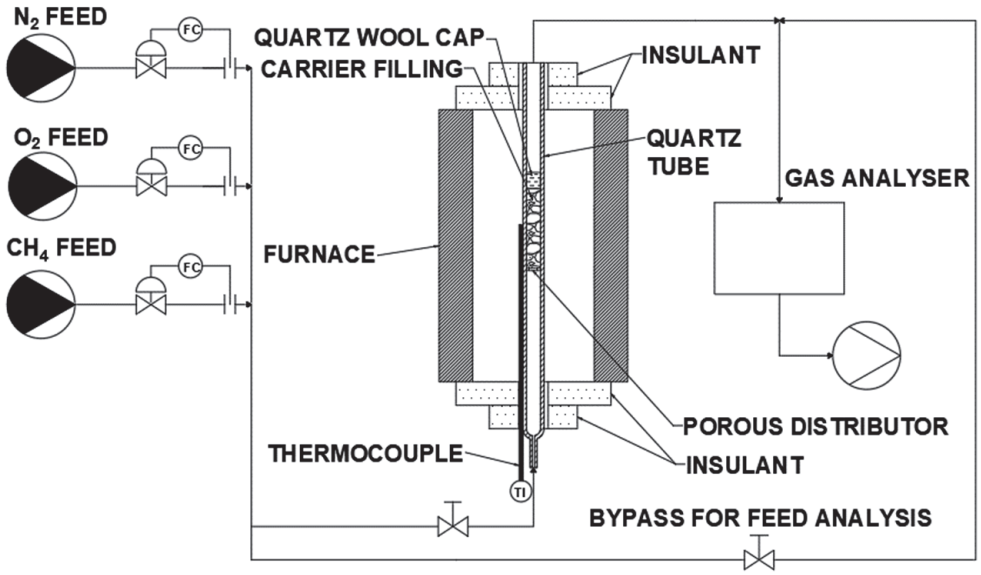

Figure 1. Schematic of the experimental apparatus. Flowrate Controller (FC) indicates the flowmeters. Temperature Indicator (TI) indicates the thermocouple.

In a typical experiment, a mass of 14 to 16 g of oxygen carrier is loaded in the reactor to ensure the same bed volume for the three oxygen carriers (≈5 cm^3), with a layer of ceramic wool on the top of the bed to limit fluidization and avoid the entrainment of particles outside the reactor. The residence time of the gas stream in the fixed bed was lower than 0.1 s. For the half cycle of reduction, streams of 1 NL/min of CH_4 at 5, 10 and 20 vol.% in N_2 were selected to study the effect of methane concentration on reaction selectivity, while for carrier regeneration, streams of O_2 at 3, 5, or 21 vol.% in N_2 at a total 1 NL/min flow rate were evaluated. The main factor in the choice of oxygen concentration during regeneration was the necessity to avoid overheating triggered by the exothermic reaction without loss in regeneration efficiency.

Reduction experiments were carried out by varying the time between 2 and 10 min, while for regeneration the reactor was kept on stream until a breakthrough in the inlet oxygen molar fraction was obtained.

2.3. Data Elaboration

The CH_4 conversion, ξ_{CH_4}, is evaluated by the integration of the difference between the inlet and outlet methane flow rate divided by the methane fed during the reduction step of length t_c = 2, 5 or 10 min (Equation (1)). The outlet molar flow rate is calculated using N_2 balance as a reference.

$$\xi_{CH_4} = \int (q_{in} \times y_{CH_4,in} - q_{out} \times y_{CH_4,out})dt/(q_{in} \times y_{CH_4,in} \times t_c) \quad (1)$$

The CO and CO_2 selectivity (η_{CO}, η_{CO_2}) are computed (Equations (2) and (3)) based on the converted CH_4 by integration of their molar fraction profiles,

$$\eta_{CO} = \int (q_{out} \times y_{CO,out})dt/(q_{in} \times y_{CH_4,in} \times t_r) \quad (2)$$

$$\eta_{CO_2} = \int (q_{out} \times y_{CO_2,out})dt/(q_{in} \times y_{CH_4,in} \times t_r) \quad (3)$$

Carbon deposition is calculated from carbon balance by considering the amount of CO and CO_2 released during the regeneration stage, also calculated by integrating the molar fraction profile. Carbon selectivity can therefore be obtained as

$$\eta_C = \int (q_{out} \times y_{CO,out} + q_{out} \times y_{CO_2,out})dt/(q_{in} \times y_{CH_4,in} \times t_c) \quad (4)$$

The equivalence factor of a single run corresponds to

$$e = n_{O_2\ av,i}/n_{O_2\ stoich,\ CH_4} \quad (5)$$

where $n_{O_2\ stoich,\ CH_4}$ indicates the moles of oxygen necessary for stoichiometric total combustion of the total fed methane, while $n_{O_2\ av,i}$ is the total amount of oxygen which can be released from the carrier i.

$$n_{O_2\ stoich,\ CH_4} = 2(q_{in} \times y_{CH_4,in} \times t_c) \quad (6)$$

The reactions considered for carrier reduction are

$$2CeO_2 \rightarrow Ce_2O_3 + 1/2O_2 \quad (R1)$$

$$Fe_2O_3 \rightarrow 2FeO + 1/2O_2 \quad (R2)$$

$$CuO \rightarrow Cu + 1/2O_2 \quad (R3)$$

Therefore, for cerium dioxide, the amount of available oxygen was calculated considering complete reduction to Ce_2O_3:

$$n_{O_2\ av,\ CeO_2} = 1/4(m_{CeO_2}/M_{CeO_2}) \quad (7)$$

For chromite, the amount of oxygen was calculated considering the FeO content of chromite only (Table 1), the reduction of the other oxides contained in chromite being thermodynamically hindered at the investigated temperature. The maximum releasable O_2 content derives from converting FeO to Fe_2O_3 and then reducing it back to FeO (Equation (8)), ω_i being the generic mass fraction of the component i. The reduction of FeO to metallic Fe was excluded,

$$n_{O_2\ av,\ Chro} = 1/4(m_{Chro} \times \omega_{FeO})/M_{FeO} \quad (8)$$

While the thermodynamic formation of completely reduced Fe would be feasible, metallic iron was not observed in the XRD patterns of reduced samples. Similarly, Leion et al. also excluded the total reduction of iron when discussing the use of ilmenite as an oxygen carrier [21].

For the Ce–Cu carrier, both reactions R1 and R3 were considered,

$$n_{O_2\ av,\ Ce\text{-}Cu} = 1/4(m_{Ce\text{-}Cu} \times \omega_{CeO_2})/M_{CeO_2} + 1/4(m_{Ce\text{-}Cu} \times \omega_{CuO})/M_{CuO} \quad (9)$$

The oxygen capacity (Table 1), reported as mmol of O_2 per gram, is also used to evaluate the conversion degree of the carrier, $\xi_{carrier}$, obtained by evaluating the total oxygen released during the reduction step through oxygen balance for CO, CO_2, O_2 and H_2O species, H_2O production being estimated via hydrogen balance.

$$\xi_{carrier} = \int \{q_{out} \times [0.5 \times y_{CO,\ out} + y_{CO_2,out} + y_{O_2,out}] + 0.5[2 \times q_{in} \times y_{CH_4,in} - q_{out} \times (2 \times y_{CH_4,out} - y_{H_2,out})]\}dt/n_{O_2,av,carrier} \quad (10)$$

where "carrier" indicates Chro, CeO_2, or Ce–Cu.

Experimental errors are mainly caused by the intrinsic transient character of the looping operation and are estimated in ±10% of the reported data.

3. Results

3.1. Reaction Test Results

Figure 2 shows the volumetric fraction profiles of CH_4, CO, CO_2, H_2 and O_2 for both oxidation (t = 1 ÷ 3 min) and regeneration (t = 4 ÷ 9 min) on the Chro carrier for a 2′ reduction step in 10% methane followed by 6′ regeneration in 3% O_2. A 1′ flushing with N_2 was performed in the passage from oxidation to regeneration and vice versa. It is clearly visible how the volume fractions change as reaction proceeds, with CO_2 production decreasing during the reduction step, whilst the H_2 and CO volume fractions increase. Similar profiles are also observed over CeO_2, while for the Ce–Cu carrier, CO and H_2 production were found to be almost completely absent, even for longer reduction steps. Considering an equal mass of carriers, the Ce–Cu carrier theoretically offers the highest oxygen availability compared to the other two tested (see Table 1). Also, the Ce–Cu carrier is the only one that shows the release of gaseous oxygen due to thermal dissociation at the investigated temperature, thus providing oxygen in a larger amount for reaction with methane.

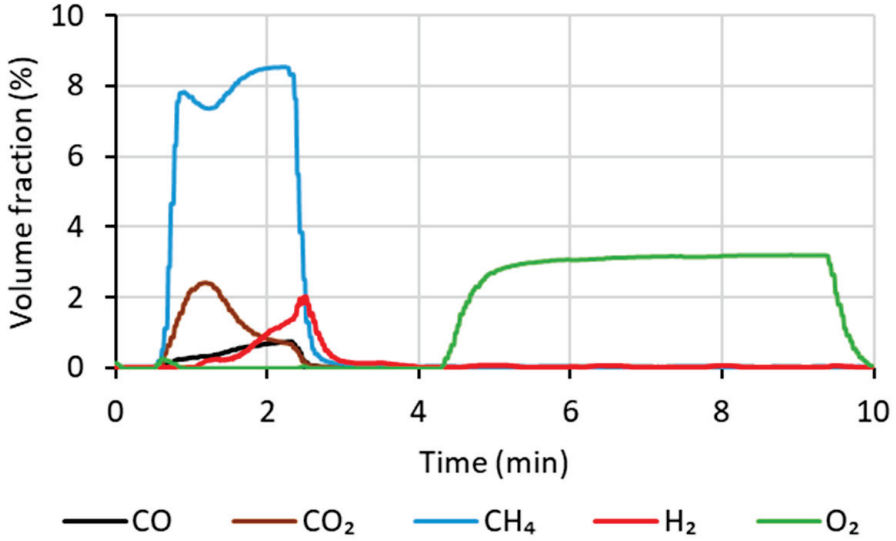

Figure 2. Volume fraction profiles of CH_4, CO, CO_2, H_2 and O_2 during a test at 950° (Chro, y_{CH_4} = 0.10, Y_{O2} = 0.03).

Figure 3 shows the comparison among Chro, CeO_2 and Ce–Cu carriers in terms of CH_4 conversion for tests carried out at 850 and 950 °C with reduction time of 2 or 5 min. It is clear that, in terms of maximum methane conversion, the rank of the carrier is Ce–Cu > CeO_2 > Chro, as a consequence of the difference in O_2 capacity and availability. Oxygen is the most widely available in the Ce–Cu carrier, both in terms of the quantity of available oxygen (Table 1) and of the easiness of oxygen release, as it is the only investigated material that releases gaseous oxygen at the investigated reaction temperature. Therefore, it is not surprising that methane conversion is greatest for this material, as the combustion reaction is not strictly surface-mediated, but can also involve fully gaseous species. It is worth noting that this Chemical Looping Oxygen Uncoupling (CLOU) mechanism [22] is also likely responsible for the similar values of ξ_{CH_4} at 850 and 950 °C for Ce–Cu, owing to the capability of this carrier to make available gaseous molecular O_2 imposing a less strict limit on process kinetics compared to the strictly surface-mediated oxidation on the other carriers, with the presence of metallic Cu further favoring the reaction by providing active sites for methane C–H bond cleavage.

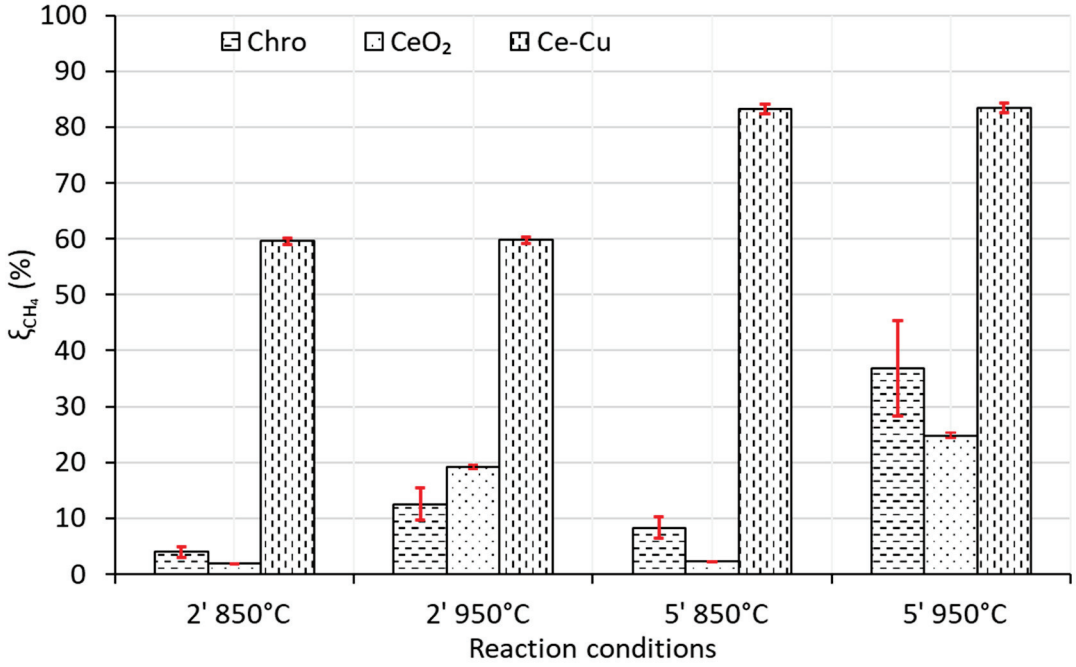

Figure 3. Average CH_4 conversion in Chro, CeO_2 and Ce–Cu carriers at 850 and 950 °C (y_{CH_4} = 0.10); the error bars reported in red in the plot indicate the standard deviation in triplicate tests.

On the contrary, the very low values of ξ_{CH_4} obtained for Chro and CeO_2 carriers at 850 °C moved the investigation preferably to the temperature of 950 °C. Furthermore, Chro carrier exhibited greater instability in performance, particularly after undergoing cycles at 950 °C. After undergoing reaction at 950 °C, the material appeared more effective even at a lower temperature: the observed average ξ_{CH_4} for 2 min partial oxidation steps at 850 °C was 1.7 ± 0.2% for fresh material, while it increased to 7.4 ± 0.4% after the material underwent reaction at a higher temperature. It is likely that the material undergoes structural changes during operation at higher temperatures. Once extracted from the reactor, Chro carrier was found to be partly sintered, and this could be the reason for the differences in performance.

Table 2 reports the selectivity and yield data for Chro, CeO_2 and Ce–Cu at 950 °C and y_{CH_4} = 0.10. The equivalence factor changes largely due to the difference in oxygen capacity of the three carriers. The greater availability of oxygen in Ce–Cu clearly appears, resulting in conversion up to 0.83 and the total combustion of methane regardless of the

total reduction time. The catalytic activity was retained over repeated cycles (>10) of reduction and oxidation for all samples.

Table 2. CH_4 conversion, CO selectivity and CO_2 selectivity for Chro, CeO_2 and Ce–Cu carriers (y_{CH_4} = 0.10, 950 °C).

	Time, min	e	ξ_{CH_4}	η_{CO}	η_{CO_2}
Chro	2	0.81	0.13	0.12	0,29
	5	0.32	0.37	0.45	0,00
CeO_2	2	1.25	0.19	0.24	0.78
	5	0.50	0.25	0.58	0.54
Ce–Cu	2	2.48	0.60	0.00	1.00
	5	0.99	0.83	0.00	1.00

For Chro and cerium dioxide, selectivity and conversion change throughout the reaction.

Figure 4 shows CH_4 conversion, and CO and CO_2 selectivity, at different CH_4 concentrations, as well as reduction time over CeO_2 carrier. The trends in the changes of these variables are mutually consistent: ξ_{CH_4} decreases as the mole fraction of CH_4 increases, corresponding to a lower equivalence factor in the whole test. Selectivity towards partial oxidation also increases with a longer reduction time.

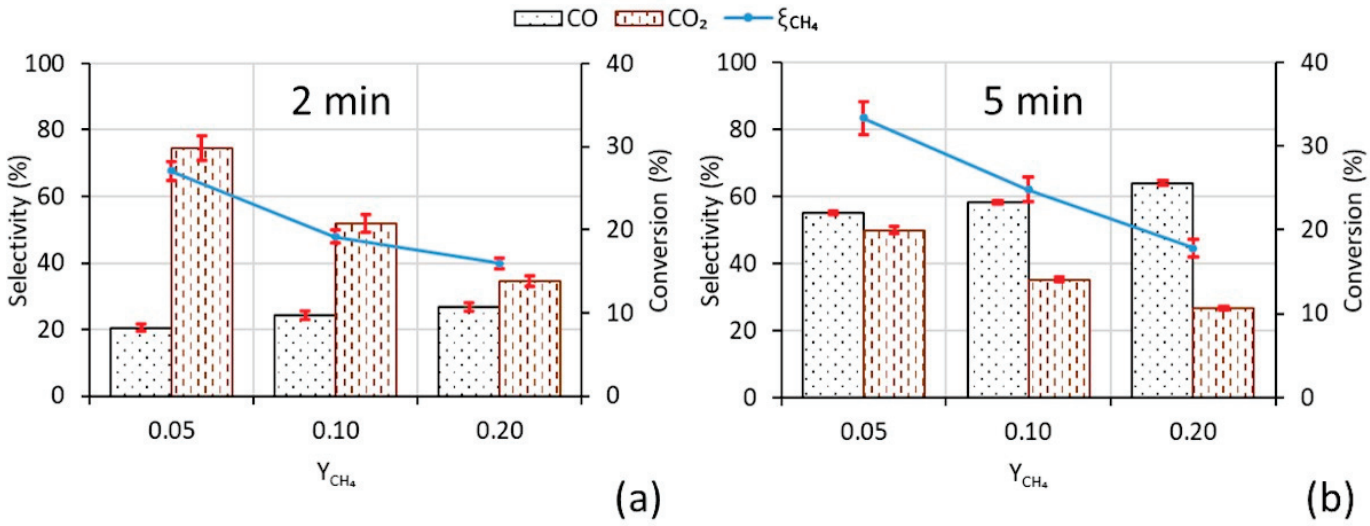

Figure 4. CH_4 conversion, CO selectivity and CO_2 selectivity over CeO_2 carrier at 950 °C, Y_{CH_4} = 0.05, 0.10 and 0.20: (**a**) reduction time 2 min, (**b**) reduction time 5 min; the error bars in the plot indicate the standard deviation in triplicate tests; the error bars reported in red in the plot indicate the standard deviation in triplicate tests.

The selectivities of CO and CO_2 clearly exhibit opposite trends when increasing the mole fraction of CH_4 for both reduction times. Therefore, the conditions required to achieve total combustion, over CeO_2, are those corresponding to a short reduction time and low y_{CH_4}, i.e., a higher equivalence factor.

Experimental data, for all carriers, have also been evaluated to allow for consideration of carbon deposition. Coke formation was appreciable only for experiments carried out at 950 °C, where the presence of carbon lowered the selectivity towards CO_2 and CO. Table 3 reports the carbon selectivity, η_C, for these tests, which is always below 10%, with the exception of the test with Chro at y_{CH_4} = 0.10 and t = 5′ (η_C = 11.9%), which was affected by a partial agglomeration of the fixed-bed particles. The accumulated carbon was readily converted during carrier regeneration, without causing apparent problems to carrier regeneration.

Table 3. Carbon (coke) selectivity (%) in Chro, CeO_2 and Ce–Cu at different y_{CH_4} and oxidation times (T = 950 °C).

y_{CH_4}	0.05	0.05	0.10	0.10	0.20	0.20
Time, min	**2**	**5**	**2**	**5**	**2**	**5**
Chro	3.5	0.7	1.3	11.9	-	-
CeO_2	7.7	2.4	4.4	1.1	1.0	0.7
Ce–Cu	0.8	0.1	0.5	1.4	4.6	2.6

Mean standard deviation ±0.3.

Figure 5 displays the instantaneous selectivity towards CO and CO_2 for tests carried out with CeO_2 carrier at 950 °C and increasing y_{CH_4}. The reported behavior is consistent with the changes in operating conditions and the transient character of the test. CO_2 selectivity was the highest at the initial time, i.e., at maximum equivalent factor ($e \rightarrow +\infty$), and declined with decreasing e, corresponding to the progressive depletion of oxygen sites in the carrier. The increase in the mole fraction of CH_4 leads to a shift in the CO_2 curves towards lower values due to the lower equivalence factor and the lower availability of oxygen. Congruently, the selectivity behavior of CO is perfectly symmetrical with that of CO_2.

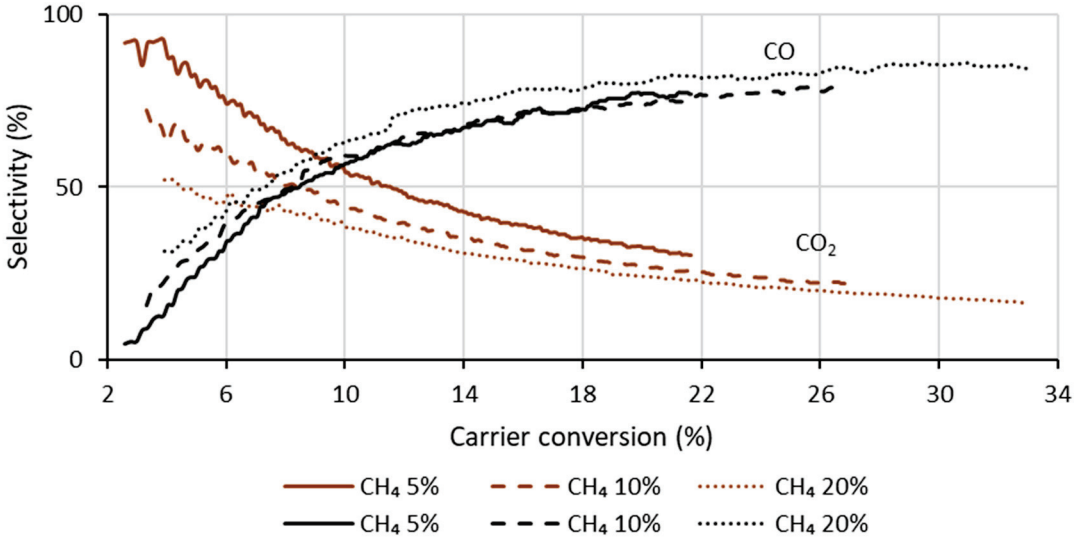

Figure 5. Instantaneous CO and CO_2 selectivity in CeO_2 carrier at Y_{CH_4} = 0.05, 0.10 and 0.20 as a function of carrier conversion degree (t_c = 5′, T = 950 °C).

3.2. Characterization of the Samples

Oxygen carriers, before and after use in the reactor, have been characterized by SEM and XRD analyses.

Figure 6 displays the SEM images of the granules at different magnifications. Low-magnification images (Figure 6a,b) demonstrate that for the CeO_2 and Ce–Cu carrier, the granules remain almost unchanged before and after use in the reactor. No fine particles were formed during reaction, which is reasonable, as the tests were carried out in a fixed bed without abrasion and rather limited thermal stress. In general, all granules are dense with well-defined external surfaces. Therefore, we have confirmed the good mechanical stability of both synthetic CeO_2 and Ce–Cu carriers. The morphology of Chro carrier granules recalls the cubic-octahedral symmetry of the material with isometric/rounded granules with smooth surfaces and without microstructures, a bit like crystalline faces. Some particle agglomerates are also evident in the case of chromite use (Figure 6b). In this regard, a rather large agglomerate was recovered after unloading the chromite bed, while the other two materials did not present similar problems.

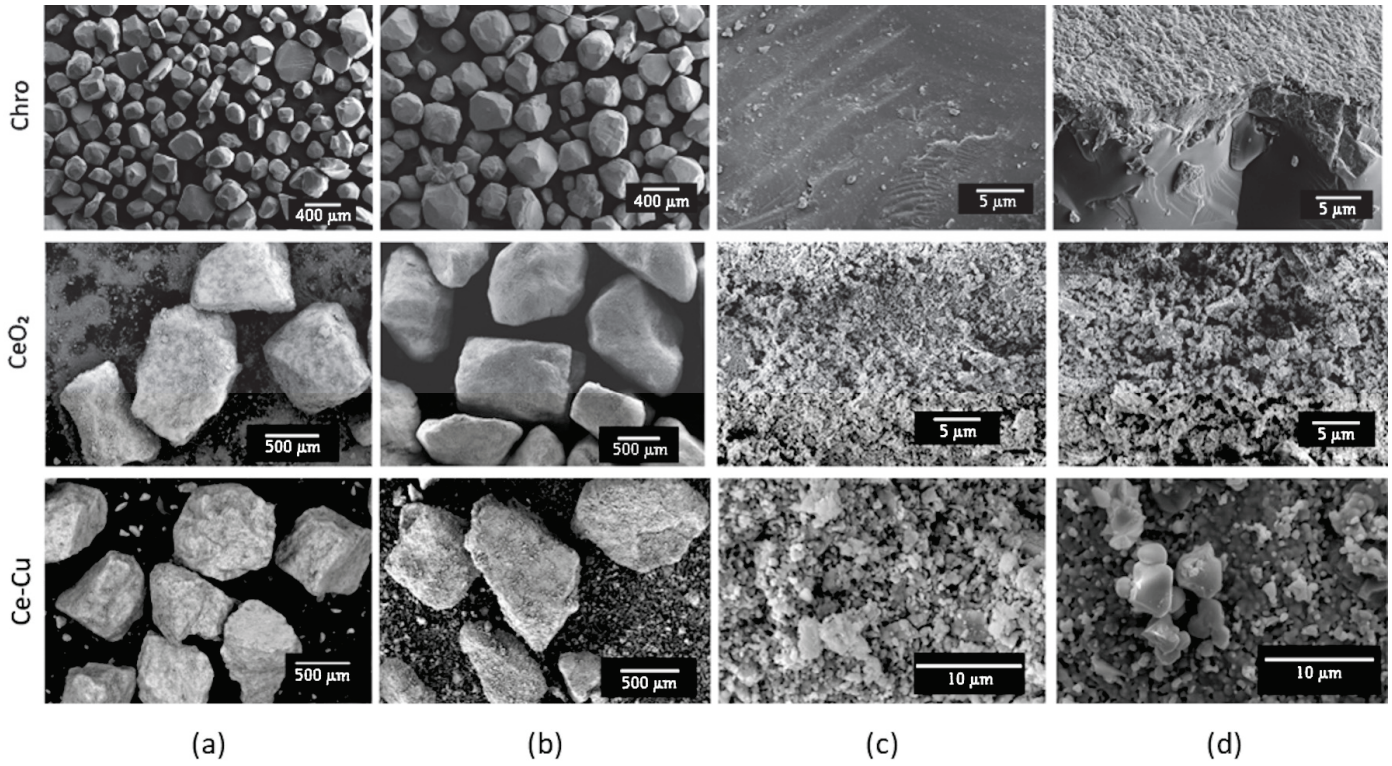

Figure 6. SEM images of Chro, CeO_2 and Ce–Cu granules at 10× (**a**,**b**) and 10,000× (**c**,**d**) magnification before (**a**,**c**) and after (**b**,**d**) utilization in the reactor.

The XRD analysis (Figure 7) proves that before and after the test, the CeO_2 and Ce–Cu samples were very similar, without substantial crystallographic–structural and crystalline difference. Only a certain difference can be seen in terms of crystallite size. The Ce–Cu carrier exhibits some peaks of CuO (pristine oxide) and Cu_2O, as a consequence of the reduction step and incomplete regeneration. Conversely, before and after the test, chromite samples exhibit large differences with clear oxidation phenomena and the presence of Fe_2O_3 peaks in the one subjected to chemical looping. Some spinel structures between Fe and Chro oxides also appear for the used Chro carrier. Also, a higher baseline for chromite is present due to the lower degree of crystallinity of this natural material.

Ceria samples do not exhibit a substantial presence of any additional phases or Cerium oxide with different oxidation states (e.g., Ce_2O_3), and they appear quite pure and composed of a single phase according to XRD analysis. Even after undergoing several reaction steps, the material does not display any relevant change, either from the chemical or structural point of view (e.g., entry or loss of oxygen), with no apparent change in cell parameters. Both the spacing and intensity of reflections are completely coherent before and after treatment. This finding suggests very good stability and regeneration efficiency.

Ce–Cu samples are also very similar before and after reaction, without substantial crystallographic–structural and crystalline difference in the present CeO_2, before and after treatment. The only changes in Ce–Cu carrier are exhibited concerning the copper phase, with some peaks of Cu_2O (cuprite) appearing together with CuO (tenorite, as pristine oxide) peaks in the spent material, as a consequence of the reduction step and incomplete regeneration. Concerning this regeneration process, some traces of the presence of an intermediate oxidative phase, where copper is present with both oxidation numbers as Cu_4O_3 (paramelaconite, where $Cu^{1+}{}_2Cu^{2+}{}_2O_3$), have been found [23]. Even a certain difference could be appreciated in terms of crystallite size before and after treatment.

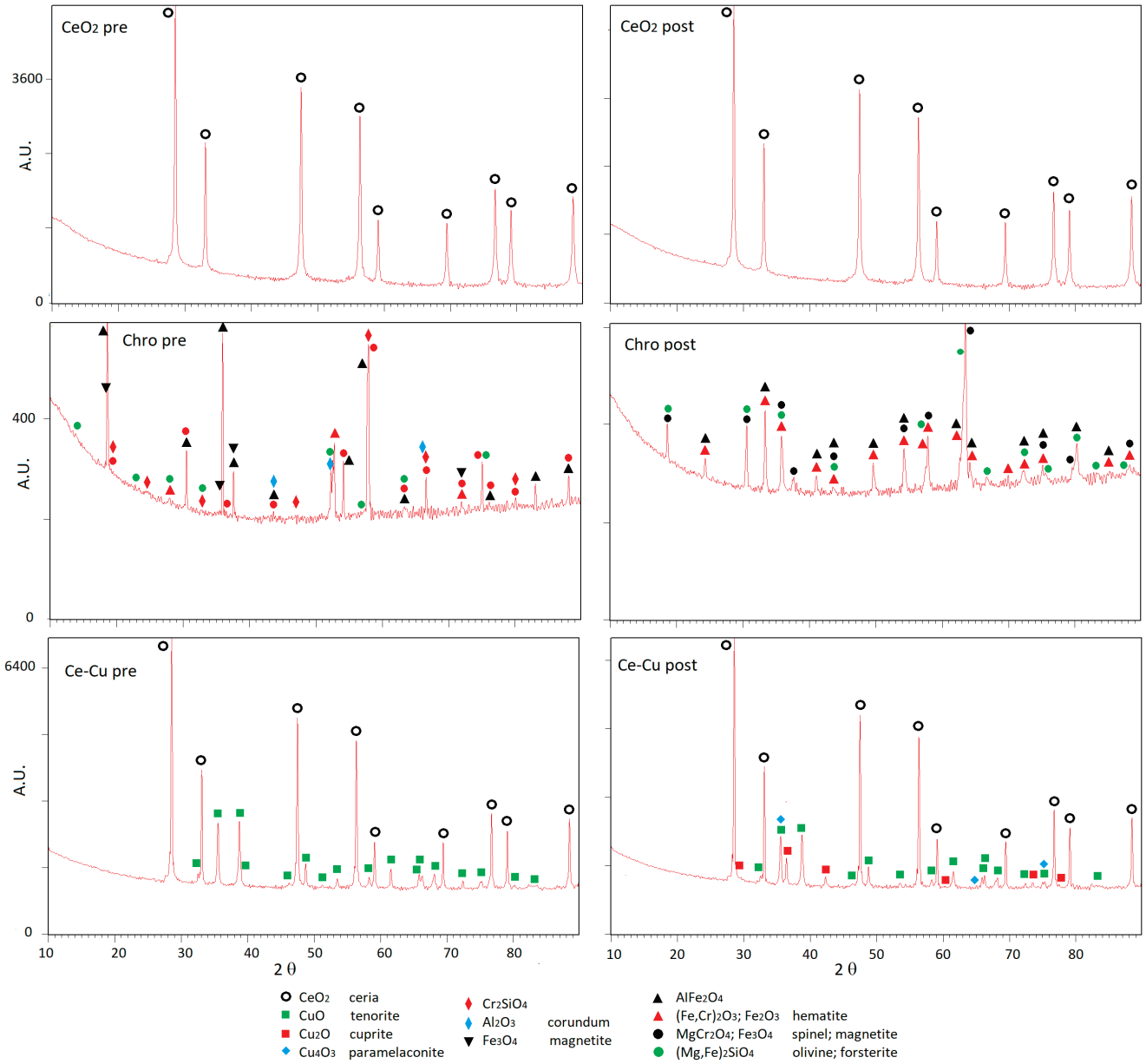

Figure 7. XRD patterns of Chro, CeO_2 and Ce–Cu before and after utilization in the reactor.

The chromite sample comes from mineral natural sand collecting several spinel phases with a complex stoichiometry $(Mg,Fe)(CrAl)_2O_4$, $Fe(Cr,Al)_2O_4$, $AlFe_2O_4$, etc., according to the main elements already found in the chemical analyses. The higher baseline of the patterns is due to a fluorescence effect of XRD in the presence of transition metals (Mn, Co, Ni, Fe, Cr, and others). Only a few traces of accessory residual and refractory mineral phases have been found (e.g., corundum, magnetite, olivine).

4. Discussion

Table 4 provides a comparison of methane conversion and selectivity as the input mole fraction and carrier conversion vary for the three materials investigated. The cells in which there are high values (0.50) of selectivity in CO_2 and CO have been highlighted in dark and light grey, respectively. Despite some inconsistencies due to the limits of the experimental technique, especially regarding short conversion times, it can be noted that the initial phases of reaction ($\xi_{carrier}$ = 0.1) favor the total oxidation of methane with the production of CO_2, while the progress of the carrier conversion ($\xi_{carrier}$ = 0.2) leads to the

partial oxidation and formation of CO. For the values investigated, Ce–Cu always promotes total combustion with the formation of CO_2 and CO present only in traces. This can be attributed to the high O_2 capacity of the carrier, as well as its CLOU behavior due to the release of gaseous oxygen. These results could be linked to the different activities of oxygen sites in the carrier [8], depending on their ease of accessibility.

Table 4. CH_4 conversion, CO and CO_2 selectivity in Chro, CeO_2 and Ce–Cu at different y_{CH_4} values and conversion degrees of the carrier (T = 950 °C).

	y_{CH_4}	0.05	0.05	0.10	0.10	0.20	0.20
	$\xi_{carrier}$	0.10	0.20	0.10	0.20	0.10	0.20
Chro	ξ_{CH_4}	0.18	(-)	0.21	0.14	(-)	(-)
	η_{CO}	0.15	(-)	0.39	0.58	(-)	(-)
	η_{CO_2}	0.85	(-)	0.36	0.35	(-)	(-)
CeO_2	ξ_{CH_4}	0.29	0.28	0.22	0.21	0.17	0.16
	η_{CO}	0.47	0.33	0.59	0.74	0.63	0.80
	η_{CO_2}	0.53	0.77	0.44	0.27	0.39	0.24
Ce–Cu	ξ_{CH_4}	0.73	0.73	0.74	0.74	0.74	0.74
	η_{CO}	0.00	0.00	0.00	0.00	0.00	0.00
	η_{CO_2}	1.00	1.00	1.00	1.00	0.87	0.88

The microstructural analysis showed different behaviors among the three carriers (Figure 6c,d). The granules of CeO_2 retain their surface characteristics well even after exposure to high temperature and redox atmosphere. On the contrary, chromite gives rise to an evident modification of the exposed surface with fractures and the formation of an amorphous layer, while the crystalline structure remains unchanged in the internal core of the granule (Figure 6d). An intermediate behavior occurs for Ce–Cu granules, where some formations of sintered micro-granules are evident (Figure 6d) upon the exposure to high temperature and chemical reaction, probably due to the less refractory character of copper oxide with respect to ceria.

Conversely, before and after the test, chromite samples exhibit large differences with clear oxidation phenomena, with a presence of peaks from neo-formed Fe_2O_3 (particularly lying on the surface of the granules where the oxidation process was more intense) in the one subjected to chemical looping, together with a rearranging of chemical compositions of the phases. Iron oxide phases appear to be segregated on the grain surface. This is consistent with phase diagrams for Fe–Cr–O systems reported in literature [24,25].

The CuO–CeO_2 oxygen carrier displayed the highest oxygen availability, while the chromite carrier showed limited activity towards methane.

Overall, the good selection of reaction step duration is crucial to ensuring the desired process selectivity for all oxygen carriers. Previous literature has suggested that the mechanism of reaction of methane on cerium dioxide changes as the material is reduced [9], and so does the selectivity. Methane was shown to be activated on surface oxygen sites over oxidated cerium dioxide, which are also active in the further oxidation of syngas. As the surface oxygen sites are depleted, methane activation starts occurring on the formed oxygen vacancies, while the lower surface oxygen availability stops the further formation of CO_2 and H_2O. This must be considered when discussing process optimization, and the extent of reduction reached by the carrier can be used to modulate reaction selectivity. Limiting reaction time allows one to reduce coke deposition, but should be accomplished with care, as an overly strict limitation in the reaction step duration can cause a noticeable overall loss in selectivity towards partial oxidation.

In the case of cerium dioxide, the present paper clearly displays the presence of a lower threshold in the extent of carrier conversion that needs to be surpassed if one is to observe a significant prevalence of partial oxidation when compared to complete combustion.

A carrier conversion lower than 10% (Figure 5) in the observed reaction conditions leads to a very high influence of total combustion on process yield. The previous literature on chemical looping over cerium dioxide showed the need for short reaction cycles to avoid excessive carbon deposition [26,27], but this tradeoff between complete and partial oxidation also needs to be addressed when selecting cycle length.

Chromite also displayed a similar behavior to CeO_2 carrier, with a first phase of reaction where complete oxidation is favored followed by a second step with prevalent syngas formation. In this case, the first phase of complete combustion is most likely attributed to the reduction of surface Fe_2O_3 to Fe_3O_4, with the further reduction to FeO being responsible for the generation of syngas, as previously reported in the literature for iron-based oxygen carriers [28]. In general, chromite sand displayed low activity and yields for both chemical looping reforming and combustion, despite its relevant content (26%) of iron species. While iron species demonstrated activity related to methane oxidation, as shown by the XRD patterns, chromium species were shown to not be active in the experimental conditions investigated, and the material displayed significant aggregation and carbon deposition during reduction, leading to an overall unsatisfying performance of the material.

Finally, in the case of the Ce–Cu process, step duration showed no effect on the selectivity towards either complete or partial oxidation for these short reaction times, as oxygen uncoupling favored complete combustion independently of the extent of carrier reduction. The Ce–Cu carrier thus appears to be unsuited for reforming, but shows excellent performance for combustion. For the Ce–Cu carrier, the selection of an ideal reduction step duration would thus mostly be determined by the rate of carbon deposition compared to the rate of oxidation as carrier conversion increases. Previously, Saddiq et al. investigated the kinetics for the oxidation of liquefied petroleum gas (propane/butane mixture) on 10% CuO/CeO_2 powder at 800 °C, and observed that a first-order kinetic model best described the reforming reaction, thanks to the high availability of oxygen, while a shrinking core model best described the reaction rate of pellets of the same material due to reduced oxygen release [29]. Nonetheless, high oxygen release was observed in both cases. He et al. also investigated the use of a 50/50 wt. % CuO/CeO_2 oxygen carrier for methane reforming [30]. They observed an almost complete selectivity towards partial oxidation above 850 °C, coupled with a very high carbon deposition, but this is not consistent with our observed results. In our experiments, the Cu–Ce oxygen carrier was almost completely selective towards complete oxidation both at 850 °C and 950 °C, and carbon deposition became relevant only for the longer-running tests at higher methane concentration. This discrepancy in results could be partly explained by the lower methane concentration and shorter reaction time used in our experiments compared to their results. The high selectivity towards complete combustion observed for our results can also be related to the preparation method employed for the Ce–Cu carrier. He et al. [30] prepared their sample through the co-precipitation method, which may allow a more intimate mixing of the two phases, allowing for cerium dioxide to play a major role in determining process selectivity. Our low carbon deposition results are closer to the observations made by Elgarni et al. [31], who also observed limited carbon deposition for CeO_2-supported CuO. Both Elgarni et al. [31] and Tijani et al. [32] observed a reduction in overall oxygen exchange capacity for CeO_2-supported Cu carriers when increasing the operation temperature above 900 °C, which would coincide with an increase in carbon deposition, but this is not immediately evident in our experimental results, as only limited aggregation was observed in our case for the Ce–Cu carrier.

5. Conclusions

The chemical looping conversion of methane was investigated in a lab-scale fixed-bed reactor. Three oxygen carriers with different oxygen capacities, one exhibiting CLOU behavior, were used. The materials showed different reactivity and oxygen transport capacity depending on their chemical composition, crystallographic phases, and microstructure.

The rank of the studied carriers in methane conversion was Ce–Cu > CeO_2 > Chro. The Ce–Cu carrier was very effective in achieving the full oxidation of methane, whilst CeO_2 allowed either full or partial oxidation. Carbon deposition on CeO_2 was appreciable only for tests carried out at 950 °C. Natural chromite was unsatisfactory because of the absence of any contribution of the prevalent Cr_2O_3 phase.

The study of the process has also shown that the operating conditions and the control of the carrier conversion degree can alternatively lead to the partial (high CO selectivity) or total (high CO_2 selectivity) oxidation of CH_4. Indeed, the selectivity towards carbon monoxide also increases with a longer reduction time. The degree of carrier conversion, tunable by an effective switching strategy between the two cyclic phases of reduction and regeneration, is therefore a key parameter in guiding the process towards the desired products.

The further development of the research will consider steady-state operation, preferably in a circulating fluidized bed where the residence times of the gas and solids in reducing and oxidizing reactors can be easily modified.

Author Contributions: Conceptualization, F.M., F.D. and M.B.; methodology, M.B., A.S. and M.M. (Matteo Minelli); investigation, M.B., A.S. and M.M. (Mauro Mazzocchi); writing—original draft preparation, F.M. and M.M. (Mauro Mazzocchi); writing—review and editing, M.M. (Matteo Minelli) and M.B. All authors have read and agreed to the published version of the manuscript.

Funding: This research was funded under the National Recovery and Resilience Plan (NRRP), Mission 04 Component 2 Investment 1.5—NextGenerationEU, Call for tender n. 3277 dated 30 December 2021 (Award Number: 0001052 dated 23 June 2022).

Data Availability Statement: Data are available upon request to the corresponding author.

Acknowledgments: Valli Granulati srl (I) is acknowledged for the free supply of samples of inert granules used in setting up the experimental equipment.

Conflicts of Interest: The authors declare no conflict of interest.

Nomenclature

Symbols	Meaning	Units
q	Molar flow rate	mmol/min
y_i	Molar fraction of compound i	dimensionless
t	time	Min
m_i	Mass of carrier i	Mg
M_i	Molar mass of compound i	g/mol
e	Equivalence factor for methane oxidation	dimensionless
$n_{O_2\ stoich,\ CH_4}$	Oxygen amount for stoichiometric combustion	mmol
$n_{O_2\ av,carrieri}$	Oxygen availability in carrier	mmol
ξ_{CH_4}	Methane conversion	dimensionless
$\xi_{carrier}$	Conversion of carrier i	dimensionless
η_i	Selectivity for compound i	dimensionless
ω_i	Mass fraction of compound i	dimensionless
Subscripts		
in	Reactor inlet	-
out	Reactor outlet	-
c	Combustion step	-
r	Regeneration step	-

References

1. Abanades, J.C.; Arias, B.; Lyngfelt, A.; Mattisson, T.; Wiley, D.E.; Li, H.; Ho, M.T.; Mangano, E.; Brandani, S. Emerging CO_2 Capture Systems. *Int. J. Greenh. Gas. Control.* **2015**, *40*, 126–166. [CrossRef]
2. Boscherini, M.; Storione, A.; Minelli, M.; Miccio, F.; Doghieri, F. New Perspectives on Catalytic Hydrogen Production by the Reforming, Partial Oxidation and Decomposition of Methane and Biogas. *Energies* **2023**, *16*, 6375. [CrossRef]

3. Lyngfelt, A.; Hedayati, A.; Augustsson, E. Fate of NO and Ammonia in Chemical Looping Combustion—Investigation in a 300 W Chemical Looping Combustion Reactor System. *Energy Fuels* **2022**, *36*, 9628–9647. [CrossRef]
4. Adanez, J.; Abad, A.; Garcia-Labiano, F.; Gayan, P.; de Diego, L.F. Progress in Chemical-Looping Combustion and Reforming Technologies. *Prog. Energy Combust. Sci.* **2012**, *38*, 215–282. [CrossRef]
5. Lu, H.; Shi, X.; Costa, M.; Huang, C. Carcinogenic Effect of Nickel Compounds. *Mol. Cell Biochem.* **2005**, *279*, 45–67. [CrossRef]
6. Otsuka, K.; Sunada, E.; Ushiyama, T.; Yamanaka, I. The Production of Synthesis Gas by the Redox of Cerium Oxide. In *Studies in Surface Science and Catalysis*; Elsevier: Amsterdam, The Netherlands, 1997; pp. 531–536. [CrossRef]
7. Chuayboon, S.; Abanades, S.; Rodat, S. Solar Chemical Looping Reforming of Methane Combined with Isothermal H_2O/CO_2 Splitting Using Ceria Oxygen Carrier for Syngas Production. *J. Energy Chem.* **2020**, *41*, 60–72. [CrossRef]
8. Cheng, Z.; Qin, L.; Fan, J.A.; Fan, L.-S. New Insight into the Development of Oxygen Carrier Materials for Chemical Looping Systems. *Engineering* **2018**, *4*, 343–351. [CrossRef]
9. Warren, K.J.; Scheffe, J.R. Role of Surface Oxygen Vacancy Concentration on the Dissociation of Methane over Nonstoichiometric Ceria. *J. Phys. Chem. C* **2019**, *123*, 13208–13218. [CrossRef]
10. Cheng, Z.; Qin, L.; Guo, M.; Xu, M.; Fan, J.A.; Fan, L.-S. Oxygen Vacancy Promoted Methane Partial Oxidation over Iron Oxide Oxygen Carriers in the Chemical Looping Process. *Phys. Chem. Chem. Phys.* **2016**, *18*, 32418–32428. [CrossRef]
11. Koleli, N.; Demir, A. Chapter 11-Chromite. In *Environmental Materials and Waste. Resource Recovery and Pollution Prevention*; Academic Press: Cambridge, MA, USA, 2016; pp. 245–263. [CrossRef]
12. Nurjaman, F.; Subandrio, S.; Ferdian, D.; Suharno, B. Effect of Basicity on Beneficiated Chromite Sand Smelting Process Using Submerged Arc Furnace. In Proceedings of the International Seminar on Metallurgy and Materials (ISMM2017): Metallurgy and Advanced Material Technology for Sustainable Development, Jakarta, Indonesia, 24–25 October 2017; p. 020009. [CrossRef]
13. Miccio, F.; Ruoppolo, G.; Russo, S.; Urciuolo, M.; De Riccardis, A. Fluidized Bed Combustion of Wet Biomass Fuel (Olive Husks). *Chem. Eng. Trans.* **2014**, *37*, 1–6. [CrossRef]
14. Prasad, R.; Singh, P. A Review on CO Oxidation Over Copper Chromite Catalyst. *Catal. Rev.* **2012**, *54*, 224–279. [CrossRef]
15. Ammendola, P.; Chirone, R.; Lisi, L.; Ruoppolo, G.; Russo, G. Copper Catalysts for H_2 Production via CH_4 Decomposition. *J. Mol. Catal. A Chem.* **2007**, *266*, 31–39. [CrossRef]
16. Warren, K.J.; Carrillo, R.J.; Greek, B.; Hill, C.M.; Scheffe, J.R. Solar Reactor Demonstration of Efficient and Selective Syngas Production via Chemical-Looping Dry Reforming of Methane over Ceria. *Energy Technol.* **2020**, *8*, 2000053. [CrossRef]
17. Storione, A.; Boscherini, M.; Miccio, F.; Landi, E.; Minelli, M.; Doghieri, F. Improvement of Process Conditions for H_2 Production by Chemical Looping Reforming. *Energies* **2024**, *17*, 1544. [CrossRef]
18. Miccio, F.; Natali Murri, A.; Landi, E. Synthesis and Characterization of Geopolymer Oxygen Carriers for Chemical Looping Combustion. *Appl. Energy* **2017**, *194*, 136–147. [CrossRef]
19. Miccio, F.; Landi, E.; Murri, A.N.; Minelli, M.; Doghieri, F.; Storione, A. Fluidized Bed Reforming of Methane by Chemical Looping with Cerium Oxide Oxygen Carriers. *Chem. Eng. Res. Des.* **2023**, *191*, 568–577. [CrossRef]
20. Liu, G.; Lisak, G. Cu-Based Oxygen Carriers for Chemical Looping Processes: Opportunities and Challenges. *Fuel* **2023**, *342*, 127828. [CrossRef]
21. Leion, H.; Lyngfelt, A.; Johansson, M.; Jerndal, E.; Mattisson, T. The Use of Ilmenite as an Oxygen Carrier in Chemical-Looping Combustion. *Chem. Eng. Res. Des.* **2008**, *86*, 1017–1026. [CrossRef]
22. Jing, D.; Arjmand, M.; Mattisson, T.; Rydén, M.; Snijkers, F.; Leion, H.; Lyngfelt, A. Examination of Oxygen Uncoupling Behaviour and Reactivity towards Methane for Manganese Silicate Oxygen Carriers in Chemical-Looping Combustion. *Int. J. Greenh. Gas. Control.* **2014**, *29*, 70–81. [CrossRef]
23. Živković, A.; Sheehama, J.; Warwick, M.E.A.; Jones, D.R.; Mitchel, C.; Likius, D.; Uahengo, V.; Dzade, N.Y.; Meenakshisundaram, S.; Dunnill, C.W.; et al. Structural and Electronic Properties of Cu_4O_3 (Paramelaconite): The Role of Native Impurities. *Pure Appl. Chem.* **2021**, *93*, 1229–1244. [CrossRef]
24. Perrot, P. Chromium–Iron–Oxygen. Ternary Alloy Systems: Phase Diagrams; Crystallographic and Thermodynamic Data. In *Ternary Alloy Systems: Phase Diagrams, Crystallographic and Thermodynamic Data Critically Evaluated by MSIT®*; Springer: Berlin/Heidelberg, Germany, 2009; Volume 11, pp. 250–276. [CrossRef]
25. Jacob, A.; Povoden-Karadeniz, E.; Kozeschnik, E. Revised Thermodynamic Description of the Fe-Cr System Based on an Improved Sublattice Model of the σ Phase. *Calphad* **2018**, *60*, 16–28. [CrossRef]
26. Otsuka, K.; Wang, Y.; Sunada, E.; Yamanaka, I. Direct Partial Oxidation of Methane to Synthesis Gas by Cerium Oxide. *J. Catal.* **1998**, *175*, 152–160. [CrossRef]
27. Fosheim, J.R.; Hathaway, B.J.; Davidson, J.H. High Efficiency Solar Chemical-Looping Methane Reforming with Ceria in a Fixed-Bed Reactor. *Energy* **2019**, *169*, 597–612. [CrossRef]
28. Zhu, M.; Song, Y.; Chen, S.; Li, M.; Zhang, L.; Xiang, W. Chemical Looping Dry Reforming of Methane with Hydrogen Generation on Fe_2O_3/Al_2O_3 Oxygen Carrier. *Chem. Eng. J.* **2019**, *368*, 812–823. [CrossRef]
29. Saddiq, H.A.; Muhammed-Dabo, I.A.; Hamza, A.; Waziri, S.M. Kinetic Modeling of CuO/CeO_2 and CuO/Nb_2O_5 as Oxygen Carriers in the Production of Syngas. *React. Kinet. Mech. Catal.* **2021**, *134*, 727–742. [CrossRef]
30. He, F.; Wei, Y.; Li, H.; Wang, H. Synthesis Gas Generation by Chemical-Looping Reforming Using Ce-Based Oxygen Carriers Modified with Fe, Cu, and Mn Oxides. *Energy Fuels* **2009**, *23*, 2095–2102. [CrossRef]

31. Elgarni, M.M.; Tijani, M.M.; Mahinpey, N. Characterization, Kinetics and Stability Studies of NiO and CuO Supported by Al_2O_3, ZrO_2, CeO_2 and Their Combinations in Chemical Looping Combustion. *Catal. Today* **2022**, *397–399*, 206–219. [CrossRef]
32. Tijani, M.M.; Aqsha, A.; Mahinpey, N. Synthesis and Study of Metal-Based Oxygen Carriers (Cu, Co, Fe, Ni) and Their Interaction with Supported Metal Oxides (Al_2O_3, CeO_2, TiO_2, ZrO_2) in a Chemical Looping Combustion System. *Energy* **2017**, *138*, 873–882. [CrossRef]

energies

MDPI

Article

Evaluation of Changes in the Chemical Composition of Grasses as a Result of the Methane Fermentation Process and Biogas Production Efficiency

Bogusława Waliszewska [1], Hanna Waliszewska [1,2], Mieczysław Grzelak [3], Leszek Majchrzak [4,*], Eliza Gaweł [5], Maciej Murawski [3], Agnieszka Sieradzka [1], Iryna Vaskina [6] and Agnieszka Spek-Dźwigała [1]

[1] Department of Chemical Wood Technology, Poznań University of Life Sciences, Wojska Polskiego 38/42, 60-637 Poznań, Poland; boguslawa.waliszewska@up.poznan.pl (B.W.); hanna.waliszewska@up.poznan.pl (H.W.); agnieszka.sieradzka@up.poznan.pl (A.S.)
[2] The National Centre for Research and Development, Chmielna 69, 00-801 Warszawa, Poland
[3] Department of Grassland and Natural Landscape, Poznań University of Life Sciences, Dojazd 11, 60-656 Poznan, Poland; mieczyslaw.grzelak@up.poznan.pl (M.G.); maciej.murawski@up.poznan.pl (M.M.)
[4] Agronomy Department, Poznań University of Life Sciences, Dojazd 11, 60-632 Poznań, Poland
[5] Department of Forage Crop Production, Institute of Soil Science and Plant Cultivation—State Research Institute, Czartoryskich 8, 24-100 Puławy, Poland; gawel@iung.pulawy.pl
[6] Department of Biosystem Engineering, Poznań University of Life Sciences, Wojska Polskiego 48, 60-637 Poznań, Poland; iryna.vaskina@up.poznan.pl
* Correspondence: leszek.majchrzak@up.poznan.pl

Abstract: Methane fermentation, which is one of the key processes in biogas production, plays an important role in the conversion of biomass to energy. During this process, changes occur in the chemical composition of organic feedstocks, including the chemical composition of grasses. The assessment of these changes is crucial for the efficiency and productivity of biogas production. The material for this study comprised fully mature grass blades with leaves and inflorescences and was collected from extensively used meadows and pastures, as well as cultivated and set-aside areas in the Wielkopolskie Voivodeship, the communes of Białośliwie and Trzcianka, Poland. The aim of this study was to compare methane fermentation efficiency in nine grass species and identify the biomass component involved in biogas production. The results indicate that the fermentation process, as expected, changed the cellulose content. The lignin content of the grasses before fermentation varied more than the cellulose content. The content of holocellulose (sum of carbohydrate components) in the grasses ranged from 59.77 to 72.93% before fermentation. Methane fermentation significantly reduced the carbohydrate content in the grasses, with a low degree of polymerization. Grassland biomass-based biogas production is a viable alternative to conventional fossil fuels.

Keywords: renewable energy; biogas plant; grasses; chemical composition

1. Introduction

Grasses from extensively managed meadows and pastures are a common source of animal feed. However, in modern livestock farming, the feed of choice has changed from species-rich forage obtained from natural grasslands typically low in energy content to cultivated crops and high-energy feed concentrates. There are vast areas of underutilized grassland that need to be managed [1]. Globally, as the focus on alternative energy sources increases and mineral fertilizer prices soar, grassland biomass could be used for biogas production. The digestate produced from agricultural biogas plants [2,3] can be used as a fertilizer that positively influences the growth and development of grasses and the soil environment. The production of biogas from biomass, waste, or by-products is recognized as renewable energy [4,5]. In Austria and Germany, about 50% of agricultural biogas plants use grass silage as a biogas source [6]. Biogas plants are RESs (Renewable Energy

Sources) installations that are completely independent of weather conditions, season, or precipitation and, considering the current energy market situation, are increasingly common and gaining importance.

The amount and composition of the biogas obtained from different grasses depends on several factors such as the type of bacteria used, process condition (temperature), type of substrate, and its chemical composition [7,8]. Biogas typically comprises about 55% methane, 45% carbon dioxide, and minor amounts of other components [9]. To optimally utilize biomass for renewable energy, Pilarski et al. [10] propose the production of bioethanol and biogas simultaneously from corn, since it is one of the most widely cultivated crops in the world and has many applications, ranging from animal and human nutrition to biofuel production. The biomass produced by corn (leaves, stalks, and ears) is used in biogas plants, while the grain is used for ethanol production. The resulting distillery digestate is reused for biogas production.

In the context of the global challenges of climate change and the demand for more sustainable forms of energy, understanding and developing grass fermentation is an important step towards achieving the Sustainable Development Goals. By deepening our understanding of the mechanisms of this process and identifying potential strategies to optimize it, we can collectively strive to create greener and more efficient energy production systems using the wealth of natural resources that are grasses.

The anatomy and chemical composition of plant biomass within the same species vary greatly. This variation is influenced by several factors: growing conditions, plant developmental stage, and its morphological parts. Understanding the chemical composition of the raw material is integral to optimizing its use. In a literature review on the influence of chemical composition on the calorific value of biomass and the correlation of the individual components, the authors report that these are very important indicators [11]. In addition, policies in the agricultural sector are driving environmentally friendly biomass energy production systems. This further emphasizes the role that cultivated grasslands can play in sustainable biogas production [12]. This study focuses on the biogas production potential of different grass species growing under different conditions.

In this study, nine grass species were investigated as a potential source of biogas. The structural and plant by-product components were analyzed and the effect of the anaerobic digestion process on the change in their respective content was also analyzed. These analyses helped identify the components primarily involved in biogas production and how they affect the composition and yield of the digestate. The species diversity of grasses in terms of their suitability for fermentation and process optimization strategies to increase biogas production efficiency is also discussed.

2. Materials and Methods

2.1. Material Collection

The material for this study was collected from extensively used meadows and pastures, as well as cultivated and set-aside areas during the 2020 growing season. The material comprised fully mature grass blades with leaves and inflorescences from the area of the Wielkopolskie Voivodeship; the communes of Białośliwie and Trzcianka. Nine grass species were selected for this study. These were reed fescue (*Festuca arundinacea* Schreb.); brome grass (*Bromus inermis* Leyss.); perennial ryegrass (*Lolium perenne* L.); westerwold ryegrass (*Lolium multiflorum* var. *westerwoldicum*); meadow fescue (*Festuca pratensis* Huds.); meadow ryegrass (*Alopecurus pratensis* L.); meadowgrass (*Poa pratensis* L.); meadow timothy (*Phleum pratense* L.); and soft hair (*Bromus hordeaceus* L.). The harvested grasses were placed in an air-conditioned laboratory until constant humidity was achieved. For chemical analyses, the raw material was manually cut into small pieces and then ground in a Retsch SM 200 laboratory cutting mill. The milled raw material was sieved to separate the analytical fraction with a particle size of 0.1–0.4 mm. The raw material prepared in this way was used for further testing.

2.2. Chemical Composition

Structural and adventitious components were determined using standard assay methods:

- Cellulose was determined according to Seifert using dioxane and acetylacetone [13];
- Lignin was determined according to Tappi using 72% sulfuric acid [14];
- Holocellulose was determined using sodium chlorite [15];
- Extractives were determined in a Soxhlet apparatus using 96% ethanol [16];
- Ash was determined according to DIN 51731;
- Hemicelluloses were calculated arithmetically based on the difference between holocellulose and cellulose. Hemicellulose content was calculated based on the difference between the contents of holocellulose and cellulose.

2.3. Batch Test

The research experiments on biogas production (batch test) were carried out in the Ecotechnologies Laboratory (Department of Biosystems Engineering, PULS)—the largest Polish biogas laboratory (encompassing over 260 reactors working in temporary or permanent mode). The fermenters used for this experiment were used within the last 15 years for analyzing the methane production efficiency of over 3500 different substrates.

Methane fermentation was performed in 2 dm^3 glass reactors according to DIN 38 414-S8 and the guidance of VDI 4630 published by the Association of German Engineers in Dresden.

In order to proceed correctly with the biogas efficiency analysis, it was important to maintain the methodological proportions of tested substrates and inoculum. For this purpose, he following analyses were indispensable: dry matter (PN-75 C-04616/01) and organic dry matter (PN-Z-15011-3). The mentioned analyses were crucial for the calculation of the methane efficiency of the checked materials expressed in units like m^3/Mg FM (fresh matter); m^3/Mg DM; and m^3/Mg ODM.

Approximately 13 g of each grass species with about 1100 g of digestate (rich in methanogenic bacteria with dry matter content of 2.7–2.9% and ash content of 28–30%) was used in the experiment. The experiment was conducted in a multi-chamber bio-fermenter (Figure 1). The materials were placed in the reactors and then flooded with digestate. The reactors, purged with nitrogen (to create anaerobic conditions), were placed in a water bath at 39 °C ± 1 (mesophilic fermentation) to ensure optimal conditions for the process. Biogas yield from each chamber was transferred to cylindrical store-equalizing reservoirs that were filled with liquid resistant to gas solubility [17,18]. The daily measurements of produced gases (methane, carbon dioxide) were made every 24 h, with an accuracy of 0.01 dm^3.

The gas yield was analyzed using an infrared sensor for methane and carbon dioxide measurement and by an electrochemical sensor for oxygen measurement (Gas analyzer—GA5000 GeoTech company, Hong Kong, China). The calibrations of the GA5000 analyzer were made every 7 days using the calibration gases (65% CH_4 and 35% CO_2 presented in one mixture).

The results are presented on a dry matter basis as the average of 3 samples after deduction of the background, which was digestate.

According to the norm DIN 38 414-S8, the criterion to finish the methane production test from analyzed substrates was the time when daily gas generation reached the level of less than 1% of the total production obtained during the whole experiment.

After the fermentation process, the chemical composition of the digestate was examined using the same determinations as for the raw test material. The results are presented on a dry matter basis as the average of 3 samples.

All analyses were performed using R Statistical Software (v4.4.0-"Puppy Cup") [19] using the agricolae package [20].

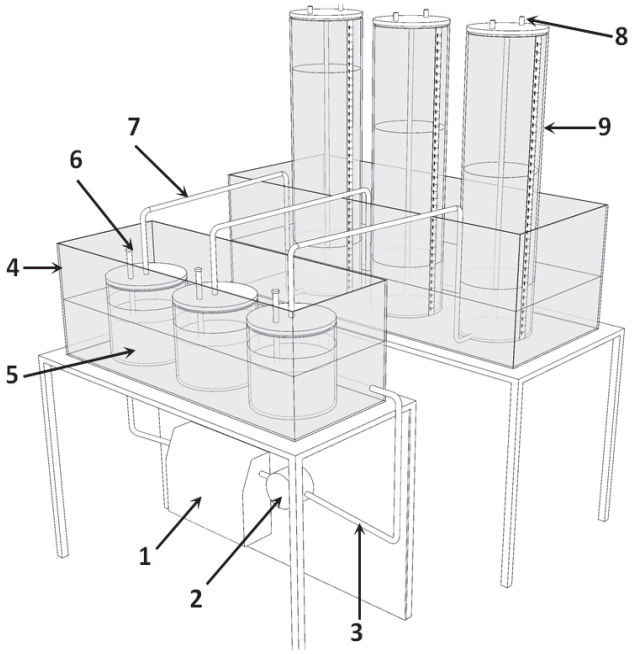

Figure 1. Scheme of bio-fermenter for biogas production research (3-chamber section): 1—water heater with temperature regulator, 2—water pump, 3—insulated conductors of calefaction liquid, 4—water coat, 5—bio-fermenter with charge capacity 2 dm^3, 6—sampling tubes, 7—biogas transporting tube, 8—gas sampling valve, 9—biogas volume-scale reservoir.

3. Results and Discussion

Below, Table 1 shows the cellulose, lignin, holocellulose, and hemicellulose content of selected grasses before fermentation and after fermentation. The cellulose content ranged from 35.17 to 36.92%, with *L. westerwoldicum* having the lowest content (31.34%) and *B. inermis* having the highest content (38.65%). Slightly higher amounts of cellulose (34%) in bagasse leaves (determined by the Kürschner–Hoffer method) were reported by Tapia-Maruri et al. [21]. Similar differences in the content of α-cellulose in genotypes of different grass species were shown by Rahaman et al. [22]. For instance, they reported 13.10–40.76% α-cellulose in *Sorghum bicolor*, 35.2140.98% in *Arundo donax*, and 17.20–27.28% in *Pennisetum purpureum*.

Table 1. Main components of selected grass species with statistically significant differences before and after methane fermentation (Tukey's test). Mean values with standard deviation for each species are presented (statistically significant at $p < 0.01$).

Grass Species	Cellulose [%]		Lignin [%]		Holocellulose [%]		Hemicellulose [%]	
	Before	After	Before	After	Before	After	Before	After
	Methane Fermentation							
Festuca arundinacea	35.56 ^{cd} ± 0.11	31.11 ^{b} ± 0.46	17.28 ^{ab} ± 0.36	44.86 ^{a} ± 0.18	67.43 ^{bc} ± 0.43	44.56 ^{ab} ± 0.54	31.87 ^{b} ± 0.51	13.45 ^{ab} ± 0.61
Bromus inermis	38.65 ^{a} ± 0.53	31.36 ^{b} ± 0.14	14.89 ^{e} ± 0.34	44.62 ^{a} ± 0.22	68.40 ^{b} ± 0.44	42.67 ^{bc} ± 0.56	29.75 ^{bc} ± 0.71	11.31 ^{bcd} ± 0.70
Lolium perenne	34.28 ^{e} ± 0.14	33.35 ^{a} ± 0.27	15.58 ^{de} ± 0.18	41.50 ^{b} ± 1.32	65.48 ^{bcd} ± 1.35	43.36 ^{bc} ± 1.20	31.20 ^{b} ± 1.23	10.01 ^{cd} ± 1.47
Lolium westerwoldicum	31.34 ^{f} ± 0.02	30.41 ^{bc} ± 0.19	16.12 ^{bcde} ± 0.39	44.55 ^{a} ± 0.06	59.77 ^{e} ± 0.63	44.44 ^{ab} ± 0.69	28.43 ^{c} ± 0.62	14.03 ^{a} ± 0.73
Festuca pratensis	35.17 ^{d} ± 0.12	29.96 ^{c} ± 0.23	15.90 ^{cde} ± 0.24	44.26 ^{a} ± 0.72	63.69 ^{d} ± 0.68	41.66 ^{bcd} ± 0.15	28.52 ^{c} ± 0.60	11.70 ^{abc} ± 0.38
Alopecurus pratensis	36.42 ^{bc} ± 0.26	29.48 ^{c} ± 0.14	17.70 ^{a} ± 0.92	44.72 ^{a} ± 0.25	68.97 ^{bc} ± 2.19	41.20 ^{cd} ± 0.77	32.55 ^{b} ± 2.02	11.72 ^{abc} ± 0.78
Poa pratensis	36.13 ^{bc} ± 0.03	31.37 ^{b} ± 0.73	16.71 ^{abcd} ± 0.15	45.32 ^{a} ± 0.15	71.42 ^{a} ± 0.23	42.37 ^{bc} ± 0.64	35.29 ^{a} ± 0.20	11.00 ^{bcd} ± 1.25
Phleum pretense	36.92 ^{b} ± 0.52	31.28 ^{b} ± 0.50	17.02 ^{abc} ± 0.25	39.67 ^{c} ± 0.49	65.48 ^{cd} ± 0.60	40.06 ^{d} ± 2.60	28.56 ^{c} ± 0.78	8.78 ^{d} ± 1.18
Bromus hordeaceus	36.39 ^{bc} ± 0.45	33.67 ^{a} ± 0.44	12.44 ^{f} ± 0.22	44.74 ^{a} ± 0.41	72.93 ^{a} ± 0.62	47.01 ^{a} ± 0.41	36.54 ^{a} ± 0.57	13.34 ^{ab} ± 0.78

^{a}, ^{b}, ^{c}, ^{d}, ^{e}, ^{f}—homogeneous groups.

The fermentation process, as expected, altered the cellulose content. The loss of cellulose mass varied widely, depending on the grass species. The smallest loss was observed in *L. perenne* (2.71%) and *L. westerwoldicum* (2.97%), while the largest was observed in *A. pratensis* (19.06%) and *B. inermis* (18.86%). A slight loss of 7.47% was observed in *B. hordeaceus*. The loss of cellulose content in the remaining species ranged from 12.51 to 15.28% (Figure 2).

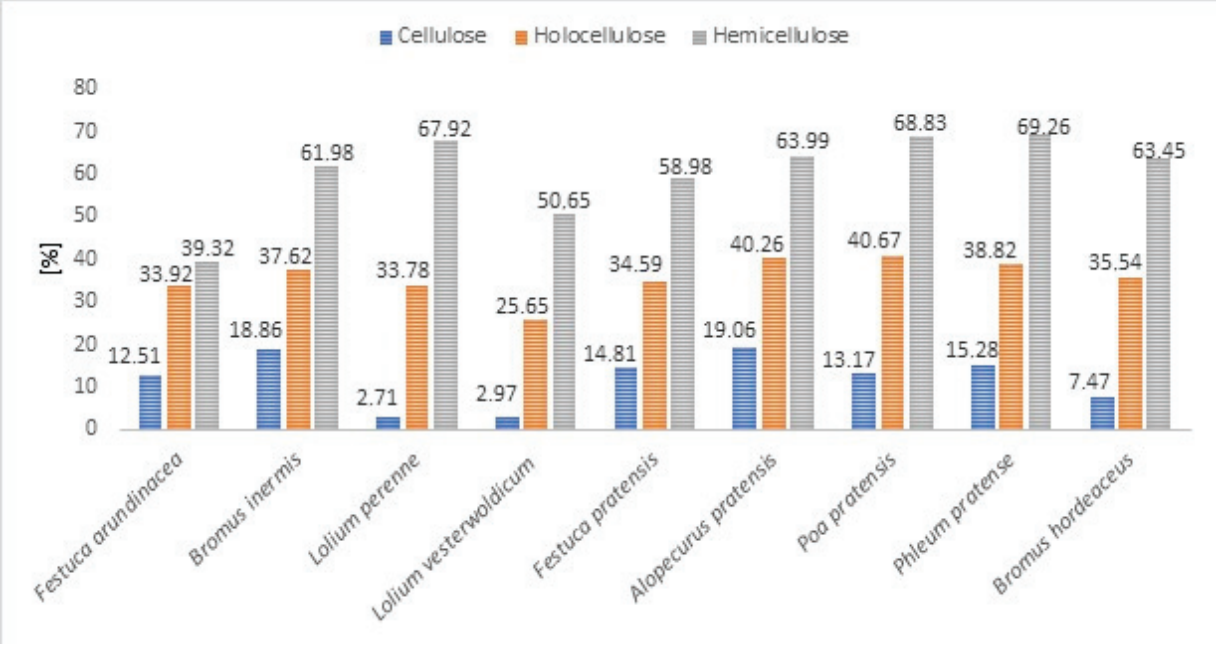

Figure 2. Mass loss of cellulose, holocellulose, and hemicelluloses because of the methane fermentation process [%].

The lignin content of the grasses before fermentation varied more than that of cellulose. It ranged from 12.44% for *B. hordeaceus* to 17.70% for *Alopecurus pratensis* (Table 1). For most species, the lignin content ranged from 15.58% to 17.02%. A very low lignin content (only 4.81%) in bagasse leaves was determined by Tapia-Maruri et al. [21]. Perhaps their modified method of determining lignin influenced the amount. Large discrepancies in lignin content, ranging from 13.41% to 26.25%, were shown by Rahaman et al. [22] in the genotypes of six grass species tested. Even the same species showed different contents of lignin. For instance, the lignin content in *Saccharum spontaneum* ranged from 17.20% to 23.01%, while in *Arundo donax* it ranged from 18.77% to 22.40%. After the fermentation process, significantly higher amounts of lignin were observed. For most grasses, the amount of lignin in the digest was 44–45%, with the exception of *Phl. pratense* (39.67%) and *L. perenne* (41.5%). The increased lignin content in the digestate is due to the mass loss of carbohydrate compounds during the fermentation process. The apparent increase in lignin content ranged from 133 to 200% (Figure 3).

The content of holocellulose before fermentation ranged from 59.77% to 72.93% (Table 1). *L. westerwoldicum* had the lowest content, while *B. horeaceus* had the highest content. The holocellulose content in the majority of the species ranged from 63% to 69%. After the fermentation process, the holocellulose content ranged from about 22% to 29%. Only *L. westerwoldicum* showed a reduction in holocellulose content to 15%.

The analysis carried out showed that the content of hemicelluloses in the grasses before fermentation ranged from 28% to 36.5% (Table 1). These values are higher than previously reported values and could have a positive effect on the fermentation process. Rahaman et al. [22], studying six grass species, determined the content of hemicelluloses to be between approximately 12% and 20%. According to Rahaman et al. [22], *Saccharum*

spontaneum had the highest hemicellulose content (20.19%), while *Arundo donax* had the lowest hemicellulose content (11.97%).

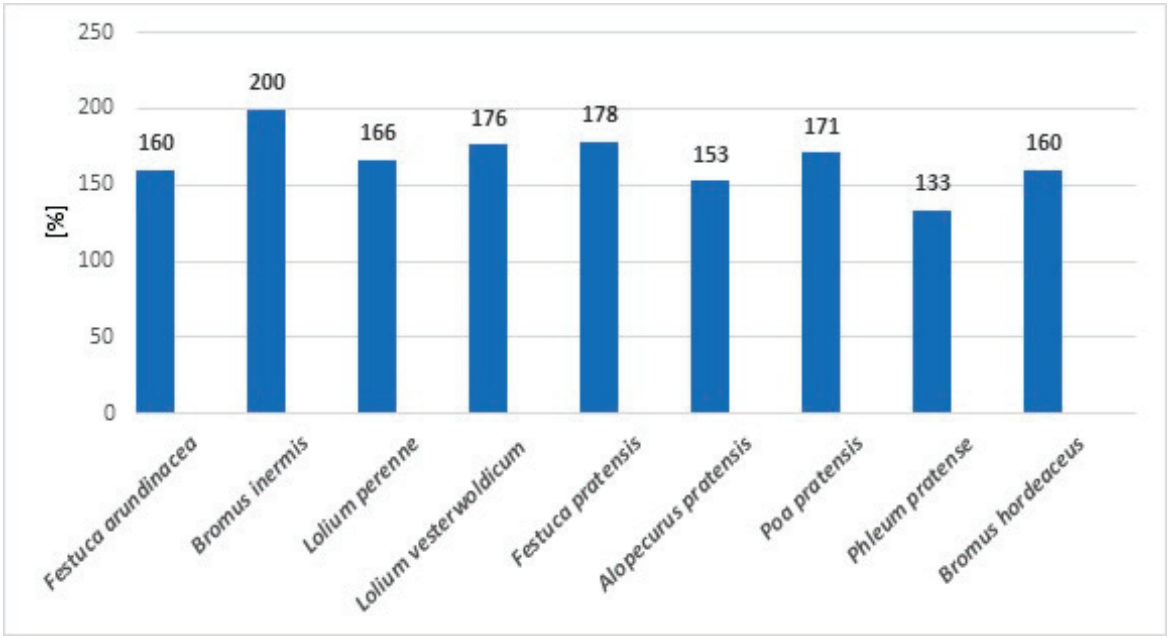

Figure 3. Apparent increase in lignin content as a result of the fermentation process [%].

The methane fermentation process significantly reduced the content of low-polymerized carbohydrates in the grasses. The concentration of hemicelluloses after fermentation ranged from 8.78% in *Phl. pretense* to 19.54% in *F. arudinacea*. The percentage loss of hemicelluloses during the fermentation process ranged from 39.32% in *F. arudinacea* to almost 70% in *Phl. pretense* (Figure 2). *P. pratensis* and *L. perenne* also showed a significant loss of hemicelluloses (68.83% and 67.92%, respectively).

Table 2 shows the content of ethanol-extractable substances in the grasses before and after the fermentation process. Analysis of the mean values of extractives and ash showed statistically significant differences for all components.

Table 2. Change in extract and ash content with statistically significant differences due to fermentation (Tukey's test). Mean values with standard deviation for each grass species are presented (statistically significant for $p < 0.01$).

Grass Species	Extraction Substances [%]		Ash [%]	
	Before	After	Before	After
	Methane Fermentation			
Festuca arundinacea	15.95 ^{cd} ± 0.90	6.32 ^{bc} ± 0.27	5.39 ^{f} ± 0.02	44.40 ^{a} ± 0.47
Bromus inermis	12.02 ^{f} ± 0.62	6.24 ^{c} ± 0.07	8.57 ^{b} ± 0.02	44.61 ^{a} ± 0.01
Lolium perenne	17.04 ^{c} ± 0.50	6.55 ^{bc} ± 0.22	6.14 ^{e} ± 0.01	34.21 ^{d} ± 0.33
Lolium vesterwoldicum	25.04 ^{a} ± 0.35	6.61 ^{bc} ± 0.35	9.46 ^{a} ± 0.02	41.08 ^{b} ± 0.20
Festuca pratensis	20.77 ^{b} ± 0.14	6.71 ^{bc} ± 0.30	7.40 ^{c} ± 0.54	41.97 ^{b} ± 0.26
Alopecurus pratensis	14.19 ^{de} ± 0.25	6.83 ^{bc} ± 0.26	4.51 ^{g} ± 0.01	38.77 ^{c} ± 0.61
Poa pratensis	16.01 ^{c} ± 0.34	7.63 ^{a} ± 0.12	4.21 ^{g} ± 0.02	38.10 ^{c} ± 0.24
Phleum pretense	15.76 ^{c} ± 0.30	6.91 ^{b} ± 0.03	6.33 ^{e} ± 0.02	30.60 ^{e} ± 0.14
Bromus hordeaceus	12.46 ^{ef} ± 0.81	5.61 ^{d} ± 0.11	6.93 ^{d} ± 0.06	45.12 ^{a} ± 0.14

^{a}, ^{b}, ^{c}, ^{d}, ^{e}, ^{f}—homogeneous groups.

Before fermentation, the content of ethanol-extractable substances in the different grass species ranged from 12.02% to 25.04%. After the fermentation process, the amount of

ethanol-extractable compounds ranged from 5.61% in *B. hordeaceus* to 7.63% in *P. pratensis*. The other grasses contained between 6.24% and 6.91% of these substances after fermentation. Analysis of the results showed that the loss of ethanol-extractable substances quantitatively was comparable to the decrease in the content of hemicelluloses. The loss ranged from 48.09% in the case of *B. inermis* to as much as 73.60% in *L. westerwoldicum*.

Table 2 also shows the ash content of the grasses before and after methane fermentation. Before fermentation, as with the extractives, there was a wide variation in ash content among species, ranging from 4.21% to 9.46%. Ash content depends on various factors, and the wide variability found in this study is comparable to other studies. Depending on the development stage of the plant, Herrmann et al. [23] found between 7% and 16% ash in ryegrass mixture, between 4% and 10% in *Sorghum bicolor,* and between 10 and19% in *Helianthus annuus*. The same authors showed ash content ranging from 7% to 11% in meadow fescue.

After the fermentation process, higher amounts of ash were observed in the residue than in the fresh plant material. Its amount in the digest ranged from 30.60% to 45.12%. This was more than 5–9 times the amount of mineral compounds in fresh grasses. Such a large increase in ash concentration in the assayed material was due to the addition of a fermentation inoculant, the composition of which cannot be disclosed due to analysis and potential industrial use.

The potential to produce biogas with a high methane content is an important quality parameter for plant biomass used as biogas feedstock. The main factor influencing the amount of methane yield that can be obtained under favorable process conditions in biogas plants is the choice of plant species [23]. Tilman et al. [24] concluded that biofuels derived from low-input native perennial grasses can produce more useful energy and reduce greenhouse gas emissions and agrochemical pollutants compared to arable crops such as maize or soya.

In Table 3, the authors show the data of dry matter and organic dry matter of the studied grass species. The dry matter ranged from 89.85% to 92.98%. Gobena et al. [25] found that the average dry matter of different grasses was about 92.78%. Waliszewska et al. [26] found that the average dry matter content of different grass species was about 93.53%. Both cited publications show that the authors obtained higher dry matter content in the studied grass species than this study. This could be due to the different storage conditions for the samples or the ability of the plant to retain water.

Table 3. The content of dry matter and organic dry matter in different grass samples.

Grass Species	DM [%]	ODM [%]
Festuca arundinacea	91.21	93.00
Bromus inermis	90.80	94.61
Lolium perenne	92.98	87.10
Lolium westerwoldicum	90.61	92.30
Festuca pratensis	92.07	94.73
Alopecurus pratensis	91.16	94.93
Poa pratensis	89.85	91.65
Phleum pretense	90.96	92.35
Bromus hordeaceus	91.24	92.38

The content of organic compounds in the dry matter of the studied grass species ranges from 87.10% to 94.93%. The lowest content of organic compounds was observed in *L. perenne*, while the highest content was observed in *A. pratensis*, *F. pratensis* and *B. inermis*. Platače and Adamovičs [27] examined timothy and meadow fescue in their study. They observed dry matter organic compounds in the range of 92.98% to 95.01% for timothy and 93.12% to 93.95% for meadow fescue. These values are comparable to the current study.

Amaleviciute-Volunge et al. [28] studied different grass species and reported biogas yields ranging from 63.2 to 114.3 $dm^3 \cdot kg^{-1}$ FM. Chiumenti et al. [29], who studied

perennial grasses, reported a biogas yield of 164.6 $dm^3 \cdot kg^{-1}$ FM and a methane yield of −87.4 $dm^3 \cdot kg^{-1}$ FM. Scarlat et al. [30] found that the methane yield of grass was 55–128 $dm^3 \cdot kg^{-1}$ FM. Slightly higher biogas yields of 510–560 l/kg VS were obtained by Kasulla et al. [31], with approximately 60% methane from the napier grass hybrid. Similar biogas quantities of 540–580 L/kg VS were reported from extensive grassland in a study by Korres et al. [12]. Species from which more than 400 $m^3 \cdot Mg^{-1}$ VS of biogas can be obtained are feasible to consider as biogas feedstock. The results of the present study show that many grass species from Polish grasslands can be used for biogas production.

Analyzing the data shown in Figure 4, no correlation was found between the holocellulose content and the amount of biogas obtained during the fermentation process.

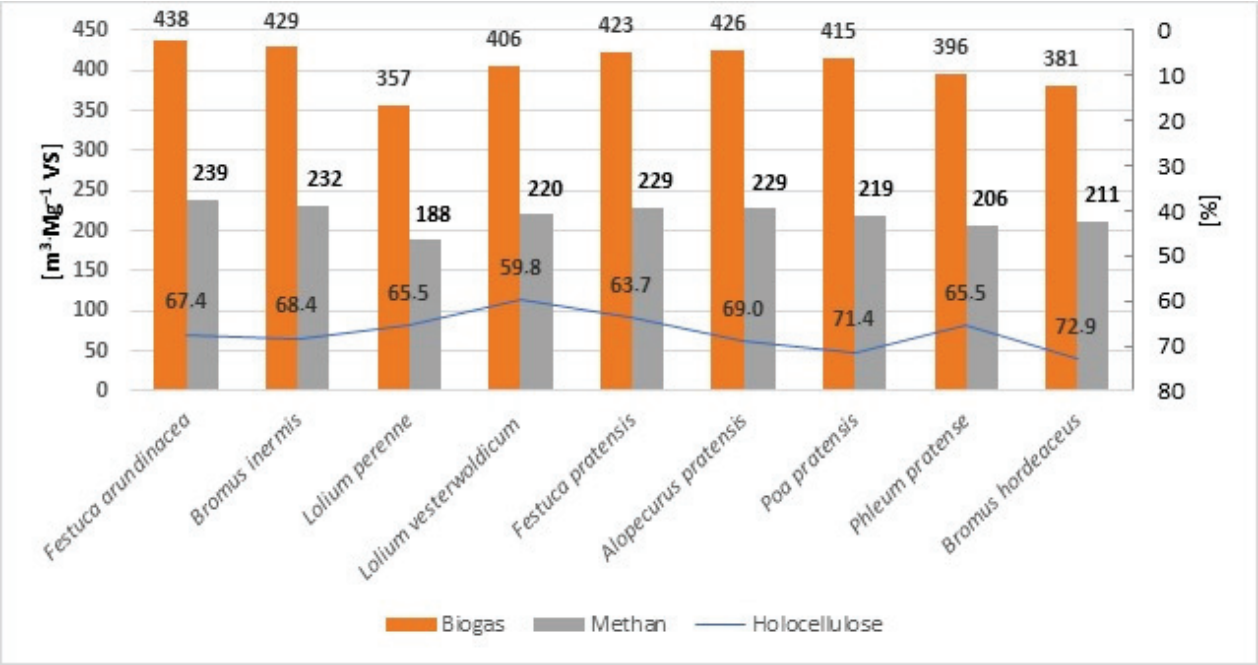

Figure 4. Amount of biogas and methane [$m^3 \cdot Mg^{-1}$ VS] obtained vs. holocellulose [%].

The species *L. westerwoldicum*, containing only 59.8% holocellulose, yielded more than 400 $m^3 \cdot Mg^1$ VS of biogas, while *B. hordeaceus*, with the highest content (almost 73%) of holocellulose, produced only 381 $m^3 \cdot Mg^{-1}$ VS of biogas. There was also no correlation between the lignin content of the grasses and biogas production (Tables 1 and 4).

Table 4. The content of methane and overall biogas yield in different grass samples.

Grass Species	Methane Yield [$m^3 \cdot Mg^{-1}$ VS]	Biogas Yield [$m^3 \cdot Mg^{-1}$ VS]
Festuca arundinacea	239.36	437.89
Bromus inermis	232.45	429.24
Lolium perenne	187.80	356.94
Lolium westerwoldicum	220.62	406.15
Festuca pratensis	229.56	423.08
Alopecurus pratensis	229.16	425.97
Poa pratensis	219.34	415.40
Phleum pretense	205.62	396.58
Bromus hordeaceus	211.00	381.36

The grass species *B. hordeaceus* containing the least lignin (12.44%) among the grasses tested had the lowest biogas yield. It is likely that other biomass components, e.g., phenolic substances with complex chemical structure, may have an inhibitory effect on biogas

production. According to literature reports, high methane production can be obtained from plants with low lignin content and high amounts of non-structural carbohydrates and soluble and easily degradable cellular components [32,33]. The authors of the present study, based on the results obtained from nine grass species, do not unequivocally support such a claim. The amount of biogas produced may depend on many other factors, hence each species should be studied individually.

4. Conclusions

The process of anaerobic digestion for biogas production results in significant changes in the structural and incidental biomass components of the grass species studied. Low-polymerized carbohydrates (hemicelluloses) were degraded to the greatest extent. Lignin was the least degradable and most prominent biomass component in the digestate.

The lack of correlation between carbohydrate and lignin content and the biogas yield suggests that only a comprehensive study of the chemical composition of the biomass can predict which species will be most favorable in terms of suitability for biogas production.

The high biogas production and methane content of the biogas indicate that grasses from Polish meadows could be an alternative source of biogas from renewable sources.

Given the well-known anaerobic digestion technology and the need for rural development and sustainable energy production, biogas production from grasses is an attractive solution that meets many legal, agronomic, and environmental requirements.

Author Contributions: Conceptualization, B.W. and M.G.; methodology, M.G.; software, H.W.; validation, L.M., E.G. and M.M.; formal analysis, B.W.; investigation, M.Gresources, M.G; data curation, B.W.; writing—original draft preparation, M.M.; writing—review and editing, L.M.; visualization, A.S.; supervision, A.S.-D.; project administration, B.W.; funding acquisition, B.W.; supervision of research, I.V. All authors have read and agreed to the published version of the manuscript.

Funding: The research conducted from budget of the Department of Chemical Wood Technology and the Department of Grassland and Natural Landscape at the Poznan University of Life Sciences. The publication was financed by the Polish Minister of Science and Higher Education as part of the Strategy of the Poznan University of Life Sciences for 2024–2026 in the field of improving scientific research and development work in priority research areas.

Data Availability Statement: The original contributions presented in the study are included in the article, further inquiries can be directed to the corresponding author.

Acknowledgments: The authors are grateful for support provided by the Poznan University of Life Sciences, Poland, including technical support and materials used for field experiments.

Conflicts of Interest: The authors declare no conflicts of interest.

References

1. Richter, F.; Fricke, T.; Wachendorf, W. Utilization of semi-natural grassland through integrated generation of solid fuel and biogas from biomass. III. Effects of hydrothermal conditioning and mechanical dehydration on solid fuel properties and on energy and greenhouse gas balances. *Grass Forage Sci.* **2010**, *65*, 185–199. [CrossRef]
2. Czekała, W. Solid Fraction of Digestate from Biogas Plant as a Material for Pellets Production. *Energies* **2021**, *14*, 5034. [CrossRef]
3. Vázquez-Rowe, I.; Golkowska, K.; Lebuf, V.; Vaneeckhaute, C.; Michels, E.; Meers, E.; Benetto, E.; Koster, D. Environmental assessment of digestate treatment technologies using LCA methodology. *Waste Manag.* **2015**, *43*, 442–459. [CrossRef] [PubMed]
4. Sobczak, A.; Chomać-Pierzecka, E.; Kokiel, A.; Różycka, M.; Stasiak, J.; Soboń, D. Economic Conditions of Using Biodegradable Waste for Biogas Production, Using the Example of Poland, and Germany. *Energies* **2022**, *15*, 5239. [CrossRef]
5. Gao, X.; Tang, X.; Zhao, K.; Balan, V.; Zhu, Q. Biogas Production from Anaerobic Co-Digestion of Spent Mushroom Substrate with Different Livestock Manure. *Energies* **2021**, *14*, 570. [CrossRef]
6. Weiland, P. Biomass digestion in agriculture: A successful pathway for the energy production and waste treatment in Germany. *Eng. Life Sci.* **2006**, *6*, 302–309. [CrossRef]
7. Dena, H.M.; Kontges, A.; Rostek, S. *Biogaspartner—A Joint Initiative. Biogas Grid Injection in Germany and Europe-Market, Technology and Players*; German Energy Agency, HP Druck: Berlin, Germany, 2009.
8. Prochnow, A.; Heiermann, M.; Plochl, M.; Linke, B.; Idler, C.; Amon, T.; Hobbs, P.J. Bioenergy from permanent grassland-A review: 1. Biogas. *Bioresour. Technol.* **2009**, *100*, 4931–4944. [CrossRef] [PubMed]

9. Korres, N.E.; Singh, A.; Nizami, A.S.; Murphy, J.D. Is grass biomethane a sustainable transport biofuel? *Biofuels Bioprod. Biorefin.* **2010**, *4*, 310–325. [CrossRef]
10. Pilarski, K.; Pilarska, A.A.; Boniecki, P.; Niedbała, G.; Witaszek, K.; Piekutowska, M.; Idzior-Haufa, M.; Wawrzyniak, A. Degree of Biomass Conversion in the Integrated Production of Bioethanol and Biogas. *Energies* **2021**, *14*, 7763. [CrossRef]
11. Esteves, B.; Sen, U.; Pereira, H. Influence of Chemical Composition on Heating Value of Biomass: A Review and Bibliometric Analysis. *Energies* **2023**, *16*, 4226. [CrossRef]
12. Korres, N.E.; Thamsiriroj, T.; Smyth, B.M.; Nizami, A.S.; Singh, A.; Murphy, J.D. Grass Biomethane for Agriculture and Energy. In *Genetics, Biofuels and Local Farming Systems*; Lichtfouse, E., Ed.; Springer Science+Business Media B.V.: Berlin/Heidelberg, Germany, 2011.
13. Seifert, K. Zur Frage der Cellulose-Schnellbestimmung nach der Acetylaceton-Methode. *Das Pap.* **1960**, *14*, 104–106.
14. *TAPPI T 222 om-06*; Acid-Insoluble Lignin in Wood and Pulp. Technical Association of the Pulp and Paper Industry (TAPPI): Atlanta, GA, USA, 2006.
15. *TAPPI T 9 wd-75*; Holocellulose in Wood. Technical Association of the Pulp and Paper Industry (TAPPI): Atlanta, GA, USA, 2006.
16. *TAPPI T 204 cm-07*; Solvent Extractives of Wood and Pulp. Technical Association of the Pulp and Paper Industry (TAPPI): Atlanta, GA, USA, 2007.
17. Cieślik, M.; Dach, J.; Lewicki, A.; Smurzyńska, A.; Janczak, D.; Pawlicka-Kaczorowska, J.; Boniecki, P.; Cyplik, P.; Czekała, W.; Jóźwiakowski, K. Methane fermentation of the maize straw silage under meso- and thermophilic conditions. *Energy* **2016**, *115*, 1495–1502. [CrossRef]
18. Lewicki, A.; Pilarski, K.; Janczak, D.; Czekała, W.; Rodríguez Carmona, P.C.; Cieślik, M.; Witaszek, K.; Zbytek, Z. The biogas production from herbs and waste from the herbal industry. *J. Res. Appl. Agric. Eng.* **2013**, *58*, 114–117.
19. de Mendiburu, F. Agricolae: Statistical Procedures for Agricultural Research, R Package Version 1.3-7; 2023. Available online: https://cran.r-project.org/web/packages/agricolae/agricolae.pdf (accessed on 20 April 2024).
20. R Core Team. *R: A Language and Environment for Statistical Computing*; R Foundation for Statistical Computing: Vienna, Austria, 2024. Available online: https://www.R-project.org/ (accessed on 20 April 2024).
21. Tapia-Maruri, D.; Evangelista-Lozano, S.; Alamilla-Beltrán, L.; Camacho-Díaz, B.H.; Ávila-Reyes, S.V.; Villalobos-Espinosa, J.d.C.; Jiménez-Aparicio, A.R. Comparative Evaluation of the Thermal, Structural, Chemical and Morphological Properties of Bagasse from the Leaf and Fruit of *Bromelia hemisphaerica* Lam. Delignified by Organosolv. *Appl. Sci.* **2022**, *12*, 3761. [CrossRef]
22. Rahaman, T.; Biswas, S.; Ghorai, S.; Bera, S.; Dey, S.; Guha, S.; Maity, D.; De, S.; Ganguly, J.; Das, M. Integrated application of morphological, anatomical, biochemical, and physico-chemical methods to identify superior, lignocellulosic grass feedstocks for bioenergy purposes. *Renew. Sustain. Energy Rev.* **2023**, *187*, 113738. [CrossRef]
23. Herrmann, C.; Plogsties, V.; Willms, M.; Hengelhaupt, F.; Eberl, V.; Eckner, J.; Strauß, C.; Idler, C.; Heiermann, M. Methane production potential of various crop species grown in energy crop rotations. *Landtechnik* **2016**, *71*, 194–208.
24. Tilman, D.; Hill, J.; Lehman, C. Carbon-negative biofuels from low-input high diversity grassland biomass. *Science* **2006**, *314*, 1598–1600. [CrossRef]
25. Gobena, G.; Urge, M.; Hundie, D.; Kumsa, D. Identification and evaluation of agro-ecological variation in dry matter yield and nutritional values of local grasses used as livestock feed in Adola Reedde. Guji Zone. Ethiopia. *J. Appl. Anim. Res.* **2022**, *50*, 369–379. [CrossRef]
26. Waliszewska, B.; Grzelak, M.; Gaweł, E.; Spek-Dźwigała, A.; Sieradzka, A.; Czekała, W. Chemical Characteristics of Selected Grass Species from Polish Meadows and Their Potential Utilization for Energy Generation Purposes. *Energies* **2021**, *14*, 1669. [CrossRef]
27. Platače, R.; Adamovičs, A. The evaluation of ash content in grass biomass used for energy production. *Energy Prod. Manag. 21st Century* **2014**, *2*, 1057–1065.
28. Amaleviciute-Volunge, K.; Slepetiene, A.; Butkute, B. Methane yield of perennial grasses with as affected by the chemical composition of their biomass. *Zemdirb.-Agric.* **2020**, *107*, 243–248. [CrossRef]
29. Chiumenti, A.; Boscaro, D.; Da Borso, F.; Sartori, L.; Pezzuolo, A. Biogas from Fresh Spring and Summer Grass: Effect of the Harvesting Period. *Energies* **2018**, *11*, 1466. [CrossRef]
30. Scarlat, N.; Dallemand, J.F.; Fahl, F. Biogas: Developments and perspectives in Europe. *Renew. Energy* **2018**, *129*, 457–472. [CrossRef]
31. Kasulla, S.; Malik, S.J.; Yadav, A.; Kathpal, G. Potential of Biogas Generation from Hybrid Napier Grass. *Int. J. Trend Sci. Res. Dev.* **2022**, *6*, 277–281.
32. Amon, T.; Amon, B.; Kryvoruchko, V.; Machmuller, A.; Hopfner-Sixt, K.; Bodiroza, V.; Hrbek, R.; Friedel, J.; Potsch, E.; Wagentristl, H.; et al. Methane production through anaerobic digestion of various energy crops grown in sustainable crop rotations. *Bioresour. Technol.* **2007**, *98*, 3204–3212. [CrossRef] [PubMed]
33. Schittenhelm, S. Chemical composition and methane yield of maize hybrids with contrasting maturity. *Eur. J. Agron.* **2008**, *29*, 72–79. [CrossRef]

energies

MDPI

Article

Energy Quality of Corn Biomass from Gasoline-Contaminated Soils Remediated with Sorbents

Agata Borowik, Jadwiga Wyszkowska *, Magdalena Zaborowska and Jan Kucharski

Department of Soil Science and Microbiology, Faculty of Agriculture and Forestry, University of Warmia and Mazury in Olsztyn, 10-719 Olsztyn, Poland; agata.borowik@uwm.edu.pl (A.B.); m.zaborowska@uwm.edu.pl (M.Z.); jan.kucharski@uwm.edu.pl (J.K.)

* Correspondence: jadwiga.wyszkowska@uwm.edu.pl

Abstract: Soil contaminated with petroleum-derived products should be used to cultivate energy crops. One such crop is *Zea mays*. Therefore, a study was performed to determine the suitability of *Zea mays* biomass obtained from gasoline-contaminated soil for energy purposes. The analysis included determining the heat of combustion and calorific value of the biomass, as well as the content of nitrogen, carbon, hydrogen, oxygen, sulfur, and ash in the biomass. Additionally, the suitability of vermiculite, dolomite, perlite, and agrobasalt for the phytostabilization of gasoline-contaminated soil was evaluated. It was found that the application of sorbents to gasoline-contaminated soil significantly reduced the severe negative effects of this petroleum product on the growth and development of *Zea mays*. Gasoline contamination of the soil caused a significant increase in ash, nitrogen, and sulfur, along with a decrease in carbon and oxygen content. However, it had no negative effect on the heat of combustion or calorific value of the biomass, although it did reduce the energy production from *Zea mays* biomass due to a reduction in yield. An important achievement of the study is the demonstration that all the applied sorbents have a positive effect on soil stabilization, which in turn enhances the amount of *Zea mays* biomass harvested and the energy produced from it. The best results were observed after the application of agrobasalt, dolomite, and vermiculite on gasoline-contaminated soil. Therefore, these sorbents can be recommended for the phytostabilization of gasoline-contaminated soil intended for the cultivation of energy crops.

Keywords: heat of combustion; biomass energy; calorific value; sorbents; gasoline; enzymes

1. Introduction

Biomass as an alternative energy source is becoming increasingly important in the context of efforts to combat global warming and reduce the use of fossil fuels [1–3]. This is justified by the fact that biobased products emit fewer greenhouse gases compared to fossil feedstocks [4,5]. Plant biomass first garnered attention as a sustainable energy source in the 1970s [4–9], and interest in the subject has grown as efforts to mitigate climate change have intensified. Current research on biomass focuses on several primary objectives: reducing greenhouse gas emissions, decreasing fossil fuel exploitation, and increasing energy self-sufficiency [10–12]. Biomass energy production holds significant potential to reduce society's dependence on fossil fuels [2,10].

The calorific value of biomass is a key parameter, particularly when considering its use as an energy source [13]. Biomass derived from agricultural residues has a calorific value of approximately 1.26×10^4 MJ Mg^{-1}, which is half the calorific value of coal and one-third that of diesel [7,14]. The calorific value of petroleum derivatives ranges from 41.5 to 47.0 MJ kg^{-1} [15]. According to Amaral [16], gasoline is composed of a variety of hydrocarbons with different molecular structures. Molecules with a higher number of atoms have higher boiling points, and their calorific value generally increases, with hydrogen having a higher calorific value compared to carbon. According to Zaharin et al. [17], gasoline blends

with ethanol and butanol (E10, E10B5, E10B10, and E10B15) result in lower calorific values, ranging from 41.7 MJ kg^{-1} to 43.1 MJ kg^{-1}.

The calorific value of biomass is significantly lower than that of gasoline [7]. The calorific value of gasoline is almost four times higher than that of biomass, indicating the relatively lower efficiency of biomass as a fuel in terms of the energy released during combustion [13]. Nevertheless, biomass has other advantages, such as a lower impact on greenhouse gas emissions, which can compensate for its lower heating value [18].

One of the main applications of biomass is the production of biofuels such as ethanol and biodiesel [2,19,20]. The European Parliament and other international institutions promote the development of advanced biofuels, which can be produced from agricultural residues, such as straw or crop leftovers [20–24]. The use of such feedstocks minimizes the impact on land use changes and does not compete with food production. In recent years, there has been particular interest in the use of corn residues, which exhibit low resistance to bioconversion processes [9,25]. This means that corn residues, such as stalks, leaves, or cobs, are relatively easy to convert into biofuels or other bioproducts through biochemical processes, such as fermentation or enzymatic decomposition. The chemical structure of plant residues is less complex and more susceptible to degradation, making bioconversion more efficient and leading to higher yields in the production of bioethanol and other forms of renewable energy [26,27]. As a result, maize biomass is one of the most popular feedstocks for biogas production in the energy sector, particularly in countries such as Germany and Austria, where biogas production is well developed [28,29]. Similarly, maize silage, from both whole plant and grain, is highly valued for its energy content, particularly in Poland, where it is used not only for biogas production but also for ethanol [30]. The growing interest in maize biomass, driven by its high biomass yield, makes it an attractive option for biogas plants and contributes to the reduction in greenhouse gas emissions by replacing fossil fuels with renewable energy sources.

One of the challenges associated with the use of biomass for energy is soil degradation [31–33], caused by the over-exploitation of agricultural land and the use of pesticides and herbicides [33–36]. Plants, sorbents, and soil microorganisms can play a crucial role in mitigating these negative effects without reducing crop yields. Finding effective methods to remediate soils contaminated with petroleum-derived products, such as gasoline, remains a major challenge [37,38].

The use of adsorbent materials capable of binding and retaining contaminants on their surface, as noted by Kapoor and Zdarta [39], has proven effective in reducing the bioavailability of toxic compounds in the soil. Petroleum products can lead to soil degradation, reduced fertility, and adverse effects on soil microbiomes and biogeochemical processes occurring in soil formations. Vermiculite, dolomite, perlite, and agrobasalt are four materials that have shown promising properties for improving the quality of soils contaminated with petroleum-derived products. Vermiculite, a natural mineral with high water and nutrient absorption capacity, can support the development of soil microorganisms by improving soil structure and increasing its water-holding capacity [40,41]. Dolomite, a mineral composed mainly of calcium and magnesium carbonate, can neutralize soil acidity [42,43]. Due to its porous structure, perlite increases air circulation in the soil. It has the ability to store water and nutrients. It consists mainly of silica (SiO_2) and oxides of potassium, magnesium, and calcium, which are essential for the development of the plant's root system [44–46]. Agrobasalt, a by-product of the basalt industry, contains numerous micro- and macroelements, such as potassium, magnesium, calcium, and iron, and can stimulate enzymatic activity in the soil, improve soil fertility, and support plant growth [47,48].

Consequently, the search for effective methods of remediating contaminated soils is of paramount importance, as abiotic factors influence the derivatives and end products of petroleum substance degradation. Sorbents can prevent the penetration of contaminants, along with water and oxygen, into deeper soil profiles, thereby affecting permeability, pH levels, and nutrient availability [49–54].

The aim of this study was to determine the suitability of *Zea mays* biomass from gasoline-contaminated soils for energy purposes. The analysis included the determination of the heat of combustion and the calorific value of the biomass, as well as the content of nitrogen, carbon, hydrogen, oxygen, sulfur, and ash in the biomass. Additionally, the effectiveness of vermiculite, dolomite, perlite, and agrobasalt in the phytostabilization of soil subjected to gasoline contamination was also assessed. This research objective prompted us to formulate the following hypotheses: (1) the energy value of *Zea mays* biomass is determined by its content of non-fuel elements; (2) the heat of combustion and calorific value of *Zea mays* biomass are functions of soil contamination with gasoline; (3) the amount of energy extracted from *Zea mays* biomass depends on soil supplementation with sorbents.

2. Materials and Methods

2.1. Research Design

The subject of the study was soil taken from an agricultural field from a depth of 0 to 20 cm. This soil was formed from loamy sand. Such soils take up an area of about 50% of arable land in Poland. Based on the classification by the International Union of Soil Sciences [55], this soil is identified as Eutric Cambisol. Its granulometric composition was as follows: sand—75.68%; silt—23.08%; clay—1.24%. The content of organic carbon (C_{org}) was 9.29 g, total nitrogen (N_{Total})—1.22 g, and pH_{KCl}—4.2. The study was carried out in the vegetation hall in a pot experiment in 4 replicates. Plastic pots were used for the experiment, the volume of which allowed to fill them with soil in the amount of 3.2 kg. The experiment was carried out in two series: uncontaminated soil and soil contaminated with unleaded gasoline 95 at 0 and 24 cm^3 kg^{-1} of soil. *Zea mays* of the DS1897B variety (producer Pioneer, Warsaw, Poland) and the following sorbents were used for phytostabilization of gasoline-contaminated soil: vermiculite with a fraction of 1–5 mm (producer Sobex, Drezdenko, Poland), dolomite with a fraction of 0.5–1 mm (producer Sobex, Drezdenko, Poland), perlite with a fraction of 3–6 mm (producer Biovita Ltd., Tenczynek, Poland), and agrobasalt with a fraction of 1–7 mm (producer Biovita Sp. z o.o., Tenczynek, Poland). The sorbents used were applied in amounts of 0 and 10 g kg^{-1} d.m. of soil (Figure 1). Unleaded gasoline 95 was purchased at a PKN Orlen (Poland) gas station. Its density varies from 0.720 to 0.775 g cm^{-3}, and its sulfur content is a maximum of 10 mg kg^{-1}. The characteristics of the petroleum substance are available on the PKN Orlen website [56].

Figure 1. Test sorbents used in the experiment (**a**) vermiculite; (**b**) dolomite; (**c**) perlite; (**d**) agrobasalt.

In the experiment, homogeneous fertilization with macronutrients was applied in the amount (mg kg^{-1} d.m. of soil): N—225 in the form of N_2H_4CO, P—50 in the form of KH_2PO_4, K—150 in the form of KH_2PO_4 and KCl, and Mg—15 in the form of $MgSO_4 \times 7H_2O$. Three days after packing the soil, eight seeds of *Zea mays* each were sown in pots. When the plants germinated, five plants were left in each pot.

The growing period of the plants was 60 days, but harvesting of the aboveground parts and roots of corn was carried out at stage 51 of the Biological Federal Institute, Bundessortenamt and Chemie (BBCH) (Figure 2).

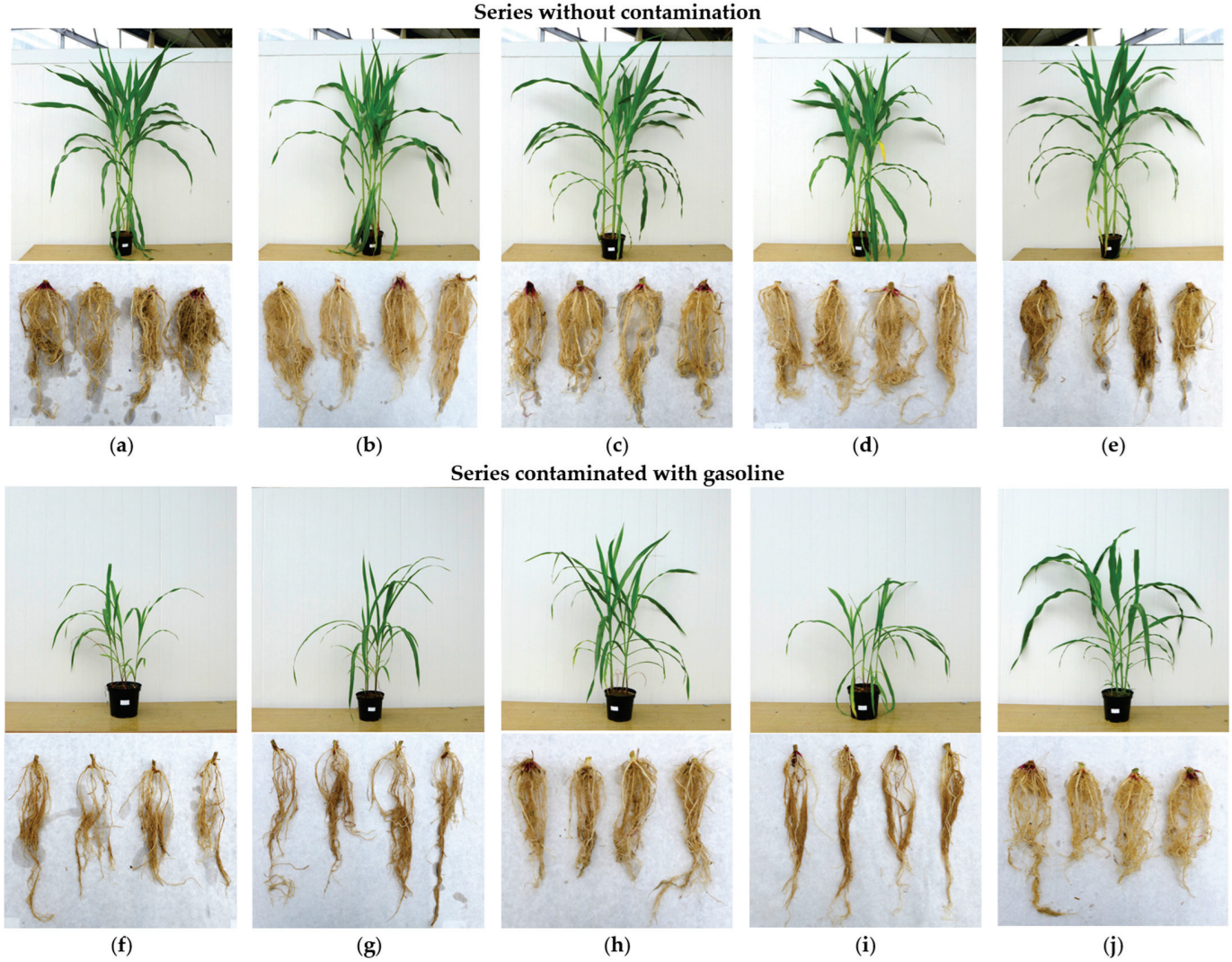

Figure 2. *Zea mays* on the day of harvest. The series without contamination: (**a**) control; (**b**) with vermiculite; (**c**) dolomite; (**d**) perlite; (**e**) agrobasalt; and series (**f**) contaminated with gasoline; (**g**) vermiculite; (**h**) dolomite; (**i**) perlite; (**j**) agrobasalt.

2.2. Laboratory Analyzes

After harvesting *Zea mays* at BBCH stage 51 and determination of biomass, the plants were ground and dried. The plant samples were then milled using a laboratory grinder (Retsch SM 200, Haan, Germany) and a sieve with a mesh diameter of 0.5 mm. The next step was to determine the heat of combustion (Q), heating value (Hv), and energy production (Yep) of the *Zea mays* biomass (Figure 3). The determination of Q was carried out according to the procedure described in PN-EN ISO 18125:2017 [57], and the calorific value (Hv) of *Zea mays* was calculated according to the formula of Kopetz et al. [58].

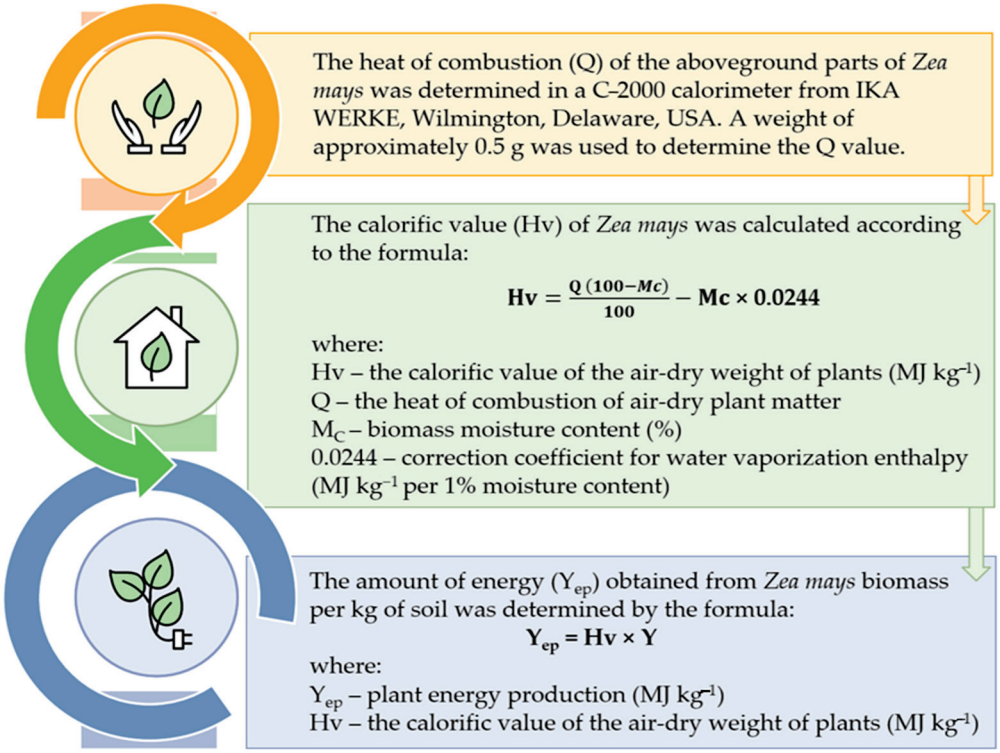

Figure 3. Methods for determining the energetic value of plants.

In order to characterize the biomass of plants for energy purposes, its carbon (C), hydrogen (H), sulfur (S), nitrogen (N), oxygen (O), and ash contents were determined (Figure 4). The contents of C, H, and N were determined according to PN-EN ISO 16948:2015-07 [59], S—PN-G-04584:2021 [60] and PN-EN ISO 16994:2016-10 [61], and ash was determined according to PN-EN ISO 18122:2016-01 [62].

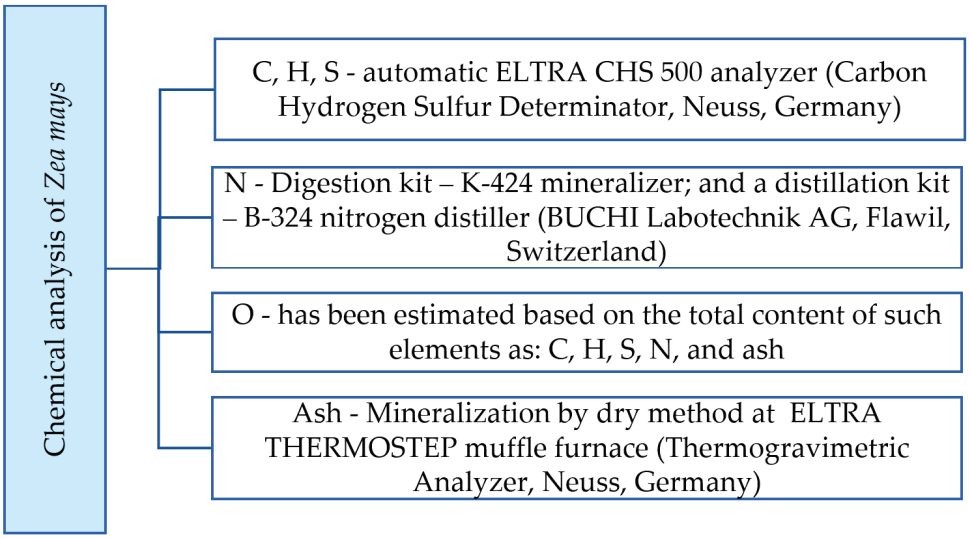

Figure 4. Methods of chemical analysis of plants.

2.3. Statistical Data Processing and Analysis

In order to evaluate the effects of gasoline (G) and vermiculite (V), dolomite (D), perlite (P), and agrobasalt (A) on *Zea mays* biomass, its Q, Hv, and Yep, as well as the content of N, C, H, S, O, and ash in the biomass, influence indices were calculated using formulae presented in our previous publications [52,63–65]. The data were illustrated on heat maps

using the RStudio 2023.06.0 [66] with the R 4.2.2 addition [67] and the gplots library [68]. Statistical analysis of the results was performed using the Statistica 13.0 package [69].

Tukey's test, principal component analysis (PCA), and Pearson's simple correlation coefficients were used for this purpose. The coefficients of η^2 were also calculated and presented in a pie chart using the Circos 0.68 package [70]. All statistical analyses were performed at a significance level of $p < 0.05$.

3. Results

3.1. Zea mays Biomass

Soil contamination with gasoline revealed the sensitivity of *Zea mays* to this xenobiotic (Table 1, Figure 5). Its application to the soil reduced the parameters characterized by the plant (Ya, Yr) by 83% and 84%, respectively. Soil not contaminated with gasoline gave an average yield of 70.26 g d.m. per pot for aerial parts and 7.52 g d.m. per pot for roots, irrespective of the sorbents used (Table 1). The ratio of Ya biomass to Yr biomass was 9.43, and the greenness index (SPAD) was 43.87. On the other hand, the soil contaminated with gasoline yielded Ya at 24.45 g d.m. per pot and Yr at 1.80 g d.m. per pot. The ratio of Ya biomass to Yr biomass was 13.33, and the SPAD index was 45.73. A slight stimulating potential of the sorbents against *Zea mays* was found in the uncontaminated soil. The exception was perlite, which reduced the amount of Ya biomass by 12%.

Table 1. *Zea mays* biomass, SPAD (6th leaf phase).

Objects	Aboveground Parts (Ya)	Roots (Yr)	Ya/Yr	Greenness Index (SPAD)
	Grams of Dry Matter per Pot			
Us	74.145 ^{a}	7.018 ^{a}	10.565	44.322 ^{ab}
V	70.961 ^{ab}	8.850 ^{a}	8.018	43.984 ^{ab}
D	72.325 ^{ab}	7.612 ^{a}	9.502	44.856 ^{ab}
P	65.447 ^{b}	7.429 ^{a}	8.810	42.322 ^{b}
A	68.428 ^{ab}	6.685 ^{a}	10.237	43.878 ^{ab}
G	12.679 ^{e}	1.114 ^{b}	11.384	45.372 ^{ab}
V_G	26.448 ^{cd}	1.749 ^{b}	15.119	45.256 ^{ab}
D_G	30.099 ^{c}	2.025 ^{b}	14.862	45.753 ^{ab}
P_G	20.080 ^{d}	1.874 ^{b}	10.713	44.278 ^{ab}
A_G	32.946 ^{c}	2.258 ^{b}	14.589	48.013 ^{a}

Explanations of the abbreviations of the sorbents tested (objects) are given in the abbreviations section. Homogeneous groups denoted with letters (a–e) were calculated separately for each part of the plant and greenness index.

On the other hand, in a series of experiments where the soil was contaminated with gasoline, all the sorbents (vermiculite, dolomite, perlite, and agrobasalt) had a positive effect and significantly reduced the toxic effects of this contaminant on *Zea mays*. For example, the use of agrobasalt in gasoline-contaminated soil increased the amount of Ya biomass by 2.6 times, dolomite by 2.4 times, vermiculite by 2.1 times, and perlite by 1.6 times. The application of sorbents to uncontaminated soil had no significant effect on root biomass, whereas it increased the size of *Zea mays* biomass in gasoline-contaminated soil. Thus, the sorbents used in the study were very effective in reducing the negative effects of gasoline on the growth and development of the plant under study. The above-mentioned relationships were also reflected in the yield ratio of aboveground parts to plant roots, which, in the gasoline-contaminated series, was highest in the sites supplemented with vermiculite, dolomite, agrobasalt, and perlite, respectively. The above statements are confirmed by the results shown in Figure 5. The positive indices of the effect of sorbents on the yield of *Zea mays* grown on gasoline-contaminated soil clearly demonstrate that they can be used to mitigate the effects of this contaminant on this plant. Their values for Ya biomass ranged from 0.584 (perlite) to 1.599 (agrobasalt), and for Yr biomass from 0.571 (vermiculite) to 1.028 (agrobasalt).

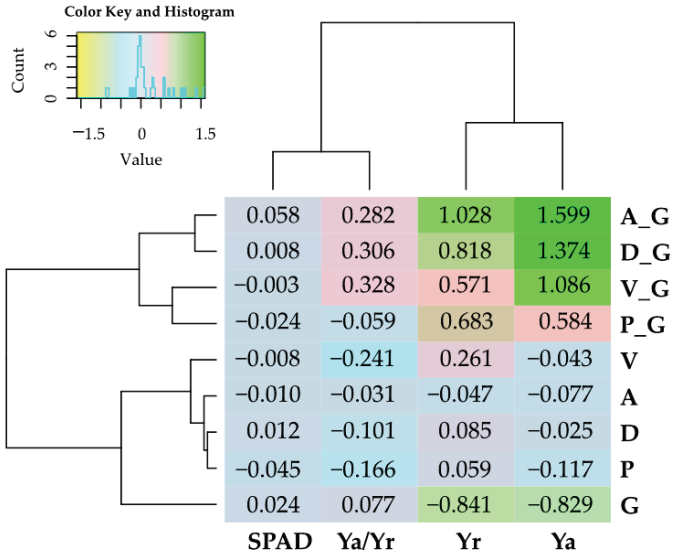

Figure 5. Indexes of the influence of gasoline (G) and sorbents on the yield of aboveground parts (Ya), roots (Yr), the ratio of yield of aboveground parts to plant roots (Ya/Yr) and the greenness index (SPAD). Explanations of the abbreviations of the sorbents tested (objects) are given in the abbreviations section.

3.2. Contents of Ash, Nitrogen, Carbon, Hydrogen, Sulfur and Oxygen in Aboveground Parts of Zea mays

Both gasoline soil contamination and sorbent application had an effect on the ash content and non-ash elements in the aboveground biomass of *Zea mays* (Table 2). Soil contamination with gasoline caused a significant increase in sulfur, nitrogen, and ash and a decrease in carbon and oxygen. For maize grown on uncontaminated soil, soil supplementation with dolomite and agrobasalt resulted in a significant increase in ash content, dolomite and perlite in nitrogen content, and perlite and agrobasalt in oxygen content. Dolomite and perlite contributed to a significant reduction in hydrogen content, while these sorbents had no statistically significant effect on sulfur content. The effect of sorbents on the content of ash and non-ash elements in maize biomass extracted from gasoline-contaminated soil was slightly different. Namely, vermiculite caused an increase in ash content, dolomite, perlite, and agrobasalt—nitrogen, perlite—sulfur and all sorbents—oxygen. In turn, all sorbents contributed to a decrease in carbon content: vermiculite, dolomite and perlite—hydrogen, dolomite and perlite—ash, and dolomite—sulfur.

Table 2. Ash content and elements determining the energy value of aboveground biomass of *Zea mays* (%).

Objects *	Ash	Nitrogen (N)	Carbon (C)	Hydrogen (H)	Sulfur (S)	Oxygen (O)
Us	4.971 ^{f}	2.044 ^{g}	51.124 ^{ab}	5.730 ^{ab}	0.092 ^{de}	36.039 ^{b}
V	4.970 ^{f}	1.940 ^{h}	51.319 ^{a}	5.788 ^{a}	0.082 ^{e}	35.901 ^{b}
D	5.710 ^{d}	2.683 ^{e}	50.865 ^{b}	5.538 ^{cd}	0.098 ^{d}	35.105 ^{c}
P	5.097 ^{f}	2.347 ^{f}	49.163 ^{c}	5.488 ^{d}	0.101 ^{d}	37.804 ^{a}
A	5.328 ^{e}	2.035 ^{g}	49.212 ^{c}	5.739 ^{a}	0.083 ^{e}	37.604 ^{a}
G	9.636 ^{b}	4.158 ^{c}	49.244 ^{c}	5.746 ^{a}	0.215 ^{b}	31.000 ^{g}
V_G	10.594 ^{a}	3.962 ^{d}	47.998 ^{d}	5.584 ^{bcd}	0.206 ^{bc}	31.657 ^{f}
D_G	9.150 ^{c}	4.615 ^{a}	47.434 ^{e}	5.459 ^{d}	0.195 ^{c}	33.146 ^{e}
P_G	9.130 ^{c}	4.316 ^{b}	47.162 ^{ef}	5.503 ^{d}	0.247 ^{a}	33.642 ^{d}
A_G	9.547 ^{b}	4.294 ^{b}	47.030 ^{f}	5.676 ^{abc}	0.212 ^{b}	33.240 ^{de}

* Explanations of the abbreviations of the sorbents tested (objects) are given in the abbreviations section. Homogeneous groups indicated by letters (a–h) were calculated separately for each parameter tested.

The described changes in the chemical composition of maize biomass extracted from soil supplemented and unsupplemented with sorbents and contaminated and uncontaminated with gasoline are well represented by the indexes of influence of gasoline (G) and sorbents on the content of ash and elements determining the energy value of the aboveground biomass of *Zea mays* presented in Figure 6. These indices show that the chemical composition of the biomass was more strongly influenced by gasoline than by sorbents. In the case of petroleum substances, the influence index for ash was 0.939, N—1.035, and S—1.322, while for C and O it was negative, respectively: −0.037 and −0.140. These indexes were significantly higher than the sorbent influence indices. The exception was the sorbent influence indices for C. Their values were low and almost always negative.

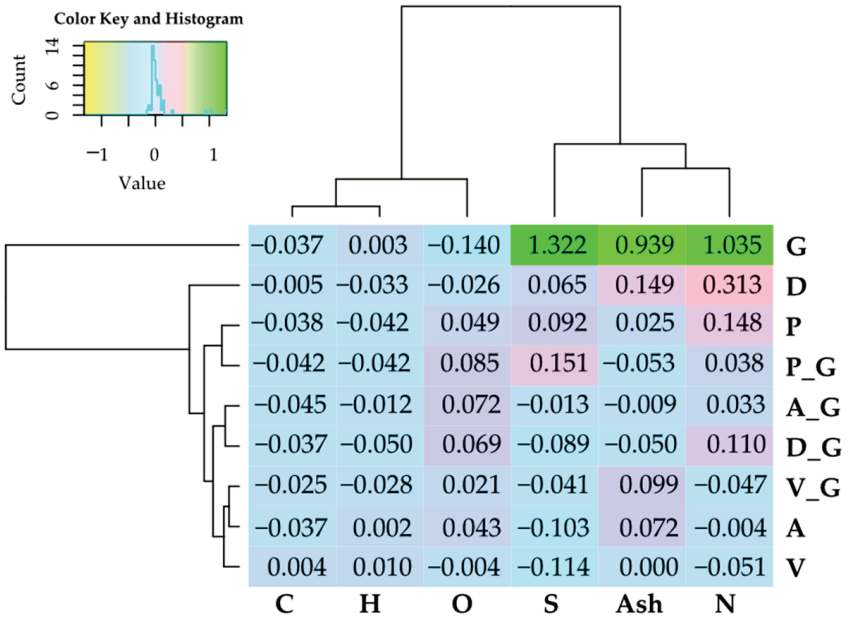

Figure 6. Indexes of the influence of gasoline (G) and sorbents on the content of ash and elements determining the energy value of aboveground biomass of *Zea mays*. Explanations of the abbreviations of the sorbents tested (objects) are given in the abbreviations section.

3.3. Energy Value of Aboveground Parts of Zea mays

All sorbents contributed to increasing the calorific value (Hv) and heat of combustion (Q) of the biomass of aboveground parts of maize grown on soil not contaminated with gasoline (Table 3). The highest Hv value was found under perlite (15.578 MJ kg^{-1}) and dolomite (15.563 MJ kg^{-1}). The heat of combustion was also highest in plant biomass extracted from soil supplemented with the mentioned sorbents. Perlite increased Q from 18.710 MJ to 19.268 MJ, while dolomite increased Q from 18.710 MJ to 19.250 MJ. The Hv and Q values of maize grown on gasoline-contaminated soil were increased only by the effect of dolomite, whereas they were decreased by the effect of vermiculite. In this series of experiments, both perlite and agrobasalt did not change the Hv and Q values. Since gasoline greatly reduced the growth and development of *Zea mays*, the amount of energy extracted (Yep) from maize on contaminated soil was reduced by 0.927 MJ per pot. This was a 5.8-fold reduction. The introduction of sorbents into gasoline-contaminated soil significantly increased Yep yields, with agrobasalt and dolomite increasing Yep production the most. The impact index for the former sorbent was 1.603, and the latter 1.388 (Figure 7). Such a spectacular effect of sorbents was not observed for maize biomass produced on uncontaminated soil.

Table 3. Heat of combustion (Q), calorific value (Hv), and amount of energy obtained (Yep) from *Zea mays* biomass.

Objects *	Heat of Combustion (Q)	Heating Value (Hv)	Energy yield of Plant Biomass (Yep), MJ pot^{-1}
	MJ kg^{-1} Air-Dry Matter Plants		
Us	18.710 ^{f}	15.115 ^{f}	1.121 ^{b}
V	18.769 ^{e}	15.163 ^{e}	1.076 ^{c}
D	19.250 ^{a}	15.563 ^{a}	1.126 ^{a}
P	19.268 ^{a}	15.578 ^{a}	1.020 ^{e}
A	19.080 ^{b}	15.422 ^{b}	1.055 ^{d}
G	18.982 ^{c}	15.340 ^{c}	0.194 ^{j}
V_G	18.820 ^{d}	15.206 ^{d}	0.402 ^{h}
D_G	19.093 ^{b}	15.432 ^{b}	0.465 ^{g}
P_G	18.979 ^{c}	15.337 ^{c}	0.308 ^{i}
A_G	19.015 ^{c}	15.368 ^{c}	0.506 ^{f}

* Explanations of the abbreviations of the sorbents tested (objects) are given in the abbreviations section. Homogeneous groups denoted with letters (a–j) were calculated separately for Q, Hv, and Yep.

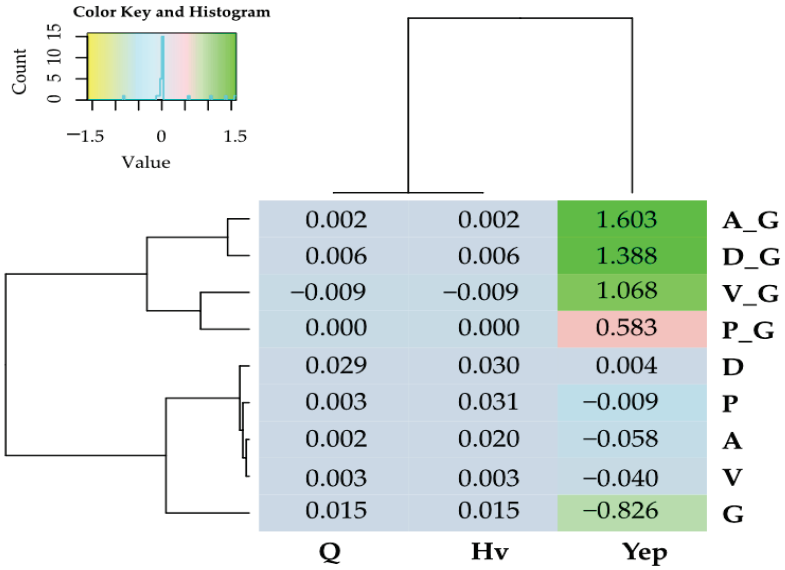

Figure 7. Indexes of the influence of gasoline (G) and sorbents on the heat of combustion (Q), calorific value (Hv), and amount of energy produced (Yep) from *Zea mays* biomass. Explanations of the abbreviations of the sorbents tested (objects) are given in the abbreviations section.

3.4. Interactions Between Zea mays Yield and Its Energy Value

Gasoline (G) had a significantly greater effect on the dependent variable than the sorbents used (Figure 8). This petroleum-based substance influenced up to 96% of the yield of the underground parts of the plants, 93% of the carbon content of the plant biomass, and the ash content. It affected the energy yield of the biomass (Yep) by 72%, the calorific value of the biomass (Hv) by 68%, the yield of the aboveground parts of the plant (Ya) by 65%, the sulfur content (S) by 58%, and the oxygen content (O) by 55%. Sorbents, on the other hand, reduced the hydrogen content (H) by 85%, the heat of combustion (Q) by 74%, and the nitrogen content of *Zea mays* biomass by 52%. Only the leaf greenness index was more dependent on the combined use of sorbents and gasoline (S × G).

Calculated Pearson's simple correlation coefficients (Figure 9) and principal component analysis (PCA) (Figure 10) allowed us to determine the strength of the interaction between the parameters studied. Thus, the amount of energy produced (Yep) was significantly positively correlated with *Zea mays* biomass, C and O content, and significantly negatively with N, S, and ash content. The heat of combustion (Q) and the calorific value (Hv) of plant biomass were negatively correlated with the H content, while they did not

form significant correlations with the other parameters studied. There was a significant positive correlation between N content and ash and S content and C, O, and H content, and a negative correlation between C and O and ash, S, and N content.

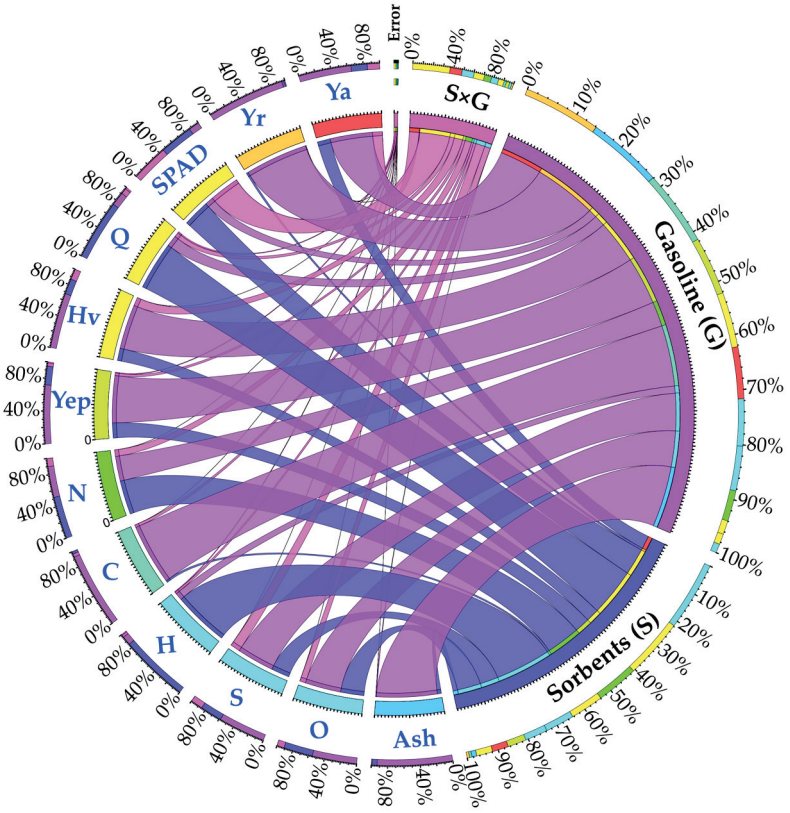

Figure 8. Share of independent variables (η^2) in determining dependent variables in *Zea mays* biomass, %. Explanations of the abbreviations of the sorbents tested (objects) are given in the abbreviations section.

Variable	Ya	Yr	Ya/Yr	SPAD	Q	Hv	Yep	N	C	H	S	O	Ash
Ya	1.000												
Yr	0.861	1.000											
Ya/Yr	0.011	−0.355	1.000										
SPAD	−0.327	−0.387	−0.006	1.000									
Q	0.064	0.055	0.047	−0.064	1.000								
Hv	0.064	0.055	0.047	−0.064	1.000	1.000							
Yep	0.994	0.862	0.021	−0.336	0.091	0.091	1.000						
N	−0.930	−0.843	−0.037	0.430	0.076	0.076	−0.932	1.000					
C	0.768	0.725	−0.105	−0.282	−0.206	−0.206	0.764	−0.829	1.000				
H	0.210	0.234	0.103	−0.072	−0.545	−0.545	0.198	−0.385	0.446	1.000			
S	−0.963	−0.854	−0.047	0.381	−0.061	−0.061	−0.968	0.957	−0.820	−0.303	1.000		
O	0.867	0.763	0.087	−0.446	0.240	0.240	0.877	−0.848	0.482	0.057	−0.842	1.000	
Ash	−0.946	−0.858	−0.001	0.432	−0.098	−0.098	−0.952	0.947	−0.789	−0.234	0.949	−0.913	1.000

Figure 9. Pearson's simple correlation coefficients. Significant at $p = 0.05$, n = 24. Red color—statistically significant, black color—statistically insignificant. Explanations of the abbreviations of the sorbents tested (objects) are given in the abbreviations section.

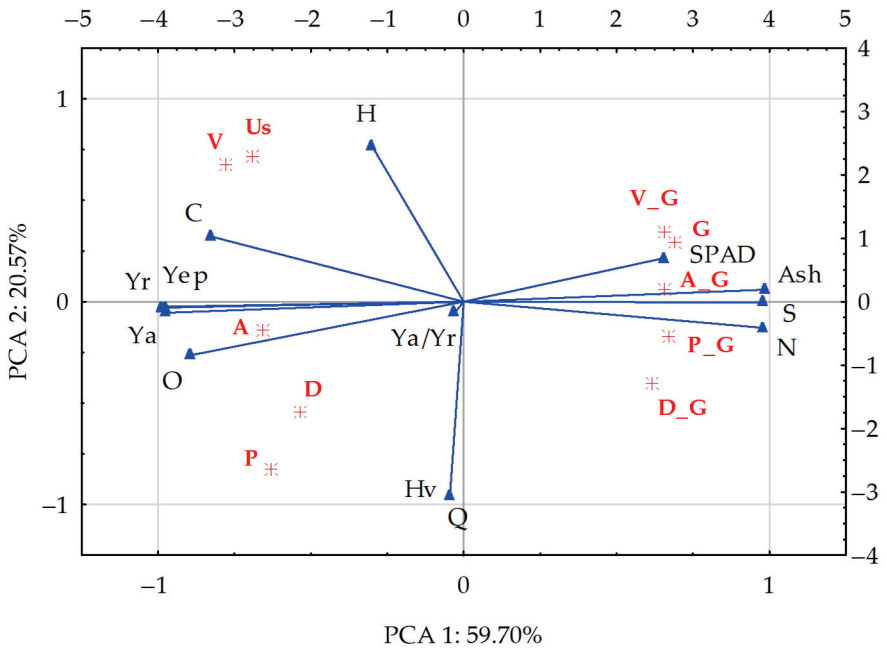

Variable	PCA 1	PCA 2
Ya	−0.972	−0.029
Yr	−0.984	−0.025
Ya/Yr	−0.029	−0.053
SPAD	0.660	0.216
Q	−0.045	−0.957
Hv	−0.045	−0.957
Yep	−0.972	−0.055
N	0.981	−0.129
C	−0.826	0.321
H	−0.301	0.771
S	0.981	−0.004
O	−0.891	−0.263
Ash	0.985	0.059

Figure 10. The interaction between the studied parameters using (PCA). Explanations of the abbreviations of the sorbents tested (objects) are given in the abbreviations section.

4. Discussion

Petroleum-derived products are toxic to all soil organisms [71,72] and plants [54,73–75]. Therefore, rapid and effective detoxification of these soils is important [37,76,77]. Our research shows that *Zea mays* is highly susceptible to the destructive effects of gasoline. Under the influence of this pollutant, plant biomass decreased by 83%. The negative effect of gasoline on maize growth and development was significantly reduced by all the sorbents used in the study, i.e., vermiculite, agrobasalt, perlite, and dolomite. This is probably due to the adsorption of gasoline by these sorbents, which limited the direct contact of gasoline with the plant roots. According to the literature [52,70,78–81], their effectiveness in revitalizing soils depends on the type of sorbent. In our study, despite the positive effectiveness of all sorbents, agrobasalt and dolomite were the most effective. The effect coefficients of these sorbents on *Zea mays* biomass were very high, being 1.599 for the first sorbent and 1.374 for the second, respectively. The effectiveness of agrobasalt and dolomite may be due to their ability to neutralize contaminants and improve soil properties by providing both calcium and magnesium, which may benefit plant growth and pH regulation [82]. According to Huang et al. [83], the particle size of the sorbent is also one of the main factors affecting its effectiveness in neutralizing soil acidity, as the reaction rate between calcium material and H^+ in the soil depends on the specific surface area. Cai et al. [84] also observed that dolomite accelerates the mineralization of nitrogenous organic compounds, thereby improving the respiration of acidic soils. On the other hand, Wu et al. [82] observed that smaller dolomite particles have a larger specific surface area, which may increase their ability to adsorb pollutants and improve soil structure; larger agrobasalt particles have a greater ability to adsorb pollutants [85,86]. These factors clearly influence interactions with the soil microbiome by promoting the growth of microorganisms that stimulate *Zea mays* growth. This is due to the different sorption capacity and chemical composition of these sorbents [87–93].

The negative effect of gasoline on *Zea mays* was not only limited to biomass production but also caused changes in its chemical composition. Under its influence, the content of N, S, and ash in the biomass increased, and the content of C and O decreased. The increase in the content of N, S, and ash was much greater than the decrease in the content of C and O. The index of the effect of gasoline on the content of S, N, and ash was 1.322, 1.035, and

0.939, respectively. Changes in the chemical composition of the biomass of gasoline-treated plants may result from the direct toxic effect of this substance on the plant, disturbances in the uptake of ions by the plants, and dysfunctions in the ion balance [94,95]. The above considerations are only appropriate for this research. However, it should be taken into account that in environmental research other issues come into play that are extremely important for the existence of ecosystems and consequently for human and animal health. These include the contamination of groundwater with benzene, toluene, ethylbenzene, and xylene (BTEX), which stresses all organisms that use the resource [96,97]. The significant amounts of carbon, hydrogen, and oxygen, as well as nitrogen and sulfur, in *Zea mays* biomass are also important for energy production. Through combustion, fermentation, or gasification, these components can be converted into heat, electricity, or biofuels such as bioethanol [98,99].

In our study, despite the variable effects of gasoline on the chemical composition of the plant, we found a positive effect of this substance on the heat of combustion and the calorific value of the biomass. Of course, this did not bridge the differences between the energy production of maize grown on uncontaminated and contaminated soil, due to the negative effect of this pollutant on the yield of corn, and thus on the amount of biomass and energy obtained [100,101].

Energy production (Yep) was positively affected by all sorbents. It was increased most by agrobasalt (influence factor of 1.603) and least by perlite (influence factor of 0.583). Thus, they can play an important role in the cultivation of plants on soils degraded with organic compounds for energy purposes. Also, Zahed et al. [102]; Vasilyeva et al. [50]; Wyszkowski and Kordala [103]; Sabitov et al. [104]; Wyszkowski et al. [105]; and Wyszkowska et al. [106] demonstrated the usefulness of sorbents (biocarbon, zeolite, kaolinite, vermiculite, diatomite, bentonite, activated carbon, molecular sieve, halloysite, sepiolite, expanded clay, biochar, and alginite) in the phytostabilization of soil contaminated with petroleum-derived products. According to Zhang and Liang [107], Qu et al. [108], and Vocciante et al. [109], the amount of energy extracted from *Zea mays* biomass depends on the soil properties, so sorbents introduced into the soil may help to modify the soil structure, increasing its capacity to retain water and nutrients, thus influencing higher biomass production. According to Ho et al. [110]; Atero-Calvo et al. [111]; Wyszkowski and Kordala [112]; and Kamenchuk et al. [113], sorbents can influence the availability of elements that are key to the intensity of the photosynthetic process, thereby increasing biomass and energy while offsetting the stress caused by soil contamination [114].

Both our results and those of other authors [100,115,116] indicate the significant potential of *Zea mays* to replace fossil fuels. Maize grown on contaminated soils has a high energy potential as an alternative energy source. A study by Morales-Máximo et al. [115] also demonstrates that *Zea mays* biomass has a high energy potential as an alternative energy source. The average calorific value determined by these authors in samples of plant material was 17.6 MJ kg^{-1}, and in our study, it ranged from 18.7 MJ kg^{-1} to 19.3 MJ kg^{-1}, which is at a comparable level compared to other biofuels [117–119]. Replacing fossil fuels with *Zea mays* biomass has numerous environmental benefits. Biomass combustion is carbon dioxide-neutral, as the CO_2 released during combustion is offset by the CO_2 absorbed by the plant during photosynthesis [4,98,99]. Additionally, biomass production can help reduce emissions of other harmful gases, such as nitrogen and sulfur oxides, which are typical of fossil fuel combustion [115,118,120].

Despite its many benefits, biomass production from *Zea mays* also poses several challenges. One of the main problems is competition for land and water resources with food production [121,122]. Therefore, it is important to develop technologies and practices that minimize these conflicts, for example by using marginal soils that are not suitable for food production. Further research into the genetic improvement of maize may in the future lead to varieties with higher energy yields and better resistance to environmental stresses [123]. Summarizing the results of our study, it can be concluded that *Zea mays* biomass has great potential as a sustainable energy source that can contribute to reducing

fossil fuel consumption. However, it is crucial that biomass production be carried out in a sustainable manner, taking into account both environmental and social aspects.

5. Conclusions

Gasoline creates unfavorable conditions for the growth and development of *Zea mays*. Growing maize on non-remediated soil limits its use for energy purposes. On the other hand, the application of agrobasalt, dolomite, vermiculite, and perlite to contaminated soil enhances both biomass production and the amount of energy obtained from it. The amount of energy obtained from *Zea mays* was significantly positively correlated with carbon and oxygen content and negatively correlated with nitrogen, sulfur, and ash content. Our research shows that all the sorbents tested represent a promising strategy for managing sites contaminated with petroleum-derived products.

Author Contributions: Conceptualization, J.W., A.B., M.Z. and J.K.; methodology, J.W., A.B., M.Z. and J.K.; formal analysis, J.W., A.B., M.Z. and J.K.; investigation, J.W., A.B., M.Z. and J.K.; writing—original draft preparation, J.W., A.B. and M.Z.; writing—review and editing, J.W., A.B., M.Z. and J.K.; visualization, J.W., A.B., M.Z. and J.K.; supervision, J.K. All authors have read and agreed to the published version of the manuscript.

Funding: This research was funded by the University of Warmia and Mazury in Olsztyn, Faculty of Agriculture and Forestry, Department of Soil Science and Microbiology (grant No. 30.610.006-110) and project financially supported by the Minister of Education and Science in the range of the program entitled Funded by the Minister of Science under the Regional Initiative of Excellence Program.

Data Availability Statement: The data presented in this study are available on request from the corresponding author.

Conflicts of Interest: The authors declare no conflicts of interest.

Abbreviations

Us—uncontaminated soil, V—uncontaminated soil with the addition of vermiculite, D—uncontaminated soil with the addition of dolomite, P—uncontaminated soil with the addition of perlite, A—uncontaminated soil with the addition of agrobasalt, G—soil contaminated with gasoline, V_G—soil contaminated with gasoline with the addition of vermiculite, D_G—soil contaminated with gasoline with the addition of dolomite, P_G—soil contaminated with gasoline with the addition of perlite, A_G—soil contaminated with gasoline with the addition of agrobasalt. Ya—yield of aerial parts, Yr—yield of roots, Ya/Yr—the ratio of aboveground parts yield to plant roots, SPAD—greenness index, Q—heat of combustion, Hv—calorific value, Yep—energy yield, C —carbon, H—hydrogen, S—sulfur, N—nitrogen, O—oxygen.

References

1. Jåstad, E.O.; Bolkesjø, T.F.; Trømborg, E.; Rørstad, P.K. The Role of Woody Biomass for Reduction of Fossil GHG Emissions in the Future North European Energy Sector. *Appl. Energy* **2020**, *274*, 115360. [CrossRef]
2. Saez de Bikuña, K.; Garcia, R.; Dias, A.C.; Freire, F. Global Warming Implications from Increased Forest Biomass Utilization for Bioenergy in a Supply-Constrained Context. *J. Environ. Manag.* **2020**, *263*, 110292. [CrossRef] [PubMed]
3. Günal, A.Ç.; Tunca, S.K.; Arslan, P.; Gül, G.; Dinçel, A.S. How Does Sublethal Permethrin Effect Non-Target Aquatic Organisms? *Environ. Sci. Pollut. Res.* **2021**, *28*, 52405–52417. [CrossRef] [PubMed]
4. Ahmed, S.F.; Rafa, N.; Mofijur, M.; Badruddin, I.A.; Inayat, A.; Ali, M.S.; Farrok, O.; Yunus Khan, T.M. Biohydrogen Production from Biomass Sources: Metabolic Pathways and Economic Analysis. *Front. Energy Res.* **2021**, *9*, 753878. [CrossRef]
5. Anwar, M.N.; Fayyaz, A.; Sohail, N.F.; Khokhar, M.F.; Baqar, M.; Yasar, A.; Rasool, K.; Nazir, A.; Raja, M.U.F.; Rehan, M.; et al. CO_2 Utilization: Turning Greenhouse Gas into Fuels and Valuable Products. *J. Environ. Manag.* **2020**, *260*, 110059. [CrossRef] [PubMed]
6. Sahoo, G.; Sharma, A.; Chandra Dash, A. Biomass from Trees for Bioenergy and Biofuels—A Briefing Paper. *Mater. Today Proc.* **2022**, *65*, 461–467. [CrossRef]
7. Antar, M.; Lyu, D.; Nazari, M.; Shah, A.; Zhou, X.; Smith, D.L. Biomass for a Sustainable Bioeconomy: An Overview of World Biomass Production and Utilization. *Renew. Sustain. Energy Rev.* **2021**, *139*, 110691. [CrossRef]

8. Gyamfi, B.A.; Ozturk, I.; Bein, M.A.; Bekun, F.V. An Investigation into the Anthropogenic Effect of Biomass Energy Utilization and Economic Sustainability on Environmental Degradation in E7 Economies. *Biofuels Bioprod. Biorefining* **2021**, *15*, 840–851. [CrossRef]
9. Cadillo-Benalcazar, J.J.; Bukkens, S.G.F.; Ripa, M.; Giampietro, M. Why Does the European Union Produce Biofuels? Examining Consistency and Plausibility in Prevailing Narratives with Quantitative Storytelling. *Energy Res. Soc. Sci.* **2021**, *71*, 101810. [CrossRef]
10. Yang, L.; Wang, X.-C.; Dai, M.; Chen, B.; Qiao, Y.; Deng, H.; Zhang, D.; Zhang, Y.; Villas Bôas de Almeida, C.M.; Chiu, A.S.F.; et al. Shifting from Fossil-Based Economy to Bio-Based Economy: Status Quo, Challenges, and Prospects. *Energy* **2021**, *228*, 120533. [CrossRef]
11. Vijay, V.; Chandra, R.; Subbarao, P.M.V. Biomass as a Means of Achieving Rural Energy Self-Sufficiency: A Concept. *Built Environ. Proj. Asset Manag.* **2022**, *12*, 382–400. [CrossRef]
12. Noorollahi, Y.; Janalizadeh, H.; Yousefi, H.; Jahangir, M.H. Biofuel for Energy Self-Sufficiency in Agricultural Sector of Iran. *Sustain. Energy Technol. Assess.* **2021**, *44*, 101069. [CrossRef]
13. Huang, Y.-F.; Lo, S.-L. Predicting Heating Value of Lignocellulosic Biomass Based on Elemental Analysis. *Energy* **2020**, *191*, 116501. [CrossRef]
14. Mao, G.; Huang, N.; Chen, L.; Wang, H. Research on Biomass Energy and Environment from the Past to the Future: A Bibliometric Analysis. *Sci. Total Environ.* **2018**, *635*, 1081–1090. [CrossRef] [PubMed]
15. de Paulo, E.H.; dos Santos, F.D.; Folli, G.S.; Santos, L.P.; Nascimento, M.H.C.; Moro, M.K.; da Cunha, P.H.P.; Castro, E.V.R.; Cunha Neto, A.; Filgueiras, P.R. Determination of Gross Calorific Value in Crude Oil by Variable Selection Methods Applied to 13C NMR Spectroscopy. *Fuel* **2022**, *311*, 122527. [CrossRef]
16. Amaral, L.V.; Santos, N.D.S.A.; Roso, V.R.; de Oliveira Sebastião, R.d.C.; Pujatti, F.J.P. Effects of Gasoline Composition on Engine Performance, Exhaust Gases and Operational Costs. *Renew. Sustain. Energy Rev.* **2021**, *135*, 110196. [CrossRef]
17. Zaharin, M.S.M.; Abdullah, N.R.; Masjuki, H.H.; Ali, O.M.; Najafi, G.; Yusaf, T. Evaluation on Physicochemical Properties of Iso-Butanol Additives in Ethanol-Gasoline Blend on Performance and Emission Characteristics of a Spark-Ignition Engine. *Appl. Therm. Eng.* **2018**, *144*, 960–971. [CrossRef]
18. Stöcker, M. Biofuels and Biomass-To-Liquid Fuels in the Biorefinery: Catalytic Conversion of Lignocellulosic Biomass Using Porous Materials. *Angew. Chem. Int. Ed.* **2008**, *47*, 9200–9211. [CrossRef]
19. Zahed, M.A.; Movahed, E.; Khodayari, A.; Zanganeh, S.; Badamaki, M. Biotechnology for Carbon Capture and Fixation: Critical Review and Future Directions. *J. Environ. Manag.* **2021**, *293*, 112830. [CrossRef]
20. Lee, J.-Y.; Lee, S.-E.; Lee, D.-W. Current Status and Future Prospects of Biological Routes to Bio-Based Products Using Raw Materials, Wastes, and Residues as Renewable Resources. *Crit. Rev. Environ. Sci. Technol.* **2022**, *52*, 2453–2509. [CrossRef]
21. Directive (EU) 2018/2001 of the European Parliament and of the Council of 11 December 2018 on the Promotion of the Use of Energy from Renewable Sources (Recast). 2018. Available online: https://eur-lex.europa.eu/legal-content/EN/TXT/PDF/?uri=CELEX:32018L2001 (accessed on 25 September 2024).
22. The Paris Agreement | UNFCCC. Available online: https://unfccc.int/sites/default/files/english_paris_agreement.pdf (accessed on 25 September 2024).
23. National Energy and Climate Plan for the Years 2021–2030—Ministerstwo Klimatu i Środowiska—Portal Gov.Pl. Available online: https://www.gov.pl/web/klimat/national-energy-and-climate-plan-for-the-years-2021-2030 (accessed on 25 September 2024).
24. Energy Policy of Poland Until 2040—Portal Gov.Pl. Available online: https://www.gov.pl/web/klimat/polityka-energetyczna-polski (accessed on 25 September 2024).
25. Malacara-Becerra, A.; Melchor-Martínez, E.M.; Sosa-Hernández, J.E.; Riquelme-Jiménez, L.M.; Mansouri, S.S.; Iqbal, H.M.N.; Parra-Saldívar, R. Bioconversion of Corn Crop Residues: Lactic Acid Production through Simultaneous Saccharification and Fermentation. *Sustainability* **2022**, *14*, 11799. [CrossRef]
26. Mosier, N.; Wyman, C.; Dale, B.; Elander, R.; Lee, Y.Y.; Holtzapple, M.; Ladisch, M. Features of Promising Technologies for Pretreatment of Lignocellulosic Biomass. *Bioresour. Technol.* **2005**, *96*, 673–686. [CrossRef] [PubMed]
27. Ashokkumar, V.; Venkatkarthick, R.; Jayashree, S.; Chuetor, S.; Dharmaraj, S.; Kumar, G.; Chen, W.-H.; Ngamcharussrivichai, C. Recent Advances in Lignocellulosic Biomass for Biofuels and Value-Added Bioproducts—A Critical Review. *Bioresour. Technol.* **2022**, *344*, 126195. [CrossRef] [PubMed]
28. Bielik, P.; Belinska, S.; Bajusová, Z.; Adamičková, I.; Bullová, T.; Belinska, Y.; Husárová, P. Economic Impact of Using Biomass for Biogas Production in the Context of Sustainable Development. *WSEAS Trans. Bus. Econ.* **2024**, *21*, 1684–1697. [CrossRef]
29. Bórawski, P.; Bełdycka-Bórawska, A.; Kapsdorferová, Z.; Rokicki, T.; Parzonko, A.; Holden, L. Perspectives of Electricity Production from Biogas in the European Union. *Energies* **2024**, *17*, 1169. [CrossRef]
30. Czekała, W.; Pulka, J.; Jasiński, T.; Szewczyk, P.; Bojarski, W.; Jasiński, J. Waste as Substrates for Agricultural Biogas Plants: A Case Study from Poland. *J. Water Land Dev.* **2023**, *56*, 45–50. [CrossRef]
31. Kumar, A.; Ramamoorthy, D.; Kumar, N.; Verma, R.; Kumar, A.; Verma, D.K.; Jayabalan, I.; Marwein, B.M.; Jaiswal, K.K. Investigation on the Potential of Eco-Friendly Bio-Char for Amendment in Serpentine Soils and Immobilization of Heavy Metals Contaminants: A Review. *Biomass Convers. Biorefinery* **2023**, *13*, 16585–16605. [CrossRef]

32. Ekka, P.; Patra, S.; Upreti, M.; Kumar, G.; Kumar, A.; Saikia, P. Land Degradation and Its Impacts on Biodiversity and Ecosystem Services. In *Land and Environmental Management Through Forestry*; John Wiley & Sons, Ltd.: Hoboken, NJ, USA, 2023; pp. 77–101, ISBN 978-1-119-91052-7.
33. Gonçalves, J.; Freitas, J.; Fernandes, I.; Silva, P. Microalgae as Biofertilizers: A Sustainable Way to Improve Soil Fertility and Plant Growth. *Sustainability* **2023**, *15*, 12413. [CrossRef]
34. Wyszkowska, J.; Kucharski, J.; Kucharski, M.; Borowik, A. Applicability of Biochemical Indices to Quality Assessment of Soil Polluted with Heavy Metals. *J. Elem.* **2014**, *18*, 733–756. [CrossRef]
35. Wyszkowska, J.; Boros-Lajszner, E.; Kucharski, J. The Impact of Soil Contamination with Lead on the Biomass of Maize Intended for Energy Purposes, and the Biochemical and Physicochemical Properties of the Soil. *Energies* **2024**, *17*, 1156. [CrossRef]
36. Baćmaga, M.; Wyszkowska, J.; Borowik, A.; Kucharski, J. Effect of Sulcotrione and Terbuthylazine on Biological Characteristics of Soil. *Appl. Soil Ecol.* **2024**, *195*, 105232. [CrossRef]
37. Gertsen, M.M.; Arlyapov, V.A.; Perelomov, L.V.; Kharkova, A.S.; Golysheva, A.N.; Atroshchenko, Y.M.; Cardinale, A.M.; Reverberi, A.P. Environmental Implications of Energy Sources: A Review on Technologies for Cleaning Oil-Contaminated Ecosystems. *Energies* **2024**, *17*, 3561. [CrossRef]
38. Ambaye, T.G.; Chebbi, A.; Formicola, F.; Prasad, S.; Gomez, F.H.; Franzetti, A.; Vaccari, M. Remediation of Soil Polluted with Petroleum Hydrocarbons and Its Reuse for Agriculture: Recent Progress, Challenges, and Perspectives. *Chemosphere* **2022**, *293*, 133572. [CrossRef] [PubMed]
39. Kapoor, R.T.; Zdarta, J. Fabrication of Engineered Biochar for Remediation of Toxic Contaminants in Soil Matrices and Soil Valorization. *Chemosphere* **2024**, *358*, 142101. [CrossRef] [PubMed]
40. Yu, M.; Tariq, S.M.; Yang, H. Engineering Clay Minerals to Manage the Functions of Soils. *Clay Miner.* **2022**, *57*, 51–69. [CrossRef]
41. Garbowski, T.; Bar-Michalczyk, D.; Charazińska, S.; Grabowska-Polanowska, B.; Kowalczyk, A.; Lochyński, P. An Overview of Natural Soil Amendments in Agriculture. *Soil Tillage Res.* **2023**, *225*, 105462. [CrossRef]
42. Mota, J.; Merlo, E.; Martínez-Hernández, F.; Mendoza-Fernández, A.J.; Pérez-García, F.J.; Salmerón-Sánchez, E. Plants on Rich-Magnesium Dolomite Barrens: A Global Phenomenon. *Biology* **2021**, *10*, 38. [CrossRef]
43. Bolan, N.; Sarmah, A.K.; Bordoloi, S.; Bolan, S.; Padhye, L.P.; Van Zwieten, L.; Sooriyakumar, P.; Khan, B.A.; Ahmad, M.; Solaiman, Z.M.; et al. Soil Acidification and the Liming Potential of Biochar. *Environ. Pollut.* **2023**, *317*, 120632. [CrossRef]
44. Abdul-Sahib, A.M.; Golbashy, M.; Abbass, J. Effect of Date Palm Wastes, Perlite and Magnesium on Growth and Flowering in Gerbera Plants (*Gerbera jamesonii* L.). *Int. J. Hortic. Sci. Technol.* **2023**, *10*, 375–386. [CrossRef]
45. Wyszkowska, J.; Borowik, A.; Zaborowska, M.; Kucharski, J. The Potential for Restoring the Activity of Oxidoreductases and Hydrolases in Soil Contaminated with Petroleum Products Using Perlite and Dolomite. *Appl. Sci.* **2024**, *14*, 3591. [CrossRef]
46. Cedeño, J.M.; Magán, J.-J.; Thompson, R.B.; Fernández, M.-D.; Gallardo, M. Comparison of Methods to Determine Nutrient Uptake of Tomato Grown in Free-Draining Perlite Substrate—Key Information for Optimal Fertigation Management. *Horticulturae* **2024**, *10*, 232. [CrossRef]
47. Ramos, C.G.; dos Santos de Medeiros, D.; Gomez, L.; Oliveira, L.F.S.; Schneider, I.A.H.; Kautzmann, R.M. Evaluation of Soil Re-Mineralizer from By-Product of Volcanic Rock Mining: Experimental Proof Using Black Oats and Maize Crops. *Nat. Resour. Res.* **2020**, *29*, 1583–1600. [CrossRef]
48. Luchese, A.V.; Leite, I.J.G.d.C.; Giaretta, A.P.d.S.; Alves, M.L.; Pivetta, L.A.; Missio, R.F. Use of Quarry Waste Basalt Rock Powder as a Soil Remineralizer to Grow Soybean and Maize. *Heliyon* **2023**, *9*, e14050. [CrossRef]
49. Bandura, L.; Woszuk, A.; Kołodyńska, D.; Franus, W. Application of Mineral Sorbents for Removal of Petroleum Substances: A Review. *Minerals* **2017**, *7*, 37. [CrossRef]
50. Vasilyeva, G.; Mikhedova, E.; Zinnatshina, L.; Strijakova, E.; Akhmetov, L.; Sushkova, S.; Ortega-Calvo, J.-J. Use of Natural Sorbents for Accelerated Bioremediation of Grey Forest Soil Contaminated with Crude Oil. *Sci. Total Environ.* **2022**, *850*, 157952. [CrossRef] [PubMed]
51. Aspectos Ecológicos Del Uso de Sorbentes Para Mejorar La Eficiencia de Bioremediación de Suelos Contaminados Por Petróleo | Fuentes, El Reventón Energético. Available online: https://revistas.uis.edu.co/index.php/revistafuentes/article/view/12501 (accessed on 27 September 2024).
52. Wyszkowska, J.; Borowik, A.; Zaborowska, M.; Kucharski, J. The Usability of Sorbents in Restoring Enzymatic Activity in Soils Polluted with Petroleum-Derived Products. *Materials* **2023**, *16*, 3738. [CrossRef]
53. Islam, T.; Li, Y.; Cheng, H. Biochars and Engineered Biochars for Water and Soil Remediation: A Review. *Sustainability* **2021**, *13*, 9932. [CrossRef]
54. Mohanta, S.; Pradhan, B.; Behera, I.D. Impact and Remediation of Petroleum Hydrocarbon Pollutants on Agricultural Land: A Review. *Geomicrobiol. J.* **2024**, *41*, 345–359. [CrossRef]
55. IUSS Working Group. World Reference Base for Soil Resources 2014, Update 2015. International Soil Classification System for Naming Soils and Creating Legends for Soil Maps. *World Soil Resour. Rep.* **2015**, *106*, 192.
56. EuroSuper 95—Unleaded Gasoline—ORLEN. Available online: https://www.orlen.pl/pl/dla-biznesu/produkty/paliwa/benzyna/benzyna-bezolowiowa-95 (accessed on 8 July 2024).
57. *PN-EN ISO 18125:2017-07*; Solid Biofuels—Determination of Calorific Value. Polish Standardization Committee: Warsaw, Poland, 2017.

58. Kopetz, H.; Jossart, J.; Ragossnig, H.; Metschina, C. *European Biomass Statistics 2007*; European Biomass Association: Brussels, Belgium, 2007.
59. *PN-EN ISO 16948:2015-07*; Solid Biofuels—Determination of Total Content of Carbon, Hydrogen and Nitrogen. Polish Standardization Committee: Warsaw, Poland, 2015.
60. *PN-G-04584:2001*; Solid Fuels—Determination of Total and Ash Sulfur Content with Automatic Analyzers. Polish Standardization Committee: Warsaw, Poland, 2006.
61. *PN-EN ISO 16994:2016-10*; Solid Biofuels—Determination of Total Content of Sulfur and Chlorine. Polish Standard-Ization Committee: Warsaw, Poland, 2016.
62. *PN-EN ISO 18122:2016-01*; Solid Biofuels—Determination of Ash Content. Polish Standardization Committee: War-Saw, Poland, 2016.
63. Wyszkowska, J.; Borowik, A.; Zaborowska, M.; Kucharski, J. Calorific Value of Zea Mays Biomass Derived from Soil Contaminated with Chromium (VI) Disrupting the Soil's Biochemical Properties. *Energies* **2023**, *16*, 3788. [CrossRef]
64. Wyszkowska, J.; Borowik, A.; Kucharski, J. The Role of Grass Compost and Zea Mays in Alleviating Toxic Effects of Tetracycline on the Soil Bacteria Community. *Int. J. Environ. Res. Public Health* **2022**, *19*, 7357. [CrossRef] [PubMed]
65. Wyszkowska, J.; Borowik, A.; Zaborowska, M.; Kucharski, J. Mitigation of the Adverse Impact of Copper, Nickel, and Zinc on Soil Microorganisms and Enzymes by Mineral Sorbents. *Materials* **2022**, *15*, 5198. [CrossRef] [PubMed]
66. Citing RStudio. Available online: https://www.posit.co/ (accessed on 8 July 2024).
67. R Core Team. *R: A Language and Environment for Statistical Computing*; R Foundation for Statistical Computing: Vienna, Austria, 2019. Available online: https://www.r-project.org (accessed on 8 July 2024).
68. Warnes, G.R.; Bolker, B.; Bonebakker, L.; Gentleman, R.; Huber, W.; Liaw, A.; Lumley, T.; Maechler, M.; Magnusson, A.; Moeller, S.; et al. Gplots: Various R Programming Tools for Plotting Data. R Package Version 2.17.0. 2020. Available online: https://CRAN.R-Project.org/package=gplots (accessed on 8 July 2024).
69. Tibco Software Inc. *Statistica*, version 13 Data Analysis Software System; Tibco Software Inc.: Palo Alto, CA, USA, 2021. Available online: https://www.tibco.com/ (accessed on 8 July 2024).
70. Krzywiński, M.; Schein, J.; Birol, İ.; Connors, J.; Gascoyne, R.; Horsman, D.; Jones, S.J.; Marra, M.A. Circos: An Information Aesthetic for Comparative Genomics. *Genome Res.* **2009**, *19*, 1639–1645. [CrossRef] [PubMed]
71. Udume, O.A.; Abu, G.O.; Stanley, H.O.; Vincent-Akpu, I.F.; Momoh, Y.; Eze, M.O. Biostimulation of Petroleum-Contaminated Soil Using Organic and Inorganic Amendments. *Plants* **2023**, *12*, 431. [CrossRef]
72. Mishra, P.; Kiran, N.S.; Romanholo Ferreira, L.F.; Yadav, K.K.; Mulla, S.I. New Insights into the Bioremediation of Petroleum Contaminants: A Systematic Review. *Chemosphere* **2023**, *326*, 138391. [CrossRef]
73. Aziz, Z.S.; Jazza, S.H.; Dageem, H.N.; Banoon, S.R.; Balboul, B.A.; Abdelzaher, M.A. Bacterial Biodegradation of Oil-Contaminated Soil for Pollutant Abatement Contributing to Achieve Sustainable Development Goals: A Comprehensive Review. *Results Eng.* **2024**, *22*, 102083. [CrossRef]
74. Wei, Z.; Wei, Y.; Liu, Y.; Niu, S.; Xu, Y.; Park, J.-H.; Wang, J.J. Biochar-Based Materials as Remediation Strategy in Petroleum Hydrocarbon-Contaminated Soil and Water: Performances, Mechanisms, and Environmental Impact. *J. Environ. Sci.* **2024**, *138*, 350–372. [CrossRef]
75. Abbaspour, A.; Zohrabi, F.; Dorostkar, V.; Faz, A.; Acosta, J.A. Remediation of an Oil-Contaminated Soil by Two Native Plants Treated with Biochar and Mycorrhizae. *J. Environ. Manag.* **2020**, *254*, 109755. [CrossRef]
76. Dahiya, P.; Behl, M.; Kumari, D.; Arya, E.; Rathour, R.K.; Kumar, V.; Bhatia, R.K. Detoxification of Contaminated Soil to Restore Its Health for Sustainable Agriculture. In *Advancements in Microbial Biotechnology for Soil Health*; Bhatia, R.K., Walia, A., Eds.; Springer Nature: Singapore, 2024; pp. 295–322, ISBN 978-981-9994-82-3.
77. Vasilyeva, G.K.; Strijakova, E.R.; Ortega-Calvo, J.J. Remediation of Soils Polluted by Oil Industries. In *Soil Remediation Science and Technology*; Ortega-Calvo, J.J., Coulon, F., Eds.; Springer Nature: Cham, Switzerland, 2024; pp. 191–234, ISBN 978-3-031-60192-7.
78. Wyszkowski, M.; Kordala, N. Trace Element Contents in Petrol-Contaminated Soil Following the Application of Compost and Mineral Materials. *Materials* **2022**, *15*, 5233. [CrossRef]
79. Murtaza, G.; Ahmed, Z.; Eldin, S.M.; Ali, I.; Usman, M.; Iqbal, R.; Rizwan, M.; Abdel-Hameed, U.K.; Haider, A.A.; Tariq, A. Biochar as a Green Sorbent for Remediation of Polluted Soils and Associated Toxicity Risks: A Critical Review. *Separations* **2023**, *10*, 197. [CrossRef]
80. Van Nguyen, T.T.; Phan, A.N.; Nguyen, T.-A.; Nguyen, T.K.; Nguyen, S.T.; Pugazhendhi, A.; Ky Phuong, H.H. Valorization of Agriculture Waste Biomass as Biochar: As First-Rate Biosorbent for Remediation of Contaminated Soil. *Chemosphere* **2022**, *307*, 135834. [CrossRef] [PubMed]
81. Borowik, A.; Wyszkowska, J.; Zaborowska, M.; Kucharski, J. Soil Enzyme Response and Calorific Value of Zea Mays Used for the Phytoremediation of Soils Contaminated with Diesel Oil. *Energies* **2024**, *17*, 2552. [CrossRef]
82. Wu, H.; Hu, J.; Shaaban, M.; Xu, P.; Zhao, J.; Hu, R. The Effect of Dolomite Amendment on Soil Organic Carbon Mineralization Is Determined by the Dolomite Size. *Ecol. Process.* **2021**, *10*, 8. [CrossRef]
83. Huang, J.; Fisher, P.R.; Argo, W.R. Container Substrate-pH Response to Differing Limestone Type and Particle Size. *HortScience* **2007**, *42*, 1268–1273. [CrossRef]
84. Cai, W.K.; Liu, J.H.; Zhou, C.H.; Keeling, J.; Glasmacher, U.A. Structure, Genesis and Resources Efficiency of Dolomite: New Insights and Remaining Enigmas. *Chem. Geol.* **2021**, *573*, 120191. [CrossRef]

85. Qi, S.; Xue, Q.; Niu, Z.; Zhang, Y.; Liu, F.; Chen, H. Investigation of Zn^{2+} and Cd^{2+} Adsorption Performance by Different Weathering Basalts. *Water. Air. Soil Pollut.* **2016**, *227*, 126. [CrossRef]
86. Ai, H.; Li, X.; Chen, C.; Xu, L.; Fu, M.-L.; Sun, W.; Yuan, B. Immobilization of β-FeOOH Nanomaterials on the Basalt Fiber as a Novel Porous Composite to Effectively Remove Phosphate from Aqueous Solution. *Colloids Surf. Physicochem. Eng. Asp.* **2022**, *632*, 127815. [CrossRef]
87. Marková, I.; Kubás, J.; Buganová, K.; Ristvej, J. Usage of Sorbents for Diminishing the Negative Impact of Substances Leaking into the Environment in Car Accidents. *Front. Public Health* **2022**, *10*, 957090. [CrossRef]
88. Sabadash, V. Adsorption of Oil Products by Natural Sorbents. In *Modern Technologies in Energy and Transport*; Boichenko, S., Zaporozhets, A., Yakovlieva, A., Shkilniuk, I., Eds.; Springer Nature: Cham, Switzerland, 2024; pp. 137–158, ISBN 978-3-031-44351-0.
89. Balidakis, A.; Matsi, T.; Karagianni, A.-G.; Ipsilantis, I. Sewage Sludge Treated with Bentonite, Vermiculite or Biochar Can Improve Soil Properties and Enhance Growth of Grasses. *Soil Use Manag.* **2023**, *39*, 1403–1421. [CrossRef]
90. Faleh, S.T.; Fahmi, A.H.; Abood, M.A. The Role of Biochar and Perlite in Improving Some Chemical Properties of Clay Loam Soil and Sandy Loam Soil. *IOP Conf. Ser. Earth Environ. Sci.* **2023**, *1262*, 082011. [CrossRef]
91. Ansari, S.; Bahmaninia, H.; Mohammadi, M.-R.; Ostadhassan, M.; Norouzi-Apourvari, S.; Schaffie, M.; Ranjbar, M.; Hemmati-Sarapardeh, A. On the Evaluation of Asphaltene Adsorption onto Dolomite Surface: The Roles of Flow Condition, Composition of Asphaltene, and Dolomite Size. *Alex. Eng. J.* **2022**, *61*, 9411–9425. [CrossRef]
92. Yuan, X.; Xia, W.; An, J.; Yin, J.; Zhou, X.; Yang, W. Kinetic and Thermodynamic Studies on the Phosphate Adsorption Removal by Dolomite Mineral. *J. Chem.* **2015**, *2015*, 853105. [CrossRef]
93. Tuchowska, M.; Wołowiec, M.; Solińska, A.; Kościelniak, A.; Bajda, T. Organo-Modified Vermiculite: Preparation, Characterization, and Sorption of Arsenic Compounds. *Minerals* **2019**, *9*, 483. [CrossRef]
94. Wojcieszak, D.; Przybył, J.; Czajkowski, Ł.; Majka, J.; Pawłowski, A. Effects of Harvest Maturity on the Chemical and Energetic Properties of Corn Stover Biomass Combustion. *Materials* **2022**, *15*, 2831. [CrossRef]
95. Wojcieszak, D.; Przybył, J.; Ratajczak, I.; Goliński, P.; Janczak, D.; Waśkiewicz, A.; Szentner, K.; Woźniak, M. Chemical Composition of Maize Stover Fraction versus Methane Yield and Energy Value in Fermentation Process. *Energy* **2020**, *198*, 117258. [CrossRef]
96. Mendes, M.P.; Cunha, D.L.; dos Santos, V.M.L.; Vianna, M.T.G.; Marques, M. Ecological Risk Assessment (ERA) Based on Contaminated Groundwater to Predict Potential Impacts to a Wetland Ecosystem. *Environ. Sci. Pollut. Res.* **2020**, *27*, 26332–26349. [CrossRef]
97. Falih, K.T.; Mohd Razali, S.F.; Abdul Maulud, K.N.; Abd Rahman, N.; Abba, S.I.; Yaseen, Z.M. Assessment of Petroleum Contamination in Soil, Water, and Atmosphere: A Comprehensive Review. *Int. J. Environ. Sci. Technol.* **2024**, *21*, 8803–8832. [CrossRef]
98. Saxena, R.C.; Adhikari, D.K.; Goyal, H.B. Biomass-Based Energy Fuel through Biochemical Routes: A Review. *Renew. Sustain. Energy Rev.* **2009**, *13*, 167–178. [CrossRef]
99. Srivastava, R.K.; Shetti, N.P.; Reddy, K.R.; Kwon, E.E.; Nadagouda, M.N.; Aminabhavi, T.M. Biomass Utilization and Production of Biofuels from Carbon Neutral Materials. *Environ. Pollut.* **2021**, *276*, 116731. [CrossRef]
100. Saleem, M. Possibility of Utilizing Agriculture Biomass as a Renewable and Sustainable Future Energy Source. *Heliyon* **2022**, *8*, e08905. [CrossRef]
101. Gao, C.; El-Sawah, A.M.; Ali, D.F.I.; Alhaj Hamoud, Y.; Shaghaleh, H.; Sheteiwy, M.S. The Integration of Bio and Organic Fertilizers Improve Plant Growth, Grain Yield, Quality and Metabolism of Hybrid Maize (*Zea mays* L.). *Agronomy* **2020**, *10*, 319. [CrossRef]
102. Zahed, M.A.; Salehi, S.; Madadi, R.; Hejabi, F. Biochar as a Sustainable Product for Remediation of Petroleum Contaminated Soil. *Curr. Res. Green Sustain. Chem.* **2021**, *4*, 100055. [CrossRef]
103. Wyszkowski, M.; Kordala, N. Role of Different Material Amendments in Shaping the Content of Heavy Metals in Maize (*Zea mays* L.) on Soil Polluted with Petrol. *Materials* **2022**, *15*, 2623. [CrossRef] [PubMed]
104. Sabitov, A.; Atamanov, M.; Doszhanov, O.; Saurykova, K.; Tazhu, K.; Kerimkulova, A.; Orazbayev, A.; Doszhanov, Y. Surface Characteristics of Activated Carbon Sorbents Obtained from Biomass for Cleaning Oil-Contaminated Soils. *Molecules* **2024**, *29*, 3786. [CrossRef] [PubMed]
105. Wyszkowski, M.; Wyszkowska, J.; Kordala, N.; Zaborowska, M. Molecular Sieve, Halloysite, Sepiolite and Expanded Clay as a Tool in Reducing the Content of Trace Elements in *Helianthus annuus* L. on Copper-Contaminated Soil. *Materials* **2023**, *16*, 1827. [CrossRef]
106. Wyszkowska, J.; Borowik, A.; Zaborowska, M.; Kucharski, J. Biochar, Halloysite, and Alginite Improve the Quality of Soil Contaminated with Petroleum Products. *Agriculture* **2023**, *13*, 1669. [CrossRef]
107. Zhang, W.; Liang, Y. Performance of Different Sorbents toward Stabilizing Per- and Polyfluoroalkyl Substances (PFAS) in Soil. *Environ. Adv.* **2022**, *8*, 100217. [CrossRef]
108. Qu, J.; Zhang, X.; Guan, Q.; Kong, L.; Yang, R.; Ma, X. Effects of Biochar Underwent Different Aging Processes on Soil Properties and Cd Passivation. *Environ. Sci. Pollut. Res.* **2022**, *29*, 57885–57895. [CrossRef]
109. Vocciante, M.; Franchi, E.; Fusini, D.; Pedron, F.; Barbafieri, M.; Petruzzelli, G.; Reverberi, A.P. Sustainable Recovery of an Agricultural Area Impacted by an Oil Spill Using Enhanced Phytoremediation. *Appl. Sci.* **2024**, *14*, 582. [CrossRef]
110. Nguyen Ho, Q.; Hidaka, T.; Rahman, M.A.; Yoshida, N. Application of Natural Zeolite Adsorption in Cooperation with Photosynthesis for the Post-Treatment of Microbial Fuel Cells. *RSC Adv.* **2024**, *14*, 26484–26493. [CrossRef]

111. Atero-Calvo, S.; Magro, F.; Masetti, G.; Navarro-León, E.; Rios, J.J.; Blasco, B.; Ruiz, J.M. Comparative Effects of Root and Foliar Leonardite-Suspension Concentrate Application on Plant Growth and Photosynthetic Efficiency of Lettuce Plants (*Lactuca sativa* L.). *J. Plant Growth Regul.* **2024**. [CrossRef]
112. Wyszkowski, M.; Kordala, N. Applicability of Compost and Mineral Materials for Reducing the Effect of Diesel Oil on Trace Element Content in Soil. *Materials* **2023**, *16*, 3655. [CrossRef] [PubMed]
113. Kamenchuk, V.; Rumiantsev, B.; Dzhatdoeva, S.; Sadykhov, E.; Kochkarov, A. Analysis of Cross-Influence of Microclimate, Lighting, and Soil Parameters in the Vertical Farm. *Agronomy* **2023**, *13*, 2174. [CrossRef]
114. Głąb, T.; Gondek, K.; Mierzwa–Hersztek, M. Biological Effects of Biochar and Zeolite Used for Remediation of Soil Contaminated with Toxic Heavy Metals. *Sci. Rep.* **2021**, *11*, 6998. [CrossRef]
115. Morales-Máximo, C.N.; López-Sosa, L.B.; Rutiaga-Quiñones, J.G.; Corral-Huacuz, J.C.; Aguilera-Mandujano, A.; Pintor-Ibarra, L.F.; López-Miranda, A.; Delgado-Domínguez, S.N.; Rodríguez-Magallón, M.d.C.; Morales-Máximo, M. Characterization of Agricultural Residues of Zea Mays for Their Application as Solid Biofuel: Case Study in San Francisco Pichátaro, Michoacán, Mexico. *Energies* **2022**, *15*, 6870. [CrossRef]
116. Priya; Deora, P.S.; Verma, Y.; Muhal, R.A.; Goswami, C.; Singh, T. Biofuels: An Alternative to Conventional Fuel and Energy Source. *Mater. Today Proc.* **2022**, *48*, 1178–1184. [CrossRef]
117. Havrland, B.; Ivanova, T.; Lapczynska-Kordon, B.; Kolaříková, M. Comparative Analysis of Bio-Raw Materials and Biofuels. *Eng. Rural. Dev.* **2013**, 541–544.
118. Gerssen-Gondelach, S.J.; Saygin, D.; Wicke, B.; Patel, M.K.; Faaij, A.P.C. Competing Uses of Biomass: Assessment and Comparison of the Performance of Bio-Based Heat, Power, Fuels and Materials. *Renew. Sustain. Energy Rev.* **2014**, *40*, 964–998. [CrossRef]
119. Zihare, L.; Soloha, R.; Blumberga, D. The Potential Use of Invasive Plant Species as Solid Biofuel by Using Binders. *Agron. Res.* **2018**, *16*, 923–935. [CrossRef]
120. Kalt, G.; Lauk, C.; Mayer, A.; Theurl, M.C.; Kaltenegger, K.; Winiwarter, W.; Erb, K.-H.; Matej, S.; Haberl, H. Greenhouse Gas Implications of Mobilizing Agricultural Biomass for Energy: A Reassessment of Global Potentials in 2050 under Different Food-System Pathways. *Environ. Res. Lett.* **2020**, *15*, 034066. [CrossRef]
121. Rocha-Meneses, L.; Luna-delRisco, M.; González, C.A.; Moncada, S.V.; Moreno, A.; Sierra-Del Rio, J.; Castillo-Meza, L.E. An Overview of the Socio-Economic, Technological, and Environmental Opportunities and Challenges for Renewable Energy Generation from Residual Biomass: A Case Study of Biogas Production in Colombia. *Energies* **2023**, *16*, 5901. [CrossRef]
122. Raza, A.; Zunaira-Tu-Zehra; Khurram, M.; Khan, M.A.P.; Durez, A.; Khan, L.A.; Raza, A.; Zunaira-Tu-Zehra; Khurram, M.; Khan, M.A.P.; et al. Comparison of Evaporation in Conventional Diesel and Bio-Fuel Droplets in Engine Cylinder. In *Exergy—New Technologies and Applications*; IntechOpen: London, UK, 2023; ISBN 978-1-83768-545-5.
123. Rocha-Meneses, L.; Ferreira, J.A.; Mushtaq, M.; Karimi, S.; Orupõld, K.; Kikas, T. Genetic Modification of Cereal Plants: A Strategy to Enhance Bioethanol Yields from Agricultural Waste. *Ind. Crops Prod.* **2020**, *150*, 112408. [CrossRef]

MDPI AG
Grosspeteranlage 5
4052 Basel
Switzerland
Tel.: +41 61 683 77 34

Energies Editorial Office
E-mail: energies@mdpi.com
www.mdpi.com/journal/energies

Academic Open
Access Publishing

mdpi.com

ISBN 978-3-7258-4562-0